Antimicrobial Peptides from Venom: Structure, Function and Toxicity

By

Kirstie Marie Rawson

Submitted in partial fulfilment of the degree of Doctor of Philosophy (PhD)

Biomolecular Sciences Research Centre

November 2019

I hereby declare that:

1. I have not been enrolled for another award of the University, or other academic or professional organisation, whilst undertaking my research degree.

2. None of the material contained in the thesis has been used in any other submission for an academic award.

3. I am aware of and understand the University's policy on plagiarism and certify that this thesis is my own work. The use of all published or other sources of material consulted have been properly and fully acknowledged.

4. The work undertaken towards the thesis has been conducted in accordance with the SHU Principles of Integrity in Research and the SHU Research Ethics Policy.

5. The word count of the thesis is 50,000.

Name	*Kirstie Marie Rawson*
Date	*November 2019*
Award	*PhD*
Faculty	*Health and Wellbeing*
Director(s) of Studies	*Dr Keith Miller*

Dedication

For Joan, Francis and Hazel who didn't get to see me do this but were with me every step of the way.

Meg Stokes (Slatcher), you were the best biology teacher anyone could ever wish for- the science is for you. You were right. I did it.

Quote

“Never be afraid of who you are”

- Leia Organa

Abstract

The need for new antimicrobials with novel mechanisms of action is becoming one of the most urgent requirements in modern medicine. Antimicrobial peptides (AMPs) are naturally occurring compounds which possess a rapid killing mechanism and low resistance potential. Consequently, they are being viewed as potential alternatives to traditional antibiotics. One of the major factors limiting further development of AMPs is off target toxicity. Enhancements to antimicrobial peptides which can maximise antimicrobial activity whilst reducing mammalian cytotoxicity would make these peptides more attractive as future pharmaceuticals.

Smp24 and Smp43 are AMPs derived from the venom of the scorpion *Scorpio maurus palmatus.* This study sought to better understand the relationship between structure, function and bacterial selectivity of these peptides by performing single amino acid substitutions. The structure-function relationship of the two AMPs has been investigated by performing N-terminal, mid-chain and C-terminal amino acid substitutions and determining the effect this has on the antimicrobial and cytotoxic activity of the peptides. The structural implications of the amino acid substitutions have been investigated via homology modelling and circular dichroism spectroscopy.

Functional improvements have been made to modified peptides when compared with native Smp24 and native Smp43, which have produced peptides with enhanced therapeutic indices.

Table of Contents

Dedication – i

Quote- ii

Abstract- iii

Table of contents- iv

List of figures- xi

List of tables- xiv

1* Introduction *1

1.1 Antibiotics and the emergence of resistant pathogens 2

1.2 Antibiotic resistance mechanisms 7

1.3 Modern antimicrobial drug discovery 9

1.4 Antimicrobial peptides 10

1.5 Antimicrobial peptide conformation 12

1.5.1 α-helical peptides 13

1.5.2 β-sheet containing peptides 14

1.5.3 Peptides with α and β elements 14

1.5.4 Linear peptides rich in particular amino acids 14

1.6 Structural characteristics of AMPs 15

1.6.1 Structure 16

1.6.2 Charge 16

1.6.3 Amphipathicity 17

1.6.4 Hydrophobicity 17

1.6.5 Polar angle 17

1.7 Mechanism of action 18

1.7.1 Barrel-stave model 21

1.7.2 Toroidal pore model 21

1.7.3 Carpet model 22

1.7.4 Other mechanisms of pore formation 23

1.7.5 Mechanism of action and cell membrane composition 25

1.7.6 Other mechanisms of action 26

1.8 Natural resistance towards AMPs 28

1.9 Antimicrobial peptides in therapeutic usage and the design of new peptides 31

1.9.1 AMPs in clinical usage 31

1.9.2 Designing new peptide analogues 35

1.10 Strategies for AMP production 37

1.11 Venoms 37

1.11.1 Scorpion venom 39

1.11.2 *Scorpio maurus palmatus* 41

1.11.3 Smp24 41

1.11.4 Smp43 44

1.12 Scope of the present study 46

2* General Methods *47

2.1 Materials 48

2.2 Peptide synthesis 48

2.3 Minimum inhibition concentration (MIC) assay 48

2.4 Minimum bactericidal concentration (MBC) assay 49

2.5 Minimum biofilm eradication concentration (MBEC) assay 49

2.6 Haemolysis assay 50

2.7 Cytotoxicity assays 50

2.7.1 Eukaryotic cell culture line maintenance 50

2.7.2 Cytotoxicity assays 51

2.7.3 LD_{50} calculations 52

2.7.4 T-test on data 52

2.7.5 Therapeutic index 52

2.8 Circular dichroism 52

2.8.1 Methodology 52

2.8.2 Data analysis 53

2.9 Modelling 53

2.9.1 Helical wheel projections 53

2.9.2 *Ab-initio* modelling 54

2.9.3 3D-modelling 54

2.9.4 Hydrophobic moment 54

2.10 Gene synthesis 54

2.10.1 Transformation of plasmids 55

2.10.2 Polymerase chain reaction (PCR) to confirm transformation 55

2.10.3 Agarose gel electrophoresis 56

2.11 Production of Smp24 with the STII leader sequence 56

2.12 Purification of the STII/Smp24 peptide 57

2.12.1 Cation exchange I 57

2.12.2 Cation exchange II 57

2.13 Sodium dodecyl sulphate polyacrylamide gel electrophoresis (SDS-PAGE) 58

2.14 Tris-tricine PAGE 59

2.14.1 TRIS-tricine gel composition (12%) 59

2.14.2 Pre-cast gels 60

2.14.3 Pre-cast gradient gel 61

2.15 MALDI 61

2.16 Immunological detection of Smp24 by anti-Smp24 antibodies 61

2.16.1 Raising antibodies in rabbits 61

2.16.2 Dot blot 61

2.17 *Galleria mellonella* pathogenicity assay 62

2.17.1 Preparation of larvae 62

2.17.2 Pathogenicity assay 62

2.17.3 Log rank reduction test. 63

2.18 Affinity tagged protein over production 63

2.18.1 Protein overproduction 63

2.18.2 Identification of fusion protein by dot blot 64

2.19 Affinity-tagged protein purification 64

2.19.1 Further optimisation 65

2.20 Site-directed mutagenesis 65

3* Elucidating the relationship between structure and. Antimicrobial activity og AMPs from venom *67

3.1 Introduction 68

3.2 Study aims 69

3.3 Experimental design 70

3.4 Results 74

3.4.1 Peptide sequences 75

3.4.2 Minimum inhibitory concentrations and Minimum bactericidal concentrations 77

3.4.2.1 Smp24 antimicrobial activity 77

3.4.2.2 Smp24 microbial inhibition 80

3.4.2.3 Smp24 bactericidal activity 81
3.4.2.4 Comparison between MIC and MBC 82
3.4.3 Smp43 antimicrobial activity 84
3.4.3.1 Smp43 microbial inhibition 85
3.4.3.2 Smp43 bactericidal activity 86
3.4.3.3 MIC: MBC ratios for Smp43 87
3.5 Anti-biofilm activity 89
3.5.1 Biofilm vs planktonic MICs 90
3.5.2 Comparison of anti-biofilm activity of Smp24 and Smp43 with commercially available lipopeptide antibiotics 91
3.6 Structural investigations: Circular Dichroism 91
3.6.1 CD spectroscopy of Smp24 91
3.6.2 TFE titration of Smp24 93
3.6.3 CD spectroscopy of Smp43 95
3.7 Discussion 96
3.7.1 Structural differences between modified peptides 97
3.7.2 Comparison of AMPs to commercially available lipopeptide antibiotics 98
3.7.3 AMPs and anti-biofilm activity 99
3.8 Conclusions 101
4* Investigating the relationship between structure, cytotoxicity and haemolysis of AMPs from venom *103
4.1 Introduction 104
4.2 Study aims 104
4.3 Experimental design 105
4.4 Results 107
4.4.1 Haemolysis 107
4.4.1.1 Haemolytic activity of modified Smp24 peptides 107
4.4.1.2 Haemolytic activity of modified Smp43 peptides 108
4.4.2 Cytotoxicity against liver and kidney cells 109
4.4.2.1 Cytotoxic activity of modified Smp24 peptides 110
4.4.2.2 Cytotoxic activity of modified Smp43 peptides 111
4.4.3 Cytotoxicity of AMPs against skin cell lines 113
4.4.3.1 Cytotoxicity of modified Smp24 peptides against human skin cells 113
4.4.3.2 Cytotoxicity of modified Smp43 peptides against immortalised keratinocytes 114
4.4.3.3 Human Urothelial Epithelial Cells (HUEPC) 116

4.5 Discussion 117
4.5.1 Haemolysis of Smp24 117
4.5.2 Haemolysis of Smp43 118
4.5.3 Haemolysis as a measure of cytotoxicity 119
4.5.4 Eukaryotic cytotoxicity 120
4.5.4.1 Membrane composition 121
4.5.4.2 Cytotoxicity of Smp24 122
4.5.4.3 Cytotoxicity of Smp43 123
4.5.5 Therapeutic applications 124
4.6 Conclusions 125
5* Modelling the relationship between structure and function *127
5.1 Structural investigations relating to antimicrobial activity 128
5.2 Study aims 128
5.3 Experimental design 129
5.4 Structural investigations relating to antimicrobial activity 129
5.4.1 Structural investigations of Smp24 K7F 129
5.4.2 Structural investigations of Smp24 S3K 131
5.4.3 Structural investigations for Smp43 W3A/W5A/W14A 132
5.4.4 Relating structure to function: Smp24 S3K and Smp24 K7F 134
5.4.5 Polar angles and hydrophobic moments 136
5.4.6 Relating structure and function: Smp43 S24K, Smp43 S43K and Smp43 W14A 140
5.4.7 Smp43 S43K 143
5.4.8 Smp43 W14A 143
5.4.9 The role of charge and hydrophobicity on Smp43 function 143
5.5 Structural investigations relating to eukaryotic toxicity 149
5.5.1 Haemolysis of Smp24-derived modifications 149
5.5.2 Haemolysis of Smp43-derived modifications 151
5.5.2.1 Cytotoxicity of Smp24-derived modifications 152
5.5.3 Cytotoxicity of Smp43 153
5.6 Therapeutic indices 155
5.6.1 Therapeutic indices of modified Smp24 peptides 155
5.6.2 Therapeutic indices of modified Smp43 peptides 156
5.6.3 Therapeutic indices of peptides against urothelial cells 158
5.6.3.1 Therapeutic indices of lipopeptide antibiotics 159
5.7 Conclusions 161

6 **Optimisation of recombinant production of venom-derived peptides in *E.coli* BL21** ***163***

6.1 Introduction 164

6.2 Study aims 165

6.3 Experimental design 165

6.3.1 Recombinant expression of antimicrobial peptides in *E. coli* 165

6.3.2 Experimental design for the overproduction of Smp24 protein 168

6.3.3 Vector design for the expression of Smp24 170

6.3.4 Transformation & Confirmation of transformation 172

6.3.5 Recombinant production of Smp24 protein 172

6.3.6 Validation of protein overproduction 173

6.3.7 Protein purification 174

6.3.8 Validating the presence of Smp24 176

6.3.8.1 SDS-PAGE 176

6.3.8.2 TRIS-tricine PAGE 177

6.3.8.3 Matrix assisted laser desorption/ionisation time of flight mass spectrometry (MALDI-TOF MS) 177

6.3.8.4 Detection of Smp24 in the presence of salt 179

6.3.9 Additional protein purification 181

6.3.10 Immunological detection of Smp24 182

6.3.11 Alternative approach for protein detection 184

6.4 Limitations of the signal peptide expression system 186

6.5 Plasmid construct design with affinity tag 189

6.5.1 Transformation 194

6.5.2 Affinity tagged protein over production 194

6.5.3 Affinity tagged protein purification 195

6.5.4 Additional optimisation 196

6.5.5 Mutagenesis of Smp peptides 197

6.6 Discussion 202

7 **General Discussion** ***208***

7.1 Improving the understanding of structure and function 209

7.2 AMPs and membrane interactions 211

7.3 Elucidating the mechanism of action 213

7.4 Development of novel antimicrobials 214

7.5 Recombinant peptide production 215

7.6 Improving the stability of AMPs..... 216

7.7 Higher resolution structural biology approaches..... 218

List of Figures

Figure 1.1: Structural classes of AMPs 13
Figure 1.2: factors influencing structure of AMPs. 15
Figure 1.3: Interactions between amphipathic AMPs and prokaryotic and eukaryotic membranes. 20
Figure 1.4: Visual representation of pore formation 23
Figure 1.5: Mechanisms of cell death by AMPs 27
Figure 1.6: Mechanisms of antimicrobial peptide resistance 29
Figure 3.1: Helical wheel projections 71
Figure 3.2: Mutation strategy for scorpion AMPs 73
Figure 3.3: Helical propensity of Smp24, S3K and K7F in aqueous (0% TFE) and membrane mimetic (60% TFE) conditions. 92
Figure 3.4: CD spectra for the titration of TFE (0-60%) for Smp24, Smp24 S3K and Smp24 K7F 94
Figure 3.5: the helical propensity of Smp43 in water (0% TFE) and in membrane mimetic conditions (60% TFE). 95
Figure 4.1: Mutation strategy for scorpion AMPs 106
Figure 5.1: Structural analysis of Smp24 and modifications 130
Figure 5.2: Structural analysis of N-terminal charge modification of Smp24 .. 131
Figure 5.3: Structural analysis of tryptophan substitutions in Smp43 133
Figure 5.4: Spatial distribution of Smp24, S3K and K7F 135
Figure 5.5: Atomic representations of Smp24 and derived modifications 137
Figure 5.6: Spatial diagrams for Smp43, Smp43 S24K, Smp43 S43K and Smp43 W14A. 141
Figure 5.7: Polar facet representation in Smp43 and derived modifications .. 142
Figure 5.8: Spatial distribution of Smp43 and Smp43 W3A/W5A/W14A 145
Figure 5.9: Sequence homology between Smp43 and Pandinin 1. 147
Figure 5.10: Structural modifications of Smp24 150
Figure 5.11: Structural modifications to Smp43. 152
Figure 5.12: Helical wheel projections of Smp24, Smp24 S3F, Smp24 K7F and Smp24 D23F 153

Figure 5.13: Helical wheel projections of Smp43, Smp43 S24K, Smp43 S43K and Smp43 W3A 154
Figure 5.14: The calculated TI's of modified Smp24 peptides against HepG2, HEK-293, HaCaT and sheep erythrocytes.. 155
Figure 5.15: The calculated TI's of modified Smp43 peptides against HepG2,, HEK-293, HaCaT and sheep erythrocytes. Statistical significance was determined by performing a T-test on the data 157
Figure 5.16: Calculated TIs for Smp24 and Smp43 against human uroepithelial cells (HUEPC). 158
Figure 5.17: Calculated TI's of daptomycin and PMB against liver, kidney, skin and red blood cells. 159
Figure 5.18: Observable differences in TI for Smp24 and Smp43 against all cell lines used in this study. 160
Figure 6.2: Vector design for the expression of neurotoxins in *E. coli*.. 167
Figure 6.1: Strategy for the production of recombinant Smp24 in a prokaryotic expression system. 169
Figure 6.3: pET22b(+) vector map and the corresponding codon usage sequences for STII and Smp24 for insertion of the gene between the HindIII and NdeI restriction sites. 171
Figure 6.4: Visualisation of the PCR product from the extraction of pET22b/STII/Smp24 from *E. coli* BL21 λDE3 172
Figure 6.5: SDS-PAGE gel of the overproduction of Smp24 in *E. coli* 173
Figure 6.6: Purification of Smp24 175
Figure 6.7: MALDI-MS spectral identification of Smp24 178
Figure 6.8: MALDI MS analysis of Smp24 180
Figure 6.9: AKTA A_{280} trace for additional purification of Smp24 181
Figure 6.10: Optimisation of antibody detection using dot blot for the detection of Smp24 183
Figure 6.11: Immunological detection of expressed proteins in *E. coli.* 184
Figure 6.12: *Galleria mellonella* pathogenicity results 188
Figure 6.14: The design of pET22b/STII/FLAG/Smp24. 191
Figure 6.15: Creation of the vector pET22b/Smp24/FLAG 193
Figure 6.16: Agarose gel electrophoresis for the transformation of FLAG-tagged vectors in to *E. coli* BL21 λDE3 195
Figure 6.18: Dot blot analysis of Smp24-FLAG purification 196

Figure 6.19: Dot blot analysis of Smp24-FLAG purification. 197
Figure 6.20: Agarose gel electrophoresis depicting the mutagenesis of Smp24. 200

List of Tables

Table 1.1: Common components of eukaryotic and prokaryotic membranes and the charge states observed. 26
Table 1.2: Membrane and intracellular targets of AMPs 28
Table 2.1: SDS-PAGE reagent composition 58
Table 2.2: Final SDS-PAGE running conditions 59
Table 2.3: Gel and buffer composition for the analysis of protein fractions by TRIS-tricine PAGE. 60
Table 2.4: PCR cycling conditions for site-directed mutagenesis 66
Table 3.1: Sequence and parameter data for Smp24 and derived modifications. 75
Table 3.2: Sequence and parameter data for Smp43 and derived modifications. 76
Table 3.3: Antimicrobial activity of Smp24 and modified peptides as determined by broth microdilution assay and bactericidal assay. 79
Table 3.4: MIC: MBC ratios for Smp24 and derived modifications 83
Table 3.5: Antimicrobial activity of Smp43 and modified peptides as determined by broth microdilution assay. 84
Table 3.6: MIC: MBC ratios for Smp43 and derived modifications 88
Table 3.7: Anti-biofilm activity of Smp24 and Smp43 as defined by MBIC and MBEC values 89
Table 4.1: Sequence and parameter data for Smp24 and derived modifications. 107
Table 4.2: Sequence and parameter data for Smp43 and derived modifications. 107
Table 4.3: Haemolytic activity presented as HC_{50} values for Smp24 and derived modifications used within this study. 107
Table 4.4: Haemolytic activities of Smp43 and the modified peptides displayed as HC_{50} values. 108
Table 4.5: Cytotoxic activities of Smp24-derived peptides against liver and kidney cell lines. 110
Table 4.6: Cytotoxic activities of Smp43 and derived modifications against liver and kidney cell lines. 112

Table 4.7: LD_{50} concentrations for modified Smp24 peptides against an immortalised human keratinocyte cell line (HaCaT)..... 113
Table 4.8: Cytotoxicity profiles of Smp43 and derived modifications displayed as LD_{50} values against the HaCaT cell line..... 115
Table 4.9: Membrane potential differences between primary and secondary cell lines..... 116
Table 4.10: Cytotoxicity assessment of native Smp24 and Smp43 against HUEPC cells 116
Table 6.1: The amino acid sequence for the signal peptide (STII) and neurotoxin II sequence (NTII) is shown in black. 168
Table 6.2: Primer design for the site-directed mutagenesis of pET22b/STII/Smp24. Primers were redesigned for the creation of the S3K mutant as previous attempts to modify the gene were unsuccessful. 199
Table 6.3: Confirmed sequences of mutated Smp24 peptides, as produced by site-directed mutagenesis. 201
Table 7.1: Comparison of prokaryotic and eukaryotic activity of Smp24, Smp43 and derived modifications that yielded peptides with enhanced TIs. 210

Abbreviations

3D	Three dimensional
3FTxs	Three-fingered toxins
A	Alanine
AAMP	Anionic antimicrobial peptide
ABC	ATP binding cassette
AFM	Atomic force microscopy
AIM	Autoinduction media
AMP	Antimicrobial peptide
AMR	Antimicrobial resistance
APS	Ammonium persulphate
ASP	Antibiotic stewardship programme
ATP	Adenosine triphosphate
bp	Base pair
BSA	Bovine serum albumin
BSAC	British Society for Antimicrobial Chemotherapy
$CaCl_2$	Calcium chloride
CARB-X	Combatting antibiotic resistant bacteria biopharmaceutical accelerator
CAUTIs	Catheter-associated urinary tract infections
CD	Circular dichroism
CH_3COONa	Sodium acetate
CHCA	α-cyano-4-hydroxycinnamic-acid
CHO	Chinese hamster ovary
CL	Cardiolipin
cm	Centimetre
CRE	Carbapenem-resistant Enterobacteriaceae
cUTI	Complicated urinary tract infection
CV	Column volume
D	Aspartic acid
$_D$-AAs	D-amino acids
Da	Dalton
DBPs	Disulphide bridged peptides
dH_2O.	Distilled water
DLA	Diffusion limited aggregation
DMEM	Dulbecco's modified Eagle's medium
DMSO	Dimethyl sulfoxide
DNA	Deoxyribonucleic acid
dNTP	Dinucleotide phosphate
DPPC	1,2-dipalmitoyl-sn-glycero-3-phosphocholine
E	Glutamic Acid
ELISA	Enzyme linked immunosorbent assay
EPS	Extracellular polymeric substances

ESBL	Extended-spectrum β-lactamase
ESKAPE	*Enterococcus faecium, Staphylococcus aureus, Klebsiella pneumoniae, Acinetobacter baumannii, Pseudomonas aeruginosa and Enterobacter species*
EUCAST	European Committee on Antimicrobial Susceptibility Testing
F	Phenylalanine
FAO	The Food and Agricultural Organisation of the United Nations
FCS	Foetal calf serum
FDA	Food and Drug Administration
GNB	Gram negative bacilli
GRAS	Generally recognised as safe
GRAVY	Grand average of hydropathy
GVG	Glycine-valine-glycine
H	Histidine
HaCat	Human keratinocyte cell line
HC_{50}	Lethal haemolysis 50% lysis
HCl	Hydrochloric acid
HEK-293	Human embryonic kidney cell line
HepG2	Hepatic cell line
HGT	Horizontal gene transfer
HM	Hydrophobic moment
HUEPC	Human urothelial epithelial cells
I	Isoleucine
IPTG	Isopropyl-1-thio-β-D-galactopyranoside
IUD	Intrauterine device
K	Lysine
kb	Kilobase
KCl	Potassium chloride
kDa	Kilodalton
KH_2PO_4	Potassium phosphate
KSI	Ketosteroid isomerase
L	Litre
LB	Luria Burtani
LD_{50}	Lethal dose 50% death
LDH	Lactate dehydrogenase
LPS	Lipopolysaccharide
LRRT	Log-rank reduction test
M	Molar
m/z	Mass to charge ration
MALDI-MS	Matrix assisted laser desorption/ionisation mass spectrometry
MALDI-TOF	Matrix assisted laser desorption/ionisation time of flight
MATE	Multi-drug and toxic compound extrusion
MBC	Minimum bactericidal concentration
MBEC	Minimum biofilm eradication concentration

MBIC	Minimum biofilm inhibition concentration
MD	Molecular dynamics
MDR	Multi-drug resistant
MF	Major facilitator
mg	Milligram
µg	Microgram
$MgCL_2$	Magnesium chloride
MGE	Mobile genetic elements
$MgSO_4$	Magnesium sulphate
MH	Muller Hinton
MIC	Minimum inhibition concentration
ml	Millilitre
mM	Millimolar
MRE	Mobile resistance elements
MRSA	Methicillin-resistant *Staphylococcus aureus*
mV	Millivolts
Na_2HPO_4	Sodium phosphate dibasic
nAchRs	Nicotinic acetylcholine receptors
NaCl	Sodium chloride
NADH	Nicotinamide adenine dinucleotide
nc	Not calculable
ND	Not determined
NDBPs	Non-disulphide bridged peptides
NDM	New Delhi metallo- beta lactamase
ng	Nanogram
NH_4Cl	Ammonium chloride
NHS	National Health Service
NI	Non-injected
NICE	National Institute of Clinical Excellence
nm	Nanometre
NMR	Nuclear magnetic resonance
NT	Not tested
NTII	Neurotoxin II
OD	Optical density
OIE	Organisation for Animal Health
PBP	Penicillin binding protein
PBS	Phosphate buffered saline
PC	Phosphatidylcholine
PCR	Polymerase chain reaction
PE	Phosphatidylethanolamine
PG	Phosphatidylglycerol
PI	Isoelectric point
PI	Phosphatidylinositol
Pin1	Pandinin-1

Pin2	Pandinin-2
PMB	Polymyxin B
PMQR	Plasmid-mediated quinolone resistance
PS	Phosphatidylserine
Q	Glutamine
QCM-D	Quartz crystal microbalance dissipation
R	Arginine
RNA	Ribonucleic acid
RND	Resistance-modulation division
ROS	Reactive oxygen species
RP-HPLC	Reversed-phase high performance liquid chromatography
rpm	Rotations per minute
RPP	Ribosomal protection protein
S	Serine
SDM	Site-directed mutagenesis
SDS	Sodium-dodecyl sulphate
SDS-PAGE	Sodium dodecyl-sulphate polyacrylamide gel electrophoresis
SM	Sphingomyelin
SMR	Small multi-drug resistance
spp	Species
SPPS	Solid-phase peptide synthesis
SRP	Signal-recognising protein
STII	Signal peptide II
subsp	Subspecies
TB	Mycobacterium tuberculosis
TBS	Tris buffered saline
TBST	Tris buffered saline with Tween-20
TEMED	Tetramethyl ethylenediamine
TFA	Trifluoroacetic acid
TFE	2,2,2-trifluoroethanol
TI	Therapeutic index
TL	Temporin L
U	Units
UBI	Ubiquicidin
µl	Microlitre
µM	Micrometre
UPEC	Uropathogenic *E. coli*
UTI	Urinary tract infection
UV	Ultraviolet
V_0	Potential difference
VRE	Vancomycin-resistant Enterococci
W	Tryptophan
WHO	World Health Organisation
Y	Tyrosine
α-KTxs	Toxins affecting K+ channels

1

Introduction

1.1 Antibiotics and the emergence of resistant pathogens

Antibiotics have been the primary treatment option for bacterial infection since their introduction in the 1940s and have saved millions of lives worldwide (Sánchez and Demain 2017). The discovery of penicillin and sulphonamides in the 1920's started the antibiotic era and spurred the 'Golden Age' of antimicrobial drug development which continued in to the 1960s and saw the discovery of almost all of the drug classes used today (Santos-Beneit *et al.* 2017). For many years antibiotics were used freely, the evolution of resistance had been foreseen but was underestimated because it would be dependent upon the rate of beneficial mutation, which was likely to be low. The unexpected capacity of bacterial populations to rapidly evolve such widespread resistance to antibiotics has severely impacted the advances in antibacterial chemotherapeutics over the past 50 years (Bell and Gouyon 2003). Antibiotics have been too frequently prescribed to treat non-bacterial conditions and prescribed at times when the drugs were unnecessary as a result of patient demand (Alumran *et al.* 2013). This has been exacerbated by the unregulated usage of antibiotics in some countries, such as Greece, in which antibiotics can be bought from markets and pharmacies without a prescription or even in the absence of a trained pharmacist or other medical professional (Karakonstantis and Kalemaki 2019). Additionally, the usage of antibiotics has spread to non-medical areas and has historically been largely unregulated (Laxminarayan *et al.* 2013, Yidong *et al.* 2017). Initially the use of antibiotics in animals was for the treatment and prevention of diseases including mastitis (Bacanlı and Başaran 2019). In the 1940's an enhanced growth rate was observed in livestock issued antibiotics, as such, the use of antibiotics as growth promoters quickly became common practice in livestock farming (Graham *et al.* 2007). The lack of understanding of the unique features of antibiotics and the subsequent risk of resistance spread has significantly contributed to the present epidemic (Laxminarayan *et al.* 2013).

In recent years, the world has come to face two important and linked problems; 1) the emergence and spread of resistance in pathogenic bacteria and 2) the lack of development of novel chemotherapeutics. The development of antimicrobial resistance not only generates an increasing economic burden in the healthcare setting, but also has a significant impact on patient morbidity and mortality

(Santos-Beneit *et al.* 2017). The World Health Organisation (WHO) has claimed antibiotic resistance is one of the greatest threats to human health, with the prospect of untreatable bacterial infections being on the horizon (MacFadden *et al.* 2015, Viens and Littmann 2015). Clinical practice was once revolutionised by the introduction of antibiotics, which enabled invasive surgery to be performed with substantially decreased risk and previously dangerous infections could be treated with minimal side effects. Sadly, it seems this era has passed and we are now entering in to what has been termed the 'resistance era' (Santos-Beneit *et al.* 2017).

Virtually all significant bacterial infections have become resistant to the first antibiotic treatment of choice, with hospital acquired infections becoming of increasing concern (Lohner and Hilpert 2016). Recent studies have also suggested that antimicrobial resistant pathogens can be more virulent than their antibiotic-susceptible counterparts, which also contributes to patient morbidity and mortality (Wang-Kan *et al.* 2017). In recent years, multidrug-resistant Gram positive organisms, such as methicillin-resistant *Staphylococcus aureus* (MRSA) are less concerning due to the introduction of daptomycin, linezolid and tigecycline to combat such infections (Chopra *et al.* 2008). Ceftaroline is a “new” cephalosporin (approved in 2010) which has activity against many Gram positive organisms including MRSA, penicillin-resistant *Streptococcus pneumoniae* and *Streptococcus pyogenes* (Kaushik *et al.* 2011, Armengol-Porta *et al.* 2016). Ceftobiprole is another cephalosporin with activity against a wide range of Gram positive and Gram negative bacteria, including MRSA, as well as penicillin- and ceftriaxone-resistant *Streptococcus pneumoniae*, Enterobacteriaceae and *Pseudomonas aeruginosa*. Ceftobiprole has been authorised for the treatment of clinical and community-acquired pneumonia (Vaneperen and Segreti 2016). The National institute for Clinical Excellence (NICE) has approved the usage of ceftobiprole in the UK for the treatment of hospital and community acquired pneumonia (excluding ventilator-associated pneumonia) (NICE, 2019) Although these drugs are welcome agents to treat bacterial infection, it does highlight that drug discovery is comparatively easier for compounds effective against Gram positive bacteria as opposed to Gram negative bacteria (Chopra *et al*., 2008).
Infections caused by Gram negative bacteria are difficult to treat due to many pathogens being intrinsically resistant to many antibiotics, which predates their

usage in the medical and agricultural setting (Blair *et al.* 2014). Gram negative bacterial infections are of increasing concern, owing to continual resistance acquisition (Brown, 2015). β-lactamase producing bacteria have been able to withstand β-lactam antibiotics, which led to the introduction of imipenem, the first carbapenem antibiotic, in 1985 (Papp-Wallace *et al.* 2011). The widespread usage of carbapenems resulted in the inevitable development of bacterial resistance, with the first isolated carbapenem-resistant Enterobacteriaceae (CRE) reported in the 1990s (Lutgring, 2019). The resistance rate of several Gram negative species toward carbapenems in some developing countries has been reported at up to 50% (Brown, 2015). Consequently, the threat of multidrug-resistant (MDR) Gram negative organisms, including CREs, is having a significant impact in the healthcare setting (Viens and Littmann 2015).

The rapid increase in Gram negative resistant bacteria is of great concern when met by a lack of compounds available to treat such infections. Most antibiotics in clinical usage today originate from discoveries made in the mid-twentieth century, and critical gaps remain in our understanding of antibiotics and their targets (Sinha and Kesselheim 2016). The issues with the need for new antibiotics in an era of continually emerging resistance coupled with a gap in our understanding of drug-target interaction and the resultant resistance development of bacteria has been exacerbated by the fact that numerous large, for-profit pharmaceutical companies have abandoned active antibiotic development groups due to concerns about returns on investment. The combination of these factors has led to the drug development pipeline being referred to as weak or broken and could lead to a threat of untreatable infection in the future (Chopra *et al.* 2008, Sinha and Kesselheim 2016). However, there is cause for optimism with new business models fostering the development of new vaccines to pre-empt potential future treatment issues (Ahmad and Khan 2019). In August 2019, the safety and immunogenicity of a chlamydia vaccine has been assessed at clinical trial level (Abraham *et al.* 2019). As the first vaccine for genital chlamydia to enter human clinical trials, it highlights the potential of utilising different strategies to prevent the “antibiotic apocalypse” which is often reported in the media (Sally Davies, 2018).

Infection management has become more challenging due to a lack of novel compounds on the market. To combat CRE infection, ceftazidime/avibactam was introduced in 2015 but reports of resistance soon followed (Livermore *et al.* 2018). In 2017, Vabomere (meropenem and vaborbactam) was granted US Food and Drug Administration (FDA) approval for the treatment of patients >18 years of age with complicated urinary tract infections (cUTIs). *In vitro* reports show a low propensity for resistance selection of meropenem-vaborbactam resistance and infrequent cross-resistance between ceftazidime/avibactam (Hackel *et al.* 2018, Peri *et al.* 2019) which is very promising for the longevity of Vabomere in clinical practice but the history of antibiotic resistance development would suggest Vabomere resistance will eventually emerge.

In addition to the problems associated with treating Gram negative bacteria, drug-resistant Mycobacteria also pose a major clinical challenge. Tuberculosis (TB) constitutes a global health burden with an estimated 1.5 million deaths annually attributed to TB. The emergence of drug-resistant TB threatened the global control of the disease, with multi-drug, extensive-drug and total-drug resistant TB being of heightened concern (Momin *et al.* 2017). In August 2019, the FDA has approved the usage of Pretomanid tablets in combination with bedaquiline and linezolid for the treatment of adults with extensively-drug resistant TB or non-responsive multidrug-resistant pulmonary TB, which accounts for an estimated 490, 000 newly diagnosed cases annually across the world (FDA, 2019 (a)).

The development of antimicrobial drugs less susceptible to bacterial resistance is one of the greatest difficulties faced by pharmaceutical companies and new approaches to drug design are required to combat the antimicrobial resistance issues (Jenssen *et al.* 2006). Additionally stricter regulation for the usage of antimicrobials is required to prevent the same limited lifespan of drugs being faced in the future (Walia *et al.* 2019).

Since the mid 1970's, the diversity and scale of the antimicrobial resistance burden has grown; initially the development of resistance was met by the introduction of new antimicrobials to bypass that resistance but since the 1990's there has been an antibiotic drug discovery void (Tang *et al.* 2014). Antimicrobial drug development has a substantial disincentive for pharmaceutical companies,

largely due to the limited financial return on the large investment required for antimicrobial drug development (Talbot *et al.* 2006). The development of new antibiotics is also more expensive, as a result of increased regulatory requirements, while newer screening methods for potential compounds have not been as successful as was first hoped (MacGowan and Macnaughton 2017). Resultantly, major pharmaceutical companies have stopped or severely restricted their investments for antimicrobial discovery and development, which has now left drug discovery efforts to small companies and universities (Sánchez and Demain 2017).

Successful control and prevention of MDR bacteria can be achieved through commitment to antibiotic stewardship programmes (ASPs) (Abbas and Stevens 2018). The United Kingdom and United States have entered a transatlantic partnership to try and combat the antimicrobial resistance issue, with the Wellcome Trust committing £125 million over 5 years. The Combatting Antibiotic Resistant Bacteria Biopharmaceutical Accelerator (CARB-X) initiative aims to fill the 'antibiotic void' to support early research into alternative antibiotics, with combined funding of $450 million (Wellcome Trust, 2017). Furthermore, Antibiotic Action is a UK-based initiative which was launched in 2011 and funded by the British Society for Antimicrobial Chemotherapy (BSAC) to raise global awareness of antibiotic resistance. Antibiotic Action seeks to inform and educate the general public in addition to clinical professionals on the importance of selective usage of antibiotics when required whilst promoting the importance of infection prevention and control (BSAC, 2019).

In addition to CARB-X and Antibiotic Action, One Health has been launched. One Health is the collaborative effort of multiple health science professions to attain optimal health for people, domestic animals, wildlife, plants, and the environment (McEwen and Collignon 2018). The World Health Organisation (WHO), the Food and Agriculture Organization of the United Nations (FAO) and the World Organisation for Animal Health (OIE) speak with one voice to take collective action to reduce the emergence and spread of AMR (WHO, 2018). As many of the antibiotic classes used in humans are also used in animals, the strategies of One Health include making improvements in antimicrobial use and regulation. This covers antimicrobial policy, surveillance, stewardship, infection control,

sanitation, animal husbandry and the search for alternatives to antimicrobials (McEwen and Collignon 2018).

The National Health Service (NHS) has launched a new scheme to test the world's first "subscription" style payment model to incentivise pharmaceutical companies to develop new antimicrobial drugs (Department of Health and Social Care, 2019). Currently, drug companies are paid by the volume of antibiotics sold and low returns on investment in development creates a disincentive for investment due to a lack of financial return (Ventola 2015). The trial will be led by NICE and NHS England and NHS Improvement which will test a model in which the NHS pays for drugs upfront based upon their usefulness. This will make the financial investment required to develop a new drug (estimated £1 billion) more attractive as they will still be paid for the drug even though it may be stored for last resort usage (Department of Health and Social Care, 2019).

All of these programmes listed above are working to promote awareness about antibiotic resistance, with emphasis on infection control, resistance surveillance and antibiotic stewardship. These factors are critical to maintain the efficacy of existing antibiotics against emerging resistant pathogens. However, the development of novel agents is a key component of the overall strategy to manage the antibiotic resistance issue. Programmes, such as the NHS pre-payment trial aiming to promote antimicrobial discovery programmes by removing the financial "risk", is an important step towards returning to a full pipeline of antimicrobials but will only address global market failure if other countries follow the UK's lead.

1.2 Antibiotic resistance mechanisms

Antibiotic resistance is a natural result of Darwinian selection. Bacteria have developed resistance to all antibiotics in clinical usage; with resistance to the last-resort antibiotic colistin being one of the latest examples (Santos-Beneit *et al.* 2017). Understanding the mechanisms by which bacteria become resistant to antibiotics contributes to the search for therapeutics which combat these

mechanisms. Mechanisms of antibiotic resistance include efflux, antibiotic inactivation, biofilm formation and target modification (Khameneh *et al.* 2016).

Antibiotic resistant bacteria can be divided in to two subsets 1) intrinsic/innate resistance and 2) acquired resistance. The former is dependent upon an individual bacterium's biological properties (Khameneh *et al.* 2016). For example, aerobic bacteria are intrinsically resistant to metronidazole as they are unable to reduce the drug anaerobically to its active form (Bendesky *et al.* 2002). Of the latter subset, bacteria can develop antimicrobial resistance via *de novo* mutations or by horizontal gene transfer of mobile genetic elements. Genetic mutations are usually random single-gene polymorphisms which occur at a rate of 10^{-9} to 10^{-10} per gene (Tang *et al.* 2014). These mutations are the result of errors in chromosomal replication or incorrect repair of damaged DNA (Khameneh *et al.* 2016).

Mobile genetic elements carrying resistances (mobile resistance elements or MRE) play a key role in the spread of antimicrobial resistance (AMR) as they spread through the bacterial population through horizontal gene transfer (HGT) (Durão *et al.* 2018). MRE typically confer antibiotic resistance by enzymatic inactivation (Wright 2005), efflux (Poole 2005), synthesis of enzymes to native targets (Wellington *et al.* 2013) or target protection (Nguyen *et al.* 2014).

Antibacterial resistance is a major problem in the clinical setting, with treatment options becoming increasingly diminished for bacterial infections. Another clinical challenge is the control and eradication of biofilm-forming bacteria, which can adhere to indwelling medical devices (Stewart and Costerton 2001) and surfaces, including sinks, within the hospital environment (Walker and Moore 2015).

Biofilms are surface-attached microbial communities able to attach to biotic or abiotic surfaces (Parrino *et al.* 2019). Bacterial cells within a biofilm are embedded in a matrix consisting of a self- synthesised layer of extracellular polymeric substances (EPS). EPS form the architecture of biofilms and are composed of polysaccharides, proteins, lipids and mucus which functions as a matrix holding the biofilm together (Kim and Lee 2016). Bacterial cells within the biofilm matrix are inherently drug resistant. Bacterial cells dwelling within the

biofilm can require up to 1000x the antimicrobial concentration required to kill their planktonic single-cell counterparts (Brandenburg *et al.* 2019). As such, biofilm treatment is of heightened clinical concern. Biofilms are often recalcitrant to both the immune response and antimicrobial treatment, making biofilm-associated infections difficult to treat (Henly *et al.* 2019).

Common biofilm-associated infections include catheter-associated urinary tract infections (CAUTIs) and biofilm formation on in-dwelling devices which in extreme circumstances can lead to biofilm-associated sepsis (Kennedy *et al.* 2010, Isabelle *et al.* 2018, Henly *et al.* 2019). Other clinically important biofilms present in chronic wounds, such as diabetic foot ulcers (Alvarado-Gomez *et al.* 2018), and biofilm contamination of burns patients by *Pseudomonas aeruginosa* (Brandenburg *et al.* 2019).

Due to the antibiotic resistance issues discussed above, there is an urgent need for new antibiotics with novel modes of action to combat the ever-growing antimicrobial resistance challenge.

1.3 Modern antimicrobial drug discovery

The rise in bacterial resistance is met by a decline in antibiotic drug development. Numerous pharmaceutical companies have abandoned the antimicrobial research and development field which has only fuelled the growing public crisis (Owens and Ambrose, 2007). The regulatory and economic barriers have caused 15 out of 18 of the larger pharmaceutical companies to completely pull out of the antibiotic field (Bartlett *et al*., 2013). The number of antibacterial drugs approved by the FDA has declined by 75% between 1983 and 2007 according to FDA statistics, with only a handful of pharmaceutical companies retaining active antimicrobial discovery programmes (Boucher *et al*., 2009). Despite this, antimicrobial drugs are still reaching the market. Three antibacterial drugs were approved by the FDA in 2018, which include plazomicin for the treatment of urinary tract infections (UTIs) (Shaeer *et al.* 2019), eravacycline for the treatment of complicated intraabdominal infections (Solomkin *et al.* 2018) and omadacycline for the treatment of community acquired pneumonia (Opal *et al.*

2019). Equally, three antibacterial drugs were approved in 2017, which included ozenoaxcin for the treatment of impetigo (Canton *et al.* 2018), Vabomere for the treatment of complicated UTIs (Hackel *et al.* 2018) and delafloxacin for the treatment of acute skin and soft tissue infections (Corey *et al.* 2019) although reports have already emerged of delafloxacin-resistant *S. aureus* isolates (Iregui *et al.* 2019). Despite reported resistance issues, the approval of new drugs offers some optimism for antimicrobial therapy, as two drugs were approved by the FDA in 2016 (Bezlotoxumab for *Clostridium difficile* infection (Bartlett 2017) and Obiltoxaximab for the treatment of inhalation anthrax (Greig 2016)) and one drug approved in 2015 (ceftazidime-avibactam) (Mosley *et al.* 2016). Three antibacterial drugs have already been approved by the FDA in 2019 (Pretomanid, Recarbrio and Lefamulin) (Momin *et al*., 2017; Rodvold, 2019, FDA 2019 (b)), which suggests, despite regulatory hurdles, new antibacterial drugs are reaching the market and this could be starting to increase.

The limited introduction of new antibiotics reaching the market, coupled with declining expertise within the field of antibiotic production demonstrates a demand for new drug discovery and development strategies (Tomaras and Dunman, 2015). The development of new antimicrobial drugs is crucial if we are to avoid a future where simple infections become life threatening once more (Butler *et al.* 2016). There have been efforts to search for alternative antimicrobial drugs over the past two decades (Irazazabal *et al*., 2016).

One group of molecules proposed to fill the antibiotic void is antimicrobial peptides (AMPs), which inhibit and kill bacteria by non-specific mechanisms (Sánchez and Demain 2017). AMPs have been extensively studied for over 40 years. The interest in the design and development of AMPs as potential therapeutic agents has resurged in recent years due to a rapid increase in drug-resistant infections (Lee *et al.* 2019).

1.4 Antimicrobial peptides

Antimicrobial peptides (AMPs) are evolutionarily conserved, vital components of innate immunity and considered a crucial aspect of the innate immune system for

almost all living organisms (Datta *et al.* 2015, Chen *et al.* 2019). The production of AMPs has been reported in numerous groups of organisms, including bacteria, fungi, plants and animals (Haugen *et al.* 2008). In microorganisms, AMPs are produced as a result of biological evolution to gain access to nutrients (Zhu *et al.* 2017a). For other organisms, AMPs are an ancient form of defence against invading pathogens and infection. AMPs act as the first line of innate defence against bacterial, fungal and viral invasion due to their location in tissues and organs commonly exposed to airborne pathogens (Datta *et al.* 2015, Zhu *et al.* 2017b). In addition to the antimicrobial activities of cationic peptides, they also demonstrate antitumor activity and growing evidence suggests cationic peptides have a role in the modulation of the immune responses, especially in inflammation and infection (Dai *et al.* 2008, Lee *et al.* 2019). It has also been suggested that the presence of AMPs in venoms can act as a weapon against both predators and prey (Falcao *et al.* 2014). Due to their selectivity for prokaryotic membranes, and their unique membrane-permeating mechanism of action for which microbes have little natural resistance, the spotlight has moved towards AMPs as potential novel antimicrobials (Zasloff 2002, Zhu *et al.* 2017a)

Despite the diversity of antimicrobial peptides and the living entities they are derived from, most AMP's share common physicochemical properties (Zhu *et al.* 2017b). They demonstrate a multitude of functions, but their main activity is bactericidal which is often achieved by the selective disruption of prokaryotic membranes (Bobone *et al.* 2012). AMPs are typically small in size, ranging from 12 to 60 amino acids in length, amphipathic, contain a net positive charge of +2 to +9 and approximately 50% hydrophobicity (Jenssen *et al.* 2006, Datta *et al.* 2015, Memariani *et al.* 2016). There has been growing interest in the discovery and investigation of AMPs due to increasing levels of antibiotic resistance in pathogenic bacteria and the aforementioned lack of therapeutic options (Barksdale *et al.* 2016).

AMPs exhibit a unique membrane-targeting mechanism of action, which compared with the single-target mechanism of action of current antibiotics, creates an interesting drug development prospect (Zhang *et al.* 2017). The hydrophobicity demonstrated by these peptides results in many AMP's forming α-helices, particularly upon interaction with phospholipid bilayers, which in turn

activates the pore forming mechanism of action (Schmidtchen *et al.* 2014). AMPs have many attractive properties such as broad-spectrum activity, a rapid killing mechanism, limited side effects, synergistic activity when used in combination therapy with antibiotics and a limited capacity to invoke resistance (Memariani *et al.* 2016). In addition to broad-spectrum antimicrobial activity, AMPs also have been shown to possess strong anti-fungal, anti-viral, anti-protozoan activity as well as exhibiting killing mechanisms towards cancer cells (Yu *et al.* 2015, Bittencourt *et al.* 2016).

1.5 Antimicrobial peptide conformation

AMPs can be classified in to four different structural groups: linear α-helical, β-sheet containing peptides (often stabilised by disulphide bonds) peptides composed of both α and β elements or linear extended structures devoid of α or β elements but commonly rich in one particular amino acid (Koehbach and Craik 2019). Of these, the most extensively studied are the α-helical peptides, which lack a tertiary structure and remain in extended, un-structured conformations until contact with the cell membrane (Dennison *et al.* 2005). Examples of structural classes of AMPs are shown in figure 1.1.

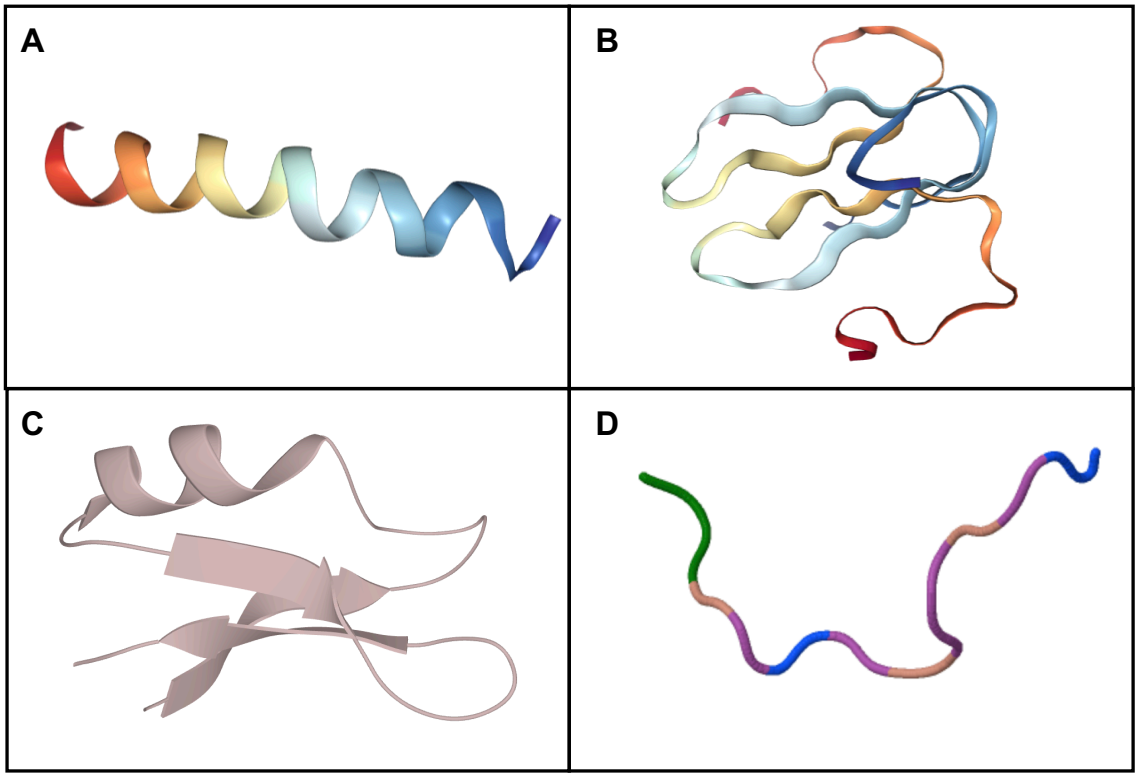

Figure 1.1: Structural classes of AMPs. (A) Magainin-2, an α-helical peptide, (B) rattusin, a β-sheet containing AMP, (C) heliomycin, an insect defensin containing α-helical and β-sheet regions and (D) bovine indolicidin, a linear AMP.

1.5.1 α-helical peptides

The α-helical peptides can be further separated into mono-helical or di-helical structures, with di-helical AMPs generally being less cytotoxic. Examples of this include the magainins isolated from the skin of the African tree frog *Xenopus laevis*. Magainin 2 adopts a di-helical structure and is less cytotoxic than other well categorised mono-helical AMPs, such as melittin (Zasloff 1987). The Pandinins isolated from the venom of the scorpion *Pandinus imperator* also demonstrate this phenomenon. Pandinin 1 is a di-helical peptide which confers a low-level of haemolysis whilst Pandinin-2 is a smaller, mono-helical peptide which demonstrates a high level of haemolysis (Corzo *et al.* 2001, Rodríguez *et al.* 2014a).

1.5.2 β-sheet containing peptides

Many of the β-sheet containing peptides are stabilised by one or more disulphide bonds. The β-sheet containing peptides can be further subcategorised in to α-defensin peptides and β-hairpin peptides based upon their cysteine content and structural characteristics (Koehbach and Craik 2019). Protegrin-1 is an example of a β-hairpin peptide. Derived from porcine blood, protegrin-1 is an 18-amino acid peptide with a charge of +7 and is stabilised by two disulphide bonds (Kokryakov *et al.* 1993). Defensins are small, cationic cysteine rich peptides which are endogenously produced by virtually all species as a first line of bacterial defence. They can be sub-categorised in to three separate groups (Zhu and Gao 2013). The α-defensins are a subgroup composed of three antiparallel β-strands which are linked by a disulphide bond in a trans arrangement. The α-defensins contain a salt bridge, which is important for proteolytic stability and folding, but is not related to antimicrobial activity (Koehbach and Craik 2019).

1.5.3 Peptides with α and β elements

Other classes of defensins often have structures containing both α and β-elements. Defensins have been found in numerous mammals, including humans, as well as invertebrates and plants. The defensins can be further subcategorised based on the arrangement of their disulphide bonds (Koehbach and Craik 2019). One group of defensins is the *cis*-defensins, where the third disulphide bond connects the N-terminal loop with the second β-sheet to form cysteine-stabilised αβ-defensins (Koehbach 2017). This motif is also commonly found in scorpion venom-derived neurotoxins, such as toxins affecting potassium channels (α-KTxs) (Zhu *et al*., 2014), which could contribute to the antimicrobial activity demonstrated by some neurotoxins.

1.5.4 Linear peptides rich in particular amino acids

Some peptides do not adopt a particular 3D structure either in solution or upon contact with membranes and are referred to as extended linear structures. These peptides are devoid of α-helices and β-sheets and are often rich in one particular

amino acid, such as glycine, proline, tryptophan or histidine (Koehbach and Craik 2019). An example of a linear AMP is bovine indolicidin. Bovine indolicidin is a tryptophan-rich 13-mer isolated from bovine neutrophils and carries a charge of +3. It demonstrates potent antimicrobial activity against *S. aureus* and *E. coli,* with almost complete sterilisation of cultures observed at 10 µg/ml (Selsted *et al.* 1992).

1.6 Structural characteristics of AMPs

The ability to selectively target prokaryotic cell membranes over host membranes is an essential factor for AMPs. As such, the biochemical composition of AMPs plays an important role in function (Yeaman and Yount 2003). The factors critical for the structure of AMPs are shown below in figure 1.2.

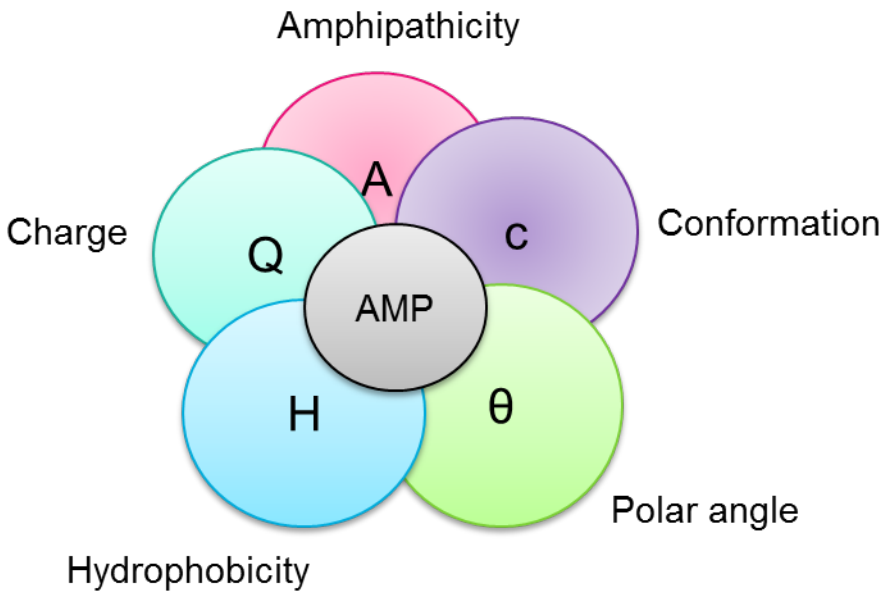

Figure 1.2: Factors influencing structure of AMPs.

The composition of AMPs and the amino acid sequence does not only influence the biochemical factors (charge, amphipathicity, hydrophobicity) but also influences the 3D-structure (conformation and polar angle). Therefore, it is postulated that changes to the primary structure can profoundly affect the structure-function relationship of the antimicrobial peptide in solution and

therefore activation at the bacterial membrane. Changes in the relative ratios of charge/hydrophobicity/amphipathicity may have a major effect on structure and function. The investigation of this relationship will enable antimicrobial peptides to be optimised for maximum antimicrobial effect and minimum host cytotoxicity (Edwards *et al.* 2016).

1.6.1 Structure

AMPs are a unique and diverse group of molecules, which can be divided in to groups based on amino acid composition and structure, as previously discussed (Section 1.5) (Travkova *et al.* 2017). Many AMPs are believed to be unstructured or adopt extended conformations prior to interaction with target cell membranes (Yeaman and Yount 2003).

1.6.2 Charge

A positive charge is generally required for antimicrobial activity and there is a strong correlation between peptide cationicity and antimicrobial activity (Travkova *et al.* 2017). The net cationic charge of AMPs is typically due to the presence of lysine and arginine residues and it facilitates membrane interaction with prokaryotic cells due to their weakly negative surface charge. These amino acids usually form highly defined cationic domains within the peptide structure (Hicks *et al.* 2013, Lakshmaiah Narayana and Chen 2015). Increasing the charge of AMPs has been demonstrated to increase the antimicrobial activity in numerous studies (Bessalle *et al.* 1992, Huang *et al.* 2015). In parallel, it has also been shown that the elimination of peptide cationic charge drastically reduces antimicrobial activity (Schmidtchen *et al.* 2014).

Whilst the majority of AMPs are cationic, anionic AMPs have been described. Dermicidin is a 47-amino acid AMP derived from human sweat glands, which carries an overall anionic charge (Schittek *et al.* 2001). The mechanism of action of anionic AMPs (AAMPs) is not fully understood, but some AAMPs use metal ions to form cationic salt bridges with anionic components of bacterial cell membranes, which facilitates AAMP-membrane interactions (Harris *et al.* 2009).

1.6.3 Amphipathicity

Amphipathicity is an essential characteristic for microbial membrane binding and can be adopted by numerous peptide conformations. Amphipathicity can be measured quantitatively via the hydrophobic moment, which is calculated as the vectoral sum of individual amino acid hydrophobicities, normalised to that of an ideal helix. An increased hydrophobic moment results in increased membrane permeabilising and haemolytic activities against target membranes. This may have an active role in host cell cytotoxicity. If the action of AMPs is considered as a combination of electrostatic and hydrophobic activity, for neutral membranes where electrostatic interactions are minimised, hydrophobic moments may have a key role (Travkova *et al.* 2017).

The amphipathic properties enable AMPs to permeabilise lipid membranes to form pores which ultimately cause cell lysis (Nakatsuji and Gallo 2012, Taute *et al.* 2015). There is growing evidence that membrane damage is only one aspect of the mechanism of action of AMPs and other targets may include inhibition of DNA, protein, cell wall and cell membrane synthesis or the stimulation of autolysis (Peschel and Sahl 2006, Taute *et al.* 2015).

1.6.4 Hydrophobicity

Peptide hydrophobicity is defined as the percentage of hydrophobic amino acids within a peptide, which for most AMPs is approximately 50%. Hydrophobicity is essential for interactions between AMPs and membranes (Travkova *et al.* 2017). However, an increase in hydrophobicity is associated with a lack of antimicrobial specificity and increased haemolysis and mammalian cell toxicity (Dathe *et al.* 1997, Tossi *et al.* 2000a). Therefore, many AMPs are moderately hydrophobic, to enable optimisation of antimicrobial activity against host toxicity.

1.6.5 Polar angle

Polar angle is a measure of the relative proportion of polar and non-polar angles of the peptide. A polar angle of near 180° is achieved when the hydrophilic and

hydrophobic fractions are approximately equal (Perrin *et al.* 2016), additionally polar angle can give some indication of the mechanism of action of AMPs (Uematsu and Matsuzaki 2000).

1.7 Mechanism of action

AMPs are effective against a wide range of bacterial pathogens, including MDR bacteria such as *Acinetobacter baumanii,* methicillin-resistant *Staphylococcus aureus* (MRSA) and MDR- *Mycobacterium tuberculosis*. The mechanisms of actions of AMPs vary depending on structure and classification and the specific mechanisms of actions of AMPs are yet to be fully understood. To avoid the same potential resistance issues which have occurred with antibiotics, understanding the mechanisms of actions of AMPs prior to introduction in the clinical setting may offer a therapeutic advantage and enable the molecules to be enhanced to further limit the potential for bacterial resistance to develop (Ong and Wiradharma 2014, Taute *et al.* 2015, Barksdale *et al.* 2016). AMPs have been shown to interact with bacterial membranes and in most instances cause membrane disruption, which has widely been thought of as the mechanism of action but other binding targets, such as DNA, peptidoglycan, lipopolysaccharide (LPS), and enzyme interference have also been noted (Juba *et al*., 2015; Barksdale *et al*., 2016; Memariani, *et al*., 2016; Peschel and Sahl, 2006). Additionally, some AMPs have demonstrated multi-targeting mechanisms of action, being active at a membrane and intracellular level (Memariani *et al.* 2016). Antibiotics generally function via targeting a single site or process and resultantly a simple mutation of modification in that target can result in the bacteria developing resistance to the antibiotic (D'Costa *et al.* 2011). As AMPs are multi-target inhibitors, the ability of bacteria to develop resistance to AMPs is also reduced. The modification of a single target would not induce total resistance to AMPs, but may cause changes to the overall efficacy (Memariani *et al.* 2016).

Most bacterial outer membranes are electronegative due to the presence of high levels of anionic phospholipids, such as phosphatidylglycerol, phosphatidylethanolamine, LPS and cardiolipin. In contrast, mammalian membranes are electroneutral due to the presence of zwitterionic phospholipids,

such as phosphatidylcholine (Li *et al.* 2016). It has been well established that initial electrostatic interactions between the positively charged peptides and the negatively charged bacterial membrane are a crucial step in the mechanism of action of the peptides (Huang 2000) and that this activity is dependent upon the structure, length and complexity of the polysaccharides found in the outer layer of the cell membrane (Samy *et al.* 2016).

The degree of amphipathicity exhibited by the peptides has also been demonstrated to be essential for membrane disruption and subsequent antimicrobial activity (Irazazabal *et al.* 2016), as shown in figure 1.3. According to the accepted model for membrane disruption, the cationic and hydrophobic surfaces of AMPs assemble by electrostatic interaction with the negatively charged lipid head groups in bacterial membranes. This leads to hydrophobic interactions upon contact with the membrane, where the peptides accumulate (Yeaman and Yount 2003). After reaching a threshold concentration, the peptides undergo conformational changes and insert in to the hydrophobic interior of the lipid bilayer, which causes pore formation and disruption to the membrane (Juba *et al.* 2015). The formation of pores can lead to the translocation of peptides to the inner leaflet of the bilayer, where they accumulate and continue to cause membrane disruption (Yeaman and Yount 2003).

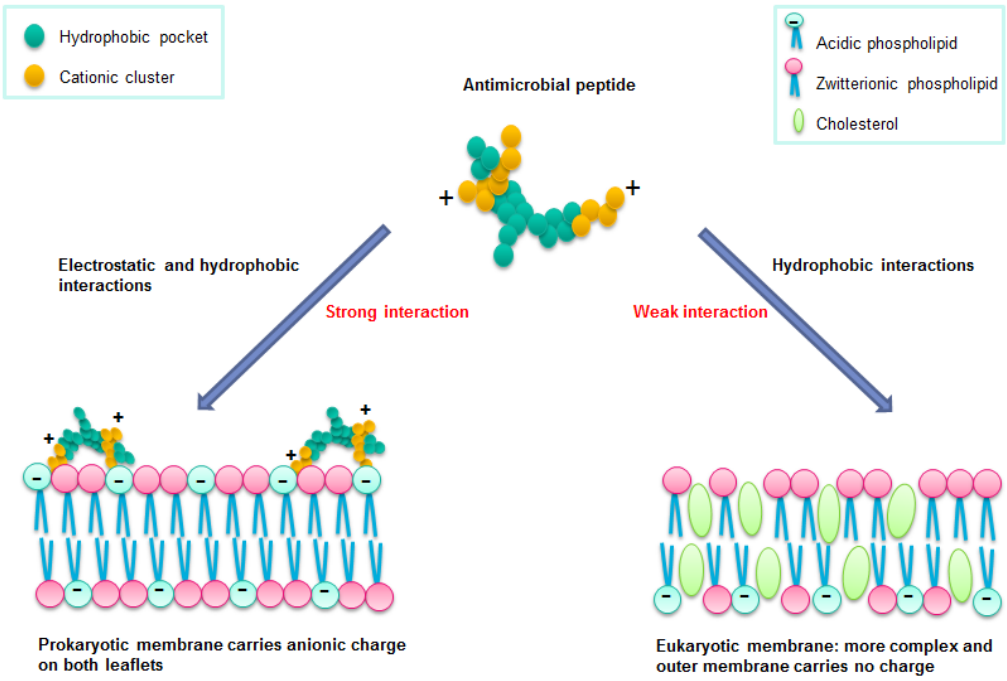

Figure 1.3: Interactions between amphipathic AMPs and prokaryotic and eukaryotic membranes. AMP organises into an amphipathic structure with discrete pockets of charge (yellow) and hydrophobicity (green) to aid insertion into the prokaryotic membrane. Prokaryotic membranes contain a high proportion of acidic phospholipid head groups, which assemble to create a membrane with an anionic charge. Electrostatic interactions between the anionic membrane and cationic peptide occur and the hydrophobic regions of the peptide insert into the membrane, which leads to pore formation. The eukaryotic membrane contains zwitterionic phospholipid head groups, which assemble to form a membrane with an overall neutral charge. The AMP is unable to form initial electrostatic interactions with the eukaryotic membrane and thus it cannot bind. Figure adapted from Zasloff, 2002.

The overall mechanism of action is more complicated than simple cation-anion interactions and is typically multi-site involving hydrophobic and hydrophilic domains of both the peptides and the membranes. The membrane disruptive mechanism of the peptides is influenced by the formation of pores. Biophysical studies have provided three general models for mechanisms of membrane disruption and pore formation (Lohner and Hilpert 2016). The formation of pores enables ions to travel through the pores, destroying the membrane potential which leads to a decline in ATP synthesis and cell metabolism which ultimately gives rise to cell death. In all proposed mechanisms of pore formation, following the initial electrostatic interactions, a threshold concentration must be reached

before membrane disruption can occur (Huang 2000, Shai 2002). The proposed models for mechanisms of pore formation are the barrel-stave, toroidal pore and carpet models.

1.7.1 Barrel-stave model

In the barrel-stave model, peptide oligomerisation induces the formation of a central lumen. AMPs reach the membrane, where they bind as a monomer and then adopt an α-helical conformation (Hancock 1999). The hydrophobic regions of the peptide align with the lipid core region of the bilayer and the hydrophilic regions of the peptides face inwards to create a central pore. This model creates a highly ordered cylindrical pore surrounded by peptides in the transmembrane orientation (figure 1.4) (Shai 2002, Brogden 2005). Alamethicin is a linear 20-amino acid long antimicrobial peptide derived from the fungus *Trichoderma viride* (Li and Salditt 2006). It's mechanism of action has been well characterised by the formation of barrel-stave pores (Perrin *et al.* 2016).

1.7.2 Toroidal pore model

In the toroidal pore model, the pore lumen is lined with both AMP and phospholipid head groups (Ong and Wiradharma 2014). The hydrophilic face of AMPs inserts into the membrane surface, inducing bending of the bilayer which causes the upper and lower leaflet to meet. This creates an ordered structure, with interactions between both lipid head groups and AMPs lining the pore, with the pore generally being smallest in the middle and larger at both ends. This creates a highly ordered pore (figure 1.4) (Brogden 2005, Mihajlovic and Lazaridis 2010). An example of a toroidal-pore forming peptide is melittin, which is derived from bee venom (Gauldie *et al.* 1976). Studies have shown that melittin adopts its α-helical structure at the membrane and then assembles in to oligomers to form toroidal pores. Additionally melittin has been shown to bind to LPS, polysachharides, chitin (from yeast) and peptidogylcan from Gram positive bacteria, which may explain the broad spectrum of activity shown by melittin as it can tranverse various bacterial cell walls to access the membrane (Park *et al.* 2006).

Other studies have suggested that in addition to the anticipated highly ordered toroidal pore structutres, irregular toroidal pores can also form. Molecular dynamics (MD) simulations with magainin revealed significantly irregular toroidal pore formation, with 1-2 monomers located in the central pore lumen and further peptides lining the rim (Mihajlovic and Lazaridis 2010). Sengupta et al., (2008) reported similar findings for melittin against 1,2-dipalmitoyl-sn-glycero-3-phosphocholine (DDPC) membranes.

1.7.3 Carpet model

In the carpet model, peptides accumulate on the surface of the bilayer until they reach a threshold concentration. Once this threshold is met, the peptides form transient pores, allowing more peptides to access the inner leaflet of the membrane. This leads to the peptides creating a 'carpet' on each layer of the membrane, with peptides spanning the transmembrane surface. This leads to membrane curvature, micelle formation and ultimately membane disintegration (figure 1.4) (Shai 2002, Brogden 2005). The cecropins were originally isolated from the haemolymph of the giant silk moth, *Hyalophora cecropia*. These AMPs possess antibacterial and anticancer activity in vitro (Moore *et al.* 1996). Cecropin is a prototype of α-helical linear AMPs which operates by a carpet mechanism (Naafs 2018).

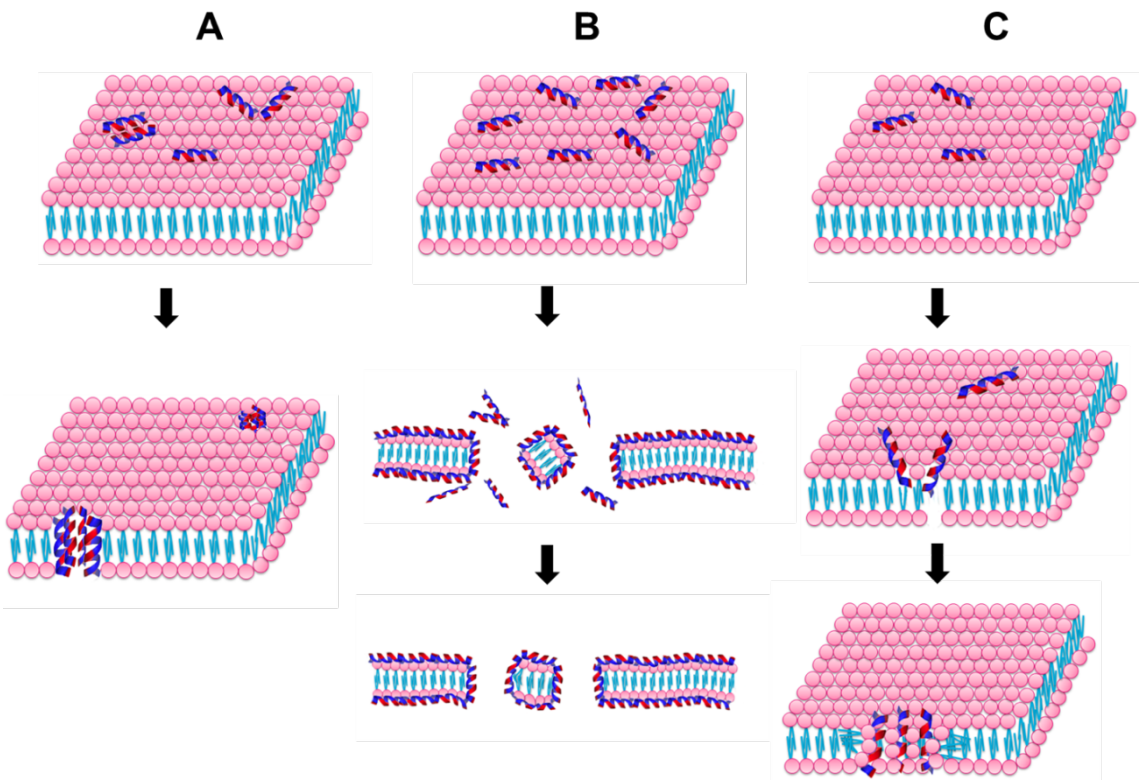

Figure 1.4: Visual representation of pore formation. Hydrophilic regions are shown in red and hydrophobic regions are shown in blue. Barrel-stave pore model (A), peptides aggregate at the membrane and insert perpendicularly into the cell membrane to create a highly ordered pore. The hydrophobic regions of the peptide align with the lipid core whilst the hydrophilic regions line the interior of the pore. The carpet model (B), peptides associate parallel to the membrane to form an extensive 'carpet.' At critical concentrations, the peptides form holes in the membrane, which allows further peptides to access the membrane. Following disruption of the bilayer curvature, the membrane disintegrates and forms micelles. The toroidal pore mechanism (C), peptide helices insert into the membrane which causes the lipid monolayers to bend continuously through the pore which creates a pore composed of phospholipid head groups and inserted peptides. Diagram adapted from Brogden, (2005).

1.7.4 Other mechanisms of pore formation

Recent models have blurred the lines between the three commonly proposed mechanisms of pore formation. Whilst the toroidal pore, barrel-stave and carpet models remain the most commonly proposed mechanisms of pore formation, a number of other mechanisms have been proposed including the interfacial, leaky

slit, aggregate, electroporation, sinking raft, lipid segregation and diffusion limited aggregation models.

The interfacial activity model is described as 'the ability of a molecule to bind to a membrane, partition in to the membrane-water interface and alter the packing and organisation of the lipids (Wimley 2010). This mechanism is dependent upon the balance of hydrophobic and electrostatic interactions between peptides, water and lipids; this model also suggests that the activity of such peptides may be more dependent on amino acid composition and physico-chemical properties as opposed to specific amino acid sequences (Wimley 2010).

The leaky slit model suggests the lipid-bound peptides form a linear, amphipathic arrangement with the hydrophobic side of the peptide aggregate facing the lipid bilayer. Toxicity would be caused by the other surface of the linear aggregate being hydrophilic, as this facet cannot seal by hydrophobic interactions with the opposing contacting bilayer. Resultantly, lipids in the hydrophilic surface are forced to adopt a highly positive curvature. The resulting leaky slit would be highly permeable to solutes and difficult for the cell to repair (Zhao *et al.* 2006).

In the aggregate model, peptides insert into the bilayer and cluster into large unstructured aggregates which span the membrane. The aggregates are proposed to be adhered to water molecules, which creates channels enabling the leakage of ions and other molecules out of the cell (Xiao *et al.* 2015). These membrane pores do not always cause membrane depolarisation and as such, are thought to arise to enable the entry of AMPs to act on intracellular targets (Wu *et al.* 1999).

The molecular electroporation method describes how a highly charged peptide in close proximity to the membrane creates an electric field to trigger pore formation. To enable pore formation, it has been suggested the AMP must bind to the lipid membrane and cause at least a 0.2 V electrostatic potential across the membrane (Miteva *et al.* 1999).

In the sinking raft model, a mass imbalance caused by the peptide binding to the outer leaflet is responsible for membrane perturbation. The mass imbalance

leads to membrane curvature and perturbation which allows small peptide aggregates to sink deeply into the bilayer and cross it, which gives rise to the “sinking raft” terminology.

The lipid segregation model is underpinned by peptide-lipid biding, which causes defects in the membrane and results in the intracellular contents leaking out of the cell (Teixeira *et al.* 2010). Epand *et al*., (2009) suggested the lipid segregation model could explain the differences in observable minimum inhibitory concentration (MIC) values between bacterial species for the same peptide, suggesting the contribution of the phospholipids affected the antimicrobial activity. Epand *et al* (2008) postulated the antimicrobial activity of some peptides was restricted to the affinity for phospholipids. They demonstrated the peptide KR-12 was effective only against bacteria composed of anionic and zwitterionic bacteria whilst the peptide GF-17 demonstrated activity against peptides composed solely of anionic phospholipids or membranes composed of both anionic and zwitterionic phospholipids.

A two-dimensional diffusion limited aggregation (DLA) model has been described whereby particles moving with Brownian motion coalesce upon contact with an aggregate. The branched structure in DLA arises as particles are captured by the extremities of the aggregate before diffusing to the centre. The DLA model assumes that a particle immediately attaches to a cluster, however in many kinetic processes in biology binding occurs with a certain probability due to required binding orientation and the need to overcome an energy barrier (Heath *et al.* 2018).

1.7.5 Mechanism of action and cell membrane composition

The mechanism of action of AMPs has been linked with membrane composition which varies between prokaryotic and eukaryotic species (Teixeira *et al.* 2010). The phospholipid content of lipid membranes differs between bacterial species, with *E. coli* membranes being composed predominantly of phosphatidylethanolamine (PE) and *S. aureus* membranes being largely composed of phosphatidylglycerol (PG) and cardiolipin (CL) (Hayami *et al.* 1979, Sohlenkamp and Geiger 2016). The phospholipid content of eukaryotic cells

varies between cell type and location (Schurer *et al.* 1993, Müller *et al.* 1996). Examples of common components of bacterial and mammalian cell membranes are listed in table 1.1.

Table 1.1: Common components of eukaryotic and prokaryotic membranes and the charge states observed.

Lipid name	Charge state (pH7)	Notes
Phosphatidylcholine (PC)	Neutral	Most abundant phospholipid in mammalian tissues
Phosphatidylglycerol (PG)	Negative	Induces negative charge into membrane surface and membrane-lipid interface
Phosphatidylethanolamine (PE)	Neutral	Second most abundant phospholipid in eukaryotic cells
Phosphatidylserine (PS)	Negative	Predominantly found on inner cytoplasmic membrane
Phosphatidylinositol	Negative	Has a role in membrane protein function
Cardiolipin (CL)	Negative	Commonly found in bacterial membranes
Sphingomyelin (SM)	Neutral	Induces presence of lipid rafts
Cholesterol	Negative	Modulates the lipid bilayer

1.7.6 Other mechanisms of action

Most studies investigating the mechanisms of action of AMPs focus on the cell membrane but limited research has been conducted to investigate mechanisms beyond cell membrane lysis (Bobone *et al.* 2012). AMPs have been discovered which target intracellular processes. Pleurocidin was isolated from the mucus of the winter flounder (*Pleuronectes americanus*) and inhibits macromolecular synthesis (Ageitos *et al.* 2017). Indolicidin binds to DNA to inhibit DNA synthesis, buforin II can bind both DNA and RNA to inhibit DNA and RNA synthesis (Shah *et al.* 2016). AMPs have been identified which can inhibit DNA synthesis, RNA synthesis, LPS synthesis, peptidoglycan synthesis, cell division whilst other AMPs have shown activation of cytolytic enzymes (Le *et al.* 2017). Examples of mechanisms by which AMPs can induce cell death are shown in figure 1.5.

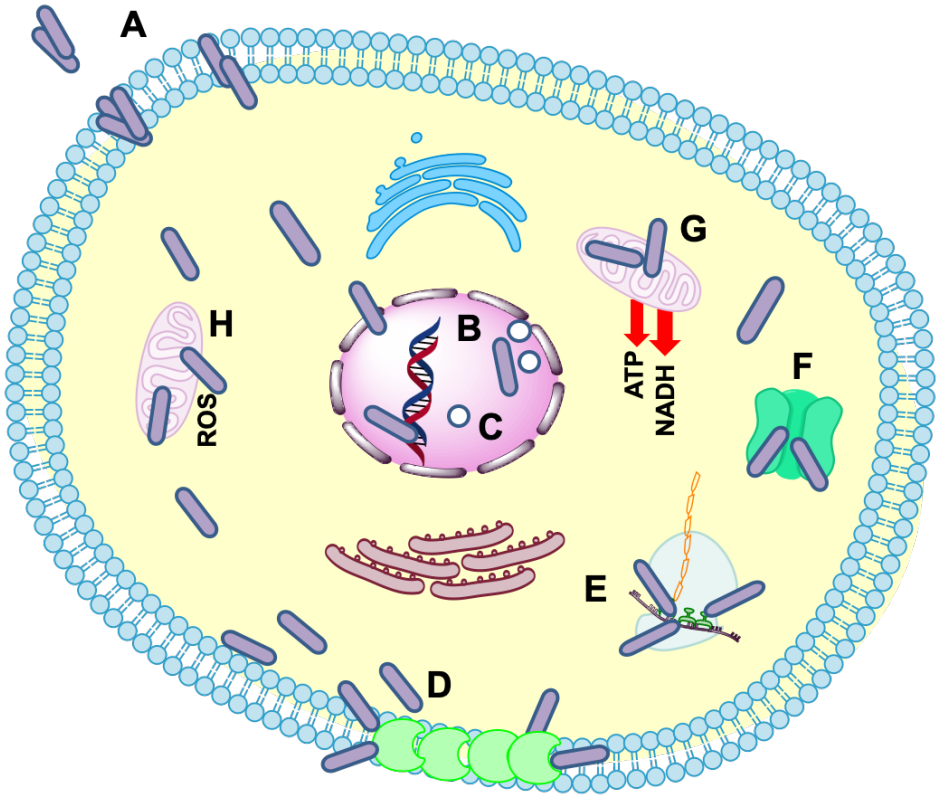

Figure 1.5: Mechanisms of cell death by AMPs. (A) Disruption of cell membrane integrity. (B) Inhibition of nucleic acid synthesis. (C) Inhibition of enzymes essential for the cross linking of cell wall proteins. (D) Inhibition of ribosome function and protein synthesis. (E & F) Blocking of chaperone proteins to inhibit protein folding. (G) Disruption of mitochondrial membrane integrity and efflux of ATP and NADH. (H) Inhibition of cellular respiration and induction of reactive oxygen species (ROS) formation. Figured adapted from Peters *et al*., 2010.

Some AMPs have demonstrated multi-target mechanisms of action, such as activity at the membrane level and via the targeting of intracellular components (Harrison, Abdel-Rahman, *et al.* 2016, Malanovic and Lohner 2016). Examples of peptides with membrane targeting and non-membrane targeting mechanisms of action are listed in table 1.2.

Table 1.2: Membrane and intracellular targets of AMPs

Mechanism of action	Peptide
Toroidal pore	Magainin 2, melittin, protegrin-1
Carpet	Cecropin, melittin, dermaseptin
Barrel-stave	Alamethicin
Inhibition of protein synthesis	Indolicidin, pleurocidin
Flocculation of intracellular components	AAMPs

1.8 Natural resistance towards AMPs

A low resistance potential makes AMPs an attractive foundation for the production of new antimicrobial drugs (Dong *et al* 2015). Bacteria have presumably been exposed to AMPs for millions of years, yet widespread resistance to these peptides has not been identified (Fjell *et al.* 2011). AMPs act on multiple cellular targets, as opposed to a particular dominant target or group of homologous targets for conventional antibiotics. As AMPs do not interact with a specific receptor, the ability of targets to develop resistant phenotypes is markedly low (Marr *et al.* 2006, Panteleev *et al.* 2015, Ageitos *et al.* 2017).

It has been suggested that bacteria would have to redesign their cell membranes, diminishing the net negative charge in order for resistance to develop (Marr *et al.* 2006, Panteleev *et al.* 2015). Although initially thought to be unlikely, the modification of bacterial membranes to prevent AMP binding has been observed. This form of passive resistance has been demonstrated in *Morganella, Proteus* and *Serratia* species which are naturally resistant to AMPs. These bacteria have an increased proportion of positively charged lipid A subunits, which diminishes the overall negative charge of the membrane and thus prevents AMP binding (Andersson *et al.* 2016). Whilst membrane changes have been observed, it is not expected that microorganisms will be able to rapidly change the lipid composition in response to AMPs targeting the cytoplasmic membrane. (Chen *et al.* 2005) This mechanism of resistance only results in a modification to the minimal inhibitory concentration, as bacteria capable of these membrane charge

modifications are inhibited by many AMPs at high concentrations. The reason for this is three-fold: 1) bacteria are incapable of completely neutralising the overall anionic charge of their membranes, 2) the binding of AMPs is not solely dependent on the physico-chemical properties of the target membrane, 3) composition and secondary structure of the AMPs is also crucial for binding to the membrane (Peschel and Sahl 2006, Ageitos *et al.* 2017). Additionally, the emergence of AMPs with a naturally high cationic charge (such as hBD3 with a charge of +10) has been attributed as a counter-evolutionary response to overcome the charge resistance mechanism displayed by certain bacteria (Peschel and Sahl 2006).

The natural mechanisms of bacterial resistance are summarised in figure 1.6.

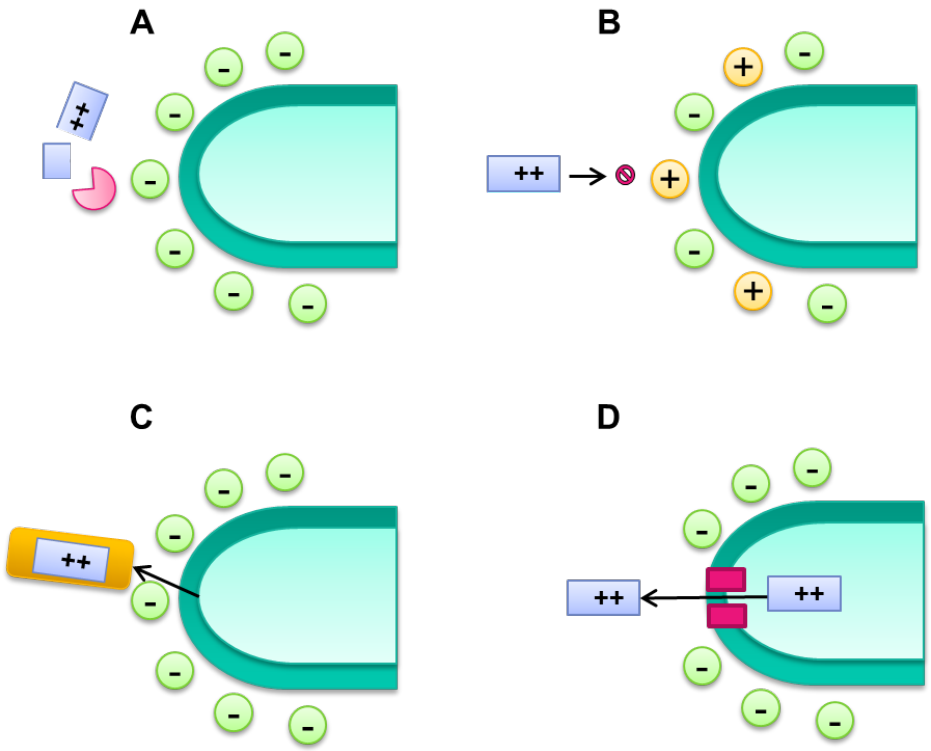

Figure 1.6: Mechanisms of antimicrobial peptide resistance. (A) Bacteria can secrete proteases which can degrade the AMP before binding occurs. (B) The membrane composition can be adjusted to reduce the anionic charge, which decreases the binding affinity the AMP has for the prokaryotic membrane. (C) Bacteria may secrete proteins which prevent AMPs from binding. (D) Some bacteria can actively remove the AMP from the cell.

Inducible resistance to AMPs has been discovered in both Gram negative and Gram positive bacteria, such as the production of peptidases capable of digesting the AMPs before binding can occur (Peschel and Sahl 2006). An example of this is the resistance developed by *S. aureus* to dermicidin by the induction of a specific protease enzyme (Ageitos *et al.* 2017).

Even though some bacterial species have demonstrated resistance to AMPs, the molecules are still present despite bacterial evolution. From a therapeutic perspective, peptides capable of resisting degradation would be attractive if oral delivery was desired. Modifications to peptides can contribute to making AMPs resistant to proteolytic degradation, thus making them even more attractive therapeutics. The inclusion of disulphide bonds, proline residues and the amidation of the C-terminus can contribute to arming AMPs with a defence strategy against proteolysis (Peschel and Sahl 2006). It has also been shown that AMPs containing D-amino acids reduce the development of microbial resistance by proteolysis whilst simultaneously having an increased biologic effect (Ageitos *et al.* 2017). The incorporation of β-amino acids in to the structure of AMPs has also demonstrated peptide enhancement by improving the selectivity (Lee *et al.* 2017).

The knowledge of resistance issues prior to the introduction of AMP-based drugs can inform the design of molecules with a reduced capacity to invoke bacterial resistance and hopefully this will mean these drugs have a more enhanced therapeutic shelf-life compared with conventional antibiotics (Ageitos *et al.* 2017). The ability to generate resistance for some AMPs in clinical trials by repeatedly exposing bacteria to AMPs at sub-inhibitory concentrations has proven unsuccessful, which further demonstrates the promise of these peptides to replace conventional antibiotics (Gottler and Ramamoorthy 2009).

1.9 Antimicrobial peptides in therapeutic usage and the design of new peptides

Previous attempts to induct AMPs into therapeutic use have been complicated, with the antimicrobial peptide Pexiganan being a primary example. Pexiganan (a 22-amino acid membrane disrupter analogue of the *Xenopus* peptide, magainin) is a broad-spectrum antimicrobial peptide which was developed for the topical use for the treatment of infection in diabetic foot ulcers, which unfortunately received a non-approval letter from the FDA in 1999 (Fox 2013). The non-approval status was issued after phase II trials demonstrated that pexiganan was no more effective at treating diabetic foot ulcers than existing antibiotics (Gottler and Ramamoorthy 2009). The usage of “noninferiority” trials for approving new antibiotics has been extensively questioned. When attempting to discover new treatments for untreatable infections, for which there is no “good” treatment option, it seems illogical that there cannot be an alternative treatment option equal to the gold standard of the current treatment when a “silver” or “bronze” treatment may have a significant impact on patient morbidity (DiNubile 2016).

1.9.1 AMPs in clinical usage

Currently, a handful of antimicrobial peptides are being used clinically, with polymyxin E and B being the most commonly used. Polymyxin E, also known as colistin, has been used over the past 50 years to control infection. Previously, the drug had been used sparingly due to nephrotoxicity and neurotoxicity complications when administered intravenously. However, a steady rise in Gram negative antimicrobial resistance has resulted in colistin being re-introduced as the last-resort drug to treat infection. This subsequent overuse of the peptide antibiotic has led to the emergence of colistin resistance (Andersson *et al.* 2016, Rhouma *et al.* 2016). A novel colistin resistance mechanism termed MCR-1 has been identified on a mobilised plasmid isolated from *E. coli, Klebsiella pneumomiae* and *Pseudomonas spp.* in China. Studies have also found the presence of this gene in human Enterobacteriaceae, suggesting the resistance is being transmitted horizontally from animals to humans (Quesada *et al.* 2016, Rhouma *et al.* 2016). Gram negative bacteria employ several mechanisms to

protect against attack from colistin. The modification of the membrane to increase the overall charge by LPS modification which reduces the membrane activity of colistin has been noted. The overexpression of efflux pumps and the overproduction of capsule polysaccharide have been demonstrated as mechanisms of bacterial defence against colistin but no mechanisms of enzymatic degradation have been reported (Aghapour *et al.* 2019).

Despite the knowledge of colistin resistance mechanisms, the presence of colistin resistance has rarely been reported in consecutive clinical isolates (Longo *et al.* 2019) and the overall prevalence of colistin resistance is low. The prevalence of colistin resistance was investigated from agricultural areas known for the usage of colistin in the meat industry. Of 647 Salmonella isolates from European broiler meat, a resistance rate of 5.5% was observed. The percentage of colistin resistance was deemed lower in isolates obtained from the intestines of agricultural animals, with a colistin resistance rate of 1% determined for *E. coli* isolates from European pigs (Kempf *et al.* 2016). 33,765 clinical isolates of Enterobacteriaceae were analysed between 2010 and 2014, 4% of Gram negative bacilli were determined as colistin resistant with MICs ranging from 2-32 mg/L (Rossi *et al.* 2017) highlighting the low prevalence of colistin resistance in the clinical setting. In Europe, the incidence of colistin resistance in *Salmonella* spp and *E. coli* spp is generally low, with sporadic incidences of high resistance levels (Apostolakos and Piccirillo 2018).

However, encouragingly, resistance issues are not present for all AMP-based antibiotics in the clinical setting. Tyrothricin was the first AMP introduced following clinical trials in the 1930s and despite widespread usage over 60 years, there has been no bacterial resistance to tyrothricin observed. Tyrothricin contains a mixture of linear and cyclic D-amino acids, which have armed the peptide with a defence strategy against bacteria (Ageitos *et al.* 2017).

Nisin is one of the most studied bacteriocins and was the first antimicrobial peptide awarded a general recognised as safe (GRAS) status for food applications by the FDA (Martins *et al.* 2010). Bacteriocins are bacterially produced, ribosomally synthesised AMPs which are small, heat-stable peptides active against other bacteria (Cotter *et al.* 2005). It is estimated that 30-99% of

bacteria and Archaea produce at least one bacteriocin, which can be narrow spectrum or broad spectrum. The bacteriocin producing organism is immune to its own bacteriocins (Cotter *et al.* 2005). Nisin is produced by *Lactococcus lactis* sub-species *lactis* and widely used as a food additive to prevent food spoilage by bacteria (Jagus *et al.* 2016). Whilst generally not active against Gram negative bacteria, it does have antimicrobial activity against Gram positive bacteria such as *Clostridium botulinum* and *Listeria monocytogenes* (Martins *et al.* 2010). The mechanism of action of nisin is exerted by the formation of pores in the bacterial cell membrane and inhibiting peptidoglycan synthesis by targeting lipid-II, the membrane-bound peptidoglycan precursor (Champak Chatterjee *et al.* 2005, Ageitos *et al.* 2017). Some Gram positive bacteria which are repeatedly exposed to increased nisin concentrations have demonstrated nisin resistance. Numerous mechanisms of resistance have been identified and differ between strains (Zhou *et al.* 2014). However, modifications to the structure of nisin have produced a peptide with enhanced antimicrobial activity (including activity against Gram negative isolates), though the mechanism of action is still not fully understood (Field *et al.* 2012). Further investigations into structural modification of nisin will provide more information on the structure, function and properties of the peptide which could result in the development of a variant less susceptible to resistance.

Bacitracin is an AMP produced by *Bacillus subtilis,* which was discovered in 1943. It is a polypeptide antibiotic, which is composed of a heptapeptide cyclic structure and a thiozalone ring stabilised by an amide link between the side chains of Lys-6 and C-terminus of Arg-12. These features of the bacitracin structure have been shown to protect it from proteolytic degradation (Nie *et al.* 2016). Its mechanism of action is dependent upon the presence of metal ions (Zn^{2+}, Mn^{2+}, Ni^{2+} and Cu^{2+}) and involves the inhibition of peptidoglycan synthesis (Ageitos *et al.* 2017). Enterococcal and Staphylococcal species isolated from animals have been shown to possess bacitracin resistance, but evidence suggests the prevalence of this resistance has not increased over time, despite widespread usage of bacitracin as a growth promoter in livestock (Aronson 2016). As widespread resistance has not been seen, this is encouraging for development of more AMPs into therapeutic usage in the future.

Daptomycin is a novel lipopeptide antibiotic, which was approved in 2003 in the United States and in 2006 in Europe, for the therapeutic treatment of skin and skin-structure infections caused by *S. aureus* (MRSA and methicillin-sensitive *S. aureus*), *Streptococcus agalactiae, Streptococcus dysgalactiae* subsp *equisimilis* and vancomycin-resistant Enterococci (VRE) (Taylor and Palmer 2016). Daptomycin displays rapid *in vitro* bactericidal activity against many clinically relevant Gram positive pathogens (Ma *et al.* 2017). The mechanism of action remains to be fully understood, but it has been well established that the mechanism involves disruption of the cytoplasmic membrane, is dependent on the presence of calcium and is limited to Gram positive bacteria. Although only being released relatively recently, daptomycin has been widely used in the clinical setting and it remains the only member of the cyclic lipid class of antibiotics approved for clinical use. Clinical resistance to daptomycin is rare, which may be in part related to the inclusion of several D-amino acids in its structure (Taylor and Palmer 2016). Unlike synthetic drug production, daptomycin has been produced recombinantly in bacterial culture. The initial strategy of production was insufficient and unsustainable due to toxicity from the expressed daptomycin towards the bacterial culture. To combat this, the recombinant production of daptomycin has been optimised to obtain a greater yield via the utilisation of strategies such as medium optimisation, fermentative strategy, genetic engineering modification, and metabolic flux analysis (Ng *et al.* 2014). The successful recombinant production of Daptomycin demonstrates a cheap and efficient strategy for the production of peptide drugs in a bacterial system, which could be utilised in the future for the production of AMPs.

Peptide 'antibiotics' are being used clinically, but there are factors which have limited their application to date, such as nephrotoxicity, but the increase in antimicrobial resistance has seen an increase in their therapeutic usage (Choi *et al.* 2016, Nie *et al.* 2016). Peptide based drugs have a wide range of applications and it is anticipated that the approval of peptide based drugs by the FDA will grow significantly. Presently, there are 140 peptide based drugs in clinical trials and over 500 therapeutic peptides undergoing preclinical development. These drugs are mostly targeted towards metabolic diseases and oncology, however, the growing antibiotic resistance crisis has demanded new strategies for the discovery of novel antimicrobial therapeutics (Fosgerau and Hoffmann 2015).

Previously, regulatory authorities were less prepared to accept adverse-side effects with antimicrobials compared with other drug classes and they have historically been required to demonstrate superiority over existing therapeutic agents. This has led to the rejection of many candidate drugs, including AMPs. After previously being rejected, pexiganan once again entered clinical trials, as Locilex, with the developers (Dipexium Pharmaceuticals) liaising with the FDA to develop pexiganan as a topical drug to treat drug-resistant bacterial infections associated with diabetic foot ulcers (Fox 2013). As of January 2019, no recent reports of development for phase IV have been reported for pexiganan for the treatment of skin and soft tissue infections in the USA. This highlights that despite the rapid clinical need for new antimicrobial drugs, the regulatory hurdles facing antimicrobials are restricting the market and slowing down an already lengthy drug development process.

Despite the regulatory issues, there is now new optimism regarding bringing these drugs to market and greater recognition is given to the challenges of translating the research and design of AMPs into a new class of antibiotics. Omiganan (Sader *et al.* 2004) has entered phase III trials for the once-daily treatment of severe papulopustular rosacea. Iseganan is in phase III trials for the treatment of oral mucositis in patients with head and neck malignancy (Mahlapuu *et al.* 2016a). In February 2019, NovaBiotics (UK) was awarded a £1.8 million grant for the advancement of the development of Novamycin (NP339) for the treatment of fungal infections caused by *Aspergillus, Cryptococcus* and *Candida* species.

1.9.2 Designing new peptide analogues

AMPs are promising alternatives to antibiotics, but many of the AMPs derived from natural sources are not optimal for therapeutic usage due to limited supply, susceptibility to acidic/enzymatic degradation and high production costs as well as eukaryotic haemolytic and cytotoxic activities. The information obtained from sequence and structural analyses of natural AMPs is providing a template for the design of more potent and less cytotoxic AMPs to be synthetically produced in order to improve the therapeutic indices (Ong and Wiradharma 2014).

There is a gap in the knowledge as to how the structure of AMPs can influence function and cytotoxicity. One method of investigating the contribution of amino acids to overall function and toxicity is to use a template-based approach to AMP design. This involves site-directed mutagenesis (SDM) of an AMP to enhance therapeutic properties. By this method, the contribution of single amino acid residues to overall function and toxicity can be determined (Panteleev *et al.* 2015). This *de novo* design approach allows increased understanding of how factors such as amphipathicity, cationicity and structural class contribute to the antimicrobial and cytotoxic properties of AMPs. Using this method, basic amino acid residues (histidine, lysine, arginine) are included to increase electrostatic interactions and are combined with non-polar amino acids (tryptophan, tyrosine, alanine) to facilitate insertion into the lipid bilayer. This approach is of great drug development interest, as it enables the identification of motifs responsible for antimicrobial activity to aid the optimisation of novel AMPs (Ong and Wiradharma 2014, Pal *et al.* 2016). The effects of structural changes have mostly been noted in terms of influence on antibacterial activity, but eukaryotic cytotoxicity is an important factor to consider if these peptides are ever to be marketed as future therapeutics (Irazazabal *et al.* 2016, Memariani, Shahbazzadeh, Ranjbar, *et al.* 2016).

Most peptide therapeutics (not limited to AMPs) are approved for delivery via the parenteral route, with 75% administered via injection (Fosgerau and Hoffmann 2015). Some AMPs are being investigated for topical administration however, it is of greater convenience for patients if orally available drugs are developed (Dean *et al.* 2011, Samy *et al.* 2015). The challenge of such drug design is susceptibility to acidic and enzymatic degradation by both the gastrointestinal tract and when crossing the intestinal mucosa alongside pharmacokinetic and pharmacodynamic parameters. As such, chemical strategies to stabilise the secondary structure must be considered when designing antimicrobial peptides for therapeutic use (Fosgerau and Hoffmann 2015). Several AMPs have been verified for their antimicrobial activity and are being used in the pharmaceutical, enzyme and food industries, demonstrating AMPs have a place in the therapeutic setting (Meng *et al.* 2016).

1.10 Strategies for AMP production

In addition to the pharmaceutical challenges relating to regulation, reducing AMP inactivation and making AMPs more drug-like, another challenge facing AMP introduction into the clinical setting is developing a strategy for large-scale protein production. AMPs are isolated from numerous organisms, but for experimental evaluation AMPs are generally synthesised by solid-phase synthesis (Lee *et al.* 2002, Edwards *et al.* 2016). Solid-phase peptide synthesis (SPPS) is considered the most mature technology available for the chemical production of peptides up to 50 amino acids in length (Mahlapuu *et al.* 2016b). Although this method can efficiently produce low quantities of peptides at high purity, it is a lengthy and expensive process that is not sustainable for large-scale production of commercial drugs.

Production systems for recombinant peptides include bacteria, yeast, insect and mammalian cells. However, these systems can require extensive optimisation and often have a long and extensive research and design phase (Mahlapuu *et al.* 2016b). Despite this, AMPs have been successfully produced recombinantly which provides optimism for up-scaling and potential drug production on a pharmaceutical scale. Plectasin has been successfully produced recombinantly in *Aspergillus oryzae* (Mygind *et al.* 2005). Snakin-1 has been recombinantly produced in *Pichia pastoris* and purified from inclusion bodies which yielded approximately 40 mg of pure snakin-1 from a one litre bacterial culture (Kuddus *et al.* 2016). Tanhaiean *et al.*, (2018) described a methodology for the recombinant production of a His-tagged camel milk lactoferrin in *E. coli,* which produced an average yield of 0.42 g of protein from a litre of bacterial culture. These studies highlight that recombinant technologies can be utilised for AMP production, which further enhance the therapeutic potential of AMPs.

1.11 Venoms

All species are subject to microbial challenge, as such numerous mechanisms to combat bacterial attack have developed (Sharma and Nagaraj 2015). The search for novel antimicrobial compounds was led by the investigations in to the bacterial

defence strategy in organisms which lack an adaptive immune system. Defensins are naturally occurring cationic, cysteine-rich polypeptides which have been isolated from numerous organisms, including mammals, insects and plants (Ye *et al.* 2010). Similarity between insect defensins and scorpion venom toxins led to the isolation of the first scorpion defensin from the haemolymph of the North African scorpion *Leiurus quinquestriatus* (Cociancich *et al.* 1993). This scorpion peptide shared a high degree of homology with insect defensins in the order Odonata, it also demonstrated antimicrobial activity against *Micrococcus luteus* (Cociancich *et al.* 1993). The isolation of antimicrobial compounds from venomous animals was not unexpected; during the envenomation process in snakes, the fangs and oral cavity is exposed to a large quantity of potentially pathogenic bacteria but despite this, snake envenomation is associated with a low level of bacterial infection (de Lima *et al.* 2005, de Latour *et al.* 2010). Fosgerau and Hoffmann, (2015), established an infection model in scorpions and detected antimicrobial activity upon bacterial challenge. This research demonstrated the expression of antimicrobial compounds in venoms may have evolved to protect the venom gland from bacterial attack (Fosgerau and Hoffmann 2015).

The venom of venomous animals represents a rich source of substances of therapeutic interest, such as AMPs, neurotoxins, defensins, antiepileptic peptides and ion-specific toxins amongst others (Zhu, Peigneur, *et al.* 2014, Memariani *et al.* 2016, Valdez-Velazquéz *et al.* 2016). Antibacterial properties of venoms had been suspected for many years, with the first reports of these venom properties emerging in 1948 and 1968 from species of *Elapidae* and *Viperidae* snakes (de Lima *et al.* 2005, de Latour *et al.* 2010). Numerous snakes have demonstrated potent antimicrobial activity in their crude venom, such as the venom of *Naja naja oxiana* which has potent antimicrobial activity towards both Gram positive and Gram negative bacteria (Samy *et al.* 2016). It has also been demonstrated that scorpion venoms are an abundant source of AMPs and the presence of such peptides in the venom may contribute to the protection of the venom gland from infection whilst also facilitating the action of neurotoxins (Hernández-Aponte *et al.* 2011, Harrison *et al.* 2014).

Components of venoms have been used as therapeutic agents since the isolation of a bradykinin-potentiating peptide from the snake *Bothrops jararaca* in the latter half of the twentieth century. This peptide was developed in to captopril® (a small molecule angiotensin converting enzyme-inhibitor) as a result of the study of structure-function relationship analysis and design, thus demonstrating that therapeutic molecules can be developed from natural venom. (Reeks *et al.* 2015) Similarly, native AMPs derived from venoms are not optimal for therapeutic application and require modification to improve the therapeutic index (Datta *et al.* 2015). Such modifications may include the substitution of amino acids or truncation to optimise the peptide to maximise antimicrobial activity and decrease host cytotoxicity (Memariani, *et al.* 2016). A greater understanding of the relationship between the structure and function of AMPs could also aid future development of novel therapeutics from naturally derived AMPs from venoms (Datta *et al.* 2015)

1.11.1 Scorpion venom

Scorpions are ancient animals and are considered one of the oldest forms of arachnids. Scorpions are characterised by an elongated body and the presence of a telson, which holds the venom glands (Abdel-Rahman *et al.* 2015). Scorpions now inhabit virtually all terrestrial habitats, except Antarctica. Over 1700 species have been described to date, with the key to their success being the production of potent venom (Ortiz *et al.* 2015). The venom of scorpions has evolved as a sophisticated weapon to aid in the capture of prey and self-defence (Abdel-Rahman *et al.* 2015) whilst also providing a means of deterring possible competitors (Ortiz *et al.* 2015). Scorpion venom provides a rich source of biological components with a range of pharmaceutical activities (Ramírez-Carreto *et al.* 2015). Venom analyses have revealed that the venom from each individual scorpion species may contain over 500 different peptides ranging from 1 to 9 kDa in mass (Newton *et al.* 2007). Peptides derived from scorpion venoms can be loosely divided in to two separate groups: disulphide-bridged peptides (DBPs) which include neurotoxins and the non-disulphide bridged peptides (NDBPs) which possess anti-cancer, immunomodulatory and antimicrobial activities (Ramírez-Carreto *et al.* 2015).

The DBPs have been more widely explored, due to the medical relevance of envenomation (Ramírez-Carreto *et al.* 2015). The majority of DBPs are cross-linked by 3-4 disulphide bridges and can specifically interact with ion channels (Machado *et al.* 2016). DBPs make up the largest constituent of scorpion venom and have been characterised as peptides which interact with ion channels (Harrison *et al.* 2014). Of the DBPs, neurotoxins have been the driving force of natural venom components. The neurotoxins can block or modify the targeted ion channels, which results in autonomic excitation, whilst α-toxins can also initiate a massive release of catecholamines. These two events combined can create a cascade of physiological events which can progress to tachycardia, heart failure and death (Ortiz *et al.* 2015).

Scorpion stings are a notorious health issue in certain countries, with over 1.2 million stings registered annually. However, scorpions have been traditionally used in medicine in Asia and Africa since the emergence of ancient cultures. (Ortiz *et al.* 2015) The isolation and chemical and functional characterisation of scorpion venom is expected to lead to the discovery of new molecules of therapeutic interest (Valdez-Velazquéz *et al.* 2016).

There has been a growing interest in the NDBPs and to date, over 40 scorpion NDBPs have been identified and functionally characterised (Ramírez-Carreto *et al.* 2015). Most of the NDBPs characterised from scorpion venom are antimicrobial peptides, which are amphipathic and generally α-helical (Machado *et al.* 2016). These peptides have been demonstrated to modify their structural conformation depending on the environmental conditions, which can facilitate their interactions with bacterial membranes and contribute to antibiotic activity (Daniele-Silva *et al.* 2016). In addition to antimicrobial properties, the NDBPs have shown multiple activities, including; insecticide, antiviral, antifungal, antimalarial, haemolytic, anti-proliferation, bradykinin-potentiating and immunomodulatory (Daniele-Silva *et al.* 2016, Machado *et al.* 2016). AMPs derived from scorpion venoms generally have a small size (13-56 amino acids), a cationic charge (+1 to +7) and distinct hydrophobic domains (Harrison *et al.* 2014). Bacteria have demonstrated a reduced ability to develop resistance to the NDBP- class of scorpion AMPs, which further demonstrates the potential of these molecules to provide a scaffold for the development of novel peptides to treat

infectious disease (Ramírez-Carreto *et al.* 2015, Daniele-Silva *et al.* 2016, Machado *et al.* 2016).

1.11.2 *Scorpio maurus palmatus*

The scorpion *Scorpio maurus palmatus* belongs to the family Scorpionidae which is commonly found in the Mediterranean, Middle East, Saudi Arabia and Jordan. *S. m. palmatus* is not dangerous to humans, but its venom possesses toxins which have neurotoxic and cytotoxic properties towards insects. Transcriptomic study of the venom milked from the venomous glands of *S. m. palmatus* has revealed the presence of antimicrobial peptides (Abdel-Rahman *et al.* 2013).

Four antimicrobial peptides have been identified and characterised from the venom of *S. m. palmatus.* Of these, Smp24 and Smp43 are of greatest interest, as Smp13 and Smp76 demonstrated no detectible antimicrobial activity (Abdel-Rahman *et al.* 2013). Smp24 and Smp43 share broad-spectrum antimicrobial activity and are promising candidates for development in to future therapeutics. Smp43 contains a helix-hinge-helix region, which is present in the group of longer-chain antimicrobial peptides all of which have high therapeutic indices. This group of AMPs has significant potential for development in to future antimicrobial therapeutics. Smp43 has demonstrated low levels of haemolysis, but it caused significant ATP release when assayed in HepG2 cells (Harrison *et al*., 2016). Modifications to the peptide to limit the host cytotoxicity would further enhance the therapeutic potential of this peptide.

1.11.3 Smp24

Smp24 is 24 amino acids in length, bactericidal, cytotoxic and belongs to the mid-chain family of scorpion antimicrobial peptides. It demonstrates broad-spectrum antimicrobial activity, including activity against methicillin-resistant *Staphylococcus aureus* (MRSA) isolates, Enterobacteriaceae and *Candida albicans* (Harrison *et al.* 2016).

Smp24 has demonstrated multiple modes of action, which vary depending upon the lipid composition of the target membrane (Harrison, *et al.* 2016). It operates by a membrane disruptive mechanism but has also demonstrated activity upon intracellular targets via disruption of DNA synthesis. Previous circular dichroism (CD) analysis determined Smp24 to be unordered in aqueous solution but adopts an α-helical structure in membrane mimetic conditions in the presence of 60% trifluoroethanol (TFE) with two helical regions of approximately 59% and 22% predicted (Harrison, *et al.* 2016).

The disruptive effects of Smp24 on membranes have been determined via numerous methodologies, which concluded the mechanisms of membrane disruption are dependent on the membrane composition (Harrison *et al.* 2016). Atomic force microscopy (AFM) is a technique which enables the visualisation of live cells in situ, which makes it a valuable tool for the study of mechanisms of action of AMPs on bacterial cell membranes (Meincken *et al.* 2005). Electrostatic interaction and lipid defect sensing may be responsible for the initial attraction of Smp24 to prokaryotic (PC:PG) and eukaryotic (PC:PE) membrane surfaces, the precise nature of peptide induced membrane disruption is different. In anionic PC:PG bilayers, pores of varying size were observed by AFM, with pores ranging between 20 and 150 nm in width and a depth of 2 – 4 nm which remained stable over a 30 minute period. Increased peptide concentration resulted in complete membrane disruption within 5 minutes. Combined with liposome leakage data, this suggests that total membrane collapse does not happen and therefore favours a pore forming mechanism as opposed to a carpet mechanism (Harrison *et al.* 2016).

Quartz crystal microbalance-dissipation (QCM-D) is a technique that enables the examination of interactions between an AMP and a biological membrane in real time and in situ, which provides information about the mass and structural changes occurring in the membrane (McCubbin *et al.* 2011). QCM-D data also supports the toroidal pore theory as increased peptide accumulation and increased dissipation was observed which is consistent with peptide induced membrane disruption. The dissipation event could be due to the peptide threshold concentration being overcome and peptide molecules mixing with the bilayer and thus resulting in reduced interaction with the aqueous phase. In conclusion, the

proposed mechanism of action for Smp24 is the classical pattern observed for AMPs: initial electrostatic interaction, peptide accumulation and membrane insertion upon meeting the threshold concentration. The collected data suggests Smp24 produces a toroidal pore, due to the presence of pores of varying sizes upon increased peptide concentration leading to complete destruction of the bilayer as opposed to increased pore formation (Harrison *et al.* 2016).

For zwitterionic PC:PE bilayers, it is proposed that Smp24 operates via a different mechanism due to observation of stratifications via AFM. Liposome leakage was also less pronounced for PC:PE membranes and combined with QCM-D data, this supports that accumulation of peptides at the bilayer does not occur. Smp24 has demonstrated the ability to cause disruption of PC:PE bilayers, forming pores between 200 and 350 nm in width depending upon Smp24 concentration, however, this does not lead to complete membrane disruption (Harrison *et al.* 2016).

Native Smp24 has a high percentage of haemolysis. Mutations have previously been applied to the structure of Smp24 to limit the percentage haemolysis. The truncation of the peptide to remove the 4 amino acids at the C-terminus (Smp24T) reduced haemolysis by 43%, but a high level of cytotoxicity was still observed (Harrison *et al*., 2016). Despite this, the decrease in haemolysis resulted in Smp24T demonstrating a higher therapeutic index overall. The incorporation of a glycine-valine-glycine (GVG) hinge has previously been postulated to reduce the haemolytic properties of venom-derived AMPs (Rodríguez *et al.* 2014b) but for Smp24 this resulted in increased haemolytic activity, increased toxicity towards HepG2 cells and decreased antimicrobial activity compared with native Smp24. For Smp24, the GVG hinge slightly decreased the selectivity of the peptide, suggesting whilst AMPs can share structural and functional characteristics, they may not be molecules which can adopt a shared strategy for therapeutic enhancement. Resultantly, this suggests further investigations in to the contribution of individual amino acids to the overall mechanism of action and cytotoxicity is required in order to fully understand how these molecules function and how they can be enhanced for therapeutic usage.

1.11.4 Smp43

Smp43 is a 43 amino acid peptide, which demonstrates broad-spectrum antimicrobial activity and a low level of haemolysis and cytotoxicity (Harrison, Abdel-Rahman, *et al.* 2016). Circular Dichroism (CD) analysis of Smp43 demonstrated that like Smp24, the peptide was disordered aqueous solution and adopted its helical structure in membrane mimetic conditions. Smp43 adopted a di-helical structure in the presence of 60% TFE with two helical regions of approximately 70% and 25% (Harrison, *et al.* 2016).

The mechanistic activity of Smp43 has been investigated by liposome leakage assays, AFM of anionic and zwitterionic membranes, QCM-D and intracellular reporter gene assays in *Bacillus subtilis.* No evidence of intracellular effects was observed for Smp43, with the stress response identified in *B. subtilis* reporter strains being limited to the cell envelope. The mechanistic information obtained by AFM analysis concluded that Smp43 is approximately 6.5 nm in length and therefore too large to span the membrane bilayer. The membrane-binding properties of Smp43 include initial binding and nucleation, defect growth by two-dimensional diffusion of surface bound peptides to existing defect sites and the convoluted geometry of the observed defects suggests Smp43 dwells at the defect boundary where it stabilises the high edge energies associated by exposing the hydrophobic phospholipid tails (Heath *et al.* 2018).

Smp43 shares 80% homology with Pandinin 1, an AMP derived from the venom of the scorpion *Pandinus imperator* (Rodríguez *et al.* 2014a). The observation of the mechanism of action of Smp43, combined with the sequence homology with Pandinin 1 suggests a mechanism by which there is initial electrostatic interaction at the membrane surface and the stabilisation of peptide-lipid bonds by the π-electron cloud of the conserved tryptophan indole groups. A threshold concentration is then reached which enables peptide insertion in to the membrane, a stable pore is formed and additional peptides are able to diffuse in to the membrane defect which results in the removal of lipid micelles. This is a rapid process, which is potentially limited by the arrival of more peptide molecules to the defect site and the probability of peptide-peptide interactions and lipid removal (Heath *et al.* 2018). Whilst it has previously been established that the

insertion of peptides in to the lipid bilayer occurs at a critical concentration (Yandek *et al.* 2007), the data obtained for Smp43 was insufficient to determine if the peptide insertion occurred before or after diffusion to the observed membrane defects (Heath *et al.* 2018).

The mechanism of action of Smp43 has been postulated as “diffusion limited disruption” which describes the growth of membrane defects as a result of peptide diffusion and accumulation. The speed and scope of this mechanism of action differs depending on membrane composition, with membrane defect growth occurring at a 30-fold faster rate in anionic PC:PG membranes than zwitterionic PC:PE membranes (Heath *et al.* 2018).

To date, no studies have investigated the relationship between structure and function of Smp43 via a mutagenesis strategy. Although Smp43 does demonstrate broad spectrum antimicrobial activity, the obtained minimum-inhibitory concentration (MIC) values for the Gram negative isolates tested were quite high (128 – 256 µg/ml) (Harrison *et al.* 2016). Modifications to the structure of Smp43 to enhance the antimicrobial properties of the peptide or truncation of the peptide in a similar methodology to that taken for Smp24 would be an interesting future direction to take.

1.12 Scope of the present study

This present study aims to improve the understanding of the relationship between structure, function and cytotoxicity of venom-derived AMPs. The study also aims to develop a recombinant protein production system for AMPs to produce large quantities of peptide "in house" and ultimately create a library of peptides.

The objectives were to:

- Characterise the relationship between structure and antimicrobial activity by performing single amino-acid substitutions in Smp24 and Smp43.

- Characterise the relationship between the Smp24 and Smp43-derived peptides and cytotoxicity and haemolytic activity with eukaryotic cells.

- Determine the effects of the amino acid substitutions on the secondary structure of the peptides via biophysical techniques.

- To develop a recombinant expression system for the over production of Smp24.

- Optimise a site-directed mutagenesis (SDM) strategy to create a library of genes which can recombinantly produce modified Smp24 peptides.

2

General Methods

2.1 Materials

All chemicals were purchased from Sigma Aldrich (Dorset, UK) unless otherwise stated.

2.2 Peptide synthesis

Smp24, Smp43 and all derived modifications were synthesised via solid-phase synthesis by David's Biotechnologie GmbH, Regensberg, Germany to a purity of 90-99%.

2.3 Minimum inhibition concentration (MIC) assay

The MIC of the antimicrobial peptides was determined against a variety of organisms using the broth microdilution method described by Andrews (2001) and performed on the Clariostar plate reader (BMG labtech, Offenburg, Germany). The following microbes were used throughout this study: *Escherichia coli* JM109, *Staphylococcus aureus* SH1000, *Pseudomonas aeruginosa* 2056 (H085180216), *Bacillus subtilis* sub species subtilis (NCIMB 3610).

Overnight cultures were diluted in Muller Hinton (MH) broth (Sigma Aldrich, Dorset, UK) to produce a bacterial suspension for antimicrobial susceptibility testing. Doubling dilutions of antimicrobial peptides (AMPs) were added to the bacterial suspension at a 1:10 ratio with a final well volume of 200 µL. AMPs were examined at a concentration of 0 - 512 µg/ml, with MH broth as a growth control. Plates were incubated statically for 18 - 24 hours at 37°C and read using a plate reader. The MIC was defined as the lowest concentration of antimicrobial peptide at which growth was inhibited when viewed as turbidity against a negative broth control. The MIC was determined by performing the assay in triplicate (or duplicate if quantity was extremely limited) on two different occasions and therefor presents the average of 4 or 6 replicates.

2.4 Minimum bactericidal concentration (MBC) assay

5 µL aliquots were taken from the wells of the 96-well MIC plate and spot plated on to MH agar in triplicate. The plates were incubated statically for 18 - 24 hours at 37°C. The MBC was defined as the lowest concentration at which the visible growth was completely inhibited by the antimicrobial peptides (Henly *et al.* 2019).

2.5 Minimum biofilm eradication concentration (MBEC) assay

Overnight cultures of bacterial isolates (*E. coli* JM109 or *E. coli* EC2) were prepared in MH broth by inoculating 2 to 3 colonies of bacteria in 10 ml MH broth and incubating at 37°C, 200 rpm for 18 – 24 hours. Overnight cultures were diluted to OD_{600} 0.008 and 100 µl was added to a 96 well plate. A peg lid was added (NUNC, Warrington, UK) and the plate was incubated at 37°C for 18 - 24 hours to enable biofilm formation.

The peg lid was twice-washed with 200 µl PBS (Gibco, Warrington, UK) for 10 seconds before being added to the “challenge plate.” The challenge plate was prepared by adding doubling dilutions of antimicrobial peptide in a 1:10 ratio with sterile MH broth to give a final well volume of 150 µl. The plate was incubated at 37°C, 100 rpm for 24 hours. The minimum biofilm inhibition concentration (MBIC) was defined as the lowest concentration at which growth was inhibited versus the turbidity of a negative broth control and determined by measuring the OD_{600} of the 96-well plate. The peg lid was then transferred to 96-well plate containing 200 µl of sterile MH broth and incubated for 24 hours at 37°C, 100 rpm. The minimum biofilm eradication concentration (MBEC) was determined as the lowest concentration required to cause no growth by reading the OD_{600} and comparing turbidity to a sterile MH broth control (Cowley *et al.* 2015).

MBEC assays were performed in triplicate on two separate occasions. Data shown represents the average of 6 replicates.

2.6 Haemolysis assay

The haemolytic activity of the peptides was tested using sheep erythrocytes as described by Corzo *et al*, (2001). A 10% (v/v) suspension of phosphate buffered saline (PBS) washed sheep erythrocytes was incubated in a 96 well plate with the antimicrobial peptides at a concentration range of 0 – 512 µg/ml. The plate was incubated at room temperature with intermittent shaking for 1 hour. Haemolysis was determined by measuring the absorbance of the supernatant at an optical density of 570 nm on a Wallac Victor2 1420 plate reader (Marshall Scientific, New Hampshire, USA). 10% Triton X-100 was used as a positive control and deionised water was used as a negative control. All samples were tested in triplicate. The percentage haemolysis was calculated using the following equation:

$$\frac{\text{Absorbance of sample} - \text{Absorbance of negative control}}{\text{Absorbance of positive control} - \text{Absorbance of negative control}} \text{ x } 100$$

Haemolysis assay results represent the average of three technical repeats. Due to the limitation of the quantity of peptide available for analysis, it was not possible to perform a biological repeat for haemolysis data.

2.7 Cytotoxicity assays

2.7.1 Eukaryotic cell culture line maintenance

All cell lines were routinely screened for the presence of mycoplasma. Cells were grown in Dulbecco's modified Eagle's medium (DMEM) with 10% foetal calf serum (FCS) and 1% penicillin-streptomycin. Cells were incubated in T-75 flasks at 37˚C in a 5% CO_2 atmosphere. Culture media was changed twice a week and cells were trypsinised upon reaching 90% confluence.

Human urothelial epithelial cells (HUEPC) were purchased from Provitro (Berlin, Germany). HUEPC cells are a primary cell line, which were cultured without the addition of antibiotics in the media. Cells were grown in urothelial cell growth media (Provitro) at 37°C with 5% CO_2 until cells reached 90% confluence. Cells

were twice washed with PBS, trypsinised using TrypLe (Gibco, UK) and neutralised with trypsin neutralising solution (Provitro). The cells were centrifuged at 300 x g for 5 minutes and re-suspended in urothelial growth medium. Culture media was changed every other day until cells reached 90% confluence.

2.7.2 Cytotoxicity assays

Cellular toxicity was determined by measuring lactate dehydrogenase (LDH) release by Pierce LDH release assay kit (Life Technologies, Paisley, UK). Peptides were assayed at a concentration range of 0.5 – 512 µg/ml against a human liver cell line (HepG2), kidney cell line (HEK-293) and keratinocyte cell line (HaCaT) to determine the potential toxic effects *in vitro*.

Cells were seeded in a 96 well plate at a density of 2 x 10^5 cells per well (HepG2 and HEK-293) and 1.6 x 10^5 cells per well (HaCaT) and 1.4 x 10^5 cells per well (HUEPC) in 90 µL of culture media and incubated for 24 hours. Peptides were then added and incubated for a further 24 hours. To determine LDH release, 50 µL of culture media was incubated with 50 µL of reaction buffer at room temperature for 30 minutes as per manufacturer's instructions. The absorbance of was measured at 490 nm and 680 nm using CLARIOstar microplate reader (BMG Labtech, Ortenberg, Germany). Deionised water was used as a spontaneous LDH control and 10% Triton X-100 was used as maximum LDH control. Prior to calculating percentage cytotoxicity, the background LDH absorbance (680 nm) was subtracted from the 490 nm absorbance. Cytotoxicity was calculated as follows:

$$\frac{Peptide\ treated\ LDH\ activity - Spontaneous\ LDH\ activity}{Maximum\ LDH\ activity - Spontaneous\ LDH\ activity}\ x\ 100$$

All cytotoxicity assays were performed in triplicate on two separate occasions. Therefore, the data represents 6 technical and 2 biological repeats for all conditions assayed.

2.7.3 LD_{50} calculations

The LD_{50} was defined as the concentration which resulted in 50% cell death. This was calculated by plotting AMP concentration versus cytotoxicity on a dose-response curve and extrapolating the value which caused 50% cell death.

2.7.4 T-test on data

A T-test (De Winter 2013) was carried out on the calculated LD_{50} values. The LD_{50} of modified peptides was compared with that of the LD_{50} of the parental peptide. p-values of less than 0.05 were deemed to be statistically significant. A T-test was chosen for the method of statistical analysis due to the usage of this test in the field of drug research and development to compare the performance of drugs. In this study, the T-test was used to assess the performance of modified Smp analogues to the parental peptides (Smp24 and Smp43) to determine superiority of inferiority.

2.7.5 Therapeutic index

Therapeutic index (TI) is a widely accepted parameter to represent the specificity of antimicrobial peptides for prokaryotic *versus* eukaryotic cells. Larger TI values represent greater specificity for prokaryotic cells. Therapeutic index values were calculated as the ratio of cytotoxicity and antimicrobial activity by dividing LD_{50} and HC_{50} values by the MIC for each peptide against *E. coli* (Jiang *et al.* 2014).

2.8 Circular dichroism

2.8.1 Methodology

All circular dichroism (CD) work was carried out at the Department of Molecular Biology and Biotechnology, University of Sheffield. The secondary structures of antimicrobial peptides were determined via CD spectroscopy. Samples were prepared to a 100 μM concentration in water and 200 μl of the peptide was added

to the cuvette. Trifluoroethanol (TFE) was titrated in the experiment in a 0 - 70% concentration (v/v). The absorbance was corrected for the changes in volume over the assay. Analysis was performed on a JASCO J-810 spectropolarimeter (Jasco, Maryland, USA) at 22°C using a 0.1 cm path-length cell.

2.8.2 Data analysis

The ellipticity signal was corrected for the volume in the cuvette by the following equation:

$$Corrected\ signal = CD\ signal\ x\ \frac{Final\ assay\ volume}{200}$$

$$E.g.\ 0.339 = 0.305189\ x\ \frac{222.2}{200}$$

Data was analysed using the following equation:

$$Molar\ ellipticity = \frac{observed\ ellipticity\ \times\ 100\ \times\ Mr}{concentration\ x\ pathlength\ x\ nA}$$

Where observed ellipticity = degrees, Mr = kDa, concentration = mg/ml, path length = 0.1 cm and nA is the number of amino acids.

2.9 Modelling

2.9.1 Helical wheel projections

Helical wheel projections were produced for all the peptides in this study using the rzlab software from the University of California (www.rzlab.ucr.edu).

2.9.2 *Ab-initio* modelling

Initial 3D-modelling was performed by inputting sequences into the Quark online server at https://zhanglab.ccmb.med.umich.edu/QUARK/. The software generated a secondary structure model and produced a file format which was compatible to be used with more complex modelling software.

2.9.3 3D-modelling

3D-modelling of AMPs and derived modifications was achieved using PyMOL 2.3 software by Schrödinger (https://pymol.org/2/). Structures were generated to display the amino acids of interest.

2.9.4 Hydrophobic moment

Hydrophobic moment and surface polarity was calculated using the software developed by Reißer *et al*., 2014, accessed at http://www.ibg.kit.edu/HM/?page=paper

2.10 Gene synthesis

STII/Smp24 gene sequences were designed based upon native peptides isolated from *Scorpio maurus palmatus* venom (Harrison, Abdel-Rahman, *et al.* 2016). Smp24 sequences were adapted for *E. coli* codon usage and fused to a signal peptide from heat-stable *E. coli* as per Lyukmanova, *et al,* (2007). The STII/peptide inserts were synthesised and fused between the HindIII and NdeI sites of the vector pET22b (+) by Eurofins (Ebersberg, Germany).

Plasmids for the expression of FLAG-tagged peptides were designed using the same methodology listed above. The codon usage for the amino acid sequence for the FLAG tag (DYKDDDDK) and the cleavage sequence (LVPRGS) was adapted for codon usage in *E. coli*. The gene inserts were spliced in to a pET22b

(+) vector between the NdeI and HindIII restriction sites by Eurofins (Ebersberg, Germany).

2.10.1 Transformation of plasmids

E. coli BL21 was prepared in 10 ml Luria Burtani (LB) broth and incubated overnight at 37°C with moderate shaking (200 rpm). To produce electro-competent cells, the overnight culture was diluted 1:500 in to 50 ml of LB broth and placed in a 37°C incubator for 90 - 120 minutes until the cells reached mid-log phase (OD_{600} 0.5). The cells were pelleted by centrifugation at 4800 x g, 4°C for 10 minutes. The cell pellet was re-suspended in 20 ml ice cold sterile dH_2O and centrifuged again under the same conditions. The cell pellet was twice washed with ice cold water before a final resuspension in 2.5 ml sterile dH_2O.

Plasmids were transformed by the addition of 1 µl of plasmid to 100 µl of electro-competent *E. coli* cells and pulsing for 1 second using an electroporator (Bio-Rad, Watford, UK). 1 ml of LB broth was added to the transformed cells and the cells were incubated at 37°C for 1 hour prior to plating out the cells on LB agar containing 100 µg/ml ampicillin and incubating at 37°C overnight. A negative control was prepared by transforming 1 µl of sterile dH_2O into electro-competent cells.

2.10.2 Polymerase chain reaction (PCR) to confirm transformation

Following transformation, the presence of plasmids was confirmed via extraction, PCR and analyses of T7 PCR fragments via agarose electrophoresis. Overnight cultures were prepared by adding one colony of transformed bacteria to 5 ml LB broth containing 100 µg/mL ampicillin. Plasmids were extracted via GeneJET Miniprep kit (Thermo Fisher Scientific, Hemel Hempstead, UK) as per manufacturer's instructions.

1 µl of plasmid was added to a PCR tube containing 47 µL MegaMix (Microzone, Stourbridge, UK), 1 µl T7 forward primer (5'-TAATACGACTCACTATAGGG-3')

and 1 µl T7 reverse primer (5'- GCTAGTTATTGCTCAGCGG-3') (Sigma-Aldrich, Dorset, UK). Amplification was performed on a Techne TC-3000 PCR thermal cycler with the following conditions: initial denaturation 95°C 3 minutes, followed by 30 cycles of 95°C 30 seconds, 42°C 1 minute, 72°C 1 minute and final extension 72°C for 5 minutes. The PCR products were visualised on a 1% agarose gel containing 0.01% Ethidium Bromide. All constructs were sent for sequencing confirmation at Eurofins (Ebersberg, Germany).

2.10.3 Agarose gel electrophoresis

PCR products were visualised on a 1% agarose gel made up in 30 ml TAE buffer containing 0.01% Ethidium bromide. The PCR product was mixed with 5 x loading dye (Bioline, London, UK) and 10 µl of this was added to the gel. A 1 kb DNA HyperLadder (Bioline, London, UK) was used as a marker to determine the size of the fragments. Gels were visualised and photographed under UV light using the NU Genius gel dock system (Syngene, Cambridge, UK).

2.11 Production of Smp24 with the STII leader sequence

An overnight culture of *E. coli* BL21 λDE3 containing the pET22b/STII/Smp24 vector was prepared by inoculating 1 colony of bacteria in to 50 ml of LB broth containing 100 µg/ml ampicillin. The culture was incubated at 37°C with moderate shaking (200 - 250 rpm) for 18 hours. The overnight culture was diluted 1:100 in to minimal mineral M9 media (0.4% glycerol, 3 g/litre KH_2PO_4, 6 g/litre Na_2HPO_4, 0.5 g/litre NaCl, 0.24 g/litre $MgSO_4$, 0.01 g/litre $CaCl_2$, 2 g/litre NH_4Cl, 1% thiamine chloride, 0.2% yeast extract) containing ampicillin (100 µg/ml). The cells were cultivated at 37°C with shaking at 250 rpm until the cells reached mid-log phase with an optical density of 0.6 at 600 nm. Gene expression was induced by the addition of isopropyl-1-thio-β-D-galactopyranoside (IPTG) to a final concentration of 0.05 mM. After 15 hours of cultivation, the growth culture was centrifuged at 14,000 x g for 30 minutes at 4°C. The growth media was then acidified to pH 4.5, heated to 70°C for 30 minutes and then centrifuged again at 14,000 x g for 30 minutes at 4°C (Lyukmanova *et al.* 2007a).

Following the overproduction of Smp24, the culture was centrifuged at 14,000 x g for 30 minutes. The supernatant was acidified to pH 4.5, heated to 70°C and centrifuged under the same conditions.

2.12 Purification of the STII/Smp24 peptide

2.12.1 Cation exchange I

Peptides were purified via Akta Design using a 20 ml Sepharose Fast Flow resign column (GE Healthcare, Buckinghamshire, UK) equilibrated with 10 mM CH_3COONa, pH 5.0 (buffer A). All buffers, the expressed protein diluted in buffer A, were de-gassed and passed through a 0.22 µM filter.

The column was equilibrated with 5 column volumes (CVs) of buffer A. The culture supernatant was diluted in 1 L of buffer A and applied to the column via peristaltic pump at a flow rate of 38. The column was washed with 5 CVs of buffer A prior to elution. Samples were eluted from the column using the Akta Design via a gradient from a range of 0 - 1 M NaCl. This was achieved via gradient elution with 10 mM CH_3COONa, 1 M NaCl pH 5.0 (buffer B) over 20 CVs. The elution of peptides and/or proteins was determined by monitoring the UV range at 215 nm and 280 nm. Fractions containing proteins were collected, freeze-dried and re-dissolved in 1 ml dH_2O (Lyukmanova *et al.* 2007a).

2.12.2 Cation exchange II

The sample was de-salted by membrane dialysis, lyophilised and re-suspended for further purification to remove any additional impurities. The sample was purified using a second cation exchange column, a MonoS HR5/5 column (GE Healthcare, Buckinghamshire, UK) equilibrated with 10 mM CH_3COONa pH 5.0. Samples were to be eluted against an NaCl gradient over 20 CVs. Purification was performed using the Akta Design system (GE Healthcare).

2.13 Sodium dodecyl sulphate polyacrylamide gel electrophoresis (SDS-PAGE)

SDS-PAGE was carried out using the Bio-Rad Mini Protean system following manufacturer's instructions. Samples for SDS-PAGE were prepared by adding 30 µl of protein sample to 30 µl of sample buffer (table 2.1) and heated at 95°C for 5 minutes. The reagents used for SDS-PAGE are listed in table 2.1.

Table 2.1: SDS-PAGE reagent composition

Solution	Contents
SDS loading buffer	45 ml 10% SDS, 2.5 ml 0.5 M TRIS pH 6.8, 5 ml $_dH_2O$, 2.5 ml glycerol, 200 µl 5% Bromophenol blue, 250 µl β-mercaptoethanol
Separating gel (10%)	3.33 ml 30% Acrylamide-bis solution (Bio-Rad laboratories Ltd, Herts, UK), 2.5 ml 1.5 M TRIS pH 8.8, 100 µl 10% SDS, 4 ml $_dH_2O$, 200 µl APS, 20 µl TEMED.
Stacking gel	750 µL Acrylamide-bis solution (Bio-Rad), 1.5 ml 0.5 M TRIS pH 6.5, 60 µl 10% SDS, 3 ml $_dH_2O$, 150 µl APS, 10 µl TEMED
Running buffer	14.4g glycine (Fisher Scientific, Loughborough, UK), 1g SDS, 3g TRIS made up to 1 litre with $_dH_2O$
Stain	200 ml methanol (Fisher Scientific) 75 ml acetic acid (Fisher Scientific), 0.1% Coomassie blue R-250, made up to 1 litre with $_dH_2O$.
Destain	200 ml methanol (Fisher Scientific), 75 ml acetic acid (Fisher Scientific) made up to 1 litre with $_dH_2O$.

A resolving gel solution of 10% acrylamide was poured between two glass plates which had previously been cleaned with iso-propanol. 100 µl of water saturated butanol was added to the top of the gel to allow the gel to set with an even surface. Once set, the butanol and non-polymerised acrylamide was poured off and the gel washed with $_dH_2O$. The stacking gel was poured on to the resolving gel and the plastic comb inserted. Once the gel was set, the comb was removed and the wells washed with $_dH2O$. The gel was then assembled in a tank with the running buffer and the samples were loaded. The gel was run at 200V with 30 µl of sample running against the Precision Plus Protein Dual Xtra ladder (Bio-Rad

Laboratories Ltd, Hertfordshire, UK). Gels were stained overnight and then adequately de-stained.

If AMPs were not resolved via a 10% resolving gel, an optimised gel was used with an increased concentration of acrylamide. The final gel composition is stated in table 2.2.

Table 2.2: Final SDS-PAGE running conditions

Solution	Composition
Separating gel (20 %)	1.5 ml $_{d}H_2O$, 16 ml 30% acrylamide-bis solution (Bio-Rad), 6 ml 1.5 M TRIS pH 8.8, 240 µL 10 % SDS, 240 µl 10 % APS, 24 µl TEMED.
Stacking gel	7.9 ml $_{d}H_2O$, 3 ml acrylamide-bis solution (Bio-Rad), 3.375 ml 0.5 M TRIS pH 6.8, 150 µl 10% SDS, 150 µl 10% APS, 15 µl TEMED.

Gels were prepared as previously described. Samples (30 µl) were loaded in to the gel and run against the Precision Plus Dual Xtra ladder at 200V.

2.14 Tris-tricine PAGE

Despite increasing the acrylamide concentration, the resolution of the gel remained poor in the low molecular weight range. TRIS-tricine gels were utilised to achieve better resolution at a lower molecular weight.

2.14.1 TRIS-tricine gel composition (12%)

The composition of the TRIS-tricine gels is listed in table 2.3.

Table 2.3: Gel and buffer composition for the analysis of protein fractions by TRIS-tricine PAGE.

Solution	Composition
Cathode buffer	0.1 M TRIS (Fisher Scientific), 0.1 M tricine (Fisher Scientific), 0.1 % SDS made up to 1 litre with $_dH_2O$.
Anode buffer	0.2 M TRIS (Fisher Scientific) pH 8.9 made up to 1 litre with $_dH_2O$.
Separating gel (12%)	3 ml acrylamide-bis solution (75.5:1, 40%) (Bio-Rad), 303 ml TRIS 3 M pH 8.45, 1 ml glycerol, 3.2 µl TEMED, 80 µl APS, 2.2 ml $_dH_2O$
Stacking gel	0.43 ml acrylamide-bis solution (Bio-Rad), 1.24 ml TRIS 3 M, 3.32 ml $_dH_2O$, 5 µl TEMED, 50 µl APS.

Gels were prepared as per section 2.12 using the Bio-Rad Mini Protean system. The gel was then assembled in a tank with the anode buffer applied to the upper tank and the cathode buffer applied to the lower tank. Samples were mixed in a 1:1 ratio with sample buffer and loaded to the gel. The gel was run at 200V with 30 µl of sample running against the Precision Plus Protein Dual Xtra ladder (Bio-Rad Laboratories Ltd, Hertfordshire, UK). Gels were stained overnight and then adequately de-stained as per section 2.12.

2.14.2 Pre-cast gels

As an alternative to the TRIS-Tricine gels, pre-cast gels from Bio-Rad were purchased. Initially, the 16.5% Mini Protean TRIS-Tricine gel (Bio-Rad) was purchased. The gel was assembled in the Mini Protean tank and filled with TRIS-tricine running buffer (Bio-Rad). Protein samples were mixed with tricine sample buffer for protein gels (Bio-Rad) in a 1:1 ratio and applied to the gel. Gels were run at 200V against the Precision Plus Dual Xtra ladder. Samples were stained using a Pierce Silver Stain kit (Life Technologies Ltd, Paisley, UK) as per manufacturer's instructions.

2.14.3 Pre-cast gradient gel

10 - 20% gradient Mini Protean TRIS Tricine gels were also used for the identification of Smp24. Samples were run as per section 2.13.2 at 200V under the same conditions and stained using the Pierce Silver Stain kit (Life Technologies, Paisley, UK).

2.15 MALDI

α-cyano-4-hydroxycinnamic-acid (CHCA) was used as the sample matrix and prepared to a concentration of 5 mg/ml in 70:30 ratio of acetonitrile: 0.5% trifluoroacetic acid (TFA). 0.5 µl of sample was added to 0.5 µl of matrix on the target plate and dried until the matrix and protein co-crystallised. The plate was analysed on the Bruker Autoflex III Smartbeam MALDI-TOF (Bruker, Massachusetts, United States). Spectra were processed using mMass software to visualise peaks.

2.16 Immunological detection of Smp24 by anti-Smp24 antibodies

2.16.1 Raising antibodies in rabbits

As Smp24 is not a commercially available peptide, antibodies were raised by immunisation of animals with the antigen of interest. Polyclonal antibodies against Smp24 were raised in rabbits following a SuperFast 28 day immunisation schedule by David's Biotechnologie (Regensberg, Germany). The 28-day protocol yields antibodies with titres comparable to standard 63 or 90 day procedures.

2.16.2 Dot blot

1 µl of sample or controls was added to nitrocellulose membranes (Abcam, Cambridge, UK) and allowed to air dry. Bovine serum albumin (BSA) at a concentration of 1 mg/ml was used as a negative bind control. Samples were blocked in 5% milk in TBST (20 mM TRIS, 150 mM NaCl, 0.05% Tween-20, pH

7.5) for 1 hour in a petri dish, with gentle agitation (65 rpm) at room temperature. The blot was incubated with primary antibody (1:10,000) dissolved in 2% milk in TBST and incubated at room temperature for 1 hour with gentle agitation. After 1 hour, the blot was washed with TBS (20 mM TRIS, 150 mM NaCl, pH 7.5) for 3 x 10 minute washes. A goat anti-rabbit secondary antibody IRDye 800CW (Licor, Cambridge, UK) was added at a 1:10,000 dilution in 2% milk in TBST and incubated in the dark, at room temperature with gentle agitation for 1.5 hours. The blot was then washed for 5 minutes in TBS prior to being visualised on an Odyssey imaging system (Licor, Cambridge, UK).

2.17 *Galleria mellonella* pathogenicity assay

2.17.1 Preparation of larvae

Final larval stage *G. mellonella* larvae (Whole Foods Ltd, Sheffield, UK) were stored in the dark at 4˚C for less than 7 days before being randomly assigned to each construct-containing bacterial isolate. The larvae were assigned 12 to each condition and the death was monitored over a 7 day period.

2.17.2 Pathogenicity assay

The larvae were incubated at 37˚C for 30 minutes prior to injection. Overnight cultures of each test bacteria were centrifuged at 12000 x g and twice washed with sterile PBS (Gibco, Paisley, UK). Samples were diluted to an OD_{600} of 0.1 (5 x 10^8 to 8 x 10^8 CFU/ml) in 1ml. 5 µl of each suspension was injected in to the hemocoel of each larva via the second to last left proleg with a Hamilton syringe. Larvae were incubated at 37˚C in sealed petri dishes and the numbers of surviving larvae were recorded daily. A non-injected group and a group injected with sterile PBS were used as negative controls.

The experiment was run for a 7 day period or until 2 of the control group had died, whichever came first. Two independent bacterial replicates were used to inoculate 24 larvae (12 in each replicate).

2.17.3 Log rank reduction test.

A log-rank reduction test was performed on the data to determine the statistical significance. Log-rank reduction tests (LRRTs) are used to compare the survival between different groups. LRRTs are widely used in clinical trials to establish the efficacy of a new treatment compared with a control when the measurement is the time to event. In the scope of this study, the event is death of the larvae. The significance in death rate was calculated using a log rank reduction test ($p \leq 0.05$).

2.18 Affinity tagged protein over production

2.18.1 Protein overproduction

A 50 ml culture of *E. coli* BL21 λDE3 containing the vector of interest was prepared in 250 ml conical flask in LB broth containing 100 µg/ml ampicillin and incubated at 37°C, 200 rpm overnight. The overnight culture was diluted 1:200 in to 1L of fresh LB broth containing 100 µg/ml ampicillin and incubated at 37°C with orbital shaking at 200 rpm until the OD_{600} reached 0.5 - 0.6. The culture was rested at room temperature for 30 minutes prior to the addition of IPTG to a final concentration of 1 mM. The culture was incubated at room temperature with moderate shaking (225 rpm) overnight.

Cells were harvested by centrifugation at 5000 x g for 30 minutes at 2 - 8°C. The supernatant was discarded and the pellet was frozen at -20°C. The frozen cells were lysed by adding 10 ml of CellLytic B (Sigma-Aldrich, Dorset UK) per gram of frozen cell paste. The lysis buffer and protein pellet solution was incubated at room temperature with rocking as per manufacturer's instruction for 15 minutes to fully extract the soluble proteins from the cells. Following protein extraction, the cells were centrifuged at 16,000 x g for 10 minutes to remove the insoluble material. The supernatant (soluble) fraction was separated from the pellet (insoluble) fraction. Both fractions were analysed by dot blot to determine the location of the fusion protein.

2.18.2 Identification of fusion protein by dot blot

Expressed protein samples (1 µl) were added to nitrocellulose membrane (Abcam PLC, Cambridge, UK) and air dried. BSA at a concentration of 1 mg/ml was used as a negative bind control. Samples were blocked in 5% milk in TBST for 1 hour in a petri dish, with gentle agitation (65 rpm) at room temperature. The blot was incubated with anti-FLAG antibody produced in rabbit (Millipore, Watford, UK) dissolved in 2% milk in TBST incubated at room temperature for 1 hour with gentle agitation.

After 1 hour, the blot was washed with TBS for 3 x 10 minute washes. A goat anti-rabbit secondary antibody IRDye 800CW (Licor, Cambridge, UK) was added at a 1:10,000 dilution in 2% milk in TBST and incubated in the dark, at room temperature with gentle agitation for 1.5 hours. The blot was then washed for 5 minutes in TBS prior to being visualised on the Odyssey imaging system (Licor, Cambridge, UK).

2.19 Affinity-tagged protein purification

M2 affinity gel was prepared as per manufacturer's instructions. The protein containing supernatant was added to M2 affinity gel and incubated on a rocking platform with protease inhibitors (Fisher Scientific, Leicestershire, UK) at 4°C overnight to enable the fusion proteins to bind to the agarose beads. The following morning, the gel was centrifuged at 1000 x g for 5 minutes to separate the gel from the unbound supernatant. The supernatant was removed and stored for dot blot analysis; the gel was washed by adding 2 ml of TBS and centrifuging at 500 x g for one minute. This process was repeated until the A_{280} reached 0.05. The bound protein was eluted from the gel using 0.1 M glycine HCl pH 3.5. The gel was incubated with the glycine at room temperature with gentle agitation (200 rpm) for 5 minutes. This was centrifuged at 800 x g for 1 minute, the supernatant (eluted protein) was eluted in to three 1 ml fractions in to tubes containing 20 µl of TRIS HCl (pH 8.0) and the M2 resin regenerated as per manufacturer's instructions.

2.19.1 Further optimisation

Where no protein was detected to have eluted from the affinity gel, the cell lysate was diluted 2-fold in to lysis buffer before binding to the M2 affinity gel at 4°C overnight. The gel was pelleted by centrifugation, the supernatant was again kept for dot blot analysis and the gel washed with TBS until to A_{280} reached 0.05. Any bound protein was eluted from the gel by incubation with 0.1 M glycine pH 3.5 with gentle rocking at room temperature for 15 minutes. The gel was again centrifuged and the eluted proteins were assayed for FLAG-content via dot blot.

2.20 Site-directed mutagenesis

Site-directed mutagenesis (SDM) was performed using the Agilent Quik Change II mutagenesis kit (Agilent Technologies, Cheshire, UK). Primers were designed using Agilent Primer Design software and synthesised by Life Technologies Ltd, (Paisley, UK).

Mutagenesis reactions were optimised from the initial manufacturer's instructions, with the addition of 5% DMSO to prevent the formation of primer secondary structures. Mutagenesis conditions were as follows:

- 5 µl of 10 x reaction buffer
- X µl of pET22b/STII/Smp24 plasmid (to add ~45 ng)
- 1.25 µl forward primer (100 ng/µl)
- 1.25 µl reverse primer (100 ng/µl)
- 1 µl dNTP mix
- 2.5 µl dimethyl sulfoxide (DMSO)
- dH_2O to a final volume of 50 µl
- 1 µl *PfuUltra* High Fidelity DNA polymerase (2.5 U/µl)

Amplification was performed on a Techne TC-3000 PCR amplifier under the conditions stated in table 2.4.

Table 2.4: PCR cycling conditions for site-directed mutagenesis

Segment	Cycles	Temperature	Time
1	1	95°C	30 seconds
2	16	95°C	30 seconds
		55°C	1 minute
		68°C	6 minutes

Following amplification, a restriction digest was performed. 1 µl of *Dpn*I restriction enzyme (10 U/µl) was added to each amplification reaction, mixed, centrifuged via micro-centrifuge for 1 minute and then incubated at 37°C for 2 hours.

For the transformation, 2 µl of *Dpn*I treated DNA (the plasmid with the introduced mutation) was added to a 50 µl aliquot of XL1-Blue cells and incubated on ice for 30 minutes before heat-shocking the samples at 42°C for 45 seconds and re-incubating on ice for 2 minutes. 500 µl of S.O.C. media (2% tryptone, 0.5% yeast extract, 10 mM NaCl, 2.5 mM KCl, 10 mM $MgCl_2$, 10 mM $MgSO_4$, 20mM glucose) pre-heated to 42°C was added to the transformation reaction and incubated at 37°C for 1 hour with moderate shaking (225-250 rpm). 250 µl of reaction was added to an LB agar plate containing 100 µg/ml ampicillin and incubated overnight at 37°C for a minimum of 16 hours.

3

Elucidating the relationship between structure and antimicrobial activity of AMPs from venom

3.1 Introduction

With the ever-increasing development of resistance to conventional antibiotics, there is an urgent need to develop novel compounds for infection management and treatment (Ciumac *et al.* 2019). As such, antimicrobial peptides (AMPs) are attracting increased therapeutic interest with a long-term aim of optimising the peptides to enhance potency whilst delivering safe therapeutics with minimised risk of antimicrobial resistance (AMR) development (Schmidtchen *et al.* 2014). There are currently 60 Food and Drug Administration (FDA) approved peptide drugs, with a further 140 candidates in various phases of clinical trials, highlighting the potential for novel antimicrobial peptide-based drug development (Hazam *et al.* 2019). Pharmaceutical companies are making efforts to commercialise AMPs (Alencar-Silva *et al.* 2018).

Despite the promising nature of peptide-based antimicrobial drugs, factors limiting their potential utility as therapeutic agents include a limited spectrum of activity, low cell-membrane permeability and low oral-bioavailability (Hazam *et al.* 2019). Approaches are being taken to design novel AMPs, including peptide truncation, and deletion and substitution of amino acids from the peptide chain (Harrison *et al*., 2016a; Hilpert *et al*., 2006; Rathinakumar *et al*., 2009). Structure-activity relationship studies can be used to systematically modify naturally occurring peptides or design new synthetic peptides *de novo* to determine the relationship between structure and function (Torres *et al.* 2019). The overall goal of this approach is to produce improved AMPs with enhanced antimicrobial activity and reduced mammalian cytotoxicity.

Over 5000 AMPs have been identified to date (Fan *et al.* 2016), with over 40 peptides being biologically categorised from scorpion venom alone (Harrison *et al.* 2014). Some of the peptides demonstrate strong antimicrobial activity whilst others demonstrate more species specific antimicrobial activity (Harrison *et al.* 2014, Miyashita *et al.* 2017, Li *et al.* 2019a).

Although AMPs demonstrate structural diversity, they are commonly defined as short (10-50 amino acids), cationic (+2 to +9) and have been classified in to three main groups. Linear peptides which form alpha-helices, cysteine-rich peptides

which contain one or more disulphide bonds and peptides with an over-representation of one or two amino acids (Hancock and Lehrer 1998, Zasloff 2002), such as glycine, proline, tryptophan or histidine (Koehbach and Craik 2019). As AMPs are biological molecules, some of the peptides are derived from larger pre-cursor proteins, which consist of a signal peptide, prosequence and a mature peptide (Abdel-Rahman *et al.* 2013, Kim, Go, *et al.* 2018).

Four α-helical antimicrobial peptides (Smp13, Smp24, Smp43 and Smp76) have been characterised from the venom of the Egyptian scorpion *Scorpio maurus palmatus* (Abdel-Rahman *et al*., 2013). Of these four peptides, Smp24 and Smp43 demonstrated broad-spectrum antimicrobial activity (Harrison *et al*., 2016). Smp24 is a 24-amino acid peptide carrying a charge of +3 and shares 54% sequence homology with Pandinin 2, an AMP from the venom of the scorpion *Pandinus imperator*. Smp24 displays cytotoxic and haemolytic activity which in its native form, decreases the therapeutic application of the peptide. Smp43 is a 43-amino acid peptide, which carries a charge of +4 and has broad-spectrum antimicrobial activity, though not as a potent as the sister peptide Smp24, and a more favourable cytotoxicity profile (Harrison *et al*., 2016a) . Both peptides are of therapeutic interest, Smp24 for its broad-spectrum antimicrobial activity and Smp43 for its lower level of haemolysis and cytotoxicity compared with Smp24.

3.2 Study aims

The experiments in this chapter aim to improve the antimicrobial activity of Smp24 and Smp43. Structural modifications were performed on both peptides by introducing single, double or triple amino acid substitutions and determining the effect the structural changes had on the antimicrobial function of the peptides.

This chapter also aims to investigate the mechanism of action of the modified (daughter) peptides compared with the native peptides using homology modelling and structural investigation using circular dichroism (CD) spectroscopy. Successful candidate molecules for further development in the clinical setting have been identified and potential further modifications will be made.

3.3 Experimental design

The two peptides used within this study (figure 3.1) have been modified on the basis of improving the antimicrobial activity. Single amino acid substitutions are a common methodology for investigating the relationship between structure and function (Zhu, Dong, *et al.* 2014) with strategies varying between research groups. A systematic approach to mutagenesis is required to cover as much of the sequence space as possible. Previously, increasing the charge of antimicrobial peptides has been linked with increased antimicrobial activity (Huang *et al.* 2015, Torres *et al.* 2019).

Helical wheel diagrams can be used to display the sequence of helical peptides, in this case Smp24 and Smp43. Helical wheels present the theoretical structure of alpha-helical peptides and how the helix “stacks” when looking down through the different turns of the helix. This enables the clusters of amino-acids to be visualised, to determine if the peptide adopts an area of hydrophobicity, hydrophilicity and charge (amphipathic structure). This information can be used to determine how to enhance the peptides by increasing the amphipathic structure via site-directed mutagenesis to introduce single amino acid substitutions.

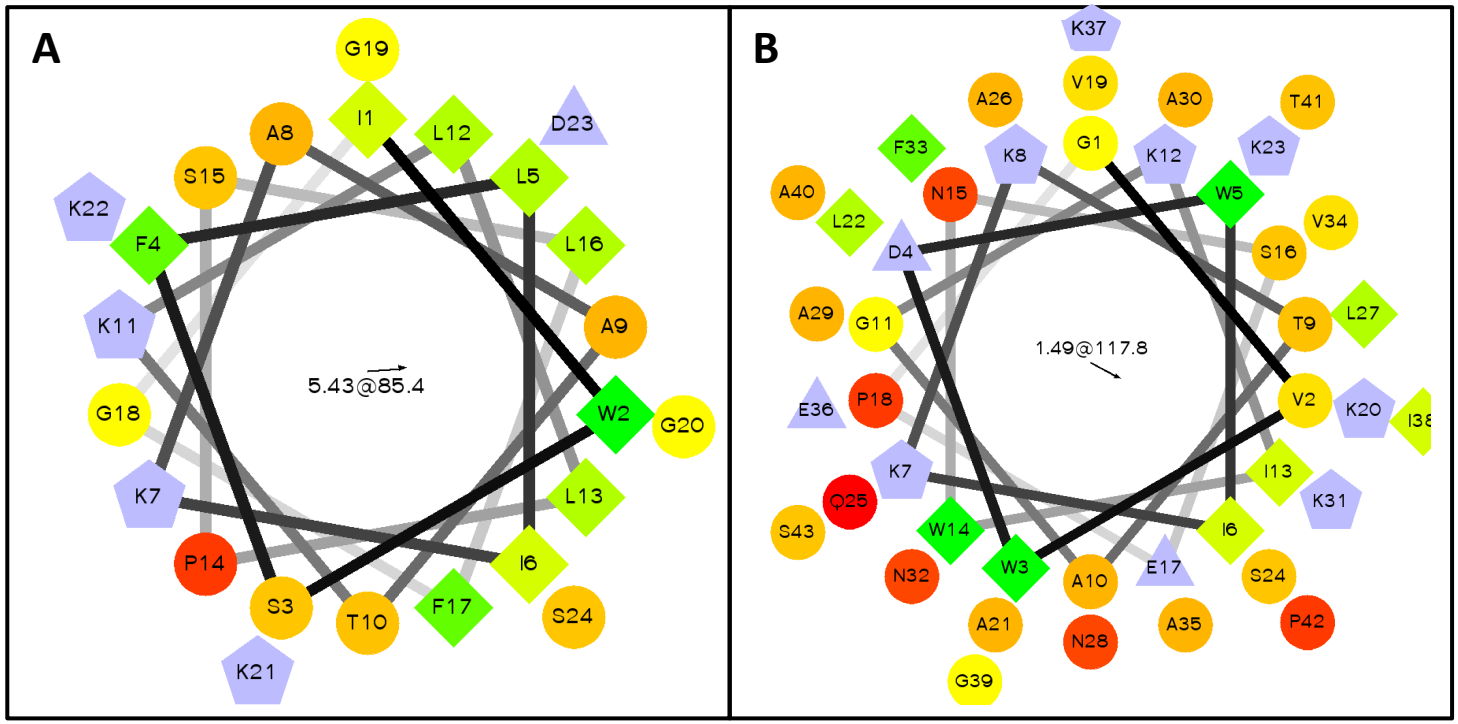

Figure 3.1: Helical wheel projections. Helical wheel diagrams were produced for Smp24 (A) and Smp43 (B) using the rzlab software from the University of California (www.rzlab.ucr.edu). Hydrophilic (circles), hydrophobic (diamonds), potentially positively charged (pentagons), potentially negatively charged (triangles). Hydrophilicity is depicted proportionally by a red-orange colour scheme, with red symbolising the greatest hydrophilic (uncharged). Hydrophobicity is shown using a green-yellow colour scheme with green being the most hydrophobic fading proportionally to yellow (zero hydrophobicity). Charged residues are light blue.

A strategy was taken to substitute serine residues (polar uncharged) for lysine residues (positively charged) to increase the overall charge of the peptides by +1. This methodology was used by (Huang *et al.* 2015) which determined increasing the charge of a porcine antimicrobial peptide resulted in increased antimicrobial activity. As such, this formed the basis for the initial mutagenesis strategy for both Smp 24 and Smp43.

Alanine scanning is a methodology commonly implemented to investigate the side chains responsible for binding and activity (Jamieson *et al*., 2013; Torres *et al*., 2019). Tryptophan residues have been demonstrated to be important for pore formation (Travkova *et al.* 2017), an approach was taken to substitute tryptophan residues for alanine across both peptides. The role of tryptophan residues in the antimicrobial peptide Pandinin-2, which shares sequence homology with Smp43, was demonstrated in a study by (Ramírez-Carreto *et al.* 2015). The substitution of tryptophan residues for alanine residues resulted in a loss of antimicrobial function. Due to the high sequence homology between Pandinin-2 and Smp43 (70%), it was an interesting research direction to determine the role of tryptophan residues in the Smp peptides. As such this could provide structural and functional information as to whether peptides with similar sequence homologies can be mutated using the same strategy and yield similar results.

The mutation strategies for the peptides are shown in figure 3.2.

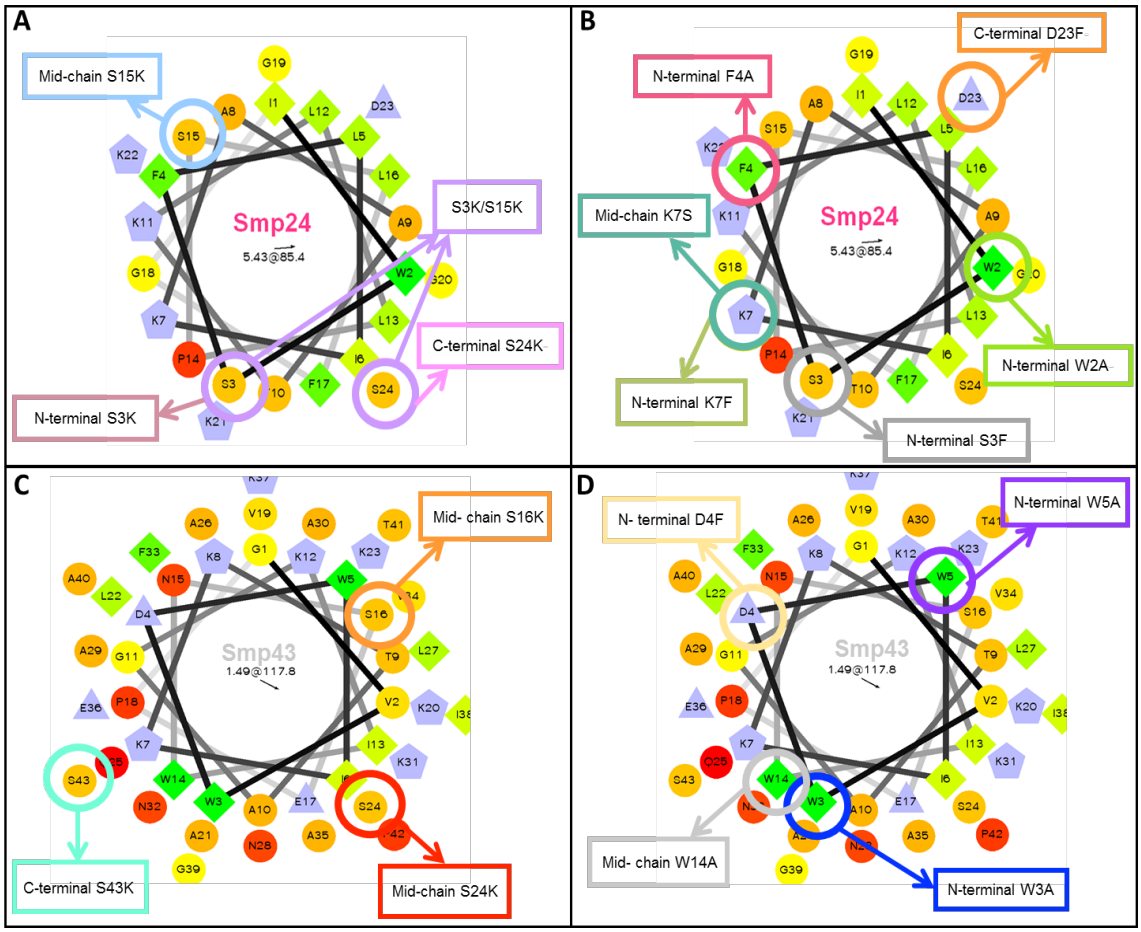

Figure 3.2: Mutation strategy for scorpion AMPs. Modifications were made to increase the charge of Smp24 (A) and Smp43 (C). Modifications were also made to increase the hydrophobicity of Smp24 (B) and Smp43 (D).

In total, 10 modifications of Smp24 were produced and 8 modifications of Smp43 were produced. A double charge modification of Smp24 (S3K/S15K) was produced to determine if charge could be increased to produce more antimicrobial activity or if charge could ultimately become a limiting factor.

A triple alanine knockout of Smp43 (W3A/W5A/W14A) was produced to determine whether tryptophan residues were essential for function following initial single substitutions by alanine scanning. Aspartic acid residues (D) were

substituted for phenylalanine (F) to simultaneously increase the charge and hydrophobicity of the peptides.

Prior to peptide production, the charge, stability, PI and grand average of hydropathy (GRAVY) of the peptides were calculated using the ProtParam tool at https://web.expasy.org/protparam/.

3.4 Results

The peptide sequences and induced changes to the charge, isoelectric point (PI) and hydrophobicity are shown in table 3.1 for Smp24 variants and table 3.2 for Smp43 derived peptides. Isoelectric point is the pH at which a protein has no net charge; significant changes to the PI can affect the charge of the peptide at physiological conditions. Proteins carry a positive charge at pH values lower than the PI, in the case of Smp24 and Smp43, the peptides are positively charged at physiological pH. Hydrophobicity is displayed as the GRAVY, which is calculated by adding the hydropathy value for each amino acid residue and dividing by the length of the peptide (Kyte and Doolittle 1982). Hydrophobicity scores below 0 are more likely globular (hydrophilic) and scores above 0 are more likely membranous (hydrophobic) (Maeda *et al.* 2012). Therefore, the higher the GRAVY score, the more hydrophobic the peptide.

3.4.1 Peptide sequences

Table 3.1: Sequence and parameter data for Smp24 and derived modifications.

Peptide	Charge	GRAVY	Molar Mass (Da)	pI	Sequence
Smp24	+3	0.31	2578	10.0	IWSFLIKAATKLLPSLFGGGKKDS
Smp24 W2A	+3	0.43	2462	10.0	I**A**SFLIKAATKLLPSLFGGGKKDS
Smp24 S3F	+3	0.46	2638	10.0	IW**F**FLIKAATKLLPSLFGGGKKDS
Smp24 S3K	+4	0.18	2619	10.2	IW**K**FLIKAATKLLPSLFGGGKKDS
Smp24 S3K/S15K	+5	0.05	2573	10.3	IW**K**FLIKAATKLLP**K**LFGGGKKDS
Smp24 F4A	+3	0.27	2502	10.0	IWS**A**LIKAATKLLPSLFGGGKKDS
Smp24 K7S	+2	0.44	2537	9.7	IWSFLI**S**AATKLLPSLFGGGKKDS
Smp24 K7F	+2	0.59	2597	9.7	IWSFLI**F**AATKLLPSLFGGGKKDS
Smp24 S15K	+4	0.18	2619	10.2	IWSFLIKAATKLLP**K**LFGGGKKDS
Smp24 D23F	+4	0.58	2610	10.5	IWSFLIKAATKLLPSLFGGGKK**F**S
Smp24 S24K	+4	0.18	2619	10.2	IWSFLIKAATKLLPSLFGGGKKD**K**

Amino acid modifications are highlighted in **bold**.

Table 3.2: Sequence and parameter data for Smp43 and derived modifications.

Peptide	Charge	GRAVY	Molar Mass (Da)	PI	Sequence
Smp43	+4	-0.32	4654	9.9	GVWDWIKKTAGKIWNSEPVKALKSQALNAAKNFVAEKIGATPS
Smp43 W3A	+4	-0.25	4539	9.9	GV**A**DWIKKTAGKIWNSEPVKALKSQALNAAKNFVAEKIGATPS
Smp43 D4F	+5	-0.17	4686	10.1	GVW**F**WIKKTAGKIWNSEPVKALKSQALNAAKNFVAEKIGATPS
Smp43 W5A	+4	-0.25	4539	9.9	GVWD**A**IKKTAGKIWNSEPVKALKSQALNAAKNFVAEKIGATPS
Smp43 W14A	+4	-0.25	4539	9.9	GVWDWIKKTAGKI**A**NSEPVKALKSQALNAAKNFVAEKIGATPS
Smp43 W3A/W5A/W14A	+4	-0.13	4310	9.9	GV**A**D**A**IKKTAGKI**A**NSEPVKALKSQALNAAKNFVAEKIGATPS
Smp43 S16K	+5	-0.39	4695	10.0	GVWDWIKKTAGKIWN**K**EPVKALKSQALNAAKNFVAEKIGATPS
Smp43 S24K	+5	-0.39	4695	10.0	GVWDWIKKTAGKIWNSEPVKALK**K**QALNAAKNFVAEKIGATPS
Smp43 S43K	+5	-0.39	4695	10.0	GVWDWIKKTAGKIWNSEPVKALKSQALNAAKNFVAEKIGATP**K**

Amino acid modifications are highlighted in **bold**.

The results of the charge modifications on both peptides yielded peptides with decreased GRAVY scores and thus made the peptides more hydrophilic. The most hydrophilic peptide for Smp24 was the S3K/S15K modification, which carried the highest charge. The increases in charge on Smp43 did increase the hydrophilicity of the peptides but to a lesser extent than the effect observed in Smp24.

All of the hydrophobic mutations introduced to both peptides increased the GRAVY score. For the most part, the hydrophobic mutations were performed without altering the charge properties of the peptides; the two exceptions to this are the K7F and K7S modifications of Smp24 which reduced the charge of the peptide to +2 due to the substitution of the positively charged lysine residue for uncharged residues.

3.4.2 Minimum inhibitory concentrations and Minimum bactericidal concentrations

3.4.2.1 Smp24 antimicrobial activity

The minimum inhibitory concentrations (MICs) of Smp24 and derived daughter peptides were determined by a broth microdilution method (Andrews 2001). Peptides were assayed in the range of 0 - 512 µg/ml, with the MIC defined as the lowest concentration of AMP which caused inhibition of bacterial growth. Strains were as follows: *Escherichia coli* JM109, *Pseudomonas aeruginosa* H085180216 and *Staphylococcus aureus* SH1000.

In addition to the inhibitory effects of the peptides, it was important to investigate the mechanistic effects of the peptides by determining if the peptides were bacteriostatic or bactericidal. The bactericidal activity of all the peptides was investigated by inoculation of MH agar with 5 µL aliquots from the MIC well plate. The minimum bactericidal concentration (MBC) was defined as the concentration which resulted in no growth of bacteria on the agar plate.

To determine the therapeutic potential of the modified peptides, the MICs were to be compared with two commercially available lipopeptide antibiotics (polymyxin B and daptomycin).

The results for MIC and MBC determination of Smp24 and the derived modifications are shown below in table 3.3.

Table 3.3: Antimicrobial activity of Smp24 and modified peptides as determined by broth microdilution assay and bactericidal assay.

Peptide	Charge	GRAVY	MIC (µg/ml)			MBC (µg/ml)		
			E. coli	*P. aeruginosa*	*S. aureus*	*E. coli*	*P. aeruginosa*	*S. aureus*
Smp24	+3	0.31	32	64	8	32	64	8
Smp24 W2A	+3	0.43	64	128	32	64	256	64
Smp24 S3F	+3	0.46	32	64	16	64	128	64
Smp24 S3K	+4	0.18	1	32	0.5	8	128	1
Smp24 S3K/S15K	+5	0.05	16	16	16	16	32	16
Smp24 F4A	+3	0.27	32	128	16	64	256	16
Smp24 K7S	+2	0.44	64	128	16	128	256	32
Smp24 K7F	+2	0.59	>512	>512	>512	>512	>512	>512
Smp24 S15K	+4	0.18	8	32	4	8	32	8
Smp24 D23F	+4	0.58	32	64	32	32	64	32
Smp24 S24K	+4	0.18	8	32	4	8	128	8
Daptomycin	-6	-1.93	>512	>512	4	>512	>512	8
Polymyxin B	+5	nc	2	2	32	4	8	64

nc = not calculable due to the mixed population of polymyxins

3.4.2.2 Smp24 microbial inhibition

The most potent antimicrobial activity was demonstrated by the S3K modification, which resulted in a 32-fold increase in bacterial inhibitory activity to 1 µg/ml against *E. coli* and a 16-fold increase in inhibition to 0.5 µg/ml against *S. aureus.* Despite the dramatic increase in activity against *E. coli* and *S. aureus*, only a 2-fold increase was observed for anti-Pseudomonal activity, with an MIC of 32 µg/ml. In contrast, the greatest decrease in antimicrobial activity was observed for the K7F modification which showed no activity at the concentrations tested against any of the organisms in this study.

All of the single charge modifications yielded peptides with increased antimicrobial activity against the Gram positive and Gram negative isolates tested, with the peptides showing the greatest increases in activity against *E. coli.* Both the S15K and S24K modifications resulted in a 4-fold increase in anti-*E. coli* activity with an MIC of 8 µg/ml and a 2-fold increase in anti-Staphylococcal and anti-Pseudomonal activity with MICs of 4 µg/ml and 32 µg/ml respectively.

The double charge modification S3K/S15K demonstrated an interesting anti-bacterial profile, with the same inhibitory value (32 µg/ml) observed for all isolates tested. S3K/S15K demonstrated a 2-fold increase in activity against *E. coli*, a 2-fold decrease in anti-Staphylococcal activity but demonstrated the greatest increase in anti-Pseudomonal inhibition with a 4-fold increase in activity.

The hydrophobicity modifications did not result in increased inhibitory activity against any of the isolates tested. Loss of activity was observed for the K7S, W2A and F4A modifications, which demonstrated reduced activity against the isolates tested. Two-fold reductions in activity were observed against *E. coli* (MIC 64 µg/ml) and *P. aeruginosa* (MIC 128 µg/ml) for K7S and W2A, with K7S and F4A showing a 2-fold reduction in anti-staphylococcal activity (16 µg/ml) and the W2A modification resulting in a 4-fold reduction in activity (32 µg/ml).

The D23F modification yielded a peptide with both increased charge and increased hydrophobicity. The activity of the peptide was similar to that of the

parental peptide with the exception of *S. aureus* activity which was a 4-fold decrease with an MIC of 32 µg/ml.

Daptomycin is commercially licensed for the treatment of skin infections caused by very specific Gram positive organisms (such as MRSA and vancomycin-resistant Enterococci), the inhibition data from this experiment demonstrates daptomycin is only effective against the Gram positive isolates tested. Promisingly, modified peptides derived from Smp24 showed inhibitory values equal to that of daptomycin (S15K and S24K), with the S3K modification demonstrating greater activity.

Polymyxin B (PMB) is primarily used for the treatment of resistant Gram negative infections, but the results of this assay demonstrate the antibiotic also possesses activity against some Gram positive species. Only one of the modified peptides demonstrated activity greater than PMB against Gram negative species, which was S3K against *E. coli.* All of the modifications of Smp24 except K7F and native Smp24 demonstrated anti-Staphylococcal activity equal to or greater than that of PMB.

3.4.2.3 Smp24 bactericidal activity

Unsurprisingly, no detectable bactericidal activity was observed with the K7F modification, which held no inhibitory activity. All of the charge modifications resulted in increased bactericidal activity against *E. coli*; despite the 32-fold increase in inhibitory activity of S3K, only a 4-fold increase in bactericidal activity was observed, a change equal to that of the other two single lysine substituted peptides. Against *S. aureus* however, an 8-fold increase in bactericidal activity was seen by S3K and the MBC value (1 µg/ml) was the lowest value observed across all modifications. Despite the increased inhibitory activity S3K and S24K against *P. aeruginosa,* both peptides demonstrated a 2-fold reduction in bactericidal activity with an MBC of 128 µg/ml.

With the exception of D23F (64 µg/ml), all of the hydrophobic modifications demonstrated reduced bactericidal activity against *P. aeruginosa* and *E. coli*

compared with native Smp24. The greatest loss of activity against *E. coli* was a 4-fold reduction by K7S (128 µg/ml), whilst K7S, W2A and F4A all demonstrated 4-fold reduction in bactericidal activity against *P. aeruginosa* (256 µg/ml). All of the hydrophobic modified peptides demonstrated reduced bactericidal activity against *S. aureus*, with the greatest loss of activity being an 8-fold reduction by W2A and S3F (64 µg/ml).

With the exception of *B. subtilis*, the lipopeptide antibiotics demonstrated a similar pattern to that observed with the AMPs with higher MBC values than the MIC. Polymyxin B demonstrated potency against *E. coli* at 4 µg/ml, a value which was not met by any of the peptides in the study, with the lowest MBC against *E. coli* being 8 µg/ml. Similarly, none of the peptides demonstrated potency against *P. aeruginosa* equal to that of PMB. Against *S. aureus*, all of serine-lysine substitutions demonstrated lethality equal to that of daptomycin. With the exception of K7S and K7F, all of the Smp24 modifications had lethality equal to or greater than that of PMB against *S. aureus*.

These results highlight that whilst some of the peptides have activity lower than that of the commercial peptide antibiotics, like antibiotics, the specificity of the peptides could be restricted. Some of the peptides demonstrated increased potency against some bacterial classes compared with others, such as S3K which demonstrated increased potency against *E. coli* and *S. aureus* but not *B. subtilis.*

3.4.2.4 Comparison between MIC and MBC

To determine the efficacy of the peptides to kill bacteria relative to the concentration required to inhibit growth, a ratio between the MIC and MBC was calculated by dividing the MBC by the MIC (table 3.4).

Table 3.4: MIC: MBC ratios for Smp24 and derived modifications

Peptide	Charge	GRAVY	MIC:MBC ratio		
			E. coli	*P. aeruginosa*	*S. aureus*
Smp24	+3	0.31	1	1	1
Smp24 W2A	+3	0.43	1	2	2
Smp24 S3F	+3	0.46	2	2	4
Smp24 S3K	+4	0.18	8	4	2
Smp24 S3K/S15K	+5	0.05	1	2	1
Smp24 F4A	+3	0.27	2	2	1
Smp24 K7S	+2	0.44	2	2	2
Smp24 K7F	+2	0.59	*NC	*NC	*NC
Smp24 S15K	+4	0.18	1	1	2
Smp24 D23F	+4	0.58	1	1	1
Smp24 S24K	+4	0.18	1	4	2
Daptomycin	-6	-1.93	*NC	*NC	2
Polymyxin B	+5	nc	2	4	2

nc - not calculable due to the mixed population of polymyxins; *NC - not calculable due to the values exceeding the limit of detection of the study

The results in table 3.4 display the increased concentration required to kill bacteria relative to the concentration to inhibit growth, e.g. the MIC of S3K is 1 µg/ml for *E. coli* but the MBC is 8 µg/ml, equal to an 8 fold increase in concentration required for bactericidal activity relative to inhibition. The differences observed could indicate mechanistic changes arising as a result of structural changes, such as a change in the pore-forming abilities of the modified peptides relative to the parental peptide.

For Smp24, all of the modifications resulting in increased charge yielded peptides with enhanced bacterial inhibition when compared with the parental peptide. For native Smp24, the MBC was equal to the MIC for all of the bacterial isolates studied.

The antimicrobial profile of Smp43 and the daughter peptides was determined (table 3.5).

3.4.3 Smp43 antimicrobial activity

Table 3.5: Antimicrobial activity of Smp43 and modified peptides as determined by broth microdilution assay.

Peptide	Charge	GRAVY	MIC (µg/ml)				MBC (µg/ml)			
			E. coli	*P. aeruginosa*	*S. aureus*	*B. subtilis*	*E. coli*	*P. aeruginosa*	*S. aureus*	*B. subtilis*
Smp43	+4	-0.32	32	64	>512	8	32	64	>512	8
Smp43 W3A	+4	-0.25	16	32	>512	16	16	128	>512	16
Smp43 D4F	+5	-0.17	64	32	>512	8	64	32	>512	16
Smp43 W5A	+4	-0.25	8	64	>512	8	8	64	>512	8
Smp43 W14A	+4	-0.13	4	64	>512	8	8	128	>512	8
Smp43 W3A/W5A/W14A	+4	-0.13	>512	>512	>512	NT*	>512	>512	>512	NT*
Smp43 S16K	+5	-0.39	32	32	>512	16	32	64	>512	16
Smp43 S24K	+5	-0.39	32	16	256	4	64	64	512	8
Smp43 S43K	+5	-0.39	16	16	>512	8	32	32	>512	8
Daptomycin	-6	-1.93	>512	>512	4	8	>512	>512	8	8
Polymyxin B	+5	nc	2	2	32	2	4	8	64	2

Nc - not calculable due to the mixed populations of polymyxins; NT* - not tested.

3.4.3.1 Smp43 microbial inhibition

The effects of charge modifications on Smp43 were less effective than the modifications observed in Smp24. This could be attributed to differences in structure between the two peptides. Whilst Smp24 and Smp43 are both derived from the venom of *Scorpio maurus palmatus,* the peptides assemble differently. Smp24 adopts a single alpha helix, whereas Smp43 adopts a di-helical protein structure (see sections 5.4.2 and 5.4.3).

None of the peptides demonstrated activity against *S. aureus*, except S24K which had an MIC of 256 µg/ml. Due to the lack of activity against *S. aureus*, the peptides were assayed against *B. subtilis* subsp *subtilis* (NCIMB 3610) to determine if the peptides held activity against Gram positive organisms. All of the peptides demonstrated anti-Bacillus activity, suggesting the spectrum of activity is more restricted for Smp43 compared with Smp24. The S24K modification was the only peptide which demonstrated increased activity against *B. subtilis* with an MIC of 4 µg/ml.

S24K and S43K modifications resulted in significant 4-fold increases in anti-Pseudomonal activity resulting in MICs of 16 µg/ml. The peptides with single tryptophan to alanine substitutions demonstrated increased activity compared with the parental peptide. The greatest increase in activity was observed for the W14A modification which demonstrated an 8-fold increase in activity against *E. coli* to gain an MIC of 4 µg/ml. Two-fold increases in activity were observed for the W3A and D4F modifications against *P. aeruginosa*, but these modifications also resulted in a 2-fold decrease in activity against *E. coli* (D4F) and *B. subtilis* (W3A).

The triple tryptophan alanine modified peptide demonstrated no detectable antimicrobial activity across the three isolates tested. The antimicrobial activity assessment of the peptide was restricted due to the small quantity of peptide synthesised and therefore the antimicrobial activity could not be assessed against *B. subtilis*.

All of the peptides except S16K and W3A had anti-Bacillus activity equal to that of daptomycin, with S24K Smp43 demonstrating a lower MIC at 4 µg/ml. None of the Smp43 modifications resulted in anti-Staphylococcal activity equal to or greater than that of daptomycin.

When comparing the activity of Smp43 and derivatives with PMB, none of the peptides demonstrated antimicrobial activity at the same range of inhibition as PMB.

3.4.3.2 Smp43 bactericidal activity

The charge modifications had little effect on the bactericidal activity of Smp43, with the peptides mostly retaining the bactericidal activity demonstrated by the parental peptide. The exceptions to this are S24K with a 2-fold decrease against *E. coli (*64 µg/ml) and detectible bactericidal activity against *S. aureus* (512 µg/ml). S43K demonstrated a 2-fold increase in activity against *P. aeruginosa* (32 µg/ml) and S16K with a 2-fold decrease in bactericidal activity against *B. subtilis* (16 µg/ml).

The hydrophobicity modifications had a more significant outcome, with increased bactericidal activity against both the Gram negative isolates tested. The greatest increases in activity were observed for W5A and W14A modifications which resulted in 4-fold increased activity (8 µg/ml) against *E. coli.* A 2-fold reduction in bactericidal activity against *P. aeruginosa* was observed for W3A and W14A (128 µg/ml), whilst a 2-fold increase in activity was observed for D4F (32 µg/ml). Only two of the hydrophobicity modifications resulted in a 2-fold reduction in activity against *Bacillus*, which are W3A and D4F.

Many of the Smp43 modified peptides had MBC values equal to that of daptomycin against *B. subtilis*, but none of the peptides demonstrated lytic activity against S*. aureus* equal to that of daptomycin. Polymyxin B was more potent than the modified Smp43 peptides used within this study, but the W5A and W14A modifications demonstrated MBC's within a 2-fold range of PMB. This is a

promising result, as the peptide is close to a therapeutic range of a commercially licensed treatment.

3.4.3.3 MIC: MBC ratios for Smp43

The bactericidal activity of native Smp43 is equal to the MIC value for all the isolates tested in this study. This did not remain consistent with the modified peptides. Despite showing increased inhibitory activity, not all of the peptides demonstrated an increase in bactericidal activity compared with Smp43 (table 3.6).

Table 3.6: MIC: MBC ratios for Smp43 and derived modifications

Peptide	Charge	GRAVY	MIC:MBC ratio			
			E. coli	*P. aeruginosa*	*S. aureus*	*B. subtilis*
Smp43	+4	-0.32	1	1	*NC	1
Smp43 W3A	+4	-0.25	1	4	*NC	1
Smp43 D4F	+5	-0.17	1	1	*NC	2
Smp43 W5A	+4	-0.25	1	1	*NC	1
Smp43 W14A	+4	-0.13	2	2	*NC	1
Smp43 W3A/W5A/W14A	+4	-0.13	*NC	*NC	*NC	NT*
Smp43 S16K	+5	-0.39	1	2	*NC	1
Smp43 S24K	+5	-0.39	2	4	2	2
Smp43 S43K	+5	-0.39	2	2	*NC	1
Daptomycin	-6	-1.93	*NC	*NC	*NC	1
Polymyxin B	+5	nc	2	4	2	1

nc - not calculable, *NC - not calculable due to values exceeding detection limits of the assay, NT* - not tested

The results from the table above demonstrate the concentration of the peptides required to kill bacteria relative to the concentration required to inhibit growth. Despite the MBC being higher than the MIC for some of the modifications, peptides were produced which overall showed improved activity compared with native Smp43. As shown in the antimicrobial assays across all of the modified peptides, there are wide differences in MIC values, with the lower MIC values typically observed against Gram positive bacteria, which mimics the activity observed by other α-helical peptides derived from scorpion venom (Bao *et al*., 2015; Bea *et al*., 2015; Miyashita *et al*., 2017b).

3.5 Anti-biofilm activity

In addition to the antimicrobial assays performed, the anti-biofilm properties of the peptides were investigated as per the methods highlighted in chapter 2, section 2.5. Briefly, biofilms were grown on peg lids which were transferred in to a "challenge plate" containing doubling dilutions of AMPs in the range of 0 - 512 µg/ml (table 3.7).

Table 3.7: Anti-biofilm activity of Smp24 and Smp43 as defined by MBIC and MBEC values

		Biofilm (µg/ml)		Planktonic (µg/ml)	
Peptide	**Strain**	**MBIC**	**MBEC**	**MIC**	**MBC**
Smp24	*E. coli* EC2	64	256	8	16
Smp24	*E. coli* JM109	32	256	32	32
Smp43	*E. coli* EC2	8	256	8	64
Smp43	*E. coli* JM109	32	256	32	32
Daptomycin	*E. coli* EC2	>512	>512	>512	>512
Daptomycin	*E. coli* JM109	>512	>512	>512	>512
Polymyxin B	*E. coli* EC2	32	64	2	4
Polymyxin B	*E. coli* JM109	8	>512	2	4

The anti-biofilm activity of the parental peptides was assayed against an *E. coli* laboratory strain (JM109) and clinical strain (EC2). EC2 is an uropathogenic *E. coli* (UPEC) strain which demonstrates antibiotic resistance against ampicillin and trimethoprim which are commonly prescribed antibiotics for urinary tract

infections (UTIs). EC2 has been previously classified as a biofilm-forming strain (Henly *et al.* 2019) and was chosen for comparison of the anti-biofilm activity of the peptides against laboratory and clinical strains.

3.5.1 Biofilm vs planktonic MICs

The MBIC for both of the peptides was markedly lower than the concentration required for eradicating the biofilm against both isolates tested. Interestingly, whilst a 2-fold increase in concentration was required to inhibit the growth of the biofilm on the biofilm-forming strain for Smp24, the MBEC remained constant. Against EC2, there was a 4-fold difference in concentration required for eradication of the biofilm compared with inhibition, whereas as an 8-fold difference was observed for JM109. When comparing the MBIC to the planktonic MIC, the values remained constant at 32 μg/ml for both AMPs against *E. coli* JM109. This could be attributed to the pore-formation mechanism of action of the AMPs, which could be uninhibited by the complexity of a biofilm in terms of growth inhibition. Differences were observed when comparing the concentration required to eradicate biofilm growth which was an 8-fold increased concentration.

Smp43 demonstrated an enhanced ability to inhibit biofilm formation compared with Smp24, but the concentration required to eradicate the biofilm was the same. The lowest MBIC of the study was noted at 8 μg/ml by Smp43 against *E. coli* EC2, equal to the anti-biofilm effect of polymyxin B. The difference in MBIC between Smp24 and Smp43 could suggest mechanistic differences between the two peptides and suggest differences in the properties possessed by both peptides. Promisingly, the activity of Smp43 is superior to that of polymyxin B, whilst both held an MBIC of 8 μg/ml, the lytic activity of Smp43 was superior (256 μg/ml) as the MBEC of polymyxin B was beyond the limit of detection of the study.

3.5.2 Comparison of anti-biofilm activity of Smp24 and Smp43 with commercially available lipopeptide antibiotics

The lowest MBIC values within this study were observed by Smp43 against *E. coli* EC2 and Polymyxin B against *E. coli* JM109 both of which were 8 µg/ml. Polymyxin B demonstrated the greatest ability to eradicate biofilm growth, with an MBEC of 64 µg/ml, though this was not consistent as Polymyxin B performed worse than the Smp peptides when eradicating growth of *E. coli* JM109.

Unsurprisingly, the anti-biofilm activity of daptomycin was not detectable for the isolates tested due to the limitation of efficacy of daptomycin's spectrum of activity being limited to Gram positive pathogens.

3.6 Structural investigations: Circular Dichroism

Circular dichroism (CD) spectroscopy is a technique which can be used to determine the secondary structure of proteins with 3-dimensional insights (Li and Arakawa 2019). Briefly, 100 µM concentrations of peptides dissolved in $_{d}H_2O$ were added to a cuvette and the absorbance was read across a 190-250 nm wavelength on a JASCO J-810 spectropolarimeter (Maryland, USA). The structure of the peptides was investigated in an aqueous environment and by titration of trifluoroethanol (TFE) to a concentration of 60% to create membrane mimetic conditions. CD spectroscopy was used to determine if the induced amino acid substitutions had affected the structure of the peptides.

3.6.1 CD spectroscopy of Smp24

CD spectra were obtained for Smp24 (see chapter 2, section 2.8) and the most and least potent modified variants (S3K and K7F) to determine if the amino acid substitutions had affected the overall secondary structure of the peptides (figure 3.3).

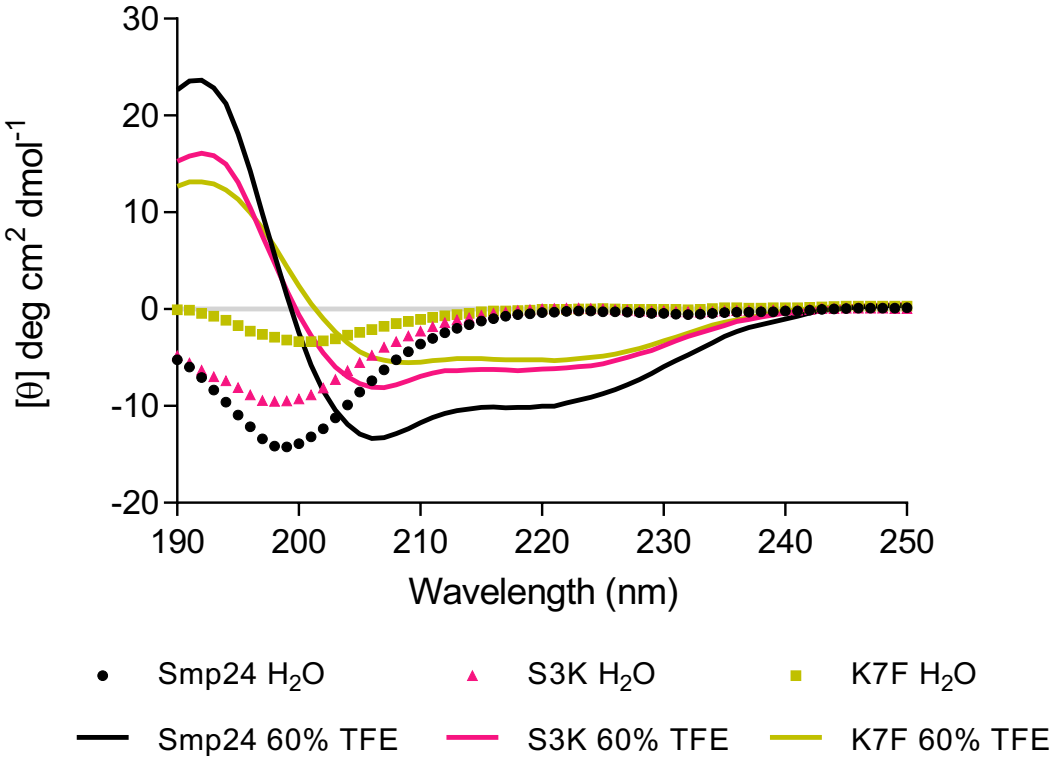

Figure 3.3: Helical propensity of Smp24, S3K and K7F in aqueous (0% TFE) and membrane mimetic (60% TFE) conditions.

As shown in figure 3.3, the peptides are disordered in an aqueous solution and adopt a helical conformation in the presence of 60% TFE, characterised by the presence of two minima around 208 and 222 nm (Kang *et al.* 2017a). There are some structural difference between the modified peptides and native Smp24, as shown by the differences in the state of the disordered peptides in aqueous solution compared with native Smp24. S3K appears to adopt a structure similar to that of Smp24, with a random coil in the presence of water and a characteristic α-helix in the presence of 60% TFE. K7F however, demonstrates some differences compared with native Smp24. The random coil demonstrates a different MRE trace compared with native Smp24 and the minima at 208 and 222 nm are less pronounced compared with Smp24 in the presence of 60% TFE.

3.6.2 TFE titration of Smp24

To further elucidate the differences in structures observed in figure 3.3, the helical propensity of the peptides was determined by the titration of TFE over a 0 to 60% percentage range. More spectra were obtained over the 0 - 30% range in order to determine the percentage at which the peptides adopt their final alpha-helices.

The results of the structural investigations by the titration of TFE for Smp24, Smp24 S3K and Smp24 K7F are shown in figure 3.4.

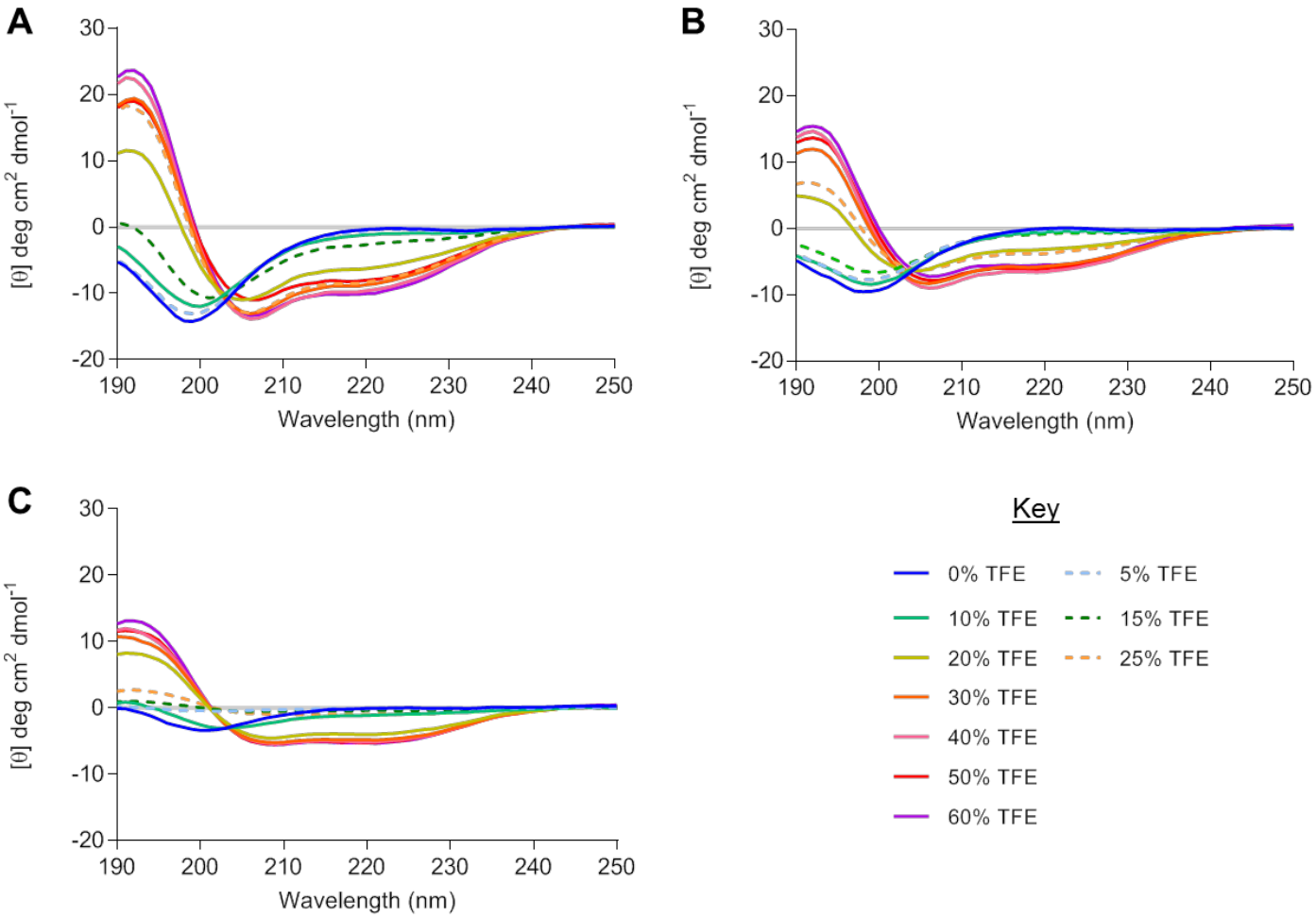

Figure 3.4: CD spectra for the titration of TFE (0-60%) for Smp24 (A), Smp24 S3K (B) and Smp24 K7F (C).

As shown in figure 3.4, the point at which the peptides adopt their final α-helices differs between the native and modified peptides. Native Smp24 adopts its α--helical structure in 25% TFE, Smp24 S3K adopts its α-helix at a higher TFE concentration (30%) and Smp24 K7F adopts α--helix at a lower concentration of TFE (20%).

3.6.3 CD spectroscopy of Smp43

CD spectra were obtained for Smp43 in the presence of 0% TFE and membrane mimetic (60% TFE) conditions (see chapter 2, section 2.8). The helical propensity of Smp43 is shown in figure 3.5.

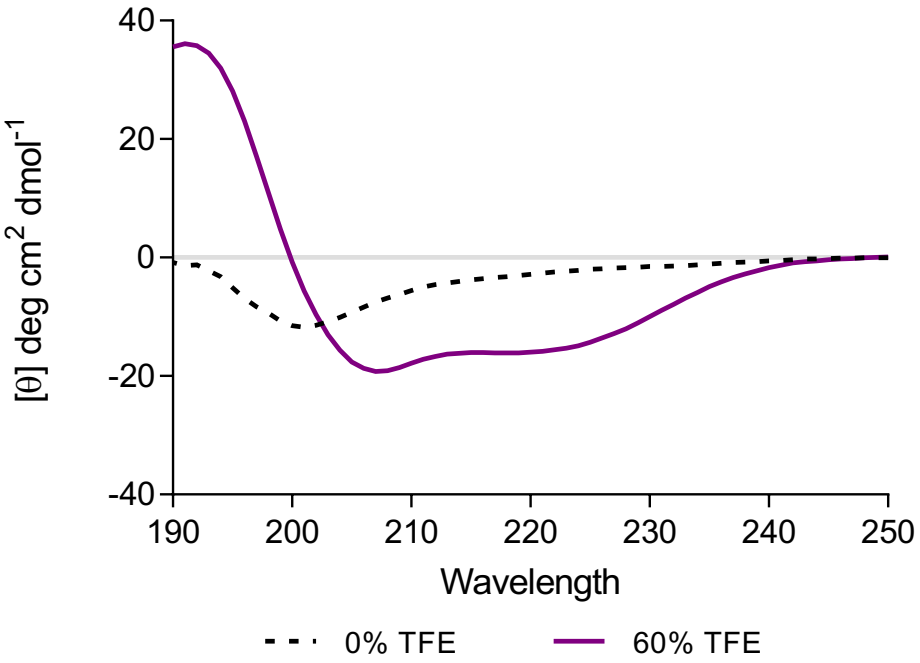

Figure 3.5: The helical propensity of Smp43 in water (0% TFE) and in membrane mimetic conditions (60% TFE).

Spectral analysis of the CD data revealed Smp43 is present as an unordered structure in aqueous conditions (H_2O) and adopts a helical structure in the presence of 60% TFE. Data analysis (Perez-Iratxeta and Andrade-Navarro 2008) revealed Smp43 held 95.39% helical content in 60% TFE.

Despite differences between Smp24 and Smp43, both peptides analysed by CD spectroscopy demonstrated a disordered structure in solution and adopted α-helical conformations in membrane mimetic environments, with the minor structural modifications resulting in small changes in helical formation. The data supports the hypothesis that peptides are disordered in solution (i.e. the extracellular environment) and adopt their final helical conformations upon interaction with the bacterial cell membrane.

3.7 Discussion

Smp24 and Smp43 have both been previously characterised in terms of biological activity (Harrison *et al*., 2016). Limited modifications have previously been performed on Smp24 in attempts to enhance the antimicrobial activity, including the truncation of Smp24 to remove the last 4 amino acid residues. The truncation was based on previous modifications to Pandinin 2 (Rodríguez *et al.* 2014a) which shares 54% sequence homology with Smp24. The truncation of Smp24 (IWSFLIKAATKLLPSLFGGG) resulted in a reduction in charge at the C-terminus to +2 and an overall 2-fold decrease in antimicrobial activity was observed against *S. aureus* and *E. coli*. Smp24 was also modified by the insertion of a glycine-valine-glycine (GVG) hinge, a modification which yielded a 2-fold decrease in potency against Gram positive species and a 4-fold reduction in activity against *Candida albicans* but retained the activity of native Smp24 against the Gram negative isolates tested (Harrison *et al*., 2016). These results highlight the effect structural changes can have on the antimicrobial activity but specific changes to the mechanism of action have not been elucidated. Whilst the mechanism of action of drugs may not be required for therapeutic licensing purposes, as demonstrated by the lack of understanding of the mode of action of daptomycin (Anderson 2008, Taylor and Palmer 2016); a greater understanding of the relationship between structure and function of AMPs could lead to the design and development of molecules with enhanced therapeutic indices.

Increases in charge have been linked to enhanced antimicrobial activity (Huang *et al.* 2015). The main lipid components of bacterial cell membranes are anionic phospholipids, such as phosphatidylglycerol (PG) and cardiolipin (CL), with the

predominant zwitterionic lipid phosphatidylethanolamine (PE) (Ciumac *et al.* 2019) which leads to an overall negative charge across the external face of the cell membrane. However, membrane composition differs between bacterial species. For example, the predominant components of *E. coli* cell membranes are PE (75%) and PG (20%) with a lower concentration of CL (5%) (Sohlenkamp and Geiger 2016, Hu and Tam 2017). The *S. aureus* membrane, however, is composed of cardiolipin (22.5%), PG (43.1%) and lysyl-PG (L-PG) (30%) (Hayami *et al.* 1979, Young *et al.* 2019) and is therefore less negative overall than the membrane of *E. coli*. The composition of the *E. coli* membrane results in an overall anionic charge, with a resting membrane potential of -220 mV during early exponential phase, which reduces to -140 mV in late exponential phase (Bot and Prodan 2010). The electrical potential across the membrane of *S. aureus* is -130 mV at pH 7.5 (Mates *et al.* 1982), making the resting membrane potential less negative than that of *E. coli.*

The overall negative charge of the outer bilayer in most models is considered to be responsible for the initial electrostatic interaction with the positively charged peptide (Torcato *et al.* 2013). Increases in the charge of AMPs increases the electrostatic binding between the peptide and cell membrane, which in turn may increase the potency of AMPs (Tossi *et al.* 2000b). This was observed in this study, as shown by the increased potency of the increased charge variants.

3.7.1 Structural differences between modified peptides

To determine the structural effect the modifications which resulted in the most and least potent antimicrobial activity, Smp24, Smp24 S3K and Smp24 K7F were analysed by CD spectroscopy. Smp24 demonstrated a disordered structure in 0 – 15% TFE and began to adopt its α-helical structure in the presence of 25% TFE, with the greatest defined helix observed in the presence of 60 – 70% TFE (conditions which mimic the cell membrane environment). Smp24 S3K demonstrated a similar structural content, with a disordered structure observed in the presence of 0 – 15% TFE, with the peptide beginning to adopt α-helical structure in the presence of 20% TFE leading to the final α-helical structure forming in the presence of 50% TFE. As Smp24 S3K adopted its helical structure

in the presence of a lower percentage of TFE, this demonstrates Smp24 S3K has a greater propensity to form an α-helical structure than native Smp24. As greater antimicrobial potency was observed for Smp24 S3K, this could be attributed to the increased ability to form α-helices due to the requirement for AMPs to adopt their final structures to exhibit antimicrobial activity (Willcox *et al.* 2008).

For Smp24 K7F the minima and maxima at 208 and 222 nm respectively are much less pronounced compared with native Smp24, suggested Smp24 K7F adopts a less defined helix. Smp24 K7F remains disordered in solution at 25% TFE, but begins to fold in to its final structure at 30% TFE. The differences in structure between native Smp24 and Smp24 K7F could provide mechanistic insights, suggesting the helical content of Smp24 is imperative for function. In the case of Smp24 K7F, a loss of helical content has resulted in a loss of antimicrobial activity.

3.7.2 Comparison of AMPs to commercially available lipopeptide antibiotics

In this study, the results of the structural modifications were compared with native peptides, but it is also important to consider the efficacy of the peptides alongside commercially available therapeutics. Daptomycin is a cyclic lipopeptide antibiotic with potent bactericidal activity against most Gram positive organisms, including vancomycin-resistant Enterococci (VRE) and methicillin-resistant Staphylococci (Galar *et al.* 2018). Whilst the mechanism of daptomycin remains unclear, it is known the mechanism involves the cytoplasmic membrane, is dependent on calcium concentration and is restricted to Gram positive bacteria (Taylor and Palmer 2016). Under broth microdilution assays, daptomycin demonstrated anti-Staphylococcal activity at an MIC of 4 μg/ml.

Although many of the peptides within this study did not demonstrate bacterial potency at similar concentrations to the lipopeptide antibiotics, there are a few candidate peptides that merit further consideration. Smp24 S3K demonstrated MIC values of 1 and 0.5 μg/ml against *E. coli* and *S. aureus* respectively. Smp24 S15K and S24K both demonstrated MIC values within a 2-fold range of

daptomycin, with MICs of 8 µg/ml for *S. aureu*s. The Smp43 modifications did not yield peptides with anti-Staphylococcal activity within an equivalent range to daptomycin, but the MIC of the S24K and W14A modifications was equal to the activity of polymyxin B. Whilst the MIC of susceptible isolates by the European Committee for Antimicrobial Susceptibility Testing (EUCAST) is usually deemed to be 2 mg/litre (2 µg/ml), this is based on colistin which has different pharmacokinetics to polymyxin B despite belonging to the same antibiotic class (Chew *et al.* 2017). A study by Sader *et al*, 2015 concluded that 41.3% of the isolates tested for MIC values against colistin and polymyxin B demonstrated higher MIC values for polymyxin B. (Albur *et al.* 2015).

3.7.3 AMPs and anti-biofilm activity

Whilst antibiotic resistance is of growing concern and new therapeutic agents are required, there is an increased observation of biofilm associated infections which contribute to 65 - 80% of all diagnosed microbial infections. Biofilms are surface-attached microbial communities able to attach to biotic or abiotic surfaces (Parrino *et al.* 2019). Biofilms are often recalcitrant to both the immune response and antimicrobial treatment, making biofilm-associated infections difficult to treat (Henly *et al.* 2019). As a result of this, new molecules are required with biofilm targeting activity. Improvements have been made to the AMPs in terms of antimicrobial activity, which is promising in the search for new antimicrobial compounds (Macià *et al.* 2018).

Several studies have reported AMPs can successfully inhibit biofilm formation. LL-73 from the cathelicidin family of AMPs showed potent inhibition of the production of biofilms by *S. aureus* at concentrations as low as 3 µg/ml (Dean *et al.* 2011) The AMP $WLBU_2$ has demonstrated anti-biofilm activity against ESKAPE (*Enterococcus faecium, Staphylococcus aureus, Klebsiella pneumoniae, Acinetobacter baumannii, Pseudomonas aeruginosa* and *Enterobacter* species) pathogens including the inhibition of growth and initial biofilm formation. In the case of $WLBU_2$, biofilm inhibition was demonstrated to be more effective than the assayed antibiotics (including colistin) at preventing biofilm formation (Lin *et al.* 2018).

The parental Smp peptides both demonstrated anti-biofilm activity, with the biofilm inhibition concentration being markedly lower than the concentration required for biofilm eradication, in keeping with other anti-biofilm studies. For example, Japonicin-2LF demonstrated an MBIC of 25 μg/ml and an MBEC of 800 μg/ml against *E. coli* biofilms (Yuan *et al.* 2019). Smp43 demonstrated greater potency than Japonicin-2LF with MBIC of 8 μg/ml against *E. coli* JM109. Both Smp24 and Smp43 demonstrated a greater ability to eradicate biofilm growth than Japonicin-2LF with MBEC values of 256 μg/ml. This highlights the potential to use the peptides as anti-biofilm agents in addition to antimicrobial compounds.

The rapid killing activity and membrane-targeting ability makes AMPs attractive molecules for antimicrobial applications, where AMPs are believed to reduce the likelihood of resistance development by bacteria. Due to this, many groups are looking at the surface immobilisation of AMPs as anti-biofilm agents (Lim and Leong 2018). Studies have demonstrated that retention of AMP secondary structure has been critical for activity and therefore the immobilisation of AMPs must be carefully considered to preserve the bactericidal activity (Willcox *et al.* 2008). As bacterial adhesion to biomaterials remains a major problem in the medical device field, the development of novel antimicrobial coatings with a reduced propensity for resistance would be worthwhile (Costa *et al.* 2011).

Future directions to investigate the anti-biofilm properties of the Smp peptides would include further screening of the compounds (particularly S3K, to ascertain if the anti-biofilm activity was more potent than that of Smp24). The incorporation of the peptides in to a coating which could potentially be used to prevent biofilm adherence on indwelling devices would also present an interesting future direction. Catheter coatings can be categorised into two groups; antifouling coatings which do not kill microbes directly but instead prevent the attachment of bacteria on the surfaces which would usually allow biofilm formation (Campoccia *et al.* 2013) and biocidal properties which are designed to kill the microbes on contact as the active compounds are not eluted from the coating (Williams and Worely 2000). The former uses steric repulsion and electrostatic repulsion to prevent the formation of conditioning films for planktonic bacteria that ultimately

form biofilms (Singha *et al.* 2017), though this could be problematic for AMP coatings due to the positive charge of the peptides.

The investigation of the anti-biofilm properties of the peptides by incorporation into a sol gel eluting the peptides into solution would be a logical next-stage approach following the observed anti-biofilm activity. Peptides could be incorporated into a sol gel and applied to the pegs of a peg lid and the abilities of the peptide sol gel to inhibit biofilm growth as per the method described in chapter 2. Alternatively, the anti-fouling properties of an AMP sol gel could be investigated by crystal violet biofilm formation assays which enable the quantification of biofilms and thus the concentration of AMP in the sol gel required to prevent biofilm formation could be determined (O'Toole 2011).

3.8 Conclusions

Both Smp24 and Smp43 demonstrate anti-biofilm activity, with biofilm inhibition being equal to the planktonic MIC, highlighting the potential for the peptides as anti-biofilm agents.

The S3K, S15K and S24K modifications to Smp24 produced peptides with enhanced antimicrobial activity compared with native Smp24. The S3K/S15K modification also demonstrated an interesting 4-fold increase in antimicrobial activity against pseudomonads. As such, these modifications are of interest for further study.

For Smp43, the W3A, W5A and W14A modifications yielded peptides with enhanced activity against *E. coli* whilst the S24K and S43K modifications resulted in increased anti-Pseudomonal activity compared with native Smp43. As such, these peptides are interesting candidates for further investigations.

Future work would involve a more intensive antimicrobial screen of the peptides of interest encompassing more bacterial strains (such as Klebsiella spp, Candida spp, clinical MRSA isolates and clinical carbapenem-resistant Enterobacteriaceae isolates). Due to cost limitations with the synthesis of

peptides by solid-phase synthesis, the antimicrobial characterisation of the peptides was restricted to two Gram positive and two Gram negative strains.

Whilst a strategy has been adopted to increase the antimicrobial properties of the peptides, it is also important to determine the effect the modifications to the peptides will have on mammalian tissues. AMPs do preferentially interact with prokaryotic membranes, but numerous venom-derived AMPs have demonstrated haemolytic properties (Yang *et al.* 2013, Hong-Ling *et al.* 2016) and significant cytotoxic effects (Lai *et al.* 2002). In order to calculate the therapeutic indices of the peptides, mammalian cytotoxicity must be performed. Calculation of the therapeutic indices will enable the peptides with significantly improved or reduced activity to be compared with the parental peptides and commercially available alternatives.

4

Investigating the relationship between structure, cytotoxicity and haemolysis of AMPs from venom

4.1 Introduction

The antimicrobial activity of the parental Smp peptides and the derived modifications has been discussed in chapter 3. Whilst improvements to antimicrobial activity have been observed, it is also important to characterise the effects of the peptides on mammalian membranes. A common limitation for the use of antimicrobial peptides (AMPs) therapeutically is the disruption of eukaryotic membranes and haemolytic side effects (Semreen *et al.* 2018).

The toxic effects of AMPs are a limiting factor for AMP drugs already in clinical usage. Polymyxins demonstrate high nephrotoxicity, neurotoxicity and neuromuscular blockage at therapeutic doses (Conway *et al.* 1997). Due to this, the usage of polymyxins and colistin is restricted to patients with serious infections caused by multi-drug resistant (MDR) Gram negative bacteria for which all other therapeutic options have been exhausted (Mirski *et al.* 2017).

A major application for AMPs in clinical usage is topical administration (Naafs 2018). Consequently, the ability of the Smp peptides and derived modifications will be assessed against a eukaryotic skin cell line to evaluate the potential the peptides may have for topical application. Additionally, the peptides will also be screened against liver and kidney cell lines to assess the cytotoxic properties of the peptides against the systems typically responsible for the processing and excretion of drugs delivered systematically.

4.2 Study aims

The experiments in this chapter aim to characterise the haemolytic and cytotoxic activity of the antimicrobial peptides Smp24 and Smp43. Structural modifications were performed on both peptides via introducing single, double or triple amino acid substitutions and the effect the structural changes had on the antimicrobial function of the peptides was also determined.

The HaCaT cell line was unfortunately found to contain mycoplasma, as such the results within this chapter for the HaCaT cell line represent only 3 technical and 1 biological repeats.

Due to cost limitations with the synthesis of peptides via solid-phase synthesis, the cytotoxicity profiles of some of the peptides were restricted. For the tryptophan knockout modification, only haemolysis data could be collected.

4.3 Experimental design

The two peptides used within this study (figure 4.1) have been modified on the basis of improving the antimicrobial activity, as discussed in chapter 3 (section 3.3).

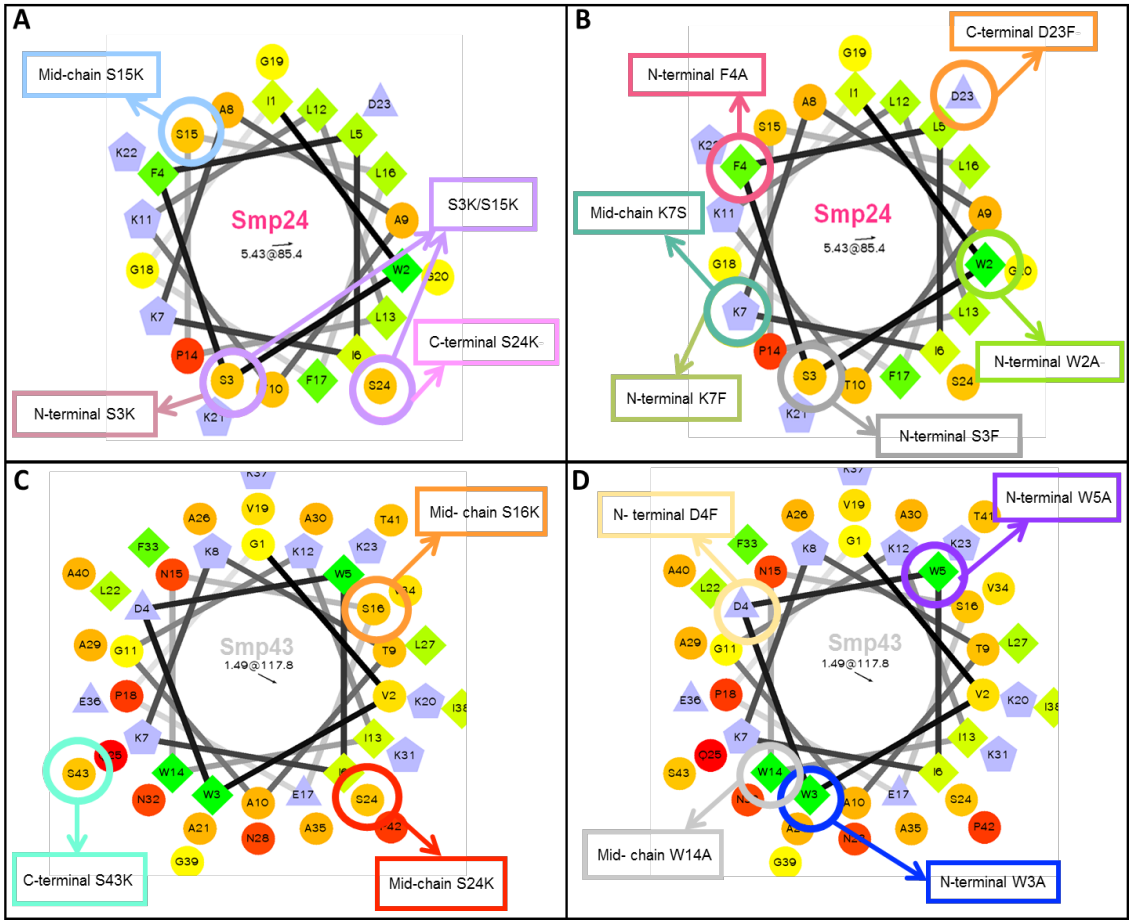

Figure 4.1: Mutation strategy for scorpion AMPs, as discussed in chapter 3, figure 3.2.

In total, 10 modifications of Smp24 were produced and 8 modifications of Smp43 were produced, as previously discussed in chapter 3 (tables 3.1 and 3.2).

4.4 Results

4.4.1 Haemolysis

The haemolytic potential of the peptides was assessed by incubation of the peptides (0 - 512 µg/ml) with sheep erythrocytes over a one hour period according to the method of Corzo *et al,* (2002). HC_{50} values were calculated as the concentration resulting in 50% haemolysis (refer to chapter 2, section 2.6).

As the antimicrobial activity of two commercially available AMP-like antibiotics (daptomycin and polymyxin B) was assessed in chapter 3 (section 3.4.2), it was deemed important to assess the activity of the AMPs used in this study compared with commercially licensed drugs.

4.4.1.1 Haemolytic activity of modified Smp24 peptides

The HC_{50} values for Smp24 and derived modified peptides are shown below in table 4.1.

Table 4.1: Haemolytic activity presented as HC_{50} values for Smp24 and derived modifications used within this study.

Peptide	Charge	GRAVY	HC_{50} (µg/ml)
Smp24	+3	0.31	76
Smp24 W2A	+3	0.43	>512*
Smp24 S3F	+3	0.46	52
Smp24 S3K	+4	0.18	11*
Smp24 S3K/S15K	+5	0.05	23*
Smp24 F4A	+3	0.27	423*
Smp24 K7S	+2	0.44	36
Smp24 K7F	+2	0.59	442*
Smp24 S15K	+4	0.18	26*
Smp24 D23F	+4	0.58	33*
Smp24 S24K	+4	0.18	15*
Daptomycin	-6	-1.93	>512
Polymyxin B	+5	nc	>512

Statistical significance was determined by performing a T-test.

* p-value ≤0.05; nc - not calculable

Native Smp24 exhibits moderate to high haemolytic activity, with an HC_{50} concentration of 76 µg/ml. All of the modifications performed to enhance the charge (which in turn enhanced the antimicrobial activity) resulted with enhanced haemolytic activity and lower HC_{50} concentrations. Interestingly, S3K which demonstrated the most potent antimicrobial activity also demonstrates the most haemolytic activity out of the peptide modifications assayed.

Unsurprisingly, both of the lipopeptide antibiotics demonstrated a low level of haemolytic activity, with HC_{50} values above the limit of detection of this study. One of the peptides within this study, W2A, demonstrated a low level of haemolysis which was observably similar to that of the lipopeptide antibiotics with a HC_{50} beyond the limit of detection (>512 µg/ml). Two of the other peptides also demonstrated a lower level of haemolysis (F4A and K7F) with HC_{50}s of 423 and 442 µg/ml respectively.

4.4.1.2 Haemolytic activity of modified Smp43 peptides

The haemolytic activity of the modified Smp43 peptides was also determined (table 4.2).

Table 4.2: Haemolytic activities of Smp43 and the modified peptides displayed as HC_{50} values.

Peptide	Charge	GRAVY	HC_{50} (µg/ml)
Smp43	+4	-0.32	>512
Smp43 W3A	+4	-0.25	>512
Smp43 D4F	+5	-0.17	92*
Smp43 W5A	+4	-0.25	>512
Smp43 W14A	+4	-0.13	>512
Smp43 W3A/W5A/W14A	+4	-0.13	>512
Smp43 S16K	+5	-0.39	>512
Smp43 S24K	+5	-0.39	>512
Smp43 S43K	+5	-0.39	>512
Daptomycin	-6	-1.93	>512
Polymyxin B	+5	nc	>512

Statistical significance was determined by performing a T-test.

* p-value ≤0.05; nc - not calculable

The haemolytic activity of Smp43 and derived modifications demonstrates a low level of haemolysis, with increased charge demonstrating no observable increase in haemolytic activity within the concentration range investigated in this study. Interestingly, one of the peptides within this study produced an HC_{50} value within the limit of detection. The D4F modification demonstrated significantly increased haemolytic activity, demonstrating a higher charge than Smp43 (+5) and increased hydrophobicity, which appears to have resulted in a peptide with an increased propensity to interact with sheep erythrocyte membranes. The activity to all of the modified Smp43 peptides, except the D4F modification, was found to be equivalent to that of the lipopeptide antibiotics within the concentration range used within this study.

4.4.2 Cytotoxicity against liver and kidney cells

Cytotoxicity testing was carried out to assess the effect the peptides would have on mammalian cell lines. As all systemic drugs pass through the liver and a significant proportion of drug metabolism occurs in the liver, a liver cell line (HepG2) was used to assess the toxicity of the peptides. The excretion of the drug must also be considered when developing potential novel antimicrobials; as such the cytotoxicity of the peptides was also assessed on a kidney cell line (HEK-293).

Both cell lines were routinely tested for mycoplasma and determined to be mycoplasma free. Cytotoxicity was assessed by incubation of the cell lines with AMPs over the concentration range of 0 - 512 µg/ml and determining LDH release by a Pierce LDH assay (Life Technologies, Paisley, UK) (chapter 2, section 2.7.2). LD_{50} values were calculated by plotting AMP concentration against observed percentage cytotoxicity to determine the concentration of peptide to cause 50% cell death.

As the haemolytic activity of daptomycin and polymyxin B had been determined, the same approach was taken with cytotoxicity screening to compare the activity of the AMPs with the cytotoxicity of the lipopeptide antibiotics.

4.4.2.1 Cytotoxic activity of modified Smp24 peptides

The cytotoxic activity of Smp24 and Smp24-derived modified peptides was determined against HepG2 and HEK-293 cell lines, as shown in table 4.3.

Table 4.3: Cytotoxic activities of Smp24-derived peptides against liver and kidney cell lines.

Peptide	Charge	GRAVY	LD_{50} (µg/ml)	
			HepG2	HEK-293
Smp24	+3	0.31	37	39
Smp24 W2A	+3	0.43	121*	72*
Smp24 S3F	+3	0.46	51*	32
Smp24 S3K	+4	0.18	34	38
Smp24 S3K/S15K	+5	0.05	42	29*
Smp24 F4A	+3	0.27	63*	56*
Smp24 K7S	+2	0.44	30	15*
Smp24 K7F	+2	0.59	>512*	>512*
Smp24 S15K	+4	0.18	38	13*
Smp24 D23F	+4	0.58	>512*	38
Smp24 S24K	+4	0.18	36	23*
Daptomycin	-6	-1.93	>512	>512
Polymyxin B	+5	nc	>512	351

Statistical significance was determined by performing a T-test,
* p-value ≤0.05; nc - not calculable.

As shown by the results in table 4.3 above, significant changes have been made to the cytotoxicity profiles of the peptides. For the cytotoxicity profiles against HepG2 cells, only one modification (K7S) resulted in a non-significant increase in cytotoxicity. Four of the peptides within this study resulted in significant decreases in liver toxicity. F4A and S3F had LD_{50} concentrations at higher concentrations than that of native Smp24 and two of the modifications in this study K7F and D23F demonstrated LD_{50} concentrations beyond the limit of detection of the assay, with values exceeding 512 µg/ml.

The cytotoxicity results against the HEK-293 cell line demonstrated a different pattern, with the peptides generally having increased levels of toxicity against the HEK-293 cell line when compared with the HepG2 cell line. The peptide which exhibited the greatest degree of cytotoxicity against the kidney cell line was S15K, with an LD_{50} concentration of 13 μg/ml. Conversely, the least cytotoxic peptide within this study was K7F which again demonstrated an LD_{50} value above the limit of detection within the confines of the study. Significant decreases in cytotoxicity were observed by the W2A and F4A modifications, although the LD_{50} concentrations were both lower than those observed against HepG2 cells. Some of the peptides within this study also demonstrated significant increases in cytotoxicity, S15K, S24K, S3K/S15K and K7S all possessed lower LD_{50} concentrations compared with native Smp24.

Both daptomycin and polymyxin B demonstrated low levels of toxicity against mammalian cell lines with LD_{50} values above the concentration range limit used within this study. The exception to this was the assessment of polymyxin B against the HEK-293 cell line, which demonstrated an LD_{50} within the limit of detection at 351 μg/ml. Two of the modified Smp24 peptides (K7F and D23F) demonstrated low levels of cytotoxicity equal to that of both polymyxin B and daptomycin. Against the kidney cell line, one of the peptides within the study demonstrated less cytotoxicity than polymyxin B and equal cytotoxicity to daptomycin, which was the K7F modification.

4.4.2.2 Cytotoxic activity of modified Smp43 peptides

Following the characterisation of the Smp24 peptides, the LD_{50} of Smp43 and derived modifications was assayed (table 4.4).

Table 4.4: Cytotoxic activities of Smp43 and derived modifications against liver and kidney cell lines.

Peptide	Charge	GRAVY	LD_{50} (µg/ml)	
			HepG2	HEK293
Smp43	+4	-0.316	162	36
Smp43 W3A	+4	-0.25	172	76*
Smp43 D4F	+5	-0.17	68	40
Smp43 W5A	+4	-0.25	46*	39
Smp43 W14A	+4	-0.13	77*	29
Smp43 W3A/W5A/W14A	+4	-0.13	ND	ND
Smp43 S16K	+5	-0.39	49	31
Smp43 S24K	+5	-0.39	29*	17
Smp43 S43K	+5	-0.39	39*	21
Daptomycin	-6	-1.93	>512	>512
Polymyxin B	+5	nc	>512	351

Statistical significance was calculated by performing a T-test,

* p-value ≤0.05; ND - not determined; nc - not calculable.

Native Smp43 shares a relatively low level of cytotoxicity against the HepG2 cell line when compared with that of Smp24. The characterisation of the Smp43 modifications within this study demonstrated many peptides with significant increases to the LD_{50}. S24K, S43K, W5A and W14A modifications all yielded peptides with increased cytotoxicity compared with native Smp43. None of the Smp43 modifications produced peptides with significantly decreased cytotoxicity.

Similar to the results obtained from Smp24, lower LD_{50} concentrations were observed for the HEK-293 cell line compared with the HepG2 cell line. Native Smp43 demonstrated a much lower LD_{50} concentration against the kidney cell line compared with that observed for the liver cell line. Only one of the modifications made to Smp43 resulted in a significant change to the LD_{50}, with W3A demonstrating a significant improvement to the LD_{50} with a concentration of 76 µg/ml.

Neither native Smp43 nor any of the modified Smp43 peptides demonstrated cytotoxicity equal to the limited cytotoxicity of daptomycin or polymyxin B. The cytotoxicity of the W3A/W5A/W14A could not be determined due to the small quantity of peptide available for analysis.

4.4.3 Cytotoxicity of AMPs against skin cell lines

Following the assessment of the AMPs against liver and kidney cell lines, the cytotoxicity of the peptides was assessed against a human skin cell line for the consideration of topical application of the peptides. Cytotoxicity was determined according to previously discussed methods (chapter 2, section 2.7.2).

4.4.3.1 Cytotoxicity of modified Smp24 peptides against human skin cells

The cytotoxicity profiles of Smp24 and the derived modifications against a human keratinocyte cell line are shown below in table 4.5.

Table 4.5: LD_{50} concentrations for modified Smp24 peptides against an immortalised human keratinocyte cell line (HaCaT).

Peptide	Charge	GRAVY	LD_{50} (µg/ml)
Smp24	+3	0.31	34
Smp24 W2A	+3	0.43	104*
Smp24 S3F	+3	0.46	>512*
Smp24 S3K	+4	0.18	18*
Smp24 S3K/S15K	+5	0.05	18*
Smp24 F4A	+3	0.27	57*
Smp24 K7S	+2	0.44	22
Smp24 K7F	+2	0.59	>512*
Smp24 S15K	+4	0.18	18*
Smp24 D23F	+4	0.58	137*
Smp24 S24K	+4	0.18	142
Daptomycin	-6	-1.93	>512
Polymyxin B	+5	nc	>512

Statistical significance was calculated by performing a T-test,

* p-value ≤0.05; nc - not calculable

Native Smp24 demonstrates a moderate to high level of cytotoxicity against the HaCaT cell line with an LD_{50} concentration of 34 µg/ml. The modifications to Smp24 yielded mixed results, with the exception of S24K, all of the serine to lysine substitutions produced peptides with significantly increased cytotoxicity profiles. Interestingly, the peptide with the highest charge (S3K/S15K) carried the highest level of cytotoxicity against the HaCaT cell line.

Increasing the hydrophobicity of the peptides generally resulted in significant decreases in cytotoxicity, with the K7S modification being the only exception to this rule. The modifications which incorporated phenylalanine residues into the sequence all resulted in significant decreases in cytotoxicity against HaCaT cells. Both K7F and S3F modifications demonstrated LD_{50} values above the detection limit within the scope of this study, whilst D23F and W2A modifications both produced peptides with LD_{50} values above 100 µg/ml.

Two of the peptides demonstrated cytotoxicity equal to that of daptomycin and polymyxin B within the detection limits of this study. The S3F and K7F modifications demonstrated cytotoxicity of >512 µg/ml. Whilst other modifications may not have demonstrated cytotoxicity comparable to that of the two lipopeptide antibiotics within the concentration range of this study, 3 of the other peptides (W2A, D23F and F4A) demonstrated significantly reduced cytotoxicity. This is promising when looking to reduce cytotoxicity of the peptides overall.

4.4.3.2 Cytotoxicity of modified Smp43 peptides against immortalised keratinocytes

The results of the cytotoxicity assessment of Smp43 and the derived modifications are shown in table 4.6.

Table 4.6: Cytotoxicity profiles of Smp43 and derived modifications displayed as LD_{50} values against the HaCaT cell line.

Peptide	Charge	GRAVY	LD_{50} (µg/ml)
Smp43	+4	-0.32	179
Smp43 W3A	+4	-0.25	194
Smp43 D4F	+5	-0.17	327
Smp43 W5A	+4	-0.25	37*
Smp43 W14A	+4	-0.13	53*
Smp43 W3A/W5A/W14A	+4	-0.13	ND
Smp43 S16K	+5	-0.39	328
Smp43 S24K	+5	-0.39	>512*
Smp43 S43K	+5	-0.39	99*
Daptomycin	-6	-1.93	>512
Polymyxin B	+5	nc	>512

Statistical significance was calculated by performing a T-test

* p-value ≤0.05; ND - not determined; nc - not calculable.

As shown by the results in table 4.6, native Smp43 demonstrates a low level of cytotoxicity against keratinocytes compared with Smp24. Unlike the results obtained for the modification to Smp24, no pattern was observed for the changes in cytotoxicity for Smp43 in relation to the modifications performed.

Four of the modifications made to Smp43 demonstrated reduced cytotoxicity. D4F and W3A modifications both resulted in peptides with increased hydrophobicity and decreased cytotoxicity against HaCaT cell line, although these differences were not determined to be statistically significant.
Two of the modifications which produced peptides with increased charge (S16K and S24K) demonstrated reduced cytotoxicity against the HaCaT cell line. The S24K modification demonstrated a statistically significant decrease in cytotoxicity, with an LD_{50} greater than 512 µg/ml.

One of the peptides within this study demonstrated a low level of cytotoxicity equal to that of daptomycin and polymyxin B. The S24K modification demonstrated cytotoxicity >512 µg/ml and was the least cytotoxic variant of Smp43. Whilst the D4F and S16K modifications didn't have the low haemolysis observed for the lipopeptide antibiotics, both modifications demonstrated reduced cytotoxicity compared with the parental peptide.

4.4.3.3 Human Urothelial Epithelial Cells (HUEPC)

Following the observation of a detectable LD_{50} for the cytotoxicity of polymyxin B against HEK-293 cells, the properties of the cell membranes of the cell lines was investigated and interesting differences in the resting membrane potential of the cell lines were noted. The HEK-293 cell line has a considerably more negatively charged membrane when compared with the other cell lines; as such the cytotoxicity of the two parental peptides was re-assessed against a cell line related to excretion with a more neutral membrane potential. Primary human uroepithelial cells (HUEPCs) were used for this investigation. Differences in membrane potential between the cell lines used in this study are shown in table 4.7.

Table 4.7: Membrane potential differences between primary and secondary cell lines

Cell line	Designation	Membrane potential (mV)
Sheep erythrocytes	Primary	28-39
HepG2	Secondary	-18.25
HEK-293	Secondary	-40
HUEPC	Primary	-14.3

Following the observations that there may be an association between cell membrane potential and peptide cytotoxicity, the cytotoxicity of the parental peptides was assessed against HUEPCs (table 4.8).

Table 4.8: Cytotoxicity assessment of native Smp24 and Smp43 against HUEPC cells

Peptide	LD_{50} (µg/ml)
Smp24	>512
Smp43	>512

As shown in table 4.10, both peptides demonstrated LD_{50} profiles beyond the limit of detection of the study when assayed against the HUEPC cell line. The results

of this study are interesting, as variations in membrane charge and composition could be a crucial factor when assessing mammalian cytotoxicity.

4.5 Discussion

Previous structural modifications to Smp24 include the insertion of a GVG hinge, increasing the peptide length to 26 amino acids and the truncation of the last 5 amino acids of the chain to reduce the peptide sequence to 19 amino acids. The results of the modifications yielded contrasting outcomes; the Smp24GVG modification resulted in greater haemolytic activity compared with native Smp24 whilst Smp24T demonstrated reduced haemolytic activity (Harrison, *et al.* 2016). Cytotoxicity of the peptides has previously been determined by ATP release assay and all the peptides demonstrated cytotoxic properties. The insertion of the GVG hinge led to dramatically increased cytotoxicity whilst the truncation of the peptide resulted in a small reduction in cytotoxicity (Harrison, Abdel-Rahman, *et al.* 2016). The truncation modification resulted in an increased hydrophobicity of the peptide with a GRAVY score of 1.05 and a charge reduction to +2. One of the peptides within this study with similar physicochemical properties, K7F, demonstrated a similar level of haemolysis but was much less cytotoxic than Smp24T.

4.5.1 Haemolysis of Smp24

Most of the Smp24 modifications within this study resulted in a high level of haemolysis, which is in keeping with haemolytic properties of scorpion venom-derived antimicrobial peptides in the literature. BmKn2-7 is an antimicrobial peptide derived from the venom of *Buthus martensii karsch* and natively demonstrates a HC_{50} of 17 μg/ml (Li *et al.* 2019b). Modifications to the structure of this peptide which resulted in increased charge, reduced the HC_{50} to 90 μg/ml (Li *et al.* 2019a). The effects of increased charge on Smp24 resulted in increased haemolysis, but the charge modifications to Smp43 resulted in a non-detectable change to the HC_{50} and thus the peptide remained non-haemolytic.

As a general rule, the Smp24 peptides which demonstrated improved antimicrobial activity also demonstrated increased haemolytic activity. Similar results have previously been observed for antimicrobial peptides extracted from Australian tree frogs, with improvements in antimicrobial activity accompanied by 4-fold increases in haemolytic activity (Fernandez *et al.* 2008).

Whilst Smp24 and Smp43 are both isolated from the same venom, the differences in haemolytic and cytotoxic profiles highlight the relationship between structure and function. Smp43 is a much larger AMP, with a di-helical structure which is predicted to be globular due in aqueous solutions by the GRAVY value. Smp24 is a smaller peptide which behaves similarly to other smaller venom-derived AMPs within the literature and is predicted to be membranous in structure. VmCT1 is a 13 amino acid peptide derived from the venom of the scorpion *Vaejovis mexicanus.* The influence of charge on the antimicrobial activity of VmCT1 was investigated by the incorporation of lysine residues in to the structure. (Pedron *et al.* 2019). Similar to the results observed in this study for Smp24, the structural modifications which resulted in reduced antimicrobial activity resulted in reduced haemolytic activity, as evidenced by the reduced cytotoxicity of the W2A and K7F modifications.

4.5.2 Haemolysis of Smp43

Smp43 has previously been shown to possess a low level of haemolysis against sheep erythrocytes (Harrison, *et al.* 2016), which is thought to be related to the structure. Smp43 adopts a di-helical structure in the presence of 60% TFE and belongs to the longer-chain AMP family. Other peptides in this class with the helix-hinge-helix topology include Pandinin 1 and cecropin A (Holak *et al.* 1988, Corzo *et al.* 2001) which offer attractive therapeutic indices for future therapeutic development. Additionally, the suggested globular state of Smp43 could contribute to the behavioural differences between Smp24 and Smp43. The modifications made to the Smp43 peptides resulted in non-detectable changes to the haemolytic potential, with the HC_{50} exceeding the limit of detection at >512 μg/ml. The exception to this is the D4F modification which resulted in a HC_{50} of

92 µg/ml. Interestingly, the D4F modification did not demonstrate an improved antimicrobial pattern compared with native Smp43. D4F has a slightly increased activity against *Pseudomonas* (32 µg/ml) but decreased potency against *E. coli* (64 µg/ml) and therefore the increased haemolytic activity demonstrated by this modification created a less therapeutically appealing peptide.

4.5.3 Haemolysis as a measure of cytotoxicity

Haemolysis has previously been used to determine the cytotoxic properties of AMPs, though methods used differ between research groups. Types of blood used for the assays can vary tremendously, with blood derived from species ranging from fish (rock bream) to human (Bae *et al.* 2018, Rončević *et al.* 2019). The membrane composition can influence the percentage haemolysis (or HC_{50}) observed, as the fatty acid content of red cell membranes can vary greatly between species (Al-Qarawi and Mousa 2004). Sheep erythrocytes are commonly used to determine the HC_{50} of AMPs due to ease of availability and no requirement for ethical approval to run the assays, but the membrane composition differs to that of human red blood cells. Zwitterionic phosphatidylcholine (PC) is responsible for 1.6% of the membrane for sheep red blood cells and 39.5% of the membrane of human red blood cells (Dennison and Phoenix 2014). As lower levels of peptide insertion have been observed in the presence of the PC (Dennison and Phoenix 2014), the usage of sheep erythrocytes as a marker of haemolysis may result in an inaccurate representation of the HC_{50} which could be observed in human red blood cells. It is anticipated, due to differences in phospholipid content of red cell membranes between different species, that a lower level of haemolysis would be observed if the peptides were tested against human blood.

As a result of the membrane composition affecting the perceived haemolysis of the peptide, the modifications to the structure of the peptides could produce misleading haemolysis results when determining suitability for human application. For future investigations, haemolysis assays could be performed on human red blood cells to determine if the membrane composition of the cells is a critical factor for the haemolytic properties of the peptides.

Limited investigations have been made in to the membrane potential of sheep erythrocytes and the resting membrane potential of the cells has been linked to ion dependency. The membrane potential of sheep erythrocytes was determined to be 33-39 mV in the presence of high potassium and 28-37.8 mV in the presence of low potassium (Andreoli *et al.* 1967). Alternatively, the haemolytic propensity of the peptides could be more complex. It has previously been postulated that the interaction between AMPs and mammalian cell membranes is mostly the result of hydrophobic interactions (Mahlapuu *et al.* 2016a). As Smp24 and the derived modifications are more hydrophobic than Smp43, this could also contribute to the increased cytotoxicity observed against mammalian cells.

4.5.4 Eukaryotic cytotoxicity

Differences in LD_{50} concentrations were observed between two cell types (HEK-293 and HepG2) used within this study for both native peptides. This could offer some mechanistic insights as to how peptides interact with mammalian membranes and the importance of the ratio between AMP charge and the electrical potential of the cell membrane. Greater cytotoxicity was observed against the HEK-293 cell line than HepG2 for all of the peptides tested.

Primary cells (such as the HUEPC cells) are isolated directly from tissues, have a finite lifespan and limited expansion capacity, which can make the cell line challenging to work with in the laboratory. Primary cells have “normal” cell morphology and maintain many of the important markers and functions observed *in vivo* (Alge *et al.* 2006, Pan *et al.* 2009). Secondary cell lines, which are often derived from tumours are immortalised by chemical carcinogens or viruses which enable virtually unlimited proliferation. A question of major importance is whether the mechanism of immortalisation affects the genotype and phenotype of the cells (Smith *et al.* 1992).

The human embryonic kidney cell line (HEK-293) was obtained by exposing human embryonic kidney cells to mechanically sheared fragments of adenovirus

type 5 DNA. This resulted in 11% of the adenovirus genome being incorporated in to the 19q13.2 chromosome of the HEK cells, which is required for the genomic coding of E1A and E1B proteins for immortalisation (Stepanenko and Kavsan 2012). HepG2 cells are a human teratocarcinoma cell line obtained from a 15 year old Caucasian male and frequently used as *in vitro* alternatives to primary hepatocytes due to an unlimited lifespan, stable phenotype, high availability and ease of handling (Donato *et al.* 2015). Studies have determined gene expression can differ between primary cell lines and the relevant immortalised cell lines. Wilkening *et al*., (2003) demonstrated the expression of Phase 1 enzymes in the HepG2 cell line was considerably lower than that observed in primary liver cells. The study concluded that the HepG2 cell line could be useful for the study of drug-metabolising enzymes (such as LDH within the confines of this study) but it does pose questions about the reliability of data obtained from secondary cell lines. Resultantly, the data obtained from using primary cells has been demonstrated to be more relevant and reflective of the *in vivo* environment (Alge *et al.* 2006, Pan *et al.* 2009).

4.5.4.1 Membrane composition

HEK-293 cells have high (~35%) phosphatidylcholine (PC), high (~25%) phosphatidylserine (PS) and a moderate (~15%) phosphatidylethanolamine (PE) content compared with HepG2 cells which have a PC (~30%) enriched membrane with PE and PS almost excluded from this leaflet (Müller *et al.* 1996). Additionally, both cell lines demonstrated marked differences in cell membrane potential, with HepG2s exhibiting a membrane potential of -18.2 mV (Liu *et al.* 2003) and HEK-293 cells holding a membrane potential of -40 mV (Stott *et al.* 2015). Together these results could indicate the importance of membrane composition when determining cytotoxicity. The licensed drug Polymyxin B demonstrated a detectable LD_{50} value (351 µg/ml) against the HEK-293 cell line but no activity against the HepG2 cells, which could indicate mechanistic interactions between a positively charged peptide and more negatively charged cell membranes. The membrane of HaCaT cells is composed of 37% PC, 6.7% sphingomyelin (SM) and 18% PE/PS/phosphatidylinositol (PI) (Schurer *et al.* 1993). The HaCaT cell membrane is composed of a greater percentage of neutral

phospholipids compared with the HEK-293 cell line which could contribute to the differences observed in cytotoxicity between the cell lines.

The increased propensity for cell death with a more negatively charged membrane is perhaps unsurprising, due to the initial electrostatic interactions between positive charged AMPs and negatively charged bacterial membranes being the driving force for antimicrobial activity (Mihajlovic and Lazaridis 2010).

4.5.4.2 Cytotoxicity of Smp24

For Smp24-derived peptides, cytotoxicity against the HepG2 cell line remained constant for all peptides with modifications that increased the net charge, with LD_{50} concentrations around 37 μg/ml. Some of the modifications which resulted in increased hydrophobicity (and decreased antimicrobial activity) resulted in reduced cytotoxicity against HepG2 cells. The incorporation of phenylalanine residues significantly reduced the cytotoxicity. Phenylalanine substitutions were performed at the N-terminus (S3F), mid-chain (K7F) and C-terminal (D23F), with the latter two resulting in the greatest reduction in cytotoxicity to >512 μg/ml. Whilst the reduction of the cytotoxicity of K7F modification is statistically significant, the lack of antimicrobial activity demonstrated by this modification renders this peptide therapeutically unattractive, though this could suggest the antimicrobial activity and the cytotoxicity activity of Smp24 could be linked.

The reduction of cytotoxicity upon incorporation of phenylalanine residues in to the AMP structure has been observed previously (Saint Jean *et al.* 2018). The modification of the AMP C18G where leucine residues were substituted with phenylalanine residues improved the percentage viability of the HEK-293 cell line (Saint Jean *et al.* 2018). As with many studies investigating modified AMPs (Oddo *et al.* 2015, Bae *et al.* 2018, Rončević *et al.* 2019), the cytotoxicity screen was limited to one cell line which creates difficulties when observing cytotoxicity patterns. For Smp24, the incorporation of phenylalanine residues reduced cytotoxicity against the HepG2 and the HaCaT cell lines but the effect on HEK-293 cells was more varied, with only the K7F modification demonstrating a reduction in cytotoxicity.

Modifications to the C-terminal of Smp24 appeared to result in contrasting outcomes. The D23F modification was less cytotoxic against HepG2 and HaCaT cells, whilst the S24K modification resulted in increased cytotoxicity against HEK-293 cells and non-significant differences against the HepG2 and HaCaT cell lines. Rodríguez *et al*., (2014) determined the cytotoxicity of Pandinin 2 was linked with the KKD residues at the C-terminal. As Smp24 shares sequence homology with Pandinin 2, the results from this study suggest the KKD residues at the C-terminal of Smp24 are also linked with cytotoxicity and substitution of these peptides results in contrasting outcomes.

4.5.4.3 Cytotoxicity of Smp43

For Smp43, the incorporation of phenylalanine (D4F) had a more varied result. Reduced cytotoxicity against HaCaT cells and non-significant changes against the HepG2 and HEK-293 cell lines were observed though the LD_{50} of the D4F modification when compared with native Smp43. Though the changes were not statistically significant, the biological relevance can be determined by calculating the therapeutic index (see chapter 5, section 5.6).

All of the modifications to Smp43, with the exception of the W3A modification, resulted in increased cytotoxicity against the HepG2 cell line. Interestingly, the W3A modification resulted in an enhanced antimicrobial profile compared with native Smp43 and therefore a more therapeutically attractive peptide was produced when comparing the ration of antimicrobial activity to cytotoxicity. The most cytotoxic peptides within the study were S24K and S43K, both of which contain increased charge within the second helix of the peptide and increased clustering of charged residues within the helix. As the HepG2 membrane has a slight negative charge, the increased polarity of the peptide could have aided interaction with the membrane and the resultant cytotoxicity. Against the HEK-293 cell line, all of the modifications except the W3A modification resulted in enhanced cytotoxicity. Polymyxin B, which has a charge of +5, demonstrated a detectable LD_{50} value against this cell line suggesting the cytotoxicity profile of peptide drugs can be dependent upon the cell line used for screening.

4.5.5 Therapeutic applications

The results in this study demonstrate technical limitations within the AMP field. Firstly, the screening of AMP cytotoxicity by means of haemolysis assay is not necessarily conclusive. Differences in haemolysis vs mammalian cytotoxicity have been observed for the variants of Smp24 and Smp43 against the numerous cell lines used. For example, the HC_{50} of Smp43 is >512 µg/ml but the LD_{50} against HEK-293 cells is 36 µg/ml which would have a significant impact when calculating the therapeutic index. Erythrocyte membrane composition differs between species, thus making data sets between studies directly incomparable. Dennison and Phoenix, (2014) determined the effect of the antimicrobial peptide modelin 5 on sheep, pig and human erythrocytes. The study determined that the greatest haemolysis was observed against sheep erythrocytes (12% at 500 µM) and much lower haemolysis was observed against human erythrocytes (<2% at 500 µM). Taking the results of this study and the results of Dennison and Phoenix, (2014) in to account, the data suggests the activity of AMPs is much more complicated than initially anticipated and a more comprehensive screen of AMPs is required in order to gain a cytotoxicity profile that may be representative against relevant cell types in humans.

Secondly, the choice of cell lines can affect the cytotoxicity. This study highlights that differences in the membrane potential of eukaryotic cell lines can affect the observed cytotoxicity, with cell lines that have a more negative membrane potential demonstrating greater susceptibility to AMPs. This could potentially lead to peptides being labelled as more cytotoxic if a single cell line is used in validating drug leads. For this study, the cell line hypothesis was tested by performing cytotoxicity screening of the parental peptides against the HUEPC cell line. The resting membrane potential of HUEPC is -14.3 mV (Laaris *et al.* 2012), which is less negative than the membrane potential of both the HepG2 and HEK-293 cell lines (Liu *et al.* 2003, Stott *et al.* 2015). This resulted in calculated LD_{50}s of >512 µg/ml for both Smp24 and Smp43, which was not observed against the other cell lines tested.

Thirdly, a general strategy to reduce cytotoxicity across AMPs may not be possible. The results of this study highlight how similar modifications introduced to peptides derived from the same venom have had contrasting effects. For example, tryptophan to alanine substitutions in Smp24 resulted in reduced cytotoxicity, but typically result in an increase in cytotoxicity following equivalent substitutions in Smp43. From this it can be concluded that it is essential to perform numerous modifications on parent peptides to determine which residues can be modified to produce enhanced peptides, but that this can be varied and a successful approach for one AMP may not be suitable for other AMPs.

4.6 Conclusions

Peptides with reduced cytotoxicity have been produced for both Smp24 and Smp43. The K7F, D23F, W2A and S3F modifications to Smp24 produced peptides with reduced cytotoxicity against kidney, liver and skin cells. Of these modifications, the D23F peptide is of interesting due to retaining the antimicrobial activity profile of native Smp24 whilst demonstrating reduced cytotoxicity. The W3A modification of Smp43 demonstrated reduced cytotoxicity against the kidney cell line whilst reduced cytotoxicity against the skin cell line was observed for the D4F, S16K and S24K modifications. Whilst both the S16K and S24K modifications of Smp43 resulted in increased cytotoxicity, both of these modifications demonstrated enhanced antimicrobial activity compared with native Smp43.

All of the modifications to Smp24 produced peptides with enhanced haemolysis, except W2A, F4A and K7F which all demonstrated statistically significant reduced HC_{50} values. With the exception of D23F, these modifications also resulted in decreased antimicrobial activity. The modifications to Smp43 resulted in non-detectable changes to the haemolysis, with HC_{50} values exceeding the limit of detection of the study. Resultantly, all of the peptides which demonstrated increased antimicrobial activity also demonstrated non-detectable changes in haemolysis and thus enhanced peptides were produced. The one exception to this was the D4F modification which was detectably and significantly more haemolytic with an HC_{50} of 92 μg/ml.

The results of this study highlight the importance of a comprehensive screen for cytotoxicity and how the effects of modifications can appear to have unpredictable effects on cytotoxicity. Additionally, this study has revealed it could be pertinent to assess cellular cytotoxicity against both primary and secondary cell lines.

The next step of the investigation is to analyse the structural modifications made to Smp24 and Smp43 and the effects these have had on function. Additionally, calculating the therapeutic indices of the peptides will enable candidate peptides with an enhanced antimicrobial and cytotoxicity profile to be identified from the native peptides.

5

Modelling the relationship between structure and function

5.1 Structural investigations relating to antimicrobial activity

The antimicrobial activity of Smp24, Smp43 and derived modifications has been assessed in chapter 3 and the cytotoxic and haemolytic properties have been assessed in chapter 4. Initial structural investigations were performed on the most and least active antimicrobial peptides (Smp24 S3K and Smp24 K7F) to determine if it was possible to visualise structural differences by circular dichroism (CD) spectroscopy (chapter 3, section 3.6). Smp24 was chosen for the focus of CD work due to the greatest increased and decreased antimicrobial activity observed across this investigation.

Computational modelling can be utilised to investigate the relationship between structure and the observed effects on function. *Ab-initio* modelling can be utilised to generate a 3-dimensional structure based upon the amino acid sequence. Whilst the accuracy of computational modelling could be subjective, when used in combination with CD spectroscopy, the experimental data enables the models generated via modelling software to be either supported or rejected.

5.2 Study aims

This chapter aims to investigate the relationship between structure and antimicrobial and cytotoxicity activity of the daughter peptides compared with the native peptides via homology modelling of both Smp24 and Smp43. The chapter will be identifying structural changes via helical wheel, three-dimensional structure and hydrophobic and electrostatic potential modelling.

Therapeutic indices have been calculated to identify which peptide modifications demonstrate an enhanced antimicrobial and cytotoxicity profile when compared with the native peptides.

5.3 Experimental design

To investigate the effects of the modifications of the peptides on the structure, computational modelling was used. Initially, helical wheels were generated to visualise the organisation of the peptides in terms of charge and hydrophobicity (section 2.9.4). *Ab-initio* modelling was then used to generate 3-dimensional helices. Structural files were generated using QUARK software by Zhanglab, but to obtain more complex models, the output file format from QUARK was used to process samples using PyMOL Molecular Graphics System, Version 2.0 Schrödinger, LLC (section 2.9.3).

5.4 Structural investigations relating to antimicrobial activity

Initially, structural investigations were made to determine the effects of structural changes on the antimicrobial activity of the peptides. The modifications resulting in >8 fold reductions or improvements to the antimicrobial activity of the peptides were investigated via helical wheel, surface polarity and 3-dimensional structural analysis.

5.4.1 Structural investigations of Smp24 K7F

The increased hydrophobicity of the peptides generally led to a reduction in antimicrobial activity. This has been observed in the literature before; modifications to Pandinin 2 which resulted in a GRAVY increase from 0.32 to 0.57 yielded a peptide with no detectable antimicrobial activity against the isolates tested, which included *S. aureus, E. coli* and *B. subtilis* (Rodríguez *et al*., 2011). The most hydrophobic Smp24 modification was K7F, which demonstrated no antimicrobial activity against the same species of bacteria. Structurally, this modification resulted in helical differences between K7F and the parental peptide (figure 5.1).

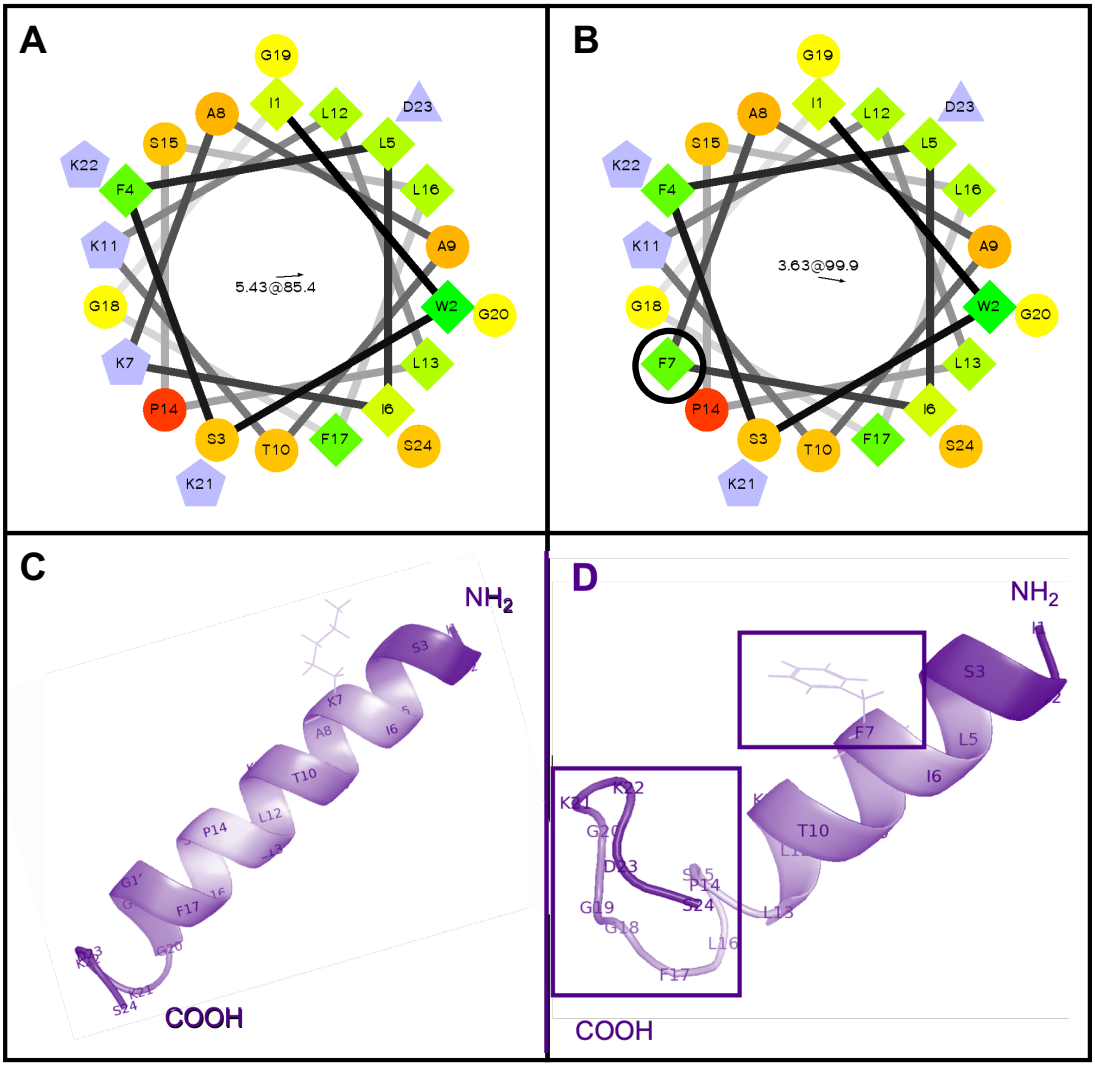

Figure 5.1: Structural analysis of Smp24 and modifications. Helical wheel analysis of (A) Smp24, (B) Smp24 K7F and 3D structural analysis of (C) Smp24 and (D) Smp24 K7F using PyMOL (Schrödinger, LLC). Differences between the modified peptide and native peptide are highlighted by rings and boxes.

From the helical wheel structures (figure 5.1 panels A and B), the K7F modification resulted in a change in the amphipathicity of the peptide compared with Smp24. The addition of the phenylalanine led to the incorporation of a hydrophobic residue towards the polar N-terminal region of the helix. The 3D modelling of the peptide also suggests significant structural changes to the peptide, with the helix region of K7F being reduced and the disordered region being more predominant. The structural changes could imply the importance of the arrangement of the secondary structure for the mechanism of action.

5.4.2 Structural investigations of Smp24 S3K

The S3K modification to Smp24 resulted in the most potent AMP within this study, with an MIC of 0.5 µg/ml against *S. aureus* and 1 µg/ml against *E. coli.* The structural analysis of the S3K modification demonstrates the effect of incorporation of a slightly longer chain and positively charged lysine residue to the N-terminus of the peptide (figure 5.2).

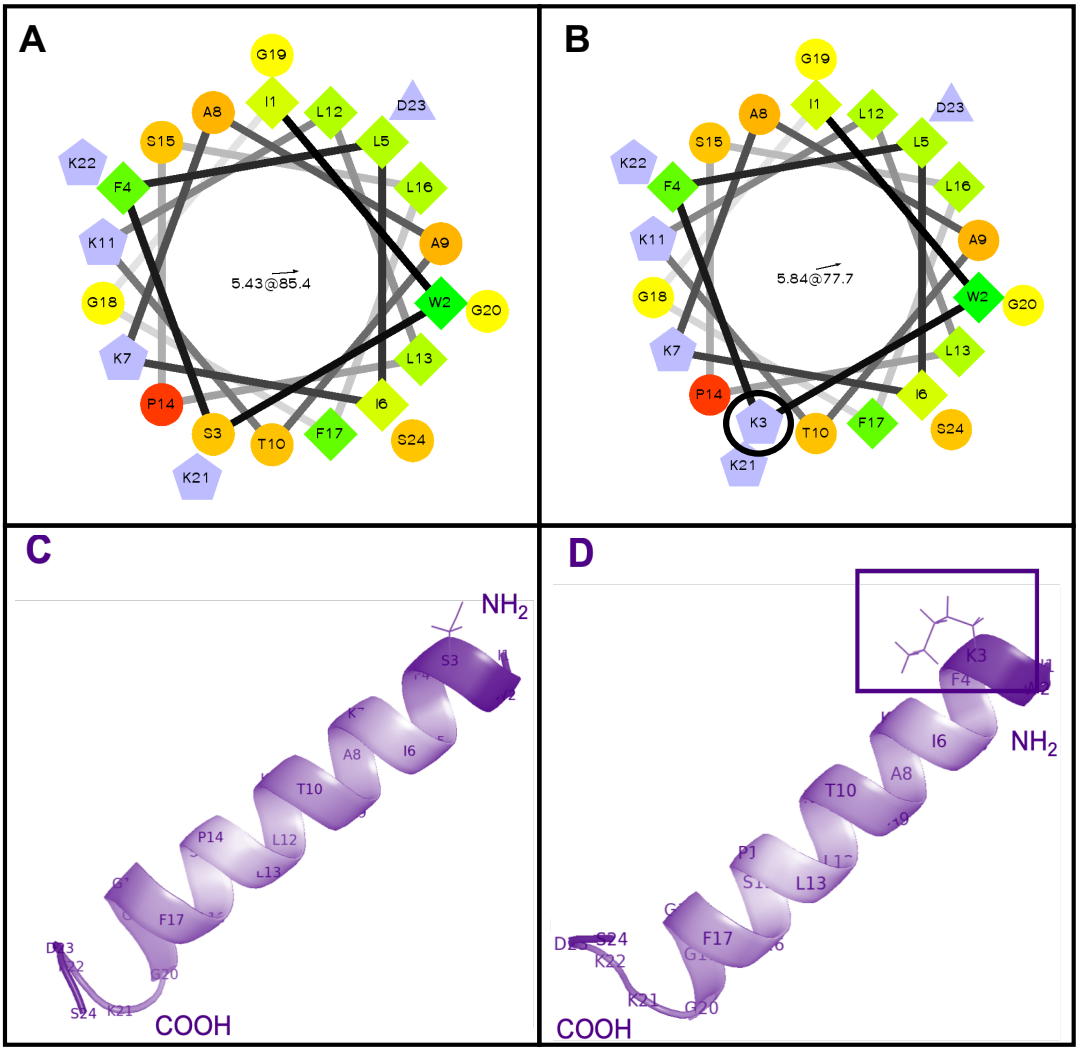

Figure 5.2: Structural analysis of N-terminal charge modification of Smp24. Helical wheel analysis of Smp24 (A) and Smp24 S3K (B); 3D structural analysis of Smp24 (C) and Sm24 S3K (D). Differences between the modified peptide and native peptide are highlighted by rings and boxes.

From helical wheel analysis, the incorporation of the lysine residue at position 3 has increased the amphipathic properties of the peptide. The amphipathicity of

peptides is widely reported as the most important physicochemical property of AMPs, as it enables the peptides to attack the cell membrane by selectively interacting with the hydrophobic-hydrophilic domains of the phospholipids (Edwards *et al.* 2016). With the S3K modification, there is an increase in charge on one side of the helix whilst the hydrophobicity on the other side of the helix remains equal to that of Smp24. This can be most readily seen in the space-filling models (figure 5.4). The change in polarity of the peptide could contribute to the observed increase in antimicrobial activity.

5.4.3 Structural investigations for Smp43 W3A/W5A/W14A

The W3A/W5A/W14A modification to Smp43 resulted in no detectable antimicrobial activity (section 3.4.3). The structural analysis of the W3A/W5A/W14A modification of Smp43 demonstrates the effect of incorporation of alanine residues, which decreased the hydrophobicity of the peptide (figure 5.3).

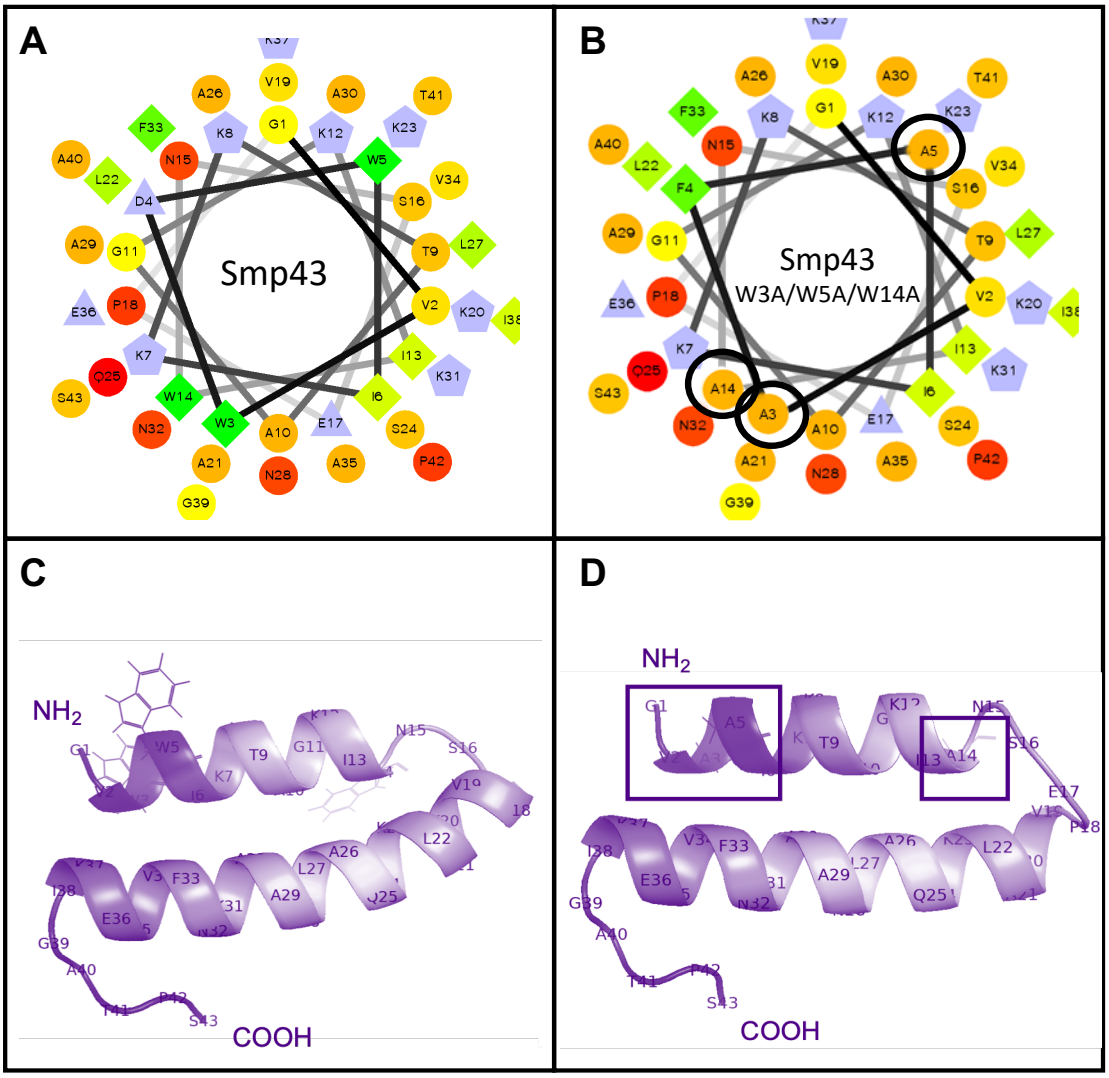

Figure 5.3: Structural analysis of tryptophan substitutions in Smp43. Helical wheel for Smp43 (A) and Smp43 W3A/W5A/W14A (B) 3D structural analysis of peptides of Smp43 (C) and Smp43 W3A/W5A/W14A (D). Differences between the modified peptide and native peptide are highlighted by rings and boxes.

From helical wheel analysis, the substitution of 3 tryptophan residues for alanine has decreased the hydrophobicity of the peptide, as demonstrated by the increase in orange circular residues. From analysis of the 3D structure, no substantial changes can be observed. The incorporation of the alanine residues has decreased the length of the side chains, but overall the peptide exhibits the same di-helical structure as the parental peptide. The decrease in the antimicrobial activity of the modification could be attributed to the decrease in hydrophobicity. Whilst the W3A/W5A/W14A modification carries the same charge as native Smp43, it retains the same propensity for electrostatic interactions with the bacterial membrane, hydrophobicity of the peptides is well documented as an

essential component for insertion in to the membrane (Zasloff 2002, Matsuzaki 2009). The decreased hydrophobicity of the peptide could be responsible for the lack of antimicrobial activity shown, as the peptide could form the initial electrostatic interactions but be unable to insert in to the membrane to create pores and the resulting cell death.

5.4.4 Relating structure to function: Smp24 S3K and Smp24 K7F

For short antimicrobial peptides, deletion or substitution of single amino acids can induce notable changes in the secondary structure (Ciumac *et al.* 2019). Numerous methods were taken to observe the effects the modifications would induce on the structure of the peptides. Structural predictions for the helical formation of Smp24 were performed using Jpred4, an update of Jpred3 previously used for the prediction of helical and coil regions of peptides (Cole *et al.* 2008). The software predicted Smp24 formed a single helix region, extending from I1 to S15 with the remaining 9 amino acids adopting an unordered structure. The most potent peptide in the study, S3K and the least potent peptide, K7F were both predicted to retain a helical structure.

Large changes to the structure were not expected from single amino acid substitutions, but small changes in the structure could affect the mechanism of action. Due to changes in the charge and hydrophobicity of the peptides, the amphipathicity and charge distribution would both be affected. Spatial distributions of the peptides were modelled using the 3D hydrophobic moment vector calculator (Reißer *et al.* 2014).

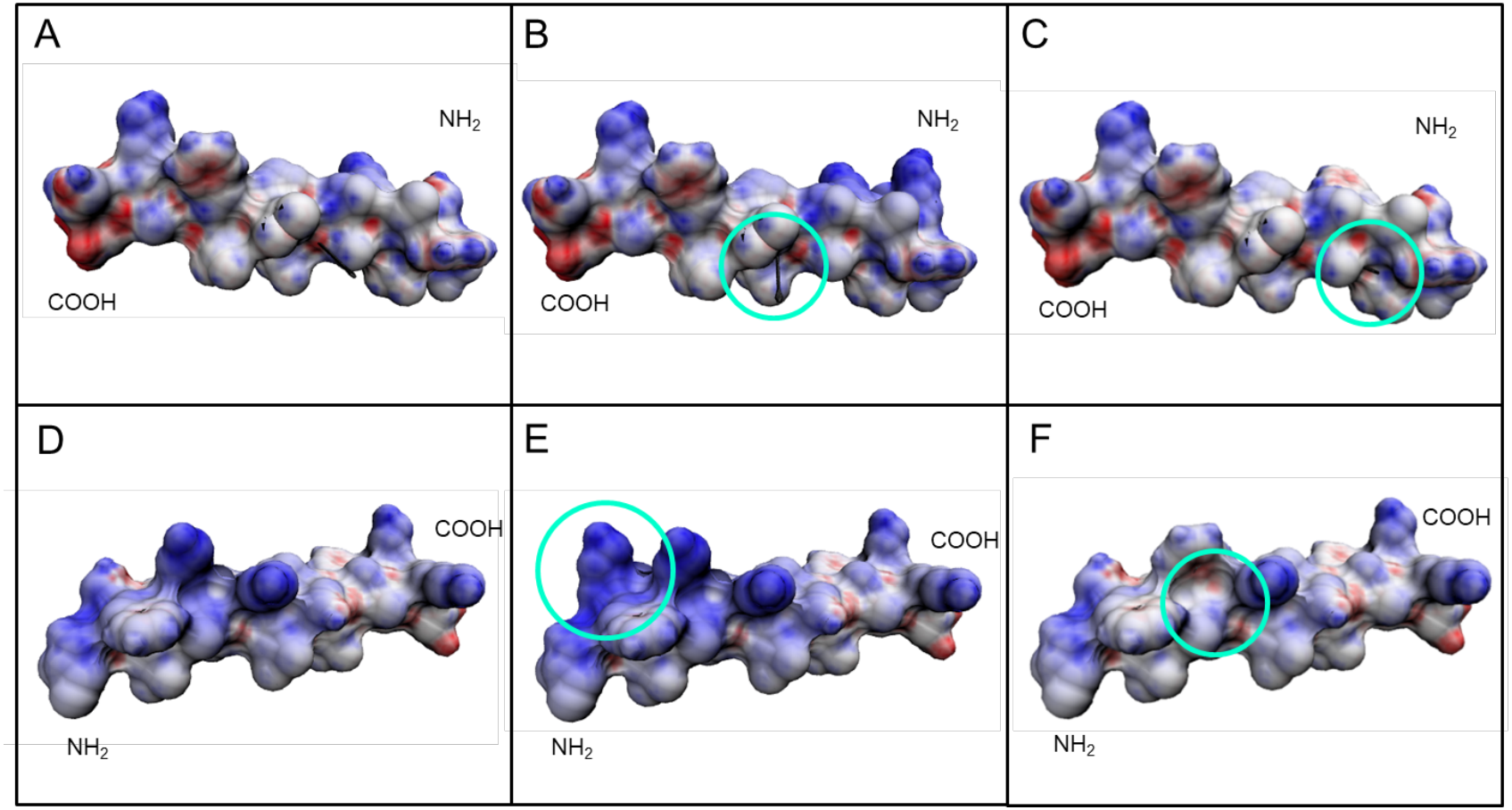

Figure 5.4: Spatial distribution of Smp24 (A, D), S3K, (B, E) and K7F (C, F) using the 3D hydrophobic moment calculator (Reißer *et al.* 2014). Polar facets are highlighted in blue and non-polar facets are highlighted in red. The rings on the images demonstrate areas of the peptides which show differences between native Smp24 and the modified peptides.

5.4.5 Polar angles and hydrophobic moments

Compared with Smp24 (figure 5.4, panels A and D), both the S3K and K7F modifications demonstrated structural changes in terms of polarity. Structural differences between the peptides are highlighted in figure 5.3, with the S3K peptide demonstrating increased polarity at the N-terminus, as expected due to the increased charge at residue 3. The hydrophobic moment (HM) vector of S3K is slightly higher when compared with native Smp24, this can be more easily visualised in figure 5.5. The angle between the HM vector and the z-axis is 127.0° for Smp24 and 139.0° for S3K. Slight structural changes can be observed around the HM vector for S3K, with other polar residues of the peptide appearing at the surface around the HM vector angle.

Increased hydrophobic moment angles have been associated with increased antimicrobial activity in previous studies. Irazazabal *et al*., (2016) observed that a modification to mastoparan, which increased the charge from +3 to +4 whilst simultaneously increasing the hydrophobic moment, yielded a peptide with enhanced antimicrobial activity compared with the parental peptide. Kim *et al* observed the inclusion of lysine residues which increased the charge and hydrophobic moment of AMPs also yielded peptides with enhanced activity against *Pseudomonas,* which was also observed in this study (Kim, Kang, *et al.* 2018). The S3K modification also follows this trend, by demonstrating an increased hydrophobic moment alongside increased antimicrobial activity.

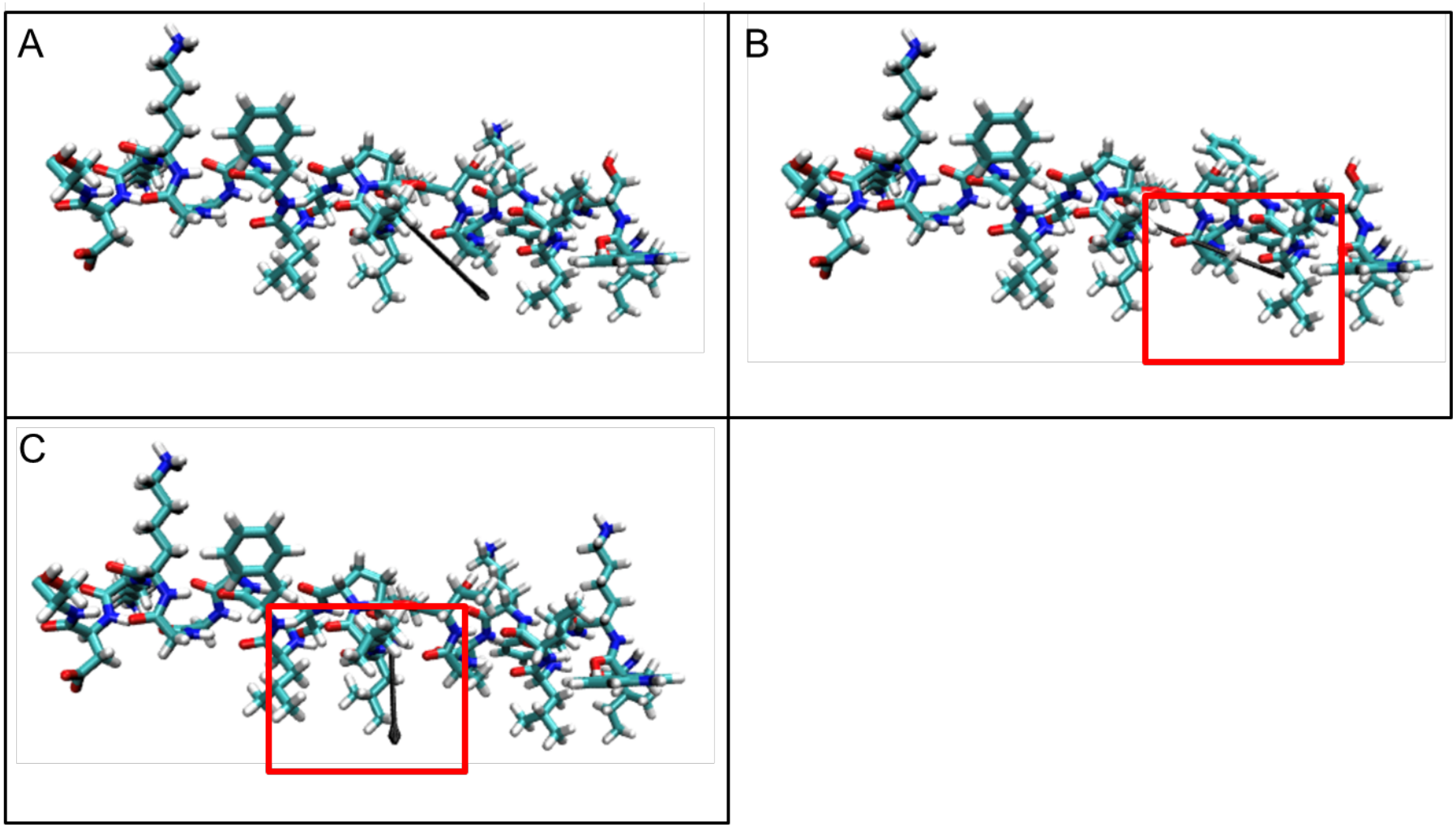

Figure 5.5: Atomic representations of Smp24 and derived modifications. Hydrophobic moment vector is shown as a black arrow. (A) Smp24, (B) K7F and (C) S3K. Observable differences in the hydrophobic moment of the daughter peptides are highlighted with by red boxes.

For K7F, the overall polarity of the peptide is reduced compared with native Smp24 (figure 5.4 panels C and F). The polarity of K7F is particularly reduced around the N-terminus, which demonstrates a significant structural change from the substitution of a single amino acid. This could contribute to the lack of activity shown, if less surface charge is available to bind with the membrane the initial electrostatic interactions would be weaker and therefore may not lead to pore formation and the resultant antimicrobial activity. K7F has a reduced HM vector angle of 111.4° as shown in figure 5.5 (panel B). Decreases in surface charge have previously been associated with a decrease in antimicrobial activity (Bluhm *et al.* 2015), which is supported by the data from this study. Both Smp24 peptides with a reduced charge (K7S and K7F) demonstrated reduced antimicrobial activity compared with the parental strain. The results highlight the importance of the initial electrostatic interaction for the overall mechanism of action.

As shown in figure 5.5, the polar angles of Smp24, S3K and K7F appear at different angles. The angle between the HM vector and the z-axis is 127.0° for Smp24 with a 12 degree increase in the polar angle resulting in the dramatic increase in antimicrobial activity of S3K. Conversely, a 16 degree decrease in the polar angle resulted in a dramatic decrease in antimicrobial activity, as the K7F peptide demonstrated no detectable antimicrobial activity. The results highlight the importance of polar angle for membrane insertion and resultant pore formation which lead to the antimicrobial activity.

The charge at the N-terminal of toroidal-pore forming peptides is thought to be critical for pore formation (Mihajlovic and Lazaridis 2012). Smp24 has previously been demonstrated to cause membrane disruption by toroidal pore formation (Harrison *et al*., 2016). When lysine 7 of melittin was replaced with glutamine or alanine, this resulted in the initial formation of a cylindrical pore but did not lead to full toroidal pore formation or membrane depletion when investigated using computer simulation experiments. The modification resulted in a change in the mechanism of action of the peptide and reduced the efficacy compared with native melittin. The results obtained for N-terminal modifications of Smp24 provide functional data which support the hypothesis that charge at the N-terminal is important for the mechanism of action of peptides which operate via toroidal pore. The S3K modification demonstrated increased propensity for bacterial

activity, whereas the K7F modification demonstrated reduced activity. Additionally, the data from this study suggests the structure of the peptide could also be important for function. Whilst S3K has a greater N-terminal charge density, it shares a similar structure to native Smp24 (figure 5.2, panel D). K7F however demonstrated reduced charge density and therefore a lower propensity for electrostatic interactions with the anionic bacterial cell membranes. The increase in disordered structure of K7F (figure 5.1, panel D) could also contribute to the lack of activity seen, as the data suggests the peptide does not adopt a full alpha-helix and therefore is unable to insert in to bacterial membranes as efficiently as native Smp24.

To investigate the effect of the N-terminal charge modifications on pore-formation, future work would involve observing the effect of the peptides on synthetic phospholipid vesicles.

The activity of the S3K/S15K modification could be attributed to the increased charge. Increasing the charge of antimicrobial peptides has been shown to be restrictive to antimicrobial peptides above a particular threshold due to electrostatic screening. The highly charged and hydrophilic peptides lose much of their effect at increased ionic strength (Schmidtchen *et al.* 2014). The protonation states of the positively charge amino acids (lysine, arginine and histidine) differs in the membrane environment (Li *et al.* 2017). Theoretical calculations have also shown that lysine becomes deprotonated in the bilayer centre (Yoo and Cui 2008, Gleason *et al.* 2013), which could explain the restriction of antimicrobial activity observed by the double lysine substitution. The presence of salt causes deactivation of AMPs and reduces the initial electrostatic interactions required for pore formation and antimicrobial activity (Aoki and Ueda 2013). This does highlight one of the limitations of AMPs in terms of therapeutics, however, although clearly AMPs are biologically effective, playing an important role in innate immunity.

5.4.6 Relating structure and function: Smp43 S24K, Smp43 S43K and Smp43 W14A

For Smp43, the effect of the modifications were less clear. In general, the S24K modification yielded the greatest increase in antimicrobial activity, with increased activity against *P. aeruginosa, B. subtilis* and *S. aureus* (section 3.4.3*).* Structurally, this modification led to an increase in charge density around the mid chain of the peptide, which can be seen in figure 5.6 along with a decreased hydrophobic moment (9.0 A*kT/e) compared with native Smp43 (9.8 A*kT/e). The modification also resulted in an alteration of the orientation of the C-terminus of the peptide (figure 5.6). The S43K modification resulted in an increase in the spread of the charge density across the peptide, as shown in figures figure 5.6 and figure 5.7, with the greatest structural change visible at the C-terminus as expected.

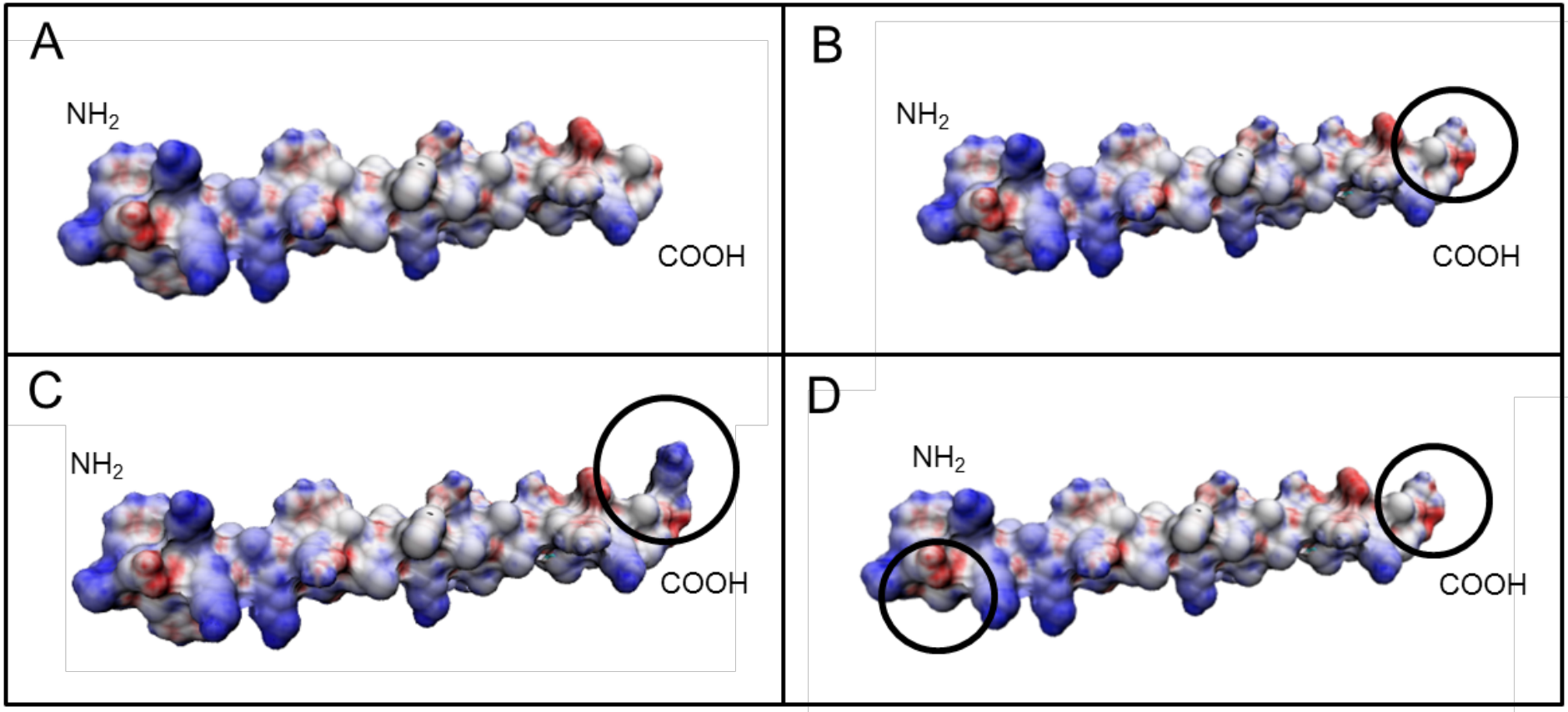

Figure 5.6: Spatial diagrams for Smp43 (A), Smp43 S24K (B), Smp43 S43K (C) and Smp43 W14A (D). The rings highlight areas of the modified Smp43 peptides which are visibly different to those of native Smp43 (A).

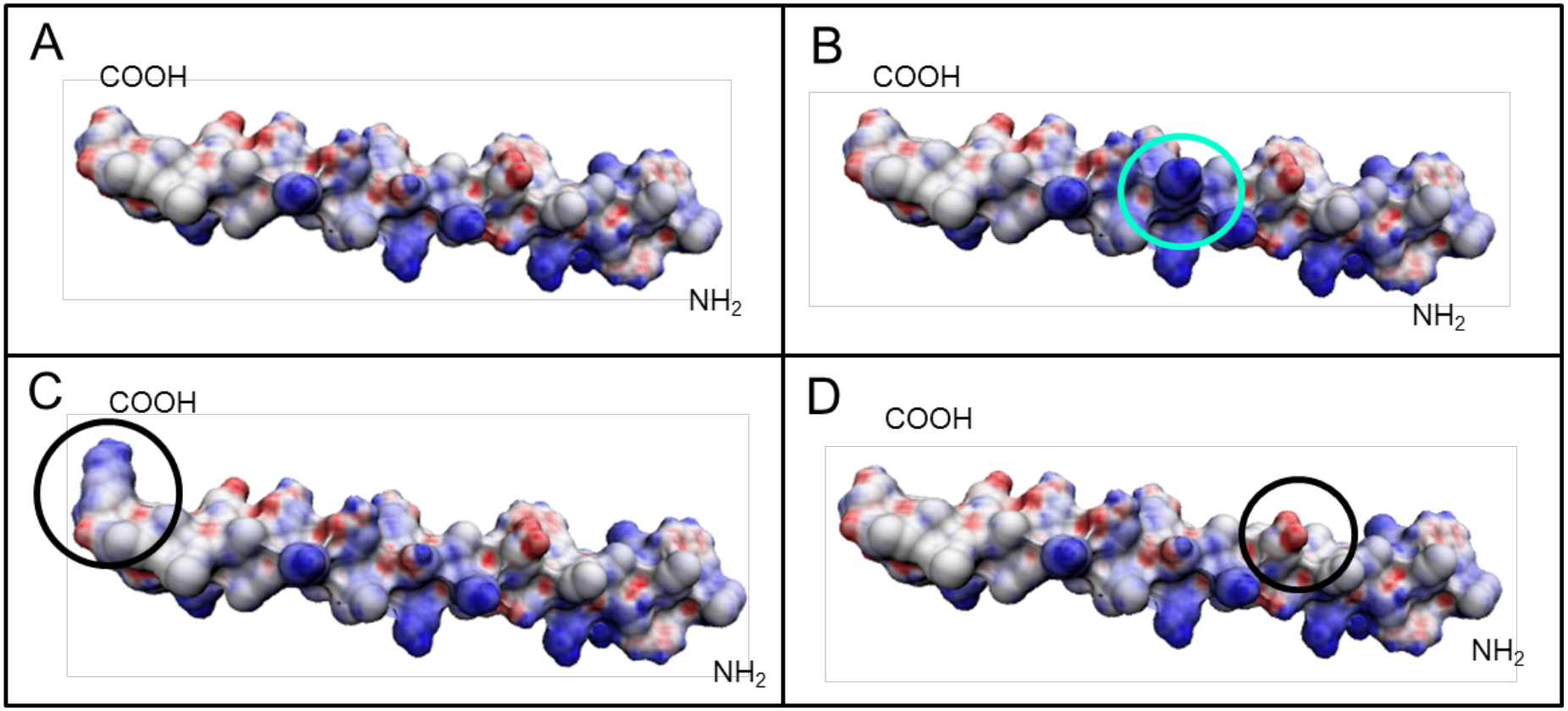

Figure 5.7: Polar facet representation in Smp43 and derived modifications. Smp43 (A), Smp43 S24K (B), Smp43 S43K (C) and Smp43 W14A (D). Regions of the modified peptides which demonstrate visible differences to the parental peptide are highlighted by the rings.

5.4.7 Smp43 S43K

The S43K modification resulted in changes to both the N and C-terminus in terms of organisation and charge distribution and demonstrated a lower hydrophobic moment (6.8 A*kT/e) than native Smp43. The changes in polarity demonstrate the importance of an AMP electrostatic interaction to the prokaryotic membrane for the pore-forming mechanism of action. Increases in surface polarity have yielded peptides with enhanced antimicrobial activity. The results of increased charge yielding enhanced antimicrobial activity are in line with results obtained with the successful modification of mucroporin-M1 (Dai *et al.* 2008). Mucroporin-M1 was modified to increase the charge compared with native mucroporin, Dai *et al* 2009, observed the increased charge resulted in greater increases to some strains tested (mostly Gram negative) and smaller fold-changes observed against *Staphylococcus* and *Bacillus* species, which was similar to the results found with this study.

5.4.8 Smp43 W14A

The W14A modification resulted in changes to the non-polar facets at both the N and C-termini (figure 5.6 and figure 5.7). The non-polar, hydrophobic components of peptides are thought to be important for the insertion of peptides in to the prokaryotic cell membrane after the initial electrostatic interaction has taken place (Hazam *et al.* 2019). The results of this study highlight a delicate balance between charge and hydrophobicity is required for optimum antimicrobial properties, as a slight increase in the hydrophobicity which resulted in small structural changes (W14A) yielded a peptide with enhanced antimicrobial activity.

5.4.9 The role of charge and hydrophobicity on Smp43 function

The hypothesis that a balance between hydrophobicity and charge is critical for antimicrobial activity is supported by the activity of the most hydrophobic peptide for the Smp43 modifications, the tryptophan knockout (W3A/W5A/W14A). The modification induced structural changes which can be visualised in figure 5.8. A

Hydrophobicity content of 50% has been stated as being desirable regarding the design of AMPs (Hazam *et al.* 2019), the W3A/W5A/W14A modification demonstrates 48.4% hydrophobic composition which is identical to the hydrophobicity content of native Smp43. With an MIC >512 μg/ml, this highlights the importance of investigating the parameters of individual AMPs to determine how each molecule can be optimised and a general approach to drug design may not be favourable for AMP design.

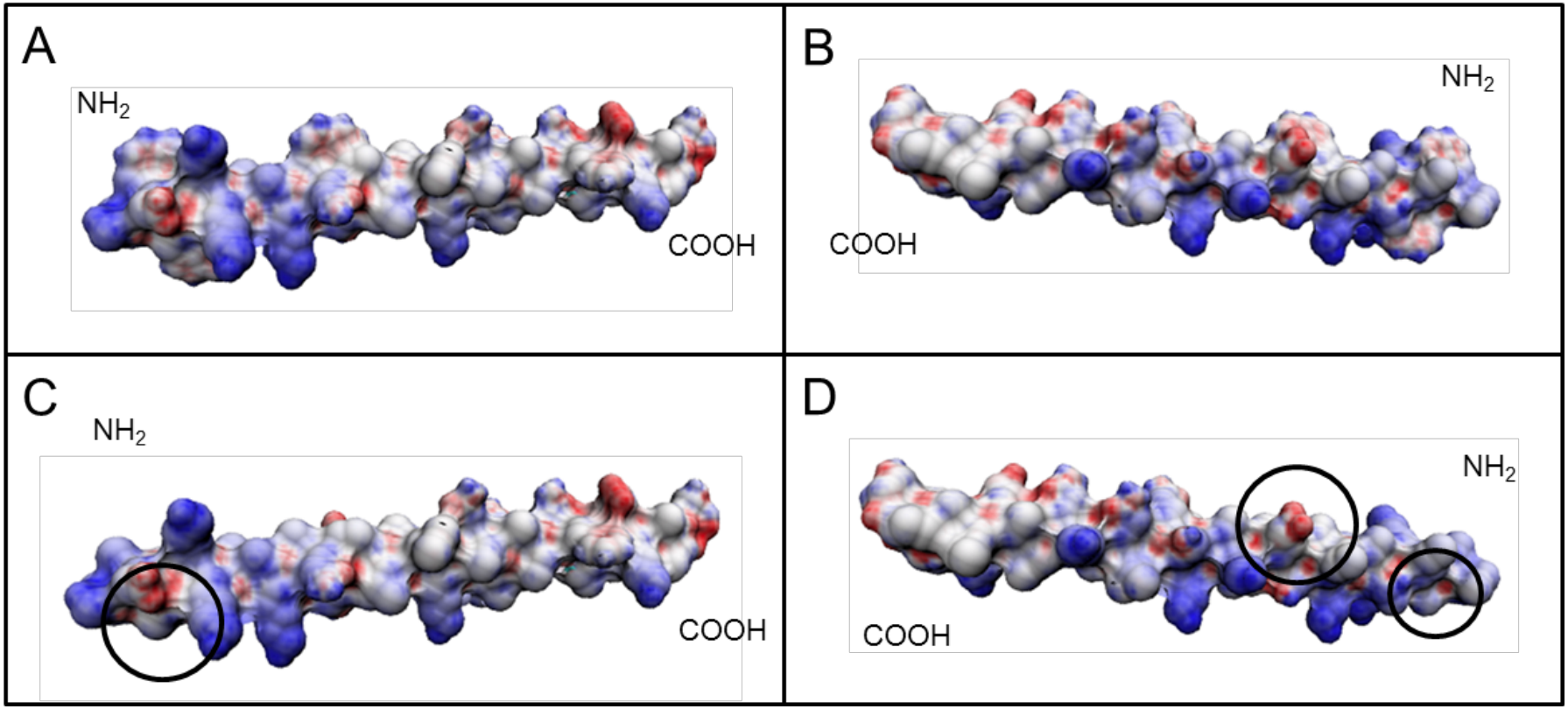

Figure 5.8: Spatial distribution of Smp43 (A and C) and Smp43 W3A/W5A/W14A (B and D). Polar facets are highlighted in blue and non-polar facets are highlighted in red. Differences between the modified peptides and native Smp43 are highlighted by the rings.

Interestingly, there are differences in the polar facets at the N terminal of the Smp43 W3A/W5A/W14A compared with native Smp43, indicating the spatial distribution of AMPs could also be critical for antimicrobial activity.

Smp43 shares high sequence homology (75%) with Pandinin 1 (Pin 1), a 44-amino acid peptide derived from the venom of *Pandinus imperator* (figure 5.9).

Peptide	Molar Mass (Da)	Sequence
Smp43	4654	G – W D W I K K T A G K I W N S E P V K A L K S Q A L N A A K N F V A E K I G A T P S
Pandinin 1	4800	G K W D W I K S A A K K I W S S E P V S Q L K G Q V L N A A K N Y V A E K I G A T P T

Figure 5.9: Sequence homology between Smp43 and Pandinin 1. The glycine residues are at the N-terminus of the peptides and the serine and threonine residues are at the C termini.

NMR experiments by Nomura *et al.*, 2005 proposed Pin 1 operated by a detergent-like mechanism. This study suggested that Pin 1 sits within the interface between the hydrophobic core and the phospholipid head groups. The N-terminal helices of Pin 1 are tilted at a 30 degree angle relative to the lipid bilayer and C-terminal helices. The interactions between the tryptophan residues at positions 4, 6 and 15 on the tilted helix and the phospholipid head groups cause the membrane disruption. The knockout of the tryptophan residues at positions 3, 5 and 14 of Smp43 resulted in a peptide with no detectable antimicrobial activity. This could suggest, due to the high sequence homology between the peptides, they both operate by a similar mechanism of action. This also implies, similar to Pin 1, the tryptophan residues have a crucial role in membrane disruption for Smp43.

The effect of the individual tryptophan modifications on the bactericidal effect, in general resulted in either no change to the lethal activity of the peptide or resulted in a 2-fold reduction. The exception to this was the lytic activity of the peptides against *E. coli*, which possessed a greater propensity to cause cell death at lower concentrations. The activity of the single tryptophan modifications resulted in up to a 4-fold increase in bactericidal activity against *E.coli* with MBCs of 8 µg/ml. This could suggest mechanistic differences of activity between bacterial species, as despite these modifications resulting in increased antimicrobial activity against other isolates, the minimum bactericidal concentration was not reduced. The improvements in the bactericidal concentrations against *E. coli* is a promising result and could suggest AMPs can be tailored for more specific treatments of bacterial strains in a similar manner to antibiotics. An interesting future direction from this work would involve observing the pore forming abilities of the peptide to determine if the incorporation of the alanine residues results in increased pore formation or the formation of larger/deeper pores. The MIC and MBC results suggest the peptides are more efficient at pore formation against *E. coli* due to the 4-fold increase in lethality. Whilst the results observed may be surprising given the “neutral” nature of alanine, studies have previously reported the importance of alanine for the pore formation mechanism of action of peptides (Ong and Wiradharma 2014)

The MIC results suggest, for Smp43, the W3, W5 and W14 residues are important for the membrane activity of the peptide. In future work, a double mutation of W5 and W14 to alanine residues would be performed in order to investigate this hypothesis.

5.5 Structural investigations relating to eukaryotic toxicity

5.5.1 Haemolysis of Smp24-derived modifications

Structurally, no particular pattern was observed for haemolysis, with the modifications appearing to have a random effect. Contrasting information has been published on the effects of modifications on the haemolytic propensity of AMPs. Some studies have previously postulated that the interaction between AMPs and mammalian cell membranes is mostly the result of hydrophobic interactions (Mahlapuu *et al.* 2016a). Whilst other studies have suggested the effects of modifications can be random. Disruption in the hydrophobic face has yielded peptides with contrasting haemolysis profiles. The hydrophobic moment is a measure of the amphipathicity of an alpha-helix (Eisenberg *et al.* 1982). The modification of pep5 by increasing the hydrophobic moment from 0.58 to 0.74 yielded a highly haemolytic variant (85% at 55 μM) compared with the parental peptide (8%). A smaller increase in the hydrophobic moment to 0.68 yielded a peptide with less haemolysis than the native peptide. Similar results were observed for the most and least haemolytic variants of Smp24. The most haemolytic modification to Smp24 was the S3K peptide, which has a hydrophobic moment vector angle of 139.0°. The least haemolytic modification was W2A, which has a hydrophobic moment angle of 139.0° compared with that of Smp24 which is 127.0°. Structurally, the peptides appear similar (figure 5.10).

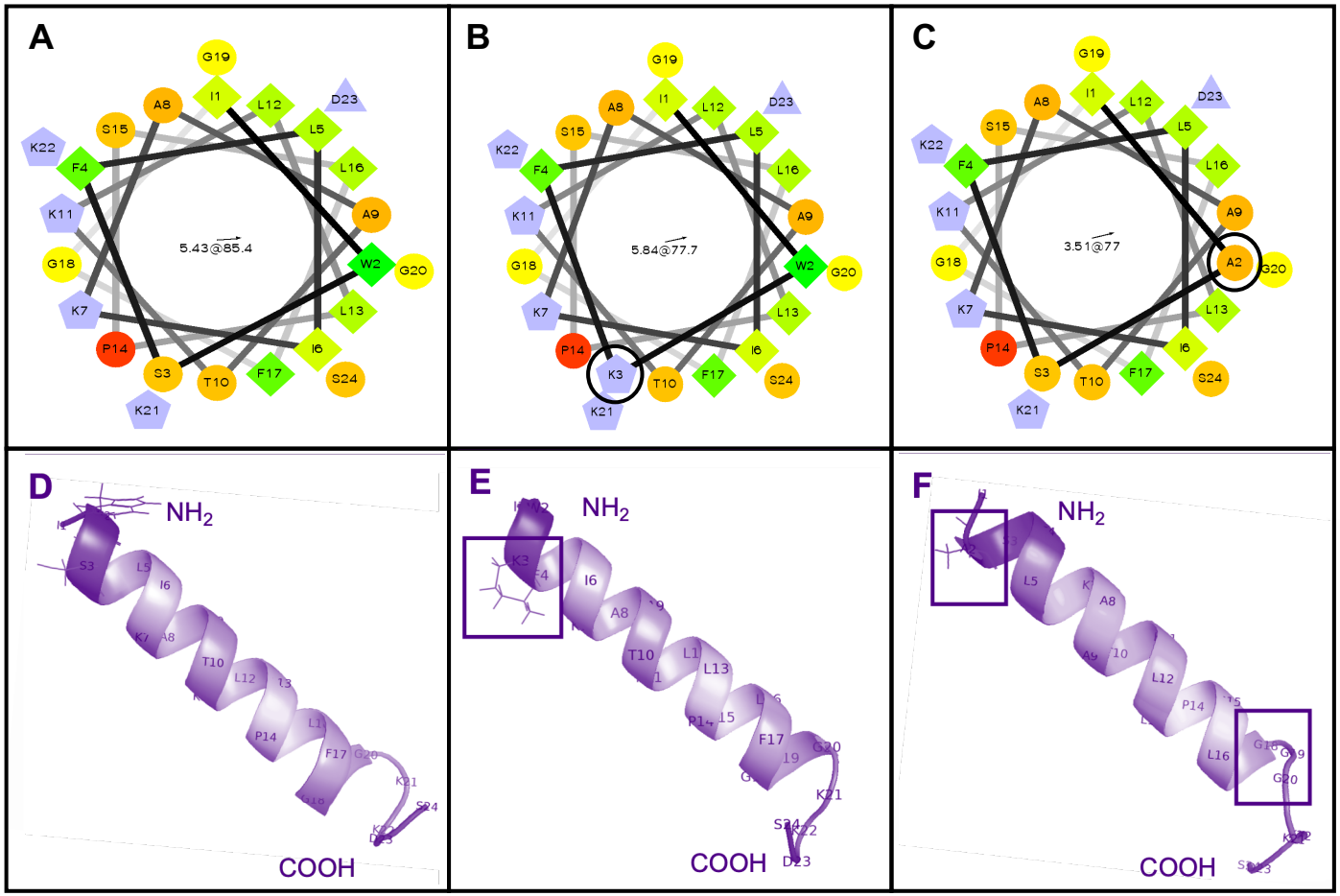

Figure 5.10: Structural modifications of Smp24. Helical wheel projections of Smp24 (A), Smp24 S3K (B) and Smp24 W2A (C). Structural changes as observed for Smp24 (D), Smp24 S3K (E) and Smp24 W2A (F). Differences in structure are highlighted by the rings and boxes.

The similarities in the structure of the modified peptides could suggest the interaction between AMPs and erythrocyte membranes is more complicated than adjusting amino acids alone to improve parameters. The W2A modification demonstrates a slightly less pronounced helix upon 3D-modelling compared with native Smp24 (figure 5.10, panel F). As the ability of the peptides to adopt their helical structure is important for the mechanism of action (Jacobs and White 1989, Shai 1999), the reduction in the helical content of the W2A modification could account for the observed decrease in haemolytic activity. The results suggest the effects of modifications on the activity of peptides could be relative to the effect on peptide structure in addition to changes in the hydrophobicity profile. In the future, CD spectroscopy could be utilised to determine the structure of the peptide under the presence of TFE titration (as per chapter 3, section 3.6.2) and this could be compared with the data for native Smp24. This would enable the visualisation of structural modifications on the helical propensity of the W2A modification.

5.5.2 Haemolysis of Smp43-derived modifications

As shown in figure 5.11, the D4F modification of Smp43 resulted in increased hydrophobicity of the peptide. The inclusion of the phenylalanine towards the N-terminal of the peptide increased the hydrophobicity of the first helical region of the peptide. As hydrophobicity has been implicated with the penetration of mammalian cell membranes (Dennison and Phoenix 2014), this could explain the increase in haemolysis observed by this modification. The D4F modification also demonstrates an increase in charge; the relationship between charge and hydrophobicity has been shown to be an important factor for antimicrobial activity and haemolytic activity of peptide mimetics (Takahashi *et al.* 2017). The results of this study are in agreement, as the alterations to the physicochemical properties of D4F yielded a peptide with similar antimicrobial activity to native Smp43 but with markedly increased haemolytic activity.

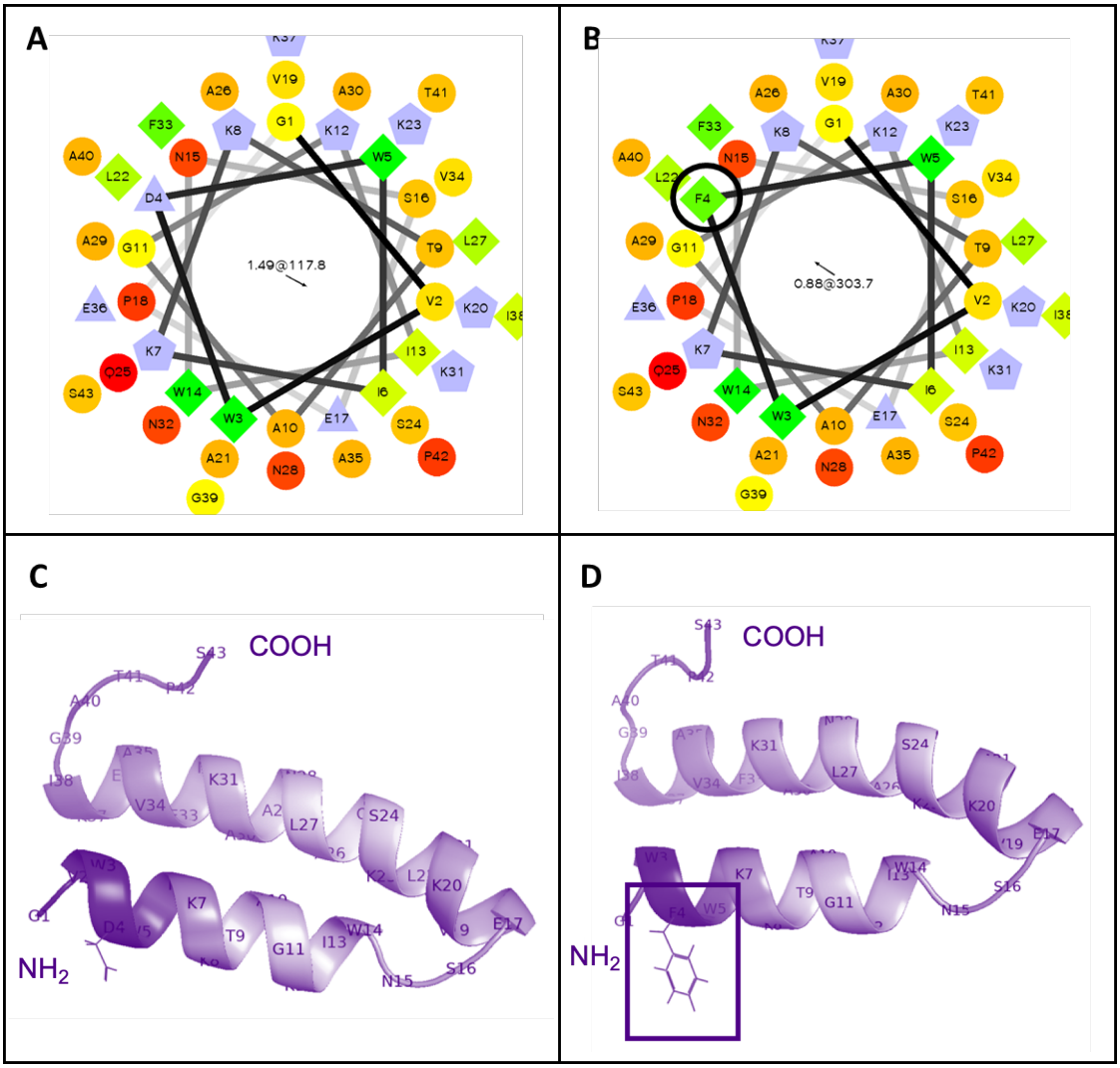

Figure 5.11: Structural modifications to Smp43. Helical wheel projections for Smp43 (A), Smp43 D4F (B). Structural changes as observed in the 3D structure of Smp43 (C) and Smp43 D4F (D).

5.5.2.1 Cytotoxicity of Smp24-derived modifications

Structurally, the incorporation of phenylalanine induced different changes. The D23F modification improved the amphipathicity of the peptide by incorporating a hydrophobic residue in place of a negatively charged residue, as shown in figure 5.12 (panel D). The K7F modification (figure 5.12, panel C) introduced a hydrophobic modification in to the charged side of the peptide, disrupting the amphipathicity and in turn reducing activity against the HepG2 cell line compared with native Smp24.

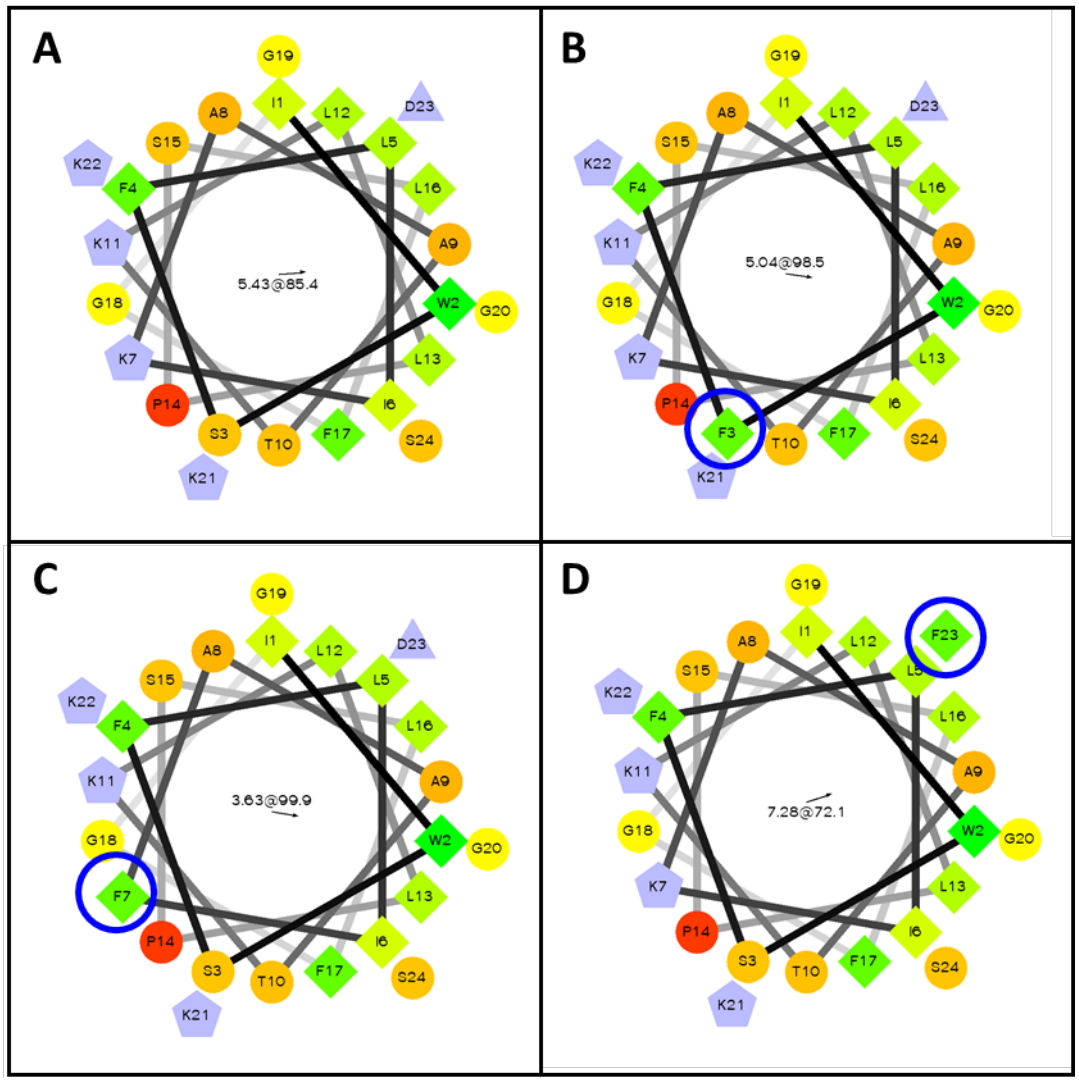

Figure 5.12: Helical wheel projections of Smp24 (A), Smp24 S3F (B), Smp24 K7F (C) and Smp24 D23F (D). The substituted residues are highlighted by rings.

5.5.3 Cytotoxicity of Smp43

All of the modifications to Smp43, except the W3A modification, resulted in increased cytotoxicity against the HepG2 cell line. The most cytotoxic Smp43 peptides within the study were S24K and S43K, both of which contain increased charge within the second helix of the peptide and increased clustering of charged residues within the helix, as shown in figure 5.13 (panels B and C). Against the HEK-293 cell line, all of the modifications except the W3A modification resulted in enhanced cytotoxicity.

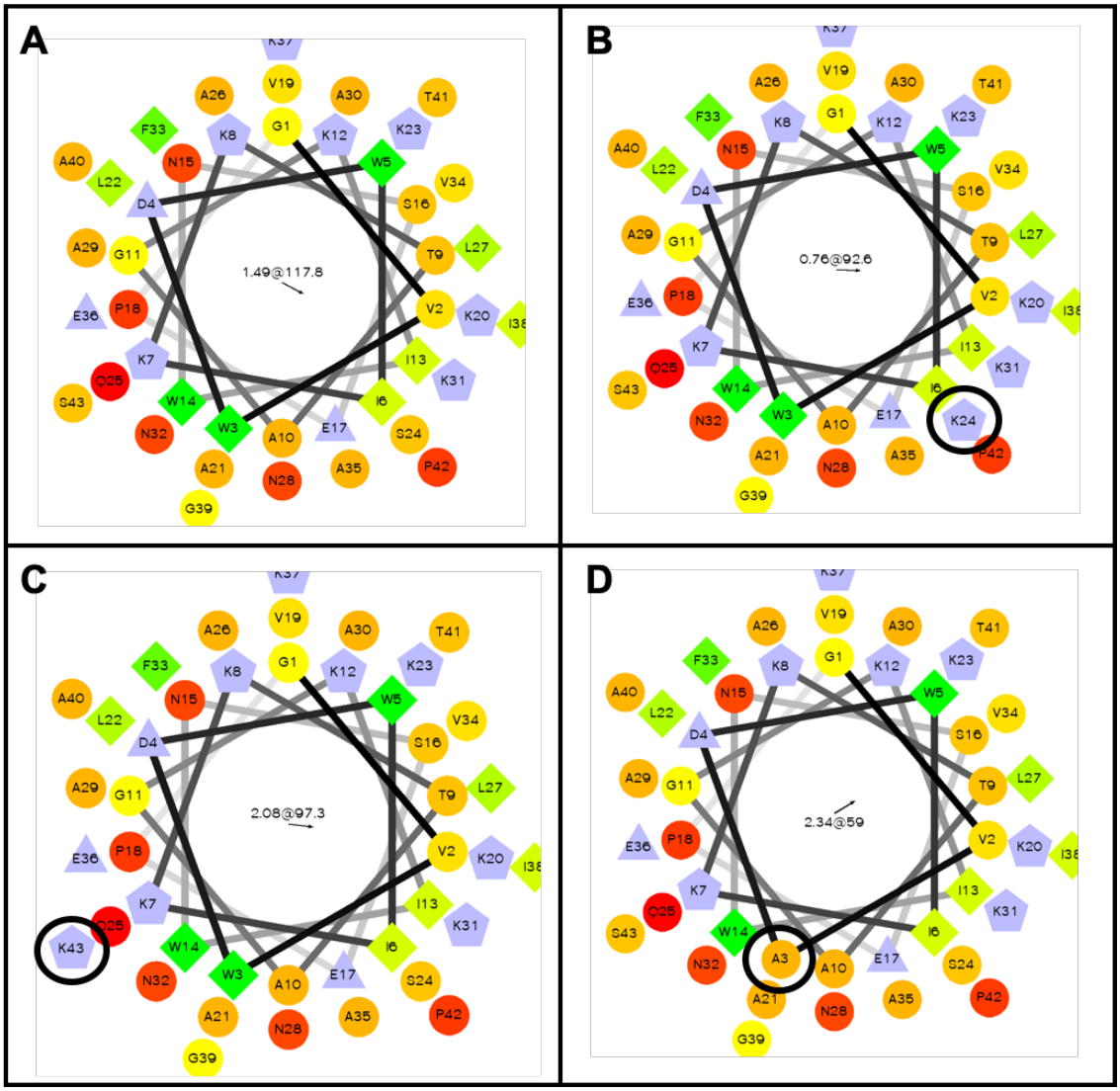

Figure 5.13: Helical wheel projections of Smp43 (A), Smp43 S24K (B), Smp43 S43K (C) and Smp43 W3A (D). The substituted residues are highlighted by rings.

As shown in figure 5.13, the W3A modification resulted in increased hydrophilicity of the helix. The reduced hydrophobic cluster of the peptide could be responsible for the reduced cytotoxicity observed by this modification. Tryptophan residues have previously been observed to be important for pore formation (Travkova *et al.* 2017), the results of this study suggest the selective substitution of tryptophan residues for alanine residues can reduce eukaryotic cytotoxicity.

5.6 Therapeutic indices

The therapeutic indices of the AMPs were calculated in order to assess any improvements or reductions to the peptides (chapter 2, section 2.7.5). Therapeutic indices were calculated by dividing the LD_{50} or HC_{50} by the calculated MIC against *E. coli.*

5.6.1 Therapeutic indices of modified Smp24 peptides

The results of the calculated therapeutic index (TI) calculations for Smp24 and derived modifications (figure 5.14).

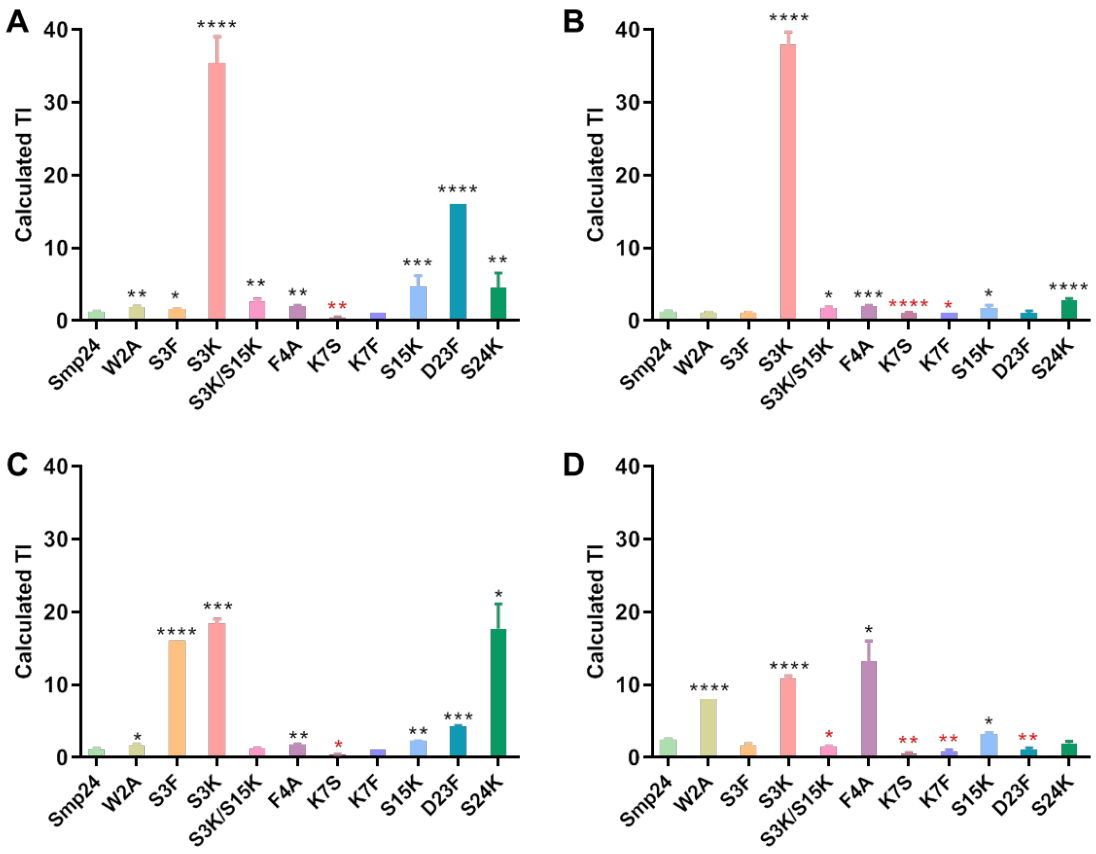

Figure 5.14: The calculated TI's of modified Smp24 peptides against HepG2 (A), HEK-293 (B), HaCaT (C) and sheep erythrocytes (D). Statistical significance was determined by performing a T-test on the data. Improvements to the TI are highlighted by the presence of black stars and reductions to the TI are highlighted by the presence of red stars .* p-value ≤0.05, ** p-value ≤0.01, *** p-value ≤0.001 and **** p-value ≤0.0001.

For the determination of the TI for peptides with a calculated LD_{50} above 512 µg/ml, 512 was used as the LD_{50} value. As shown in figure 5.14, improvements have been made to the TI of the modified peptides. The TI of the S3K and S15K modifications were significantly improved against all of the cell lines tested, with S3K demonstrating the greatest increase in TI. Similar results were observed for the S24K modification, which demonstrated significant improvements against all tested cell lines, excluding red blood cells which resulted in a non-significant decrease in the TI. The D23F modification resulted in a significant increase in TI when measured against HaCaT and HepG2 cell lines.

Conversely, significant decreases to the TI were also observed. The K7F modification demonstrated a reduced TI against all cell lines tested, though this was only deemed significant against HEK-293 and red blood cells. The K7S modification demonstrated significant reductions to the TI against all of the isolates tested.

The S3K, D23F and S24K modifications would be interesting candidates for further investigations as these modifications demonstrated enhanced therapeutic profiles compared with native Smp24.

5.6.2 Therapeutic indices of modified Smp43 peptides

The results for the TI calculations for Smp43 and the derived structural modifications are shown below in figure 5.15.

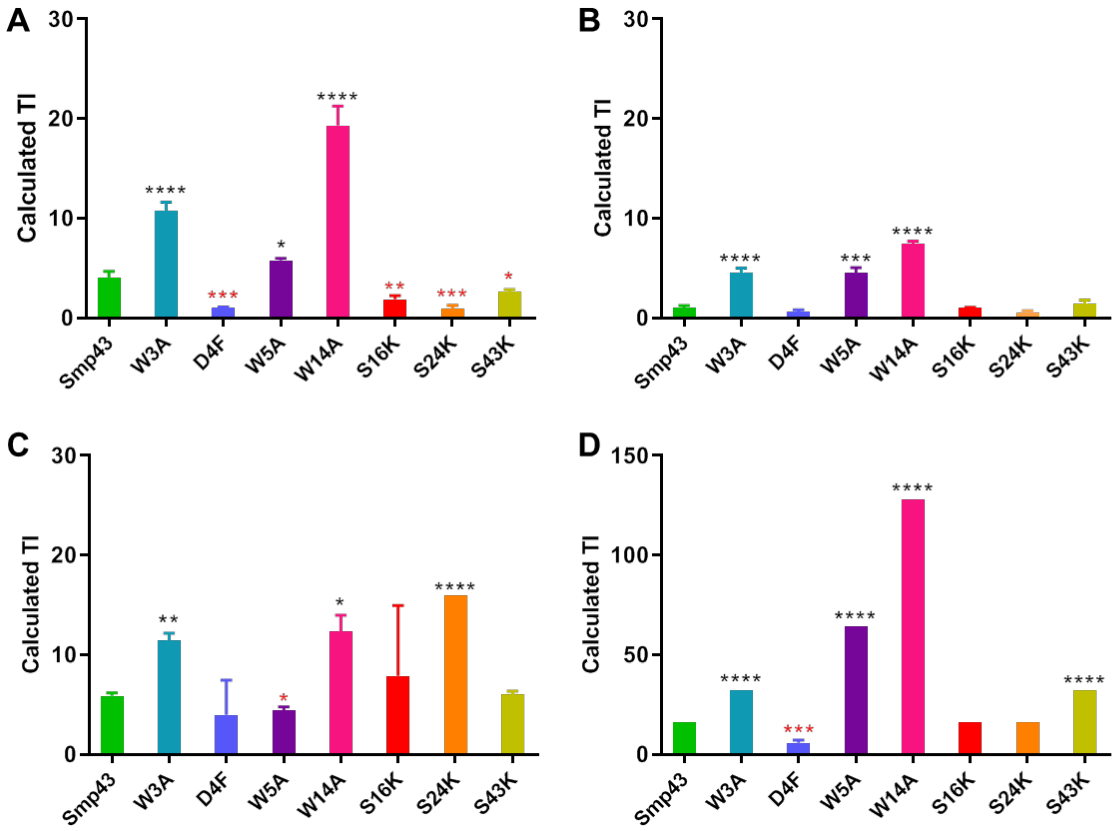

Figure 5.15: The calculated TI's of modified Smp43 peptides against HepG2 (A), HEK-293 (B), HaCaT (C) and sheep erythrocytes (D). Statistical significance was determined by performing a T-test on the data. Improvements to the TI are highlighted by the presence of black stars and reductions to the TI are highlighted by the presence of red stars. * p-value ≤0.05, ** p-value ≤0.01, *** p-value ≤0.001 and **** p-value ≤0.0001.

The structural modifications to Smp43 produced interesting results, with some of the peptides demonstrating increased TI against all cell lines tested. The W14A modification demonstrated a significantly increased TI against all cell lines tested. The W3A and W5A modifications also demonstrated increased TI against all cell lines tested, although statistical significance was only observed for three out of the four cell types for each peptide.

Reductions in the TI for the modified peptides were also observed, although no distinctive pattern was present. All of the structural modifications which increased the charge of Smp43 resulted in a decreased TI against HepG2 cells. The D4F modification reduced the TI of Smp43 against erythrocytes, whilst all the other peptide modifications resulted in an increase or a non-significant change in the TI against erythrocytes.

The W3A, W5A and W14A modifications would be interesting candidate peptides for further development as all of these peptides demonstrated increased TIs compared with native Smp43.

5.6.3 Therapeutic indices of peptides against urothelial cells

As differences in cytotoxicity were noted on the basis of membrane charge (section 4.4.4.3), the TI's of both parental peptides were calculated against the human uroepithelial cell line. As previously, the LD_{50} was calculated for both peptides using the upper limit value of 512, as the LD_{50} was calculated to be greater than 512 µg/ml.

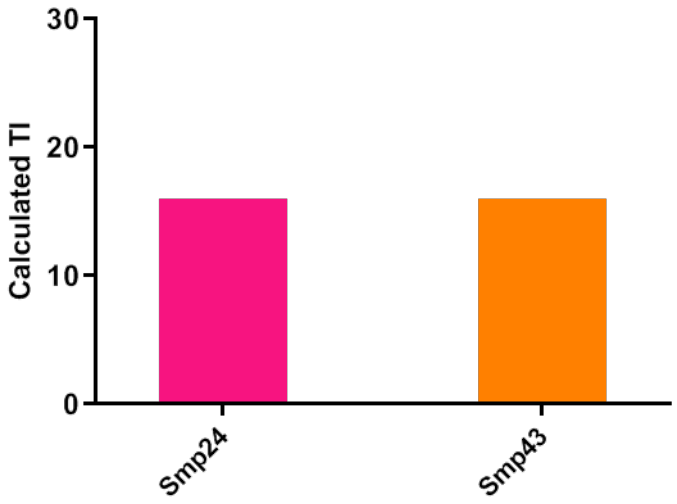

Figure 5.16: Calculated TIs for Smp24 and Smp43 against human uroepithelial cells (HUEPC).

When compared with the LD_{50} concentrations obtained for Smp24 against the other cell lines, the TI calculated against the uroepithelial cell lines was much higher. For Smp43, the TI against the uroepithelial was higher than that observed for the HaCaT, HepG2 and HEK-293 cell lines and equal to that observed for sheep erythrocytes.

5.6.3.1 Therapeutic indices of lipopeptide antibiotics

The TI's of the lipopeptide antibiotics used within this study were also calculated. As daptomycin is only commercially licensed for the treatment of Gram positive organisms and demonstrated no activity against the Gram negative isolates within this study, the TI was determined against *S. aureus.* The TI of PMB was determined against *E. coli* as per all of the other AMPs within this study (figure 5.17).

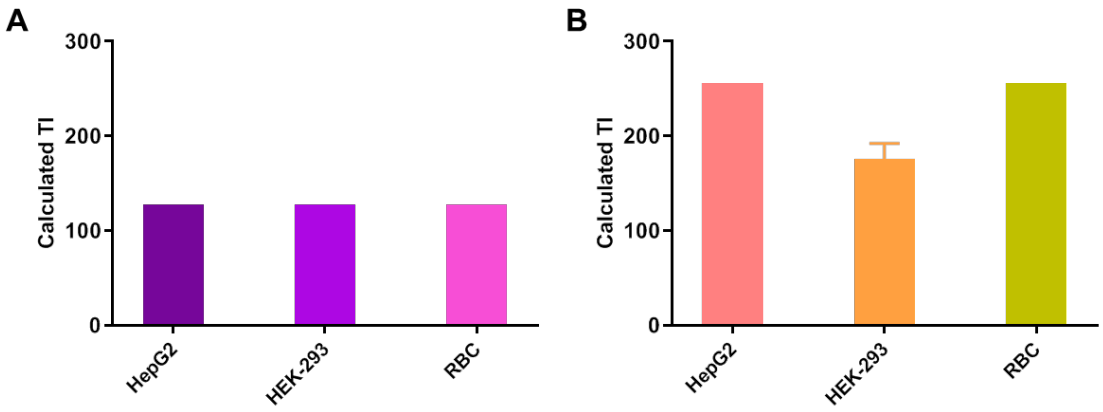

Figure 5.17: Calculated TI's of daptomycin (A) and PMB (B) against liver, kidney, skin and red blood cells.

As shown in figure 5.17 the calculated TI's of the two commercially available AMP-like drugs are very high. The drugs demonstrate high antimicrobial activity and a low level of cytotoxicity, which produces a highly desirable drug profile.

When comparing the TI of the modified Smp peptides to those obtained by the AMP-like drugs, the TI's are considerably lower. The lipopeptide antibiotics demonstrate TI's between 128 and 256, with PMB possessing the highest TI of the two lipopeptide antibiotics within this study. The activity of the W14A modified peptide produced a TI of 128 against erythrocytes, which is comparable to the calculated TI of 128 for daptomycin within this study. The highest TI observed from the Smp24 modification was 38 for S3K when calculated against HEK-293 cells.

As cytotoxicity is an important factor for the calculation of the therapeutic index, the TI varies greatly dependent upon the cell line used (figure 5.18). Greater TIs were observed for both peptides against HUEPC cells compared with the skin, liver and kidney cell lines.

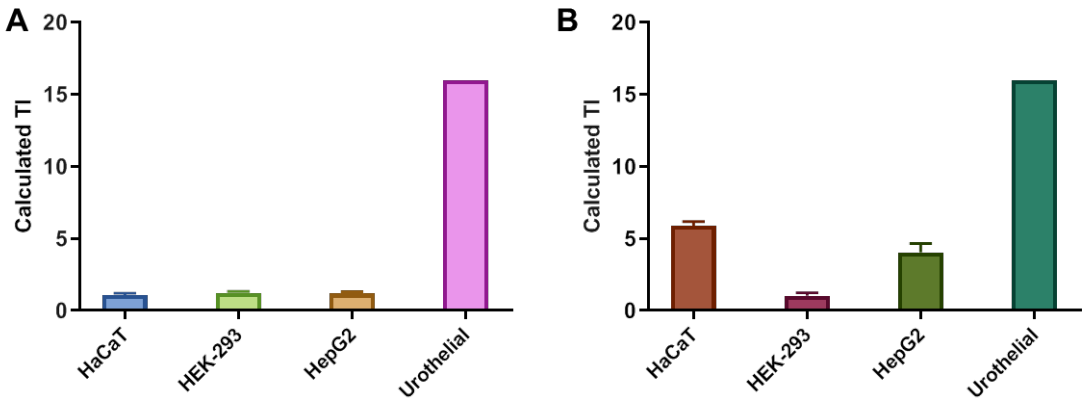

Figure 5.18: Observable differences in TI for Smp24 (A) and Smp43 (B) against all cell lines used in this study.

The TI of the AMPs varies greatly between the cell lines used with the urothelial cells producing the highest TI for both Smp24 and Smp43. This highlights the importance of a cytotoxicity screen encompassing numerous cell lines when pre-screening peptides for further development.

5.7 Conclusions

In summary, two modification strategies have been employed within this study; one was investigating the effect of charge on function and the other investigating the role of hydrophobicity. AMPs have been developed with enhanced antimicrobial activity compared with the native peptides. Currently, the peptides are rather large (Smp24: 2578 Da and Smp43: 4654 Da) when compared with the size of small molecule compounds such as penicillin (334 g/mol), gentamicin (477 g/mol) and also against the lipopeptide antibiotics daptomycin (1620 Da), polymyxin B (1301 Da). Truncation of the peptides could enable the active moiety of the peptide to be determined. If the peptides can be successfully truncated, this would reduce production costs by solid phase synthesis and potentially create a drug with greater therapeutic potential.

The modifications to Smp24 generally increased the haemolytic activity of the peptides. The only exceptions to this are the W2A, F4A and K7F modifications which had significantly improved HC_{50} concentrations. Despite the observed increased haemolysis, peptides with enhanced therapeutic indices have been produced. The S3K, F4A, D23F and S24K modifications produced enhanced TIs against all cell types tested and would be interesting candidates for further investigation.

The modifications to Smp43 resulted in increased cytotoxicity towards HepG2 cells and HEK-293 cells, with the exception of W3A. Three of the peptides within the study (D4F, S16K and S24K) demonstrated reduced cytotoxicity towards the HaCaT cell line and all of the peptides except D4F demonstrated a low level of haemolysis. Three peptides produced enhanced TIs against all cell lines tested, which are the W3A, W5A and W14A substitutions.

The incorporation of unnatural amino acids in to more potent AMPs, would be an interesting strategy to adopt to determine if peptides with a reduced susceptibility to proteolytic degradation could retain the antimicrobial profile of their naturally occurring counterparts (Kang *et al.* 2017b). Whilst resistance to AMPs is not expected, it is important to take precautionary measures to avoid facing the same issues faced with antibiotic development. The ability of bacteria to develop

resistance to AMPs was not within the scope of the study but would be an interesting future direction. Resistance to the peptides could be assayed by multiple passages of the peptides at sub-inhibitory concentrations in liquid culture and observing the effect serial passaging has on the MIC of the bacteria (Perron *et al.* 2006).

Cytotoxicity screening was limited due to the cost of peptide synthesis, which produces small quantities of peptides at high cost. The peptide synthesis also restricts the number of modifications that can be performed, due to the cost implication. The next stage of the project would be to develop a method for recombinant production of the AMPs to remove the cost and quantity factors that limit the project currently.

The "in-house" production of AMPs would enable larger quantities of the peptides to be produced, which would in turn enable a more comprehensive antimicrobial and cytotoxicity screen to take place. Additionally, the peptides could be mutated via recombinant techniques, such as site-directed mutagenesis, to produce a library of mutants. This would enable more residues within the AMPs to be substituted to more thoroughly investigate the relationship between structure and function. The development of an expression system would also be of interest from a pharmaceutical point of view, as the scaling up of the process would enable large quantities of the peptide to be produced at a low cost and thus optimising the potential financial return on the final product.

6

Optimisation of the recombinant production of venom-derived peptides in *E. coli* BL21

6.1 Introduction

Antimicrobial peptides have previously been produced using chemical synthesis, with solid-phase synthesis often being the method of choice (Münzker *et al.* 2017). This methodology is capable of producing peptides with high purity (Wanmakok *et al.* 2018) however, the production of peptides in large quantities is limited due to the high overall cost (Hancock 1997). Investigations to produce bioactive peptides under optimised conditions at a reduced cost and decreased time scale is ongoing (Agyei and Danquah 2011) and recombinant methodologies are becoming of increasing interest.

Protein production by recombinant DNA technology is much less expensive and has been used previously to successfully produce antimicrobial peptides (AMPs) (Yang *et al.* 2016, Wanmakok *et al.* 2018). *E. coli* is often used as the vector of choice due to the ease of genetic manipulation, relatively low cost and rapid growth rate (Tanhaiean *et al.* 2018b). Recombinant expression does however face its own challenges; these include proteolytic degradation by microbial cells, the protein being expressed in to inclusion bodies or cellular toxicity of the recombinant peptide on the producer cells (Ashcheulova *et al.* 2018). If these issues can be overcome, a recombinant protein production system can be used to produce large quantities of AMPs at relatively low costs.

Smp24 has previously been described in chapters 3 and 4. It demonstrates broad spectrum antimicrobial activity, making it an interesting drug development prospect. Whilst Smp43 demonstrates lower mammalian cytotoxicity than Smp24, the large size of Smp43 is a restrictive factor in terms of drug development. Due to this, the strategy to develop an “in-house” recombinant expression system has initially been limited to Smp24.

One of the major limiting factors when working with the synthetically produced peptides has been the quantity available for assay, which ranged between 10 and 15 mg for the purpose of this study. The development of a recombinant protein expression system would enable larger quantities of Smp24 to be produced, which would enable a more extensive investigation in to the antimicrobial activity of the peptide in addition to a thorough eukaryotic cytotoxicity screen.

6.2 Study aims

The main aim of this chapter was to develop a recombinant expression system for the over production of Smp24 to determine whether peptides produced in this recombinant system would retain their native activity.

The second aim of this chapter was to produce a library of mutant peptides using site-directed mutagenesis, initially based upon the results from chapter 3 (section 3.4.2.2) to inform the relationship between structure and function.

6.3 Experimental design

6.3.1 Recombinant expression of antimicrobial peptides in *E. coli*

Following the successful production of recombinant neurotoxins in an *E. coli* expression system (Lyukmanova *et al*., 2007), a similar strategy was adopted to express the previously described scorpion venom-derived peptide, Smp24. Smp24 is 24 amino acids in length with a molecular mass of 2.578 kDa and belongs to the short-chain family of scorpion AMPs (Abdel-Rahman *et al.* 2013).

The expression system described by Lyukmanova *et al,* for the recombinant production of neurotoxin II (NTII) in *E. coli* is shown in figure 6.1. The expression system was developed in the expression vector pET22b. pET22b vectors are T7 promoter vectors, which enable high-level protein expression. The system is ideal for expressing soluble, non-toxic proteins in due to the low production cost and ease of use.

In the Lyukmanova *et al*., (2007) study, the signal peptide from heat-stable *E. coli* enterotoxin (STII) was fused to the N-terminal of a gene encoding the peptide sequence for neurotoxin II (NTII). Upon protein expression, a special signal-recognising particle (SRP) binds to the signal peptide in the bacterial cytoplasm, which is then transferred to the inner membrane. Situated at the inner bacterial

cell membrane is a membrane translocation complex. The primary protein constituents of the bacterial complex are Ffh (an SRP54-like protein of eukaryotes) and FtsY (an SRP receptor [subunit]-like protein of eukaryotes) which is thought to use ATP to carry the protein to the SecYEG complex in the periplasmic space with the signal peptide acting as a membrane anchor (Saier 2006). The signal peptide is then cleaved at the external side of the internal membrane, thereby leaving the innate N-terminal of the protein of interest. The protein, or in this case neurotoxin, can then accumulate in the periplasmic space but may also accumulate in the culture media (Lyukmanova *et al*., 2010).

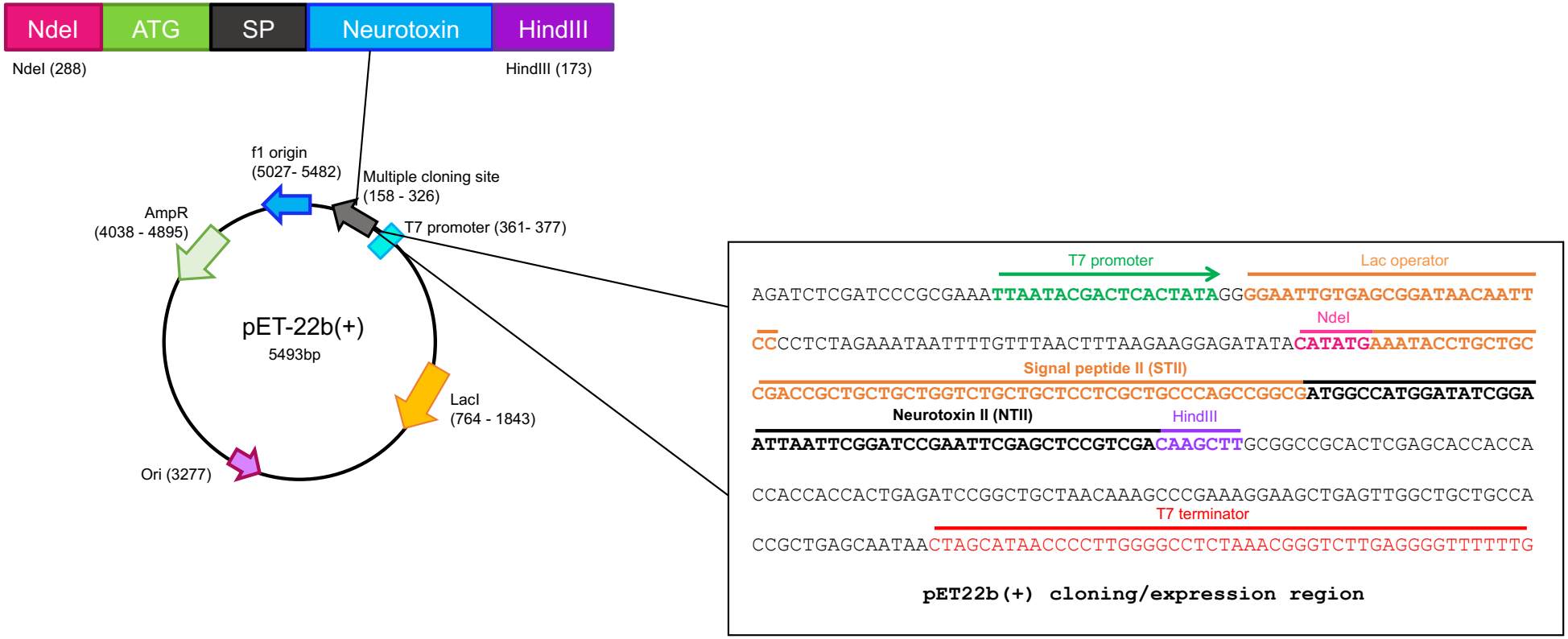

Figure 6.1: Vector design for the expression of neurotoxins in *E. coli.* The synthetic genes for neurotoxins were attached to the signal peptide of *E. coli* heat-stable enterotoxin (STII) (NCBI accession number M35729) and spliced between the NdeI and HindIII restriction sites of pET22b(+).

The gene insert for the signal peptide coded for expression of the neurotoxin shown in table 6.1.

Table 6.1: The amino acid sequence for the signal peptide (STII) and neurotoxin II sequence (NTII) is shown in black.

Construct	Amino Acid sequence
STII/NTII	MKKNIAFLLASMFVFSIATNAYALECHNQQSSQPPTTKTCSGETNCYKK WWSDHRGTIIERGCGCPKVKPGVNLNCCRTDRCNN

The amino acid sequence for STII is shown in blue and the NTII sequence is shown in black. A 252 bp insert was spliced in to the pET22b(+) vector (Novagen) between the NdeI and HindIII restriction sites.

The system used by Lyukmanova *et al,* (2007) expressed neurotoxins in minimal media (M9) to produce toxins for downstream experiments with nuclear magnetic resonance (NMR) and electrophysiology. This process yielded 1 - 20 mg quantities of neurotoxins per litre of culture media, which varied depending on the presence of disulphide bonds in the neurotoxins. Neurotoxins with more disulphide bonds typically produced smaller quantities of peptides in the recombinant system. This strategy was to be adopted for the expression of antimicrobial peptides in *E. coli* due to the previous success observed.

6.3.2 Experimental design for the overproduction of Smp24 protein

The strategy adopted for the recombinant expression of Smp24 genes and overproduction of the protein is shown in figure 6.2.

Briefly, a vector for the expression of an Smp24 gene to produce Smp24 protein was designed, transformed in to an expression vector and induced for protein overproduction. The recombinant protein was purified and the presence of the protein validated via numerous techniques, including traditional gel electrophoresis and matrix-assisted laser-desorption ionisation mass spectrometry (MALDI-MS).

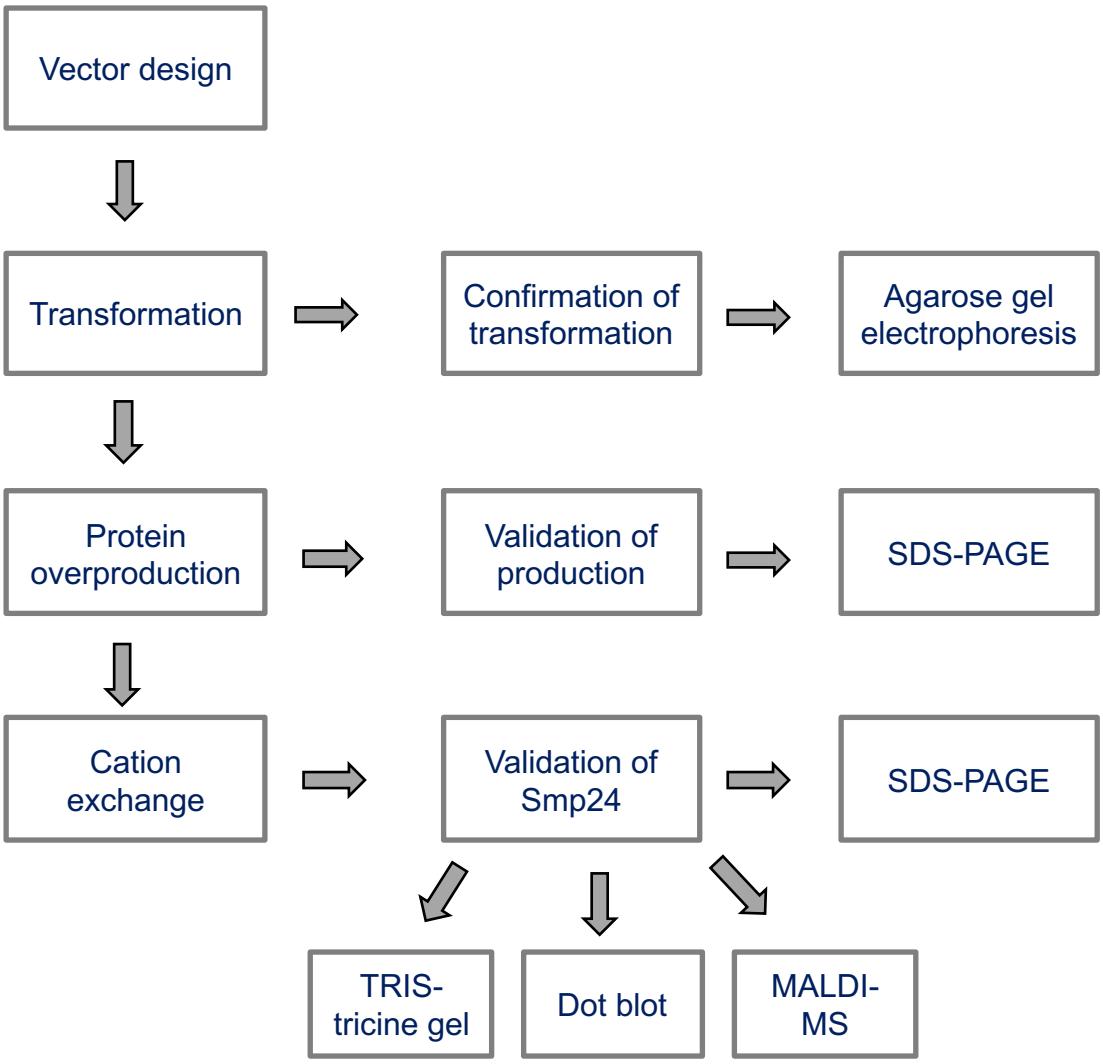

Figure 6.2: Strategy for the production of recombinant Smp24 in a prokaryotic expression system.

6.3.3 Vector design for the expression of Smp24

To enable the overproduction of Smp24, the Lyukmanova *et al,* protein expression system was modified. The genetic sequence for a gene encoding Smp24 conjugated with the STII insert was calculated using *E. coli* codon usage tables which yielded the highest frequency of successful incorporation. The sequence for the insertion of the Smp24 gene is shown in figure 6.3. Start and stop codons were included on each respective end of the gene fragment to allow the expression of the gene of interest. The genes were incorporated in to the vector by the Standard Genes gene synthesis program offered by Eurofins (Ebersberg, Germany). The pET22b vector was purchased from Novagen (Darmstadt, Germany).

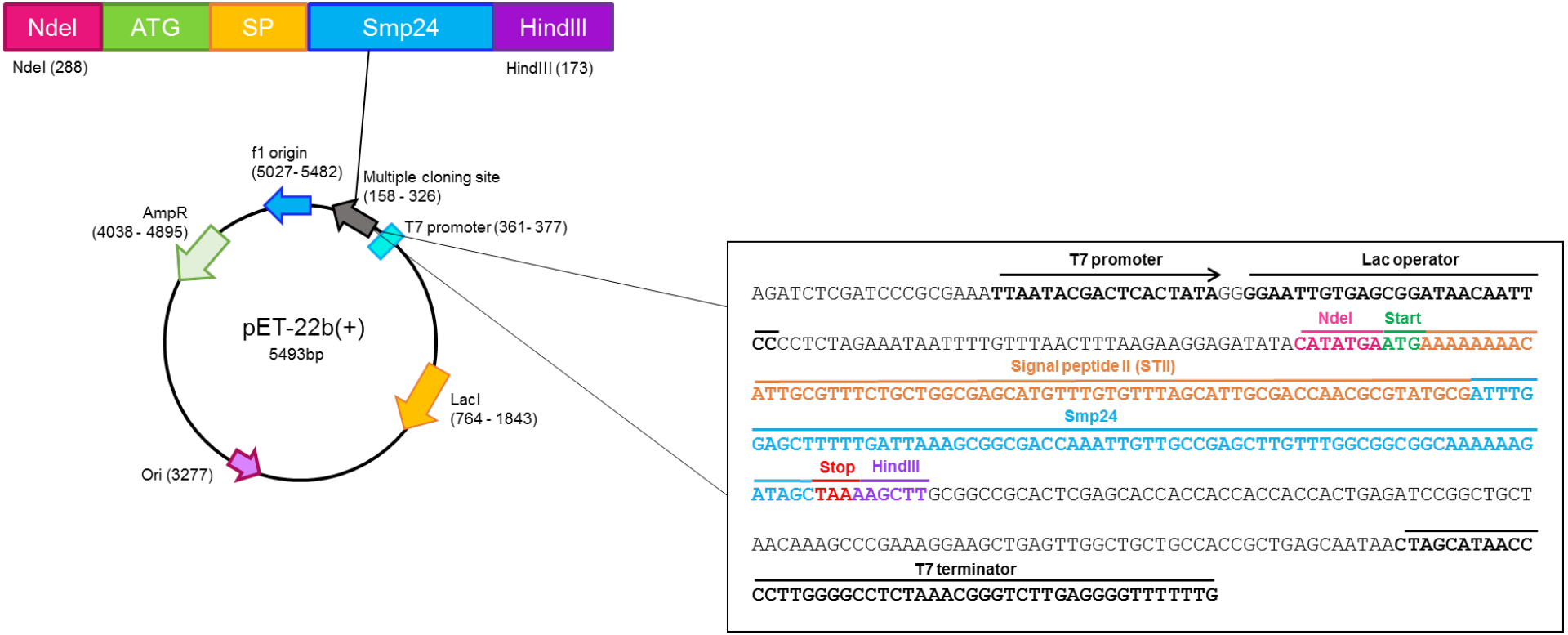

Figure 6.3: pET22b(+) vector map and the corresponding codon usage sequences for STII and Smp24 for insertion of the gene between the HindIII and NdeI restriction sites. The insert between the two restriction sites was 144 bp in length, coding for the expression of Smp24 and the signal peptide.

6.3.4 Transformation & Confirmation of transformation

To produce Smp24 in *E. coli* BL21 λDE3, the pET22b/STII/Smp24 vector was transformed into the expression strain by electroporation (section 2.10.1). To confirm successful transformation, plasmids were extracted and the T7 cloning region amplified by PCR and the PCR product was visualised on a 1% agarose gel with 0.01% ethidium bromide. The PCR product was expected to be 409 base pairs in length.

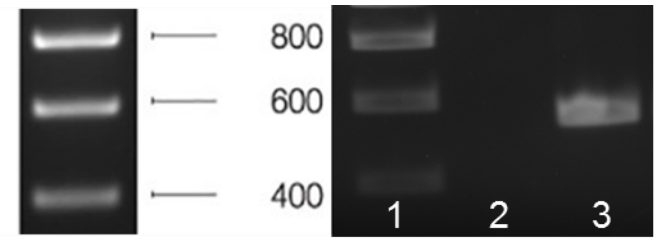

Figure 6.4: Visualisation of the PCR product from the extraction of pET22b/STII/Smp24 from *E. coli* BL21 λDE3. Primers which flanked the T7 expression region were used. Well (1) 1 kb Hyperladder (Bioline, London, UK), (2) no DNA control and (3) STII/Smp24 insert.

6.3.5 Recombinant production of Smp24 protein

E. coli BL21 λDE3 pLysS strain was chosen for the expression vector as *E. coli* BL21 strains are widely used for the expression of target proteins encoded by pET vectors. This strain is deficient in Ion and ompT proteases, which is advantageous for protein expression due to reducing the likelihood of degradation of the recombinant peptide. DE3 indicates that the host is a lysogen of λDE3, and therefore carries a chromosomal copy of the T7 RNA polymerase gene under control of the lacUV5 promoter. This enables the production of protein from target genes cloned in to pET vectors via induction with IPTG. The pLysS strains express T7 lysozyme, which suppresses basal expression of T7 RNA polymerase prior to induction, which stabilises pET recombinants encoding target proteins that affect growth and viability.

To overproduce the Smp24 protein, an overnight culture of *E. coli* containing the pET22b/STII/Smp24 vector was prepared in LB broth with ampicillin and protein production was induced by the addition of IPTG (section 2.12). Due to the presence of the STII leader sequence, it was anticipated the Smp24 protein would be transported out of the cell and in to the culture media.

6.3.6 Validation of protein overproduction

Following the overproduction of Smp24, the recombinant protein was separated from the bacterial culture (section 2.12). The results of the protein overproduction were initially visualised on a 10% standard sodium dodecyl-sulphate polyacrylamide gel electrophoresis (SDS-PAGE) gel and stained with Coomassie blue prior to purification (figure 6.5).

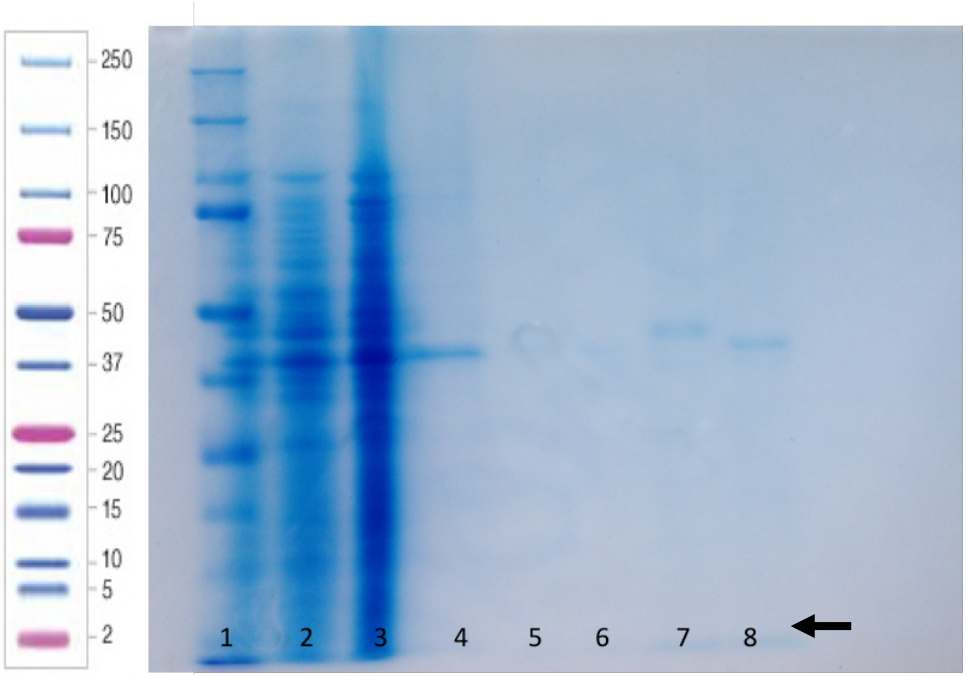

Figure 6.5: SDS-PAGE gel of the overproduction of Smp24 in *E. coli.* (1) Dual Xtra Precision Plus standard (Bio-Rad), (2) pellet before IPTG induction, (3) pellet following IPTG induction, (4) pellet from second centrifugation, (5 to 8) culture media supernatant. The arrow represents the expected size of the recombinant protein (2.5 kDa).

As shown in figure 6.5, it was not possible to identify the recombinant Smp24 protein in the culture media. The resolution of the gel in the low molecular range prevented the successful identification of the Smp24 protein (2.5 kDa). Due to the

protein being eluted in to the supernatant, it was anticipated the concentration of the produced protein would be low which would further inhibit the visualisation of the protein. Due to the low cost of purification by column chromatography, it was decided to continue with the purification process.

6.3.7 Protein purification

The next stage of the process was to purify recombinant Smp24. Due to the highly charged nature of Smp24 (+3), it was expected that the peptide would strongly bind to the column and any impurities would bind to the column more weakly and thus elute first. The culture media supernatant was diluted 2-fold with Milli-Q deionised water and applied by peristaltic pump to a Sepharose Fast Flow Resin column (GE Healthcare, Buckinghamshire, UK) for cation exchange. The protein was eluted against a sodium chloride (NaCl) gradient from 0 - 1 M NaCl at 4°C using the AKTA Design system (GE Healthcare, Buckinghamshire, UK). Protein elution was monitored by observation of the UV range at 280 nm (figure 6.6).

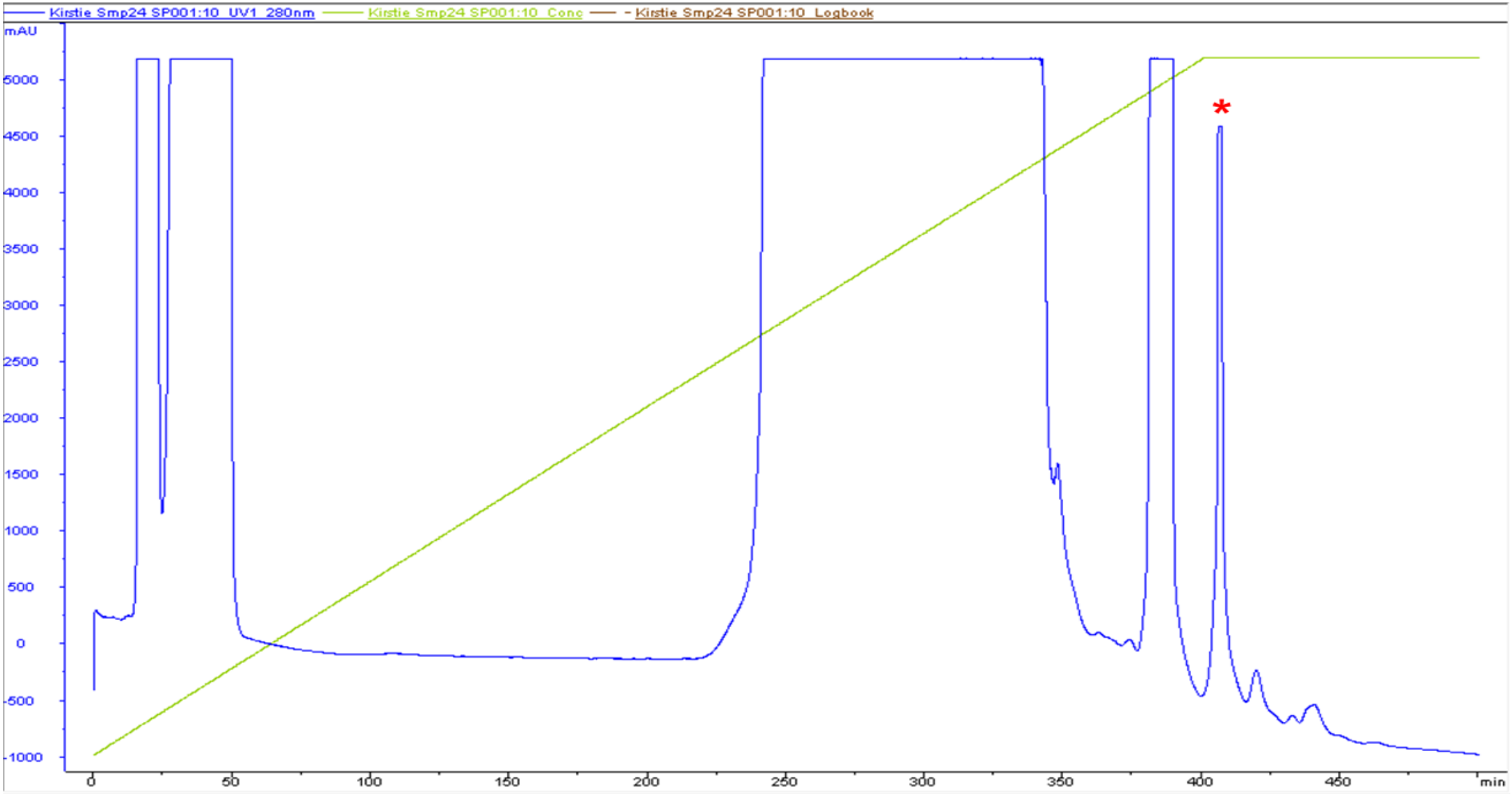

Figure 6.6: Purification of Smp24 - A_{280} trace for the purification of overproduced protein. Each peak represents the elution of peptide bound to the column. The fraction containing the asterisk denotes the fraction expected to contain Smp24, due to the highly charged nature of the peptide.

The peaks on the A_{280} AKTA trace indicate the presence of protein, specifically proteins with a cationic charge due to the cation exchange column used for purification. The more positively charged peptides bind more strongly to the column and thus require a greater salt concentration for elution. The sample suspected to contain Smp24 was strongly bound to the cation exchange column and required a 1 M NaCl concentration to elute from the column after 400 minutes.

All samples from the purification process were collected for further analysis, to confirm the identity of the protein from all of the fractions.

Whilst the above trace was cause for optimism due to the presence of large protein peaks, the results were not reproducible. The protein expression process was repeated from transformation of the plasmid in to the expression vector and the induction of protein production under the same conditions. Despite conditions remaining identical, difficulties were experienced producing replicable results for the recombinant expression and purification of Smp24 in *E. coli*. The trace depicting the elution of samples from the column was not reproducible and a peak at the retention time of 400 minutes was not observed in subsequent purification attempts.

6.3.8 Validating the presence of Smp24

6.3.8.1 SDS-PAGE

Validating the presence of the peptide in the AKTA fraction proved to be challenging. The peptide was impossible to visualise on an SDS-PAGE gel, due to the small size (2.5 kDa). The concentration of acrylamide within the SDS gel was optimised by increasing the acrylamide concentration up to 20% in the separation gel yet the resolution of the gel in the small molecular weight range was still not sufficient.

6.3.8.2 TRIS-tricine PAGE

Following unsuccessful identification of the peptide by SDS-PAGE, the next approach to visualising the peptide was TRIS-tricine gels. Tricine gels offer much higher resolution for peptides with a molecular weight below 10 kDa. The increased resolution is achieved by slowing the migration rate of peptide-SDS complexes which helps separate smaller peptides from faster moving SDS-micelles which interfere with the resolution at the smaller molecular weight range. A series of TRIS-tricine gels were produced to identify the peptide of interest.

Gels within the range of 10-20% were analysed but the resolution remained poor at the low molecular weight range. It was theorised the highly charged nature of the peptide could also contribute to the challenges of visualisation on the gel. The positive charge of the peptides could prevent the peptides from entering the gel, as they could move towards the negative electrode prior to electrophoresis. Peptides with increased hydrophilicity can also demonstrate a decreased propensity to enter the gel. The anticipated low concentration of the peptide could have also inhibited the ability to detect the peptide. Alternatively, it was also possible the peptide was not always present in the culture and therefore not possible to detect. To improve the limit of detection, a mass spectrometry approach was taken to identify the peptides.

6.3.8.3 Matrix assisted laser desorption/ionisation time of flight mass spectrometry (MALDI-TOF MS)

MALDI-TOF MS was used to identify the eluted peptides, as shown in figure 6.7. The protein samples from AKTA purification were co-crystallised with α-cyano-4-hydroxycinnamic-acid (CHCA) matrix on a target plate. The plate was analysed on the Bruker Autoflex III Smartbeam MALDI-TOF (Massachusetts, USA) (figure 6.7).

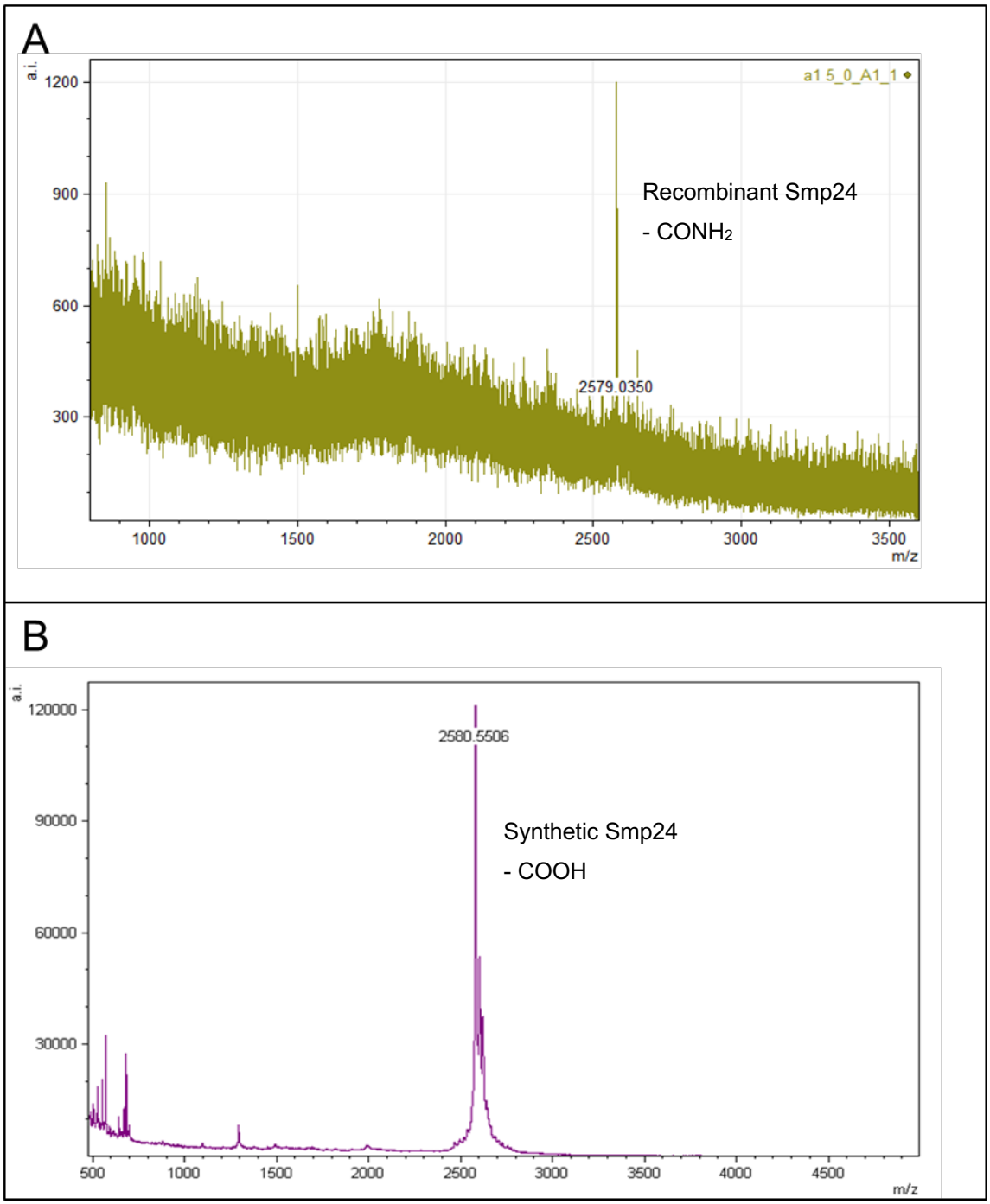

Figure 6.7: MALDI-MS spectral identification of Smp24. (A) MALDI-MS spectra from the analysis of the labelled peak from the AKTA trace from figure 6.6. (B) MALDI-MS spectra from the analysis of Smp24 as synthesised by solid-phase synthesis.

The mass of the protein fraction determined by MALDI-TOF MS (2579 Da) was consistent with that expected of Smp24 (2578 Da). Up to 2 Dalton differences have previously been observed between the natural and synthetic peptides within the literature (Kim, Kang, *et al.* 2018). Mass differences were observed within this study as the synthetically synthesised Smp24 demonstrating a mass of 2580 Daltons. The mass difference between synthetic and recombinant protein could be attributed to post-translational modifications, such as amidation, phosphorylation, hydroxylation or methylation (Grangeasse *et al.* 2015) which would result in a minor increase in the molecular mass of the peptide. Identification of a peptide of the expected size was sufficient confirmation to proceed with additional purification steps in this instance.

6.3.8.4 Detection of Smp24 in the presence of salt

As previously discussed, issues with the reproducibility of the AKTA traces were faced and peptides with a mass similar to that of Smp24 were not identified in subsequent purification attempts. Whilst initially the presence of salt had not inhibited the detection of protein, the presence of salt can influence the ionic nature of charged peptides. Two additional experiments were carried out. Synthetic Smp24, synthesised by solid phase synthesis was used as a mass control for the instrumentation. The peptide flew down the MALDI and presented at the mass range expected. The sample was then dissolved in 500mM NaCl to deduce the effect of salt. The results of this experiment are shown in figure 6.8.

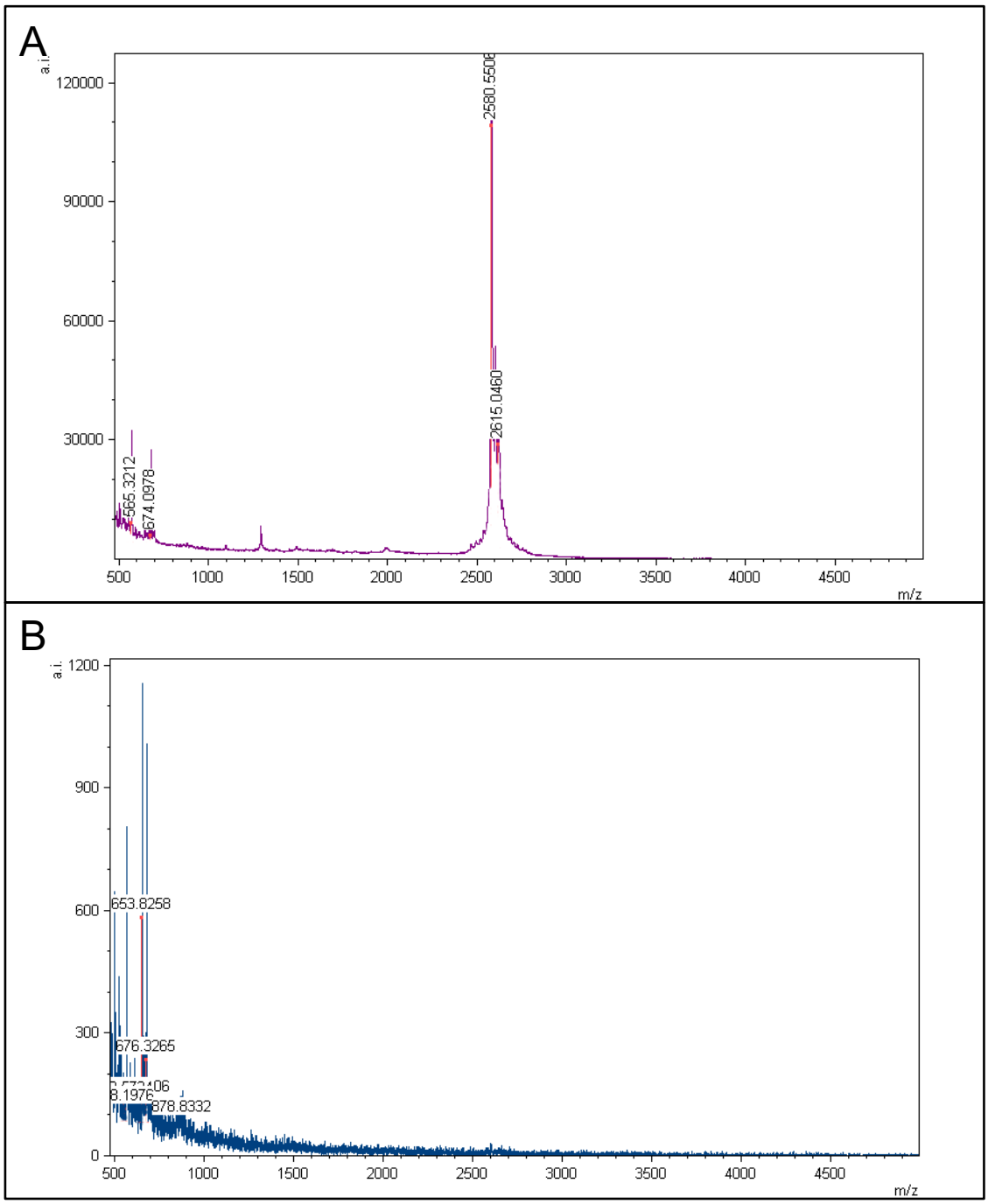

Figure 6.8: MALDI MS analysis of Smp24. Synthetic Smp24 (A) shows a peak at the mass range expected (2.5 kDa) but in the presence of 50 mM NaCl (B) the peptide can no longer be detected.

As shown in figure 6.8, the presence of salt inhibited the detection of synthetic Smp24 via MALDI MS, with no peak present in the mass range expected. As a result, the purified samples were de-salted via Zip-Tips and analysed via MALDI-MS. It was still not possible to detect peptides in the mass range expected for Smp24 via mass spectrometry methods. At this point it was not known if the issue

faced was related to detection or if there was an issue with the protein over-production and the peptide was not present at all.

6.3.9 Additional protein purification

The sample from figure 6.8 (from the AKTA purification peak containing a protein of the expected mass range) was de-salted by membrane dialysis, lyophilised and re-suspended for further purification to remove any additional impurities. The sample was purified using a second cation exchange column, a MonoS HR5/5 column (GE Healthcare, Massachusetts, USA) equilibrated with 10 mM CH_3COONa pH 5.0 (figure 6.9).

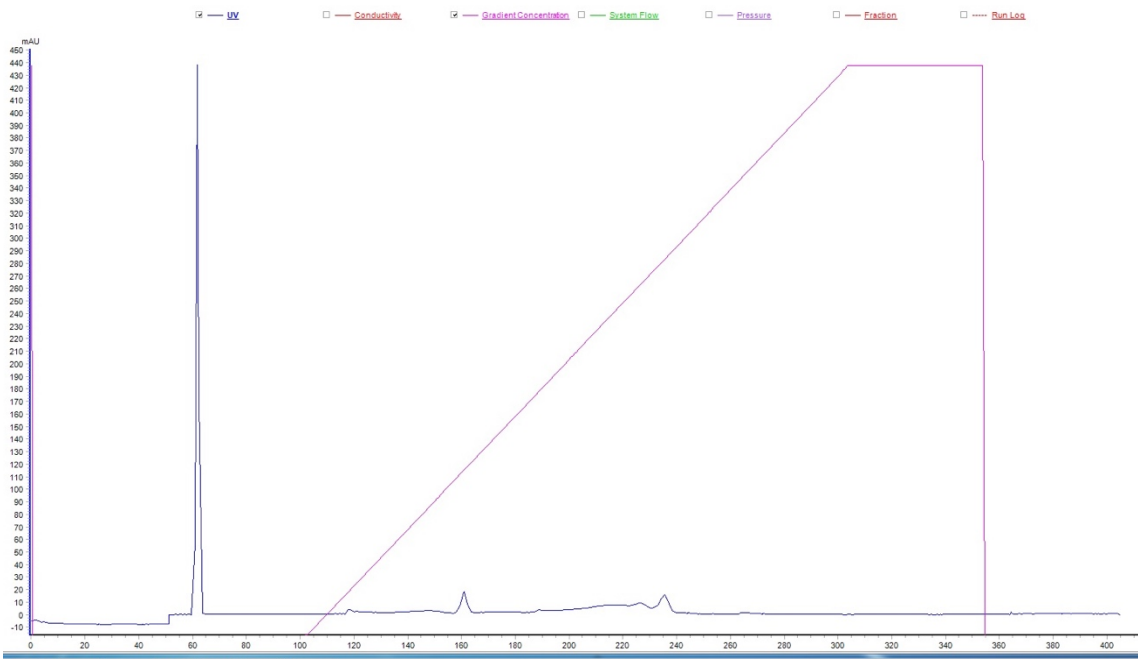

Figure 6.9: AKTA A_{280} trace for additional purification of Smp24. The column was equilibrated with sodium acetate buffer and the sample applied under the same conditions.

As shown in figure 6.9, the attempt to additionally purify Smp24 was unsuccessful. Despite the column being washed with 5 column volumes of buffer and equilibrated to the conditions required for protein binding, the sample did not bind to the column. The sample was also diluted in the same sodium acetate

buffer to further encourage binding to the column. Unfortunately, the sample not binding to the column resulted in the sample flowing straight through the column and in to the waste, preventing further analysis from being performed on this sample.

As difficulties were being faced with the detection of produced protein from the purification fractions, an immunological approach was taken.

6.3.10 Immunological detection of Smp24

Polyclonal antibodies against Smp24 were raised in rabbits following a SuperFast 28 day immunisation schedule by David's Biotechnologie (Regensburg, Germany). The 28-day protocol yields antibodies with titres comparable to standard 63 or 90 day procedures.

The sensitivity of the antibody was determined by performing dot blots with a titration of 0-10 mg/ml concentration of synthetically synthesised peptide standards (David’s Biotechnologie). It was determined the antibodies detected the presence of Smp24 to a concentration of 31 µg/ml dissolved in water. When the peptide was dissolved in broth, that the detection limit was reduced to 125 µg/ml (figure 6.10).

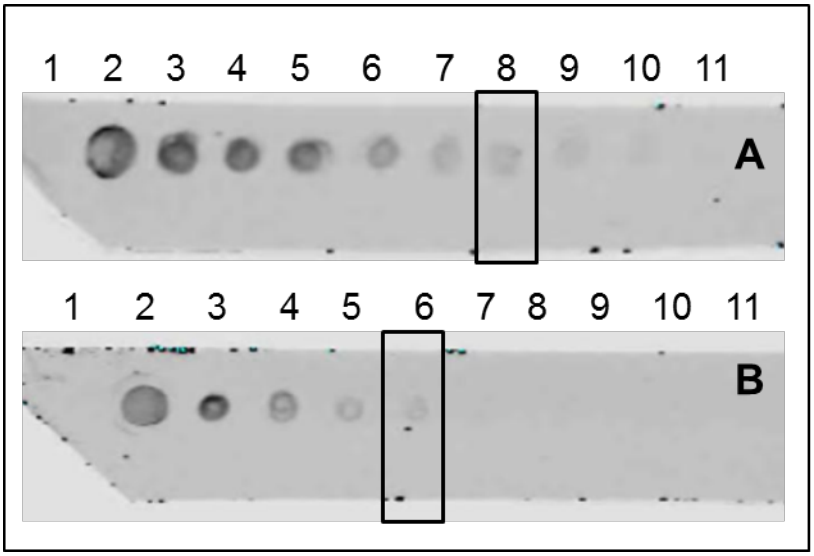

Figure 6.10: Optimisation of antibody detection using dot blot for the detection of Smp24. Synthetic peptide dissolved in H_2O is shown in A and synthetic peptide dissolved in M9 broth is shown in B. (1) BSA control. (2) Smp24 (10 mg/ml). Rows 3 - 10 - dilutions of peptides. (3) 1 mg/ml, (4) 500 µg/ml, (5) 250 µg/ml, (6) 125 µg/ml, (7) 62.5 µg/ml, (8) 31.75 µg/ml, (9) 16.125 µg/ml, (10) 8.09 µg/ml (11) Negative binding control (water or M9 broth). The limit of detection is highlighted by the box.

Following the induction of protein expression and the separation of the cell pellet and supernatant by centrifugation, the pellet and supernatant was analysed by dot blot (figure 6.11). Despite the binding affinity of the antibodies being validated from former assays, it was not possible to detect Smp24 from the overproduction samples. The protein over production system remained blind and it was not known if the peptide was being expressed or if the limit of detection for the expressed peptides was not low enough to detect the expressed proteins within the culture supernatant and therefore a lower concentration than 100 µg/ml.

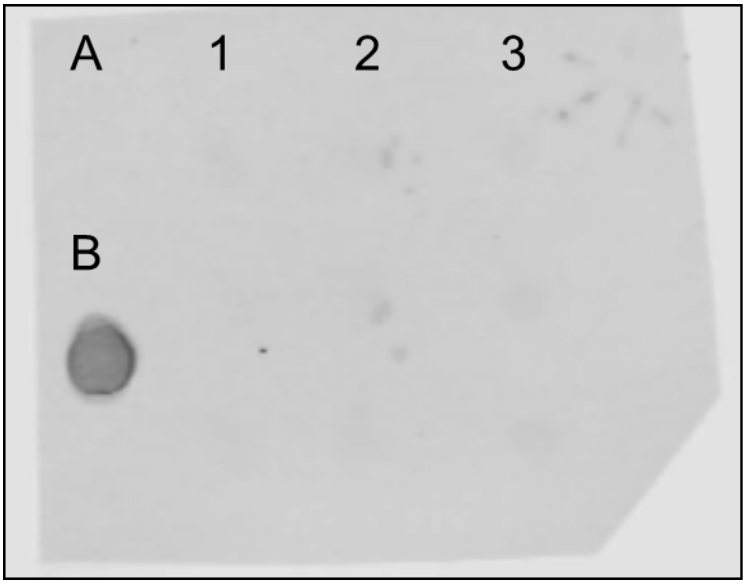

Figure 6.11: Immunological detection of expressed proteins in *E. coli.* A - BSA, B - 10 mg/ml synthetic Smp24, (1) and (2) pellets from the overproduction of Smp24 and (3) supernatant from the overproduction of Smp24.

6.3.11 Alternative approach for protein detection

Whilst the *G. mellonella* model is a marker of pathogenicity, for the purpose of this investigation it was used as method validation to determine if recombinant protein was being produced. It was hypothesised that *G. mellonella* (wax worms) injected with induction culture would demonstrate increased survival due to antimicrobial activity of the recombinant peptide against *E. coli*. Previous experimental data has shown induction with IPTG resulted in reduced growth rate (please refer to appendix 1). Samples for this assay were as follows: *E. coli* BL21 λDE3 transformed with the vector pET22b/STII/Smp24, *E. coli* BL21 λDE3 transformed with the vector and induced for protein expression with 0.05 mM IPTG an un-transformed *E. coli* BL21 λDE3 was used as a negative control.

The pathogenicity model was adapted from Peleg *et al* and Henly *et al* (Peleg *et al.* 2009, Henly *et al.* 2019). The number of surviving individuals was recorded daily. An untreated (non-injected (NI)) group and a group injected with PBS were used as negative controls.

The results of the *G. mellonella* pathogenicity model are shown in figure 6.12.

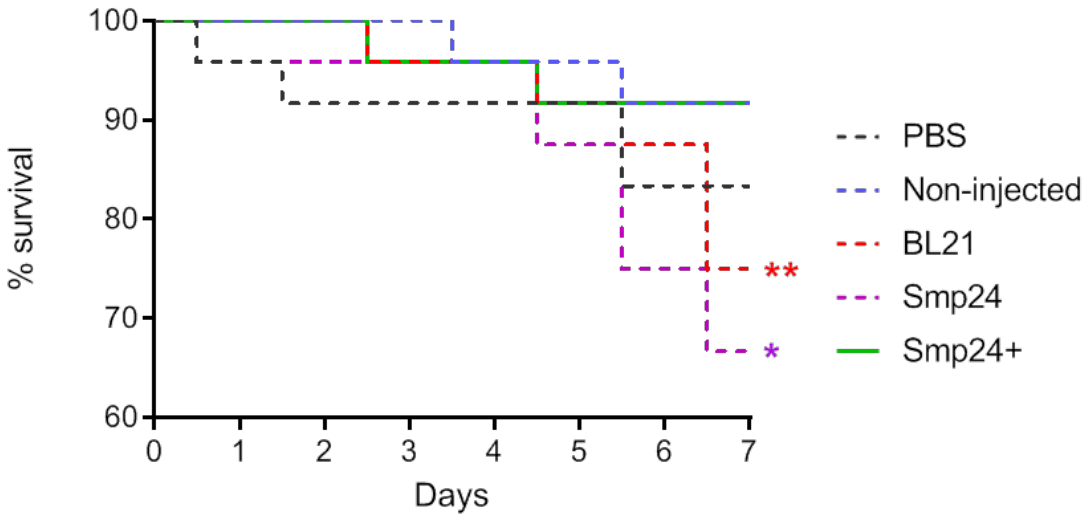

Figure 6.12: *Galleria mellonella* pathogenicity results. BL21 depicts *G. mellonella* injected with laboratory strain *E. coli* BL21 λDE3 with no vector. *E. coli* BL21 λDE3 transformed with the vector pET22b/STII/Smp24 is shown by the purple line. *E. coli* BL21 λDE3 transformed with pET22b/STII/Smp24 and induced for protein expression is shown by the green line. * p-value <0.05 as determined by log-rank reduction test. ** BL21 vs Smp24, * 24 vs 24+

A log-rank reduction test was performed on the data to determine the statistical significance (section 2.17 for methodology). Statistical difference is shown between the untransformed strain vs the strain transformed with the vector, with a p-value of 0.008. This demonstrates the presence of the expression vector in the expression strain reduced the pathogenicity overall, which could imply leaky expression of the Smp24 protein is taking place. Whilst the results could be deemed indicative of protein overproduction, the presence of the plasmid could affect the growth rate or copy number of the bacteria which in turn could have affected the pathogenicity.

Statistical significance can also be observed between the transformed strain and the induced strain, with a p-value of 0.015. The observed decrease in pathogenicity for the strain induced for protein production vs the transformed strain alone could imply that there is expression of the antimicrobial peptide. As Smp24 is an antimicrobial peptide, the production of the protein could lead to the AMP interacting with the bacteria to decrease membrane integrity. This could

result in a lower viable count within the bacteria and thus the observable differences in survival of the larvae between the induced and transformed strains. The overall pathogenicity of the induced strain was equal to that of the non-injected control, which suggests the combination of antimicrobial peptide with bacterial isolate results in lower pathogenesis than injection with bacteria alone. *E. coli* BL21 is a laboratory strain of *E. coli* commonly used for recombinant protein production (Jeong *et al.* 2015). *E. coli* BL21 demonstrates a low level of pathogenicity and is not capable of producing long-chain lipopolysaccharide (LPS) which makes the bacteria vulnerable to degradation (Chart *et al.* 2000) or potential lysis by antimicrobial peptides. Previous investigations in to the induction of cultures with IPTG resulted in reduced survival of bacteria with increased gene induction (experimental data not shown).

6.4 Limitations of the signal peptide expression system

The protein overproduction system was challenging for a number of reasons. The small size of the peptide combined with the highly charged nature of the peptide and a low overall concentration made the identification of the protein difficult and thus the process blind. The presence of peaks in the AKTA spectra confirmed the presence of protein despite some of the difficulties faced with detection. It would have been preferable to use the NTII system as a proof of concept prior to the production of antimicrobial peptides within bacteria in order to predict any issues that have since been faced, but due to genetic modification restrictions placed on this project, this was not possible.

The concentration of IPTG for induction of protein production by the bacteria was determined via growth curve analysis. For M9 media, the optimum concentration appeared to be 0.05 mM as this enabled the cells to progress through log phase steadily prior to stationary and death phase where minimal protein production is observed.

The small molecular mass of Smp24 combined with the positive charge of the peptide has caused detection issues. Despite numerous attempts at optimising gels for detection, it was not possible to detect the protein via gel electrophoresis.

The presence of salt inhibited the detection of the protein by MALDI-MS and the anti-Smp24 antibodies raised in rabbits did not exhibit a detection range sensitive enough for the detection of recombinant Smp24 in this expression system. The results from the *G. mellonella* investigation provided some evidence the protein was being produced; however, many challenges have been faced with this expression system. Whilst it is possible the issue faced is with detection, it is also possible that the protein is not being produced or the transportation system of the signal peptide is not functioning as anticipated.

Numerous observations within the investigation implied the protein was being expressed by the gene and overproduced in the bacteria. The *E. coli* growth was observed to be slower when IPTG was added to the culture media, implying more energy was spent overproducing the gene and thus less energy was available for growth and division. After induction, a decrease in pathogenicity was observed in the *G. mellonella* model, suggesting protein production was occurring and the viability of the injected bacteria was reduced. Peaks were present at 280 nm on the UV spectra from AKTA analysis, indicating the presence of protein. Additionally, a protein of the correct mass was initially identified by MALDI-MS from the first attempt of expression and purification. This suggested the protein was being produced but at a concentration below the limit of detection of the methodologies used.

As there was confidence in the production of the protein, a new detection method was adopted. A new strategy was designed to enable a recombinant production system for the expression of Smp24 in *E. coli* BL21 λDE3. This included the tagging of the peptide with a FLAG-tag to enable identification via anti-FLAG antibodies which offer a low limit of detection whilst retaining the ability to purify the protein using on-column techniques. It was anticipated the FLAG system would offer a sensitivity below 100 µg/ml as observed for the anti-Smp24 antibodies. The FLAG system was used as this incorporates a small fusion tag to the gene, which can be added at the N or C - terminal of the gene. The FLAG tag can then be cleaved by incorporating a cleavage site in to the expressed gene. The vector was to be transformed in to *E. coli* BL21 λDE3 and induced for protein production via the addition of IPTG. The recombinant protein would be detected by dot plot and purified by M2 affinity gel chromatography (figure 6.13).

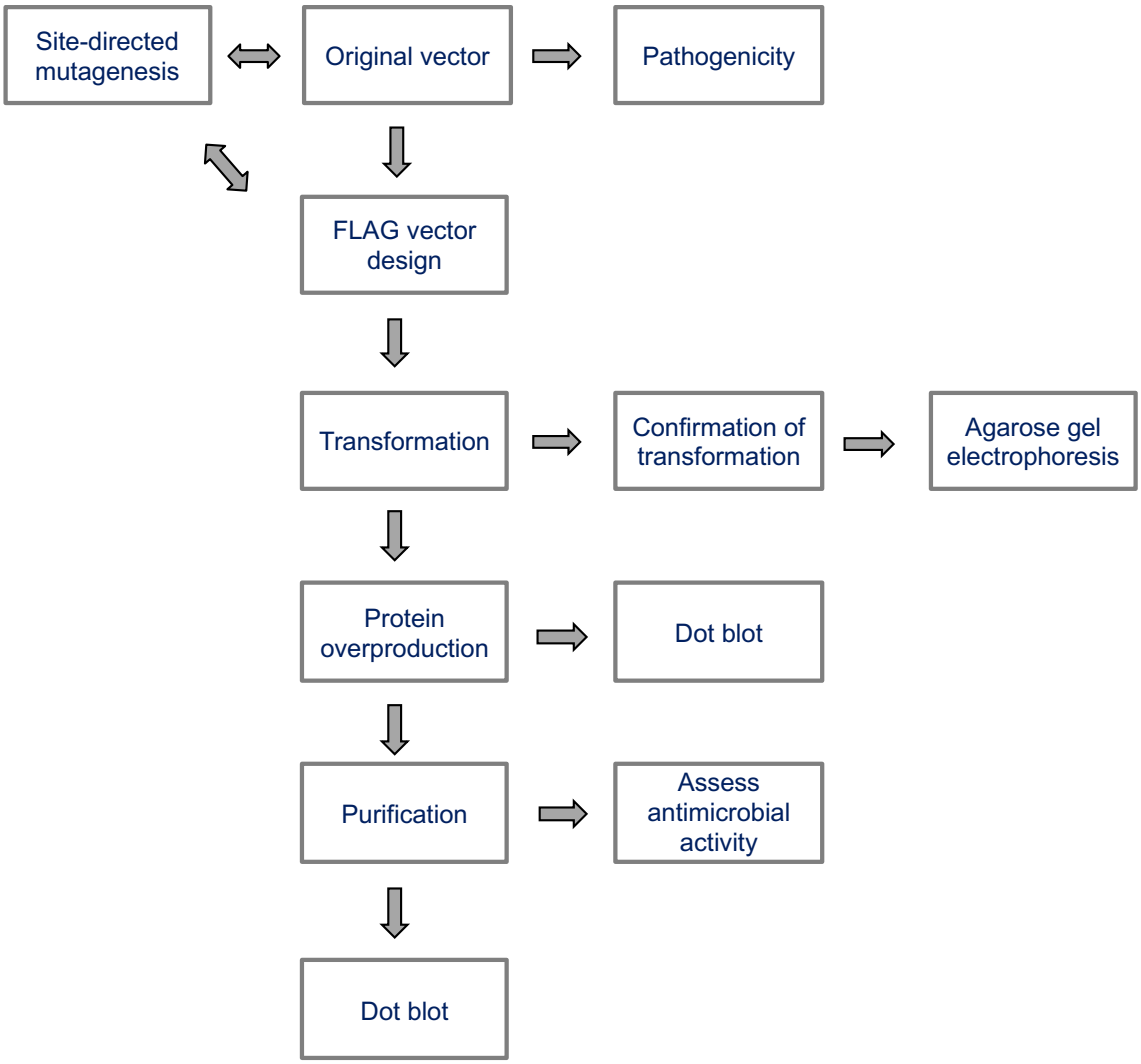

Figure 6.13: New strategy for the optimisation of production of recombinant antimicrobial peptide in *E. coli* BL21 λDE3.

6.5 Plasmid construct design with affinity tag

Producing antimicrobial peptides as fusion proteins can reduce the effects of host toxicity (Wanmakok *et al.* 2018). In addition to protecting AMPs from potential proteolytic degradation, the incorporation of a fusion tag to the peptide would assist with the detection. The FLAG system was chosen for the affinity tag due to its relatively small size (DYKDDDDK) and the ability to cleave the tag via the inclusion of a cleavage site thus reducing the likelihood of the tag interfering with protein function. The hydrophilicity of the tag was also appealing to facilitate detection of expressed proteins using antibodies. Protein fusion partners can also promote the purification process, whilst increasing the expression efficiency and solubility of the peptides (Wanmakok *et al.* 2018)

A vector was utilised for the expression of the Smp peptide in *E. coli* BL21 λDE3 with pET22b vectors as discussed previously (section 6.3.2). Expression systems were designed both with and without the signal peptide tag to determine which methodology would produce the greatest protein yield. A vector containing the signal peptide was affinity-tagged at the N-terminus and a vector without the signal peptide was tagged at the C-terminus. As the initial protein production system had faced challenges with either the production or detection of protein, the gene was tagged at the C-terminal in absence of the signal peptide leader sequence. The effect of the signal peptide on Smp24 was not known, the N-terminal tag may have had mechanistic implications for peptide functionality, or the signal peptide sequence may not have been cleaved upon transportation to the periplasm, thus affecting the detection. If the protein overproduction was successful, the concentration of peptide produced and being expressed in a large volume of liquid still remained a challenge. The tagging of the peptide at the C-terminal, if successful, would enable purification from the cell pellet from a smaller volume. This would potentially eliminate the low concentration aspect of the protein production and purification process.

A gene was designed for the expression of the Smp24 protein with the signal peptide to promote transportation of the protein out of the cell. The gene was

designed for optimum codon usage in *E. coli* and synthesised by Eurofins (Ebersberg, Germany) (figure 6.14).

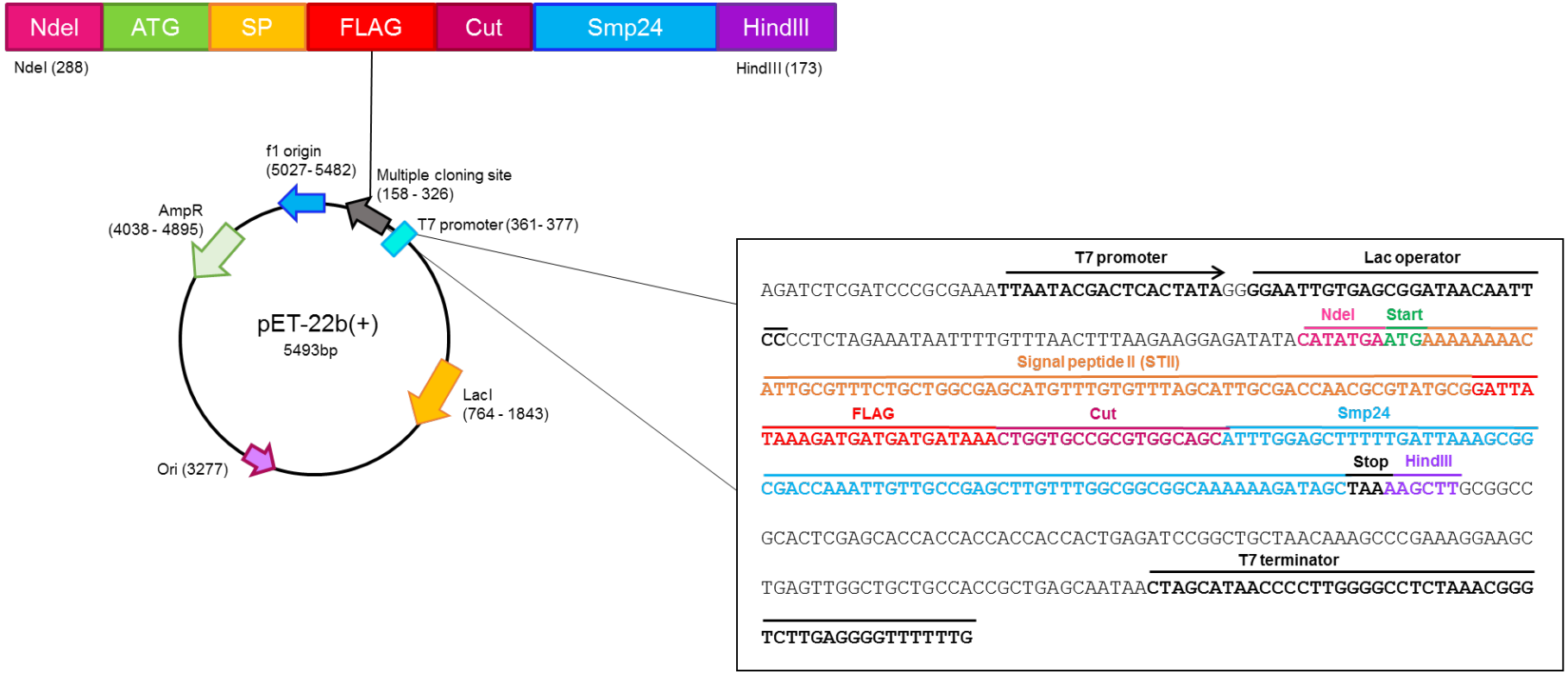

Figure 6.14: The design of pET22b/STII/FLAG/Smp24. The FLAG tag was added at the N-terminal of the sequence after the signal peptide, which is cleaved upon exit of the expressed protein from the periplasm. The gene with the affinity tag was spliced between the NdeI and HindIII restriction sites as per previously discussed methodologies.

Figure 6.14 depicts the design of the insertion region for the expression of STII/FLAG/Smp24 in a recombinant system. The FLAG tag was added upstream of the STII sequence as the signal peptide would be cleaved upon exit of the periplasm, theoretically resulting in FLAG-tagged Smp24 in to the culture supernatant. The incorporation of the cleavage site enabled the FLAG tag to be cleaved from the protein via the addition of thrombin following protein purification.

As previous experiments (section 3.4.2.1) suggested the N-terminal of Smp24 was important for the antimicrobial function, the effect of adding the fusion tag to the N-terminal of the sequence was uncertain.

A second approach was taken to observe the effect of expression of the Smp24 gene without the signal peptide at the N-terminal. A gene was designed for the expression of Smp24 with the fusion tag at the C-terminal of the peptide. A cleavage site was added prior to the FLAG tag to enable to affinity tag to be cleaved from the produced protein. The vector construction for the C-terminally tagged fusion protein is shown in figure 6.15. The codon usage was optimised for *E. coli*, the gene inserts were synthesised, and the correct sequences determined via sequencing by Eurofins (Ebersberg, Germany).

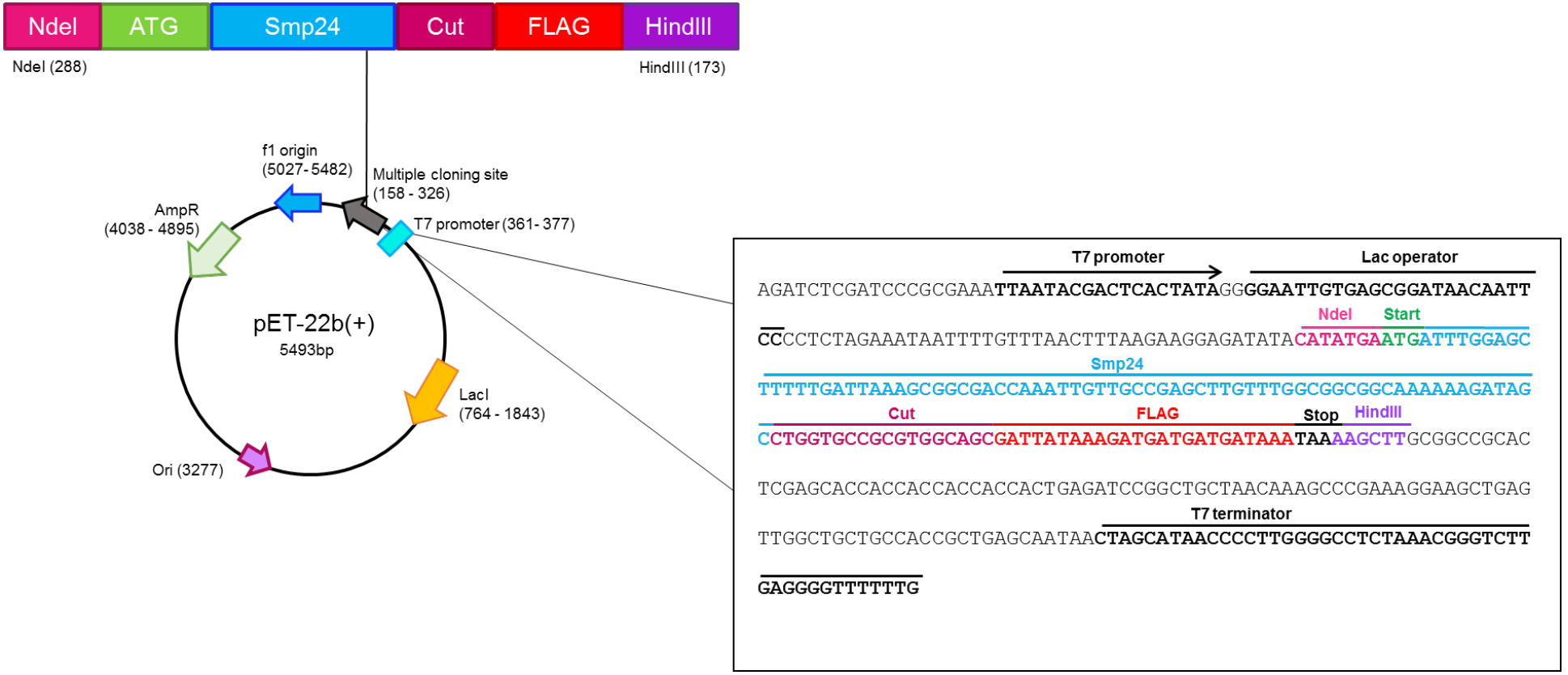

Figure 6.15: Creation of the vector pET22b/Smp24/FLAG. The FLAG tag was added to the C-terminal of the Smp24 sequence. A cleavage site was added downstream from the FLAG tag. The gene was inserted in to the pET22b vector between the NdeI and HindIII restriction site.

6.5.1 Transformation

Vectors were transformed in to *E. coli* BL21 λDE3 as per methods (section 2.10.1) confirmation of plasmid incorporation was determined via extracting the plasmids, amplifying the T7 region via PCR and running the PCR product on a 1% agarose gel (figure 6.16).

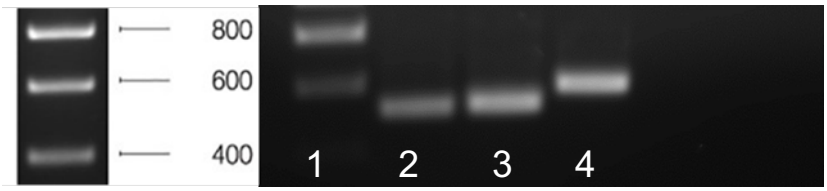

Figure 6.16: Agarose gel electrophoresis for the transformation of FLAG-tagged vectors in to *E. coli* BL21 λDE3. (1) 1kb Hyperladder (Bioline, London, UK), (2) pET22b, (3) pET22b/Smp24/FLAG, (4) pET22b/STII/FLAG/Smp24.

6.5.2 Affinity tagged protein over production

The production of affinity tagged protein was optimised to promote the maximum yield. Growth conditions were monitored in M9, auto-induction (AIM) and LB broth. It was determined that the optimal growth and expression occurred in LB broth with room temperature incubation (22°C) with 1 mM IPTG added for induction of protein production.

Cells were harvested by centrifugation according to the methodology in section 2.19.1. The pellet was frozen at -20°C and the cells were lysed by the addition of CellLytic B to extract protein. The supernatant (soluble) fraction was separated from the pellet (insoluble) fraction. Both fractions were analysed by dot blot (section 2.19.2) to determine the location of the fusion protein. The fusion protein was present in both the soluble and insoluble fractions, with the C-terminally tagged protein demonstrating a stronger signal via dot blot, as shown in figure 6.17.

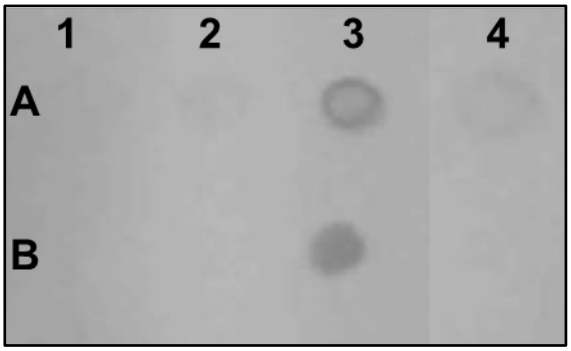

Figure 6.17: Dot blot for the analysis of Smp24 expression. (1) BSA control, (2) *E. coli* BL21, (3) Smp24-FLAG, (4) SP-FLAG-Smp24. Row A denotes the soluble fraction; row B denotes the insoluble fraction of cell free extract.

6.5.3 Affinity tagged protein purification

The soluble fraction containing the recombinant protein was added to M2 affinity gel on a rocking platform with protease inhibitors at 4°C overnight to enable the fusion proteins to bind to the agarose beads. The gel was washed and the protein eluted as per the methodology (section 2.20). The eluted protein was stored at -20°C and analysed via dot blot.

Following purification via the anti-FLAG affinity gel, samples were assayed by dot blot and visualised in the Odyssey imaging system (Licor, Cambridge, UK) (figure 6.18).

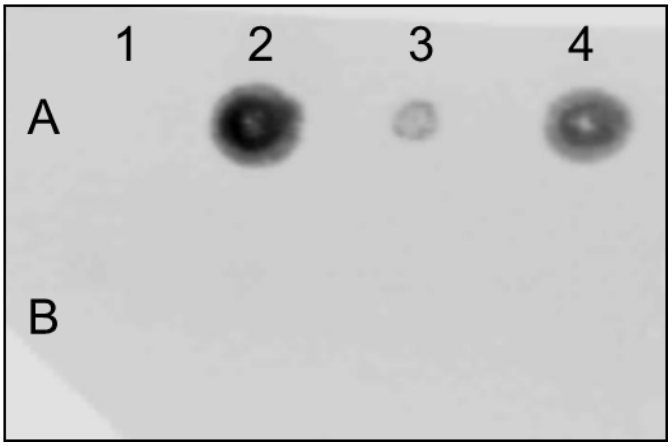

Figure 6.18: Dot blot analysis of Smp24-FLAG purification. Row A: (1) BSA, (2) unbound, (3) wash through, (4) cell lysate (pre-purification). Row B: (1 – 4) samples eluted from the affinity gel.

As shown in figure 6.18, the protein could not be detected in the post-purification samples. As shown by the spot in position A2, the sample did not bind to the column and spot A3 shows any residual FLAG-tagged Smp24 was washed from the gel. The reason for this was not known as the conditions (temperature, pH) had been adjusted as per manufacturer's instruction to enable the binding of the fusion protein to the gel and elution from the gel.

6.5.4 Additional optimisation

As it was not possible to detect Smp24 in the fraction eluted from the M2 affinity gel. The protocol was optimised, and the soluble fraction was diluted 2-fold in lysis buffer prior to binding to the M2 affinity gel at 4°C overnight. The gel was washed, and the protein eluted as per the method in section 2.20.1. All fractions, including the unbound and was through, from the purification process were kept for analysis via dot blot (figure 6.19).

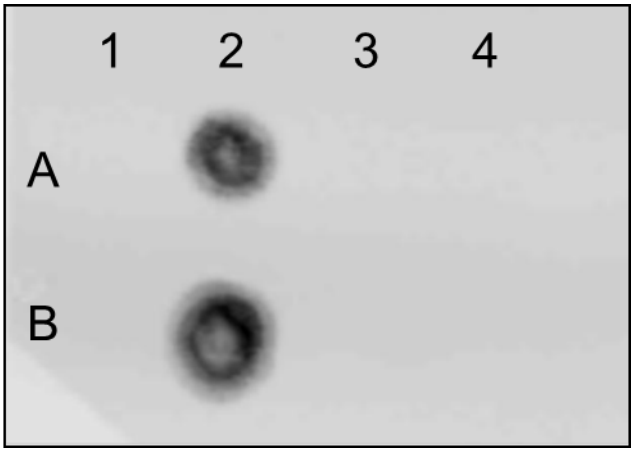

Figure 6.19: Dot blot analysis of Smp24-FLAG purification. Row A: (1) BSA, (2) cell lysate (pre-purification), (3) and (4) samples eluted from the affinity gel. Row B: (2) unbound sample and (3) wash through.

As shown in figure 6.19, challenges were still being faced with protein purification as no recombinant protein could be detected in the samples eluted from the affinity gel. The produced protein was not binding to the affinity gel beads under the conditions used and consequently, the protein could not be purified by the affinity process. As time on the project was restricted, this was the end point of the purification strategy.

6.5.5 Mutagenesis of Smp peptides

In addition to the optimisation of a methodology to produce recombinant antimicrobial peptides, a strategy was taken to modify Smp24 to express modified peptides which have demonstrated increased antimicrobial activity, as discussed in chapter 3 (section 3.7).

As solid phase synthesis is an expensive method to produce modified peptides, the optimisation of an in-house system to produce mutant peptides on a bigger scale at lower cost is appealing.

A system to produce mutant peptides within the laboratory would be low cost as the reagents required for site-directed mutagenesis (SDM) and overproduction of protein are cheap compared with the cost of solid-phase synthesis. The lead-time

on production of the peptides is reduced, as the mutants could be produced in the laboratory as and when required. This would enable a library of mutant peptides to be created for antimicrobial and cytotoxicity screening. As stated previously, the major limiting factor of solid-phase synthesis is the quantity of peptide received, as the production of protein within a recombinant system can be up-scaled, this would also remove one of the major limiting factors of this project.

As the modifications to increase the charge of Smp24 yielded peptides with enhanced antimicrobial activity, a strategy was taken to introduce single amino acid substitutions to recreate the modified peptides via SDM. The S3K, S15K and S24K modifications were selected for initial candidates for the creation of expression genes. Primers were designed which contained the codon with the highest frequency incorporation rate (table 6.2).

Table 6.2: Primer design for the site-directed mutagenesis of pET22b/STII/Smp24. Primers were redesigned for the creation of the S3K mutant as previous attempts to modify the gene were unsuccessful. The codon which to introduce the mutation in to the DNA coding sequence for the protein is shown in **bold**.

Mutation	Direction	Primer sequence	Primer length	Melting temp °C
S3K	Reverse	5'-GTCGCCGC**TTT**AATCAAAAACTTCCAAATCGCATACGCGTTG-3'	42	79.2
S3K	Forward	5'-CAACGCGTATGCGATTTGGAAGTTTTTGATT**AAA**GCGGCGAC-3'	42	79.2
S3K redesign	Reverse	5'-GGTTGCAGCTTTGATCAGGAACTTCC**AAA**TGGCATAAGCATTCG-3'	44	79.32
S3K redesign	Forward	5'-CGAATGCTTATGCCA**TTT**GGAAGTTCCTGATCAAAGCTGCAACC-3'	44	79.32
S15K	Reverse	5'-TTTCTTCCCACCACCAAACAACTTAGGTAACAG**TTT**GGTTGCAGC-3'	45	78.06
S15K	Forward	5'-GCTGCAACC**AAA**CTGTTACCTAAGTTGTTTGGTGGTGGGAAGAAA-3	45	78.06
S24K	Reverse	5'-GCGGCCGCAAGCT**TTT**ACTTGTCTTTCTTCCCACCA-3	36	78.83
S24K	Forward	5'-TGGTGGGAAGAAAGACAAGTA**AAA**GCTTGCGGCCGC-3'	36	78.83

Mutations were introduced in to the vector (section 2.11). The plasmids were extracted from the transformed *E. coli* and the T7 region amplified via PCR prior to sending the samples to Eurofins, Ebersberg for sequencing. The PCR products are shown in figure 6.20.

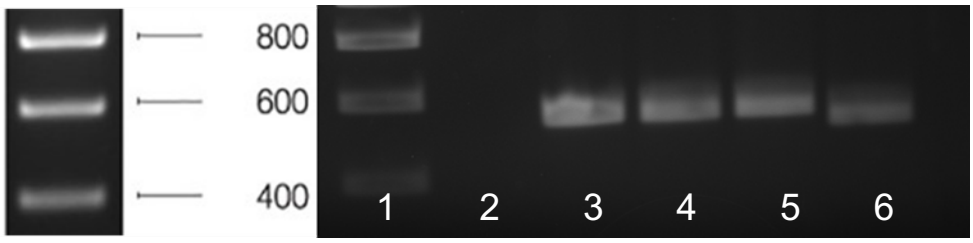

Figure 6.20: Agarose gel electrophoresis depicting the mutagenesis of Smp24. (1) 1kb Hyperladder (Bioline, London, UK), (2) negative DNA control, (3) pET22b/STII/Smp24, (4) pET22b/STII/Smp24/S15K, (5) pET22b/STII/Smp24/S24K. (6) pET22b.

The confirmed sequences of the mutated peptides are shown in table 6.3. The sequencing results confirmed successful creation of vectors capable of expressing mutant peptides with the sequences S15K Smp24 and S24K Smp24. Despite attempts to create mutant peptide with an enhanced charge at the N-terminus of the chain (S3K Smp24), this remained unsuccessful.

The SDM methodology was adapted for S3K Smp24 to enhance the elongation times of the PCR process, which remained unsuccessful. The SDM primers were redesigned and the optimisation process repeated to create the S3K mutant. None of the mutagenesis attempts revealed incorporation of the S3K mutation in the Smp24 gene. The difficulties faced with the creation of the S3K mutant could be attributed to the potent antimicrobial activity observed from the synthetically synthesised peptide discussed in chapter 3, section 3.7.1. The observable MIC for this modification against the *E. coli* strain tested (JM109) was 1 µg/ml, demonstrating the toxicity of this peptide to the expression strain. Due to this, any leaky expression within the vector would have resulted in cell death. The mutation could have been too toxic for the for the cells resulting in death and no observable incorporation of the substitution in to the gene of interest.

Table 6.3: Confirmed sequences of mutated Smp24 peptides, as produced by site-directed mutagenesis. Mutated amino acids are highlighted in **bold.**

Peptide	Charge	GRAVY	Molar Mass (Da)	PI	Sequence
Smp24	+3	0.312	2578.09	10.00	IWSFLIKAATKLLPSLFGGGKKDS
Smp24 S15K	+4	0.183	2619.19	10.18	IWSFLIKAATKLLP**K**LFGGGKKDS
Smp24 S24K	+4	0.183	2619.19	10.18	IWSFLIKAATKLLPSLFGGGKKD**K**
Smp24 S15K/S24K	+5	0.054	2573.21	10.30	IWSFLIKAATKLLP**K**LFGGGKKD**K**

Following the successful creation of the S15K and S24K mutant genes, SDM was performed to create a double charge modification resulting in the expression of Smp24 S15K/S24K. This was achieved by using the S15K primers to introduce the S15K mutation to the successfully created Smp24/S24K gene. As the antimicrobial activity of a double charge modification had previously been observed (S3K/S15K in section 3.4.2), it was of interest to observe the effect of increasing the charge at the C-terminal end of the peptide.

The mutant plasmid vectors were transformed in to *E. coli* BL21 λDE3 and induced for protein expression (section 2.13). The purification and detection of the modified peptides faced the same challenges as discussed previously, with issues with reproducibility. It was not possible to detect the presence of the modified peptides in the purified fractions. The plasmids mutated contained the leader sequence, which according to the FLAG-tagged methodology in section 6.5.2 was determined to be a less efficient system for protein production. The future approach of the mutagenesis strategy would be to incorporate the described mutations in the C-terminally FLAG-tagged vectors.

6.6 Discussion

Antimicrobial peptides are of increasing therapeutic interest, with 60 peptide-based drugs approved by the FDA and a further 140 peptide candidates in various phases of clinical trials (Hazam *et al.* 2019). Whilst the properties of Smp24 and derived modifications have been investigated in peptides synthesised via solid-phase synthesis, this is not a sustainable strategy for long-term production due to the small quantities produced, the lead time on production and the high cost.

Lipopeptide antibiotics have been successfully produced by recombinant methodologies for pharmaceutical purposes. Daptomycin is recombinantly produced by *Streptomyces roseosporus, Streptomyces lividans* TK_{23} and *S. lividans* TK_{64} strains when the 128 kbp region of cloned *S. roseosporus* DNA containing the daptomycin gene cluster is inserted site-specifically in the ϕC31 attB site (Miao *et al.* 2005, Penn *et al.* 2006). This methodology enabled 20

- 55 mg of daptomycin to be produced per litre of bacterial culture (Penn *et al.* 2006). The success of recombinant production of daptomycin is encouraging when looking for a system to exploit the production of antimicrobial peptides via similar methodologies.

The challenges faced with expressing and purifying AMPs have previously been noted. The production of the peptides within the system needs to overcome the risk of proteolytic degradation of the peptide within the microbial cells. Conversely, the negative effects of the AMP on the microbial producer cells (in terms of toxicity) must be avoided (Ashcheulova *et al.* 2018).

Whilst the production system for Smp24 has not yet been perfected, the detection of the protein prior to purification via the fusion tag is positive and suggests further improvements to the process could yield promising results. The ability to detect the protein prior to purification was previously a limiting factor for the project, as it made the purification process blind. The inclusion of a fusion tag has improved the detection aspect of this methodology.

Difficulties were initially faced with the detection of the produced peptide. A gel methodology was unsuccessful for the detection of the peptide; due to the small mass of the protein combined with its positive charge. Whilst SDS binds with proteins to create a negatively charged protein, the efficiency at which this occurs differs between proteins. Highly hydrophobic proteins bind SDS more efficiently, as Smp24 is a peptide with an abundance of hydrophilic residues, the ability to bind SDS could be reduced.

Several factors were considered when choosing a fusion system for the detection and purification of Smp24. The main consideration when choosing a tag is that it should not interfere with the native folding of the protein. Whilst structural investigations revealed Smp24 is disordered in solution and adopts its alpha-helical conformation upon membrane binding (see chapter 3, section 3.5.3), the effect of a tag of the N or C-terminus remains unknown. Whilst the produced protein was found to lack antimicrobial activity and this could be due to the FLAG-tag, it is most likely due to the low concentration. Secondly, the tag should be water soluble; this is an important factor when considering the antimicrobial

property of the peptide and the potential future application as a therapeutic. Thirdly, the tag should be suitable for an inexpensive purification procedure, to make the procedure more cost-effective than solid-phase synthesis. Finally, the tag should be easy to remove in order to gain the native peptide. Taking all of these factors in to consideration, the FLAG tag was chosen for the purification of Smp24.

The FLAG tag was originally designed as a hydrophilic tag which could be removed from the target protein by enterokinases (Sasaki *et al.* 2012). FLAG tags were added to the N and C-terminal of Smp24 to determine the effect on function as N-terminal tags have previously been shown to inhibit the functionality of proteins (Sandhu *et al.* 2019).

The addition of the FLAG tag aided the identification of expressed Smp24 from bacterial overproduction. The C-terminally tagged peptide was ultimately chosen for protein overproduction due to a higher level of expression as determined by dot blot analysis when compared with the N-terminally tagged protein. The sensitivity of the commercially available antibodies is not always sufficient to detect low-level protein expression (Sandhu *et al.* 2019), which could explain the lack of detection for the N-terminally tagged protein within the culture supernatant. It is also possible the N-terminally tagged protein did not express, though the reason for this is unknown.

The detection of the protein via anti-FLAG antibodies supported results previously observed in this study. The decrease in pathogenicity of the overproduction strain of *E. coli* vs the control strain was indicative of successful production of Smp24. The difficulty faced creating the S3K mutation via site-direct mutagenesis was also supportive of protein expression due to the microbial potency observed in chapter 3, section 3.4.2. With leaky expression within the system potentially resulting in lethality.

Issues have been faced with the purification of the protein from the M2 agarose beads. This could potentially be due to the batch purification process adopted, as each time the gel beads were centrifuged, a volume of the beads was lost. As it is anticipated that small quantities of protein are produced with the overproduction

system, volume losses could be crucial to this project. The future direction with this work would be to purify the fusion proteins via a column method. Packing the gel in a column format would prevent loss of the affinity gel and the associated fusion protein. This would also enable an upscale on production, which would maximise protein recovery. The M2-conjugated agarose bead system has been used for the pull down of proteins on small and large scales. Gerace and Moazed, 2015 described an immunoprecipitation method for affinity purification combined with elution with a 3x FLAG peptide which could be adopted.

The elution method adopted could have also contributed to the lack of recovery from the purification process. Lowering the pH was chosen as the initial method for elution due to ease of use and low cost. Other methods of elution from the gel include antibody-mediated affinity chromatography in a calcium-dependent manner and elution with synthetic peptides (Einhauer and Jungbauer 2001). Competition with a 3x FLAG peptide has previously been describe to elute FLAG-tagged fusion proteins from M2 affinity gel (Gerace and Moazed, 2015). This methodology operates via competition of the 3x FLAG protein with the FLAG-tagged fusion protein for binding to the M2 agarose beads, which releases the protein in to the eluate. In future experiments, these elution methods would be considered.

Following the optimisation of the purification process for Smp24, the activity of the peptide would initially be assayed whilst leaving the FLAG tag on the peptide. The antigenicity of the FLAG tag is essential for the detection of the Smp24 peptide, due to previous issues encountered. It has been previously reported that for small scale laboratory production the FLAG tag may be left on if the tag is shown not to interfere with the activity of the protein or peptide (Einhauer and Jungbauer 2001).

Whilst protein production via inclusion body formation was avoided during this project, this strategy has been shown to be successful in the literature. Ashcheolova *et al* (2018) utilised both the fusion tag and inclusion body formation to produce large quantities of an antimicrobial peptide. A ketosteroid isomerase (KSI) fusion tag was combined with protein production through insoluble inclusion bodies for recombinant production of ubiquicidin (UBI). This strategy was

optimised to benefit the fusion protein and the microbial host. The produced protein which was protected from proteolytic degradation by being forced in to inclusion bodies which in turn protected the host cell from the activity of the peptide. The procedure was optimised to yield up to 72 mg of an ubiquicidin variant (KSI-2xUBI$_{18-35}$) at 95% purity (Ashcheulova *et al.* 2018). The production of Smp24 via inclusion body formation could be an interesting avenue to investigate; it was avoided in this project due to the uncertainty as to whether the recombinant protein would retain its solubility. The extraction and purification method from inclusion bodies can be complicated and often requires optimisation. It is necessary to isolate and purify inclusion body aggregates into homogeneity before solubilisation and refolding (Singh *et al.* 2015).

Other considerations for future work would involve alternative affinity tags and purification methodologies. The His-tags (consisting of at least 6-histidine residues tagged at the N or C-terminus of the peptide) have been utilised for the successful recombinant production of AMPs in *E. coli*. The coding sequence for cLF chimera was cloned in to a pET expression vector and overproduced in *E. coli* via IPTG induction in LB broth, resulting in a yield of 0.42g of protein per litre of culture media (Tanhaiean *et al.* 2018b).

When looking to upscale the project, recombinant expression in mammalian cells could be considered. 60-70% of recombinant protein pharmaceuticals are produced in immortalised mammalian cell lines, such as HEK-293 or Chinese Hamster Ovary (CHO) (Wurm, 2004).

CHO cells have been used successfully for recombinant protein expression due to being a hardy and reliable cell line. The annual global revenue from products derived from CHO cells totals $100 billion, which increases every year (Bandaranayake and Almo 2014). During recombinant production in CHO cells, the recombinant gene with the necessary transcriptional regulatory elements is transferred in to the cells. A second gene is then transferred in to the cells which confers a selective advantage. This second gene is transferred a few days after the first and only the cells containing the selector gene survive. Following the selection process, survivors are transferred as single cells in to a new vessel and expanded for recombinant expression (Wurm 2004). Optimisation of expression

within CHO cells can result in a protein yield of 2 - 6 grams per litre (Bandaranayake and Almo 2014).

Conclusions

In summary, a vector capable of expressing Smp24 has been created. The plasmid has been successfully overexpressed in *E. coli* to overproduce Smp24 protein and a purification strategy has been devised. C-terminal FLAG-tagging resulted in the greatest yield of peptide, as opposed to the original method of overproduction with a signal peptide.

Whilst issues been faced with the purification and elution of the expressed peptide, initial problems with the expression system (such as detection of the peptide) have been overcome which suggests the process could be further optimised to gain an in-house method of protein production. Additionally, SDM methodology has been established which would enable high-throughput production and screening of Smp24 mutants.

7

General Discussion

7.1 Improving the understanding of structure and function

The purpose of this study was to gain an insight in to the relationship between structure, function and cytotoxicity of antimicrobial peptides (AMPs) derived from venom. Throughout this study, two antimicrobial peptides, Smp24 and Smp43, from the venom of *Scorpio maurus palmatus* have been modified. Some of the modifications have produced peptides with enhanced antimicrobial activity, whilst other modifications resulted in reduced eukaryotic cytotoxicity.

For both Smp24 and Smp43, peptides with enhanced therapeutic indices (TIs) have been produced. The S3K, F4A, D23F and S24K modifications of Smp24 and the W3A, W5A and W14A modifications of Smp43 all had enhanced TIs when compared with the native peptides. The combined results of antimicrobial activity and eukaryotic cytotoxicity are shown in table 7.1.

Table 7.1: Comparison of prokaryotic and eukaryotic activity of Smp24, Smp43 and derived modifications that yielded peptides with enhanced TIs.

Peptide	**Charge**	**GRAVY**	**MIC (µg/ml)**		**LD_{50} (µg/ml)**			**HC_{50} (µg/ml)**	**Therapeutic index**			
			E. coli	*S. aureus*	HepG2	HEK-293	HaCaT	RBCs	HepG2	HEK-293	HaCaT	RBCs
Smp24	**+3**	**0.31**	**32**	**8**	**37**	**39**	**34**	**76**	**1***	**1**	**1**	**2**
Smp24 S3K	+4	0.18	1	0.5	34	38	18*	11*	35*	39*	19*	11*
Smp24 F4A	+3	0.27	32	16	63*	56*	57*	423*	2*	2*	2*	13*
Smp24 D23F	+4	0.58	32	32	>512*	38	137*	33*	16*	1*	4*	1
Smp24 S24K	+4	0.18	8	4	36	23*	142	15*	5*	3*	18*	2
Smp43	**+4**	**-0.316**	**32**	**>512**	**161.95**	**35.86**	**179**	**>512**	**4**	**1**	**6**	**16**
Smp43 W3A	+4	-0.25	16	>512	172	76*	194	>512	11*	5*	11*	32*
Smp43 W5A	+4	-0.25	8	>512	46*	39	327	>512	6*	5*	4*	64*
Smp43 W14A	+4	-0.13	4	>512	77*	29	53*	>512	19*	7*	12*	128*
Daptomycin	-6	-1.93	>512	4	>512	>512	>512	>512	128	128	nc	128
Polymyxin B	+5	nc	2	32	>512	351	>512	>512	256	256	nc	178

nc - not calculable. Statistical significance was determined by performing a T-test, * p-value ≤ 0.05. Native peptides are highlighted in **bold**.

The modified Smp24 peptides which demonstrated improved antimicrobial activity also demonstrated increased haemolytic activity. The greatest increase in antimicrobial activity was observed for the S3K modification which was also the most potent peptide against red blood cells out of all of the peptides in this study. Similar results have previously been observed for antimicrobial peptides extracted from Australian tree frogs, with improvements in antimicrobial activity accompanied by 4-fold increases in haemolytic activity (Fernandez *et al.* 2008). Lysine substitutions in VmCT1 which resulted in 4-fold improvements in antimicrobial activity yielded peptides with a similar fold increase in haemolytic activity (Pedron *et al.* 2019). Conversely, the structural manipulation of AMPs has also demonstrated reductions in the haemolytic propensity in the literature. Sequence modifications to pep 5, which replaced three leucine residues for alanine residues, resulted in a 4-fold decrease in potency against *Staphylococcus* spp and a 2-fold reduction in haemolysis (Hollmann *et al.* 2016).

Pedron *et al*., 2017 performed lysine substitutions across the N-, mid and C-terminal of VmCT1, with a serine-lysine substitution at position 11. All the lysine modifications to VmCT1 produced peptides with enhanced antimicrobial and haemolytic activity. A modification to incorporate a tryptophan residue in to the peptide (W9) resulted in the largest polar angle and produced a peptide with reduced haemolytic activity and reduced antimicrobial activity (Pedron *et al.* 2017). The results of this study followed a similar pattern, with the greatest decrease in antimicrobial and haemolytic activity observed by the K7F modification of Smp24. Additionally, upon CD spectroscopy, the W9 modification of VmCT1 demonstrated a similar profile to Smp24 K7F, with a less pronounced alpha-helix in membrane mimetic conditions, suggesting that the ability of AMPs to adopt their alpha-helical structure is important for the function of the peptides.

7.2 AMPs and membrane interactions

The lipid composition of bacterial cytoplasmic membranes is an important factor for the mechanism of action of AMPs. Whilst membrane composition differs between species, anionic phosphatidylglycerol (PG) and cardiolipin and zwitterionic phosphatidylethanolamine (PE) are essential for the organisation of

bacterial membranes (Epand and Epand 2009). Differences in the antimicrobial activity of the AMPs against different species was observed, which could be linked to the membrane composition of the target and the mechanism of action of the peptide. Gram positive membranes present with a lower proportion of zwitterionic PE (Pedron *et al.* 2017). Smp24 demonstrated increased potency against *S. aureus* compared with the two Gram negative strains while Smp43 demonstrated no detectible antimicrobial activity against *S. aureus*.

As the lipid composition of bacterial membranes plays a role in AMP mechanism of action, the membrane composition of mammalian cells used for cytotoxicity assays needs to be considered. Previously, haemolysis assays have been used as a marker of cytotoxicity, but the results of this study highlight the differences between HC_{50} and LD_{50} concentrations and how measuring the HC_{50} alone can be an inaccurate representation of cytotoxicity. Differences in activity were noted between the activities of the peptides against the various secondary cell lines used, which was attributed partially to the difference in membrane composition, with cancer cell membranes often having similar physicochemical properties to bacterial membranes. As such, the usage of cancer-derived cell lines could produce misleading cytotoxicity results, due to potentially greater electrostatic attraction between the AMP and cancer cell membranes. Many AMPs have demonstrated anti-cancer properties (Zhu *et al.* 2017a), further supporting the conclusion that the usage of secondary cell lines may not be an accurate marker of cytotoxicity. When this hypothesis was tested within the confines of this study, a significant reduction in cytotoxicity was observed for the primary HUEPC cell line for both peptides (LD_{50} >512 μg/ml). This highlights the importance of assessing the activity of the peptides against numerous cell types, with a preference for primary cell lines which are more representative of healthy eukaryotic cells (Wilkening *et al.* 2003). The usage of immortalised cell lines could result in potential drug targets being overlooked on the basis of inaccurate cytotoxicity results.

Future work would involve further screening of the AMPs against primary cell lines with varied membrane compositions and membrane potentials to determine the role of membrane composition on the determined cytotoxicity. Additionally, numerous bacterial cell lines would be screened to assess the spectrum of

activity of the peptides and the relationship between bacterial membrane composition and AMP activity.

7.3 Elucidating the mechanism of action

It has been established that cationic peptides play an important role in microbial defence of many species (Pedron *et al.* 2017). The peptides are generally positively charged and fold in to a helical structure enabling the clustering of hydrophilic residues which promotes interaction between the peptide and the anionic bacterial cell membrane (Jiang *et al.* 2008). The hydrophobic faces of the helix are thought to be responsible for insertion in to membranes (Kang *et al.* 2012). As differences between antimicrobial activity and cytotoxicity were observed by adjusting the charge and hydrophobicity parameters of the peptides, investigating the effect of the pore-forming mechanism of the modified peptides would be an interesting avenue to pursue.

To investigate the effect of the amino acid modifications on pore-formation, future work would involve observing the effect of the peptides on phospholipid vesicles. Giant unilaminar vesicles composed of PG:PE would be produced and a free-standing membrane prepared on a borosilicate glass chip by applying a negative pressure using the Nanion Port-a-Patch system (Song *et al.* 2013). Manzo *et al* used the Port-a-Patch system to elucidate the effect that minor sequence modifications of temporin B had on membrane activity. A similar strategy would be adopted for Smp24, S3K and K7F to determine if the structural modifications resulted in mechanistic changes in terms of pore formation. The Nanion system would enable the activity of the peptides to be distinguished on the basis of peptide concentration, latency (i.e. the time taken for conductance (pore formation) to begin after the addition of the peptides), the duration of the conductance activity, the amplitude and number of each conductance event, and whether the peptide caused the membrane to break (Manzo *et al.* 2018). Ultimately, this would enable the concentration at which pore formation occurs to be ascertained, the number and size of pores to be quantified and the breakage of the membrane to be identified. The pore-forming abilities of the membranes on eukaryotic membranes could also be determined by the usage of patch-clamp

techniques at a whole cell level. A greater understanding of the mechanisms of pore formation may lead to further modifications to the AMPs, such as truncation, to further enhance the therapeutic index.

7.4 Development of novel antimicrobials

The rational design of new antimicrobial compounds follows several rules; the drugs must be well-absorbed, non-toxic and active against a specific target. Lipinski's rules are the most recognised rules governing the industry (Durand *et al.* 2019). The "rule of 5" predicts that poor absorption or drug permeability is more likely if a drug has more than 5 H-bond donors, 10 H-bond acceptors, a molecular weight exceeding 500 Da and a calculated log P greater than 5 (Lipinski *et al.* 1997). The rule of 5 was intended to enable high-throughput screening of new drugs and identify poorly behaving drugs early in the discovery process to reduce drug development costs. Despite the original intentions, the rule of 5 has become a mainstay of decision making; drugs which fail two or more of the rules are often rejected. Only seven orally active antibiotics fit the Lipinski criteria at the time of publications (Mckerrow and Lipinski 2017). Similar to antibiotics, antimicrobial peptides also fail to follow the "rule of 5."

Previous attempts to introduce novel antimicrobials have faced many difficulties. In addition to the drug requirements listed above, antimicrobials face several other hurdles. Telithromycin (Ketek) was authorised in the European Union in 2001 and initially marketed in France in 2002 with great success. The adverse effect profile of the drug was noted and despite the claim Ketek held a novel mechanism of action, it was found to be no more effective than existing macrolide antibiotics. This led to the withdrawal of two of the three telithromycin analogues (licensing was retained for the treatment of community acquired pneumonia) from the clinical setting in 2006. The decision to withdraw Ketek was the result of a change in non-inferiority trials for the approval of antibacterial drugs by the Food and Drug Administration (FDA). In 2018, the drug was officially removed from the market by Sanofi Aventis, citing economic reasons. Echols, (2011) has argued that the withdrawal of Ketek for the treatment of acute bacterial sinusitis and acute bacterial exacerbation of chronic bronchiectasis has caused collateral damage to

the antibacterial pipeline, particularly for molecules with novel mechanisms of action. The usage of non-inferiority trials to approve new antibacterial products has resulted in a dramatic decline in the approval of new drugs (DiNubile 2016). This does present a challenge when assessing molecules for potential therapeutic application, such as within the confines of this study. Whilst comparisons have been made between the modified Smp peptides and commercially available compounds, the venom peptides are inferior. Some of the peptides, such as the W14A modification of Smp43 did produce a TI of 128 against erythrocytes, which was equal to that of daptomycin (128) but lower than the calculated TI of polymyxin B (256). For Smp24, however, the highest calculated TI was the S3K modification against HEK-293 cells (38.7) whilst this is far superior than the TI of native Smp24 (1.2) it does demonstrate inferiority against the commercially available AMP-like antibiotics used in this study.

Despite the difficulties faced with the development of novel antimicrobials, new drugs are entering clinical trials which provides some optimism. Omiganan is a topical 12-amino acid peptide (Sader *et al.* 2004) which has recently completed phase III clinical trials for the treatment of rosacea. Novexatin is a potent AMP undergoing clinical trials for the brush on treatment for onychmycosis (fungal nail infection). This AMP, developed by NovaBiotics, has demonstrated safety, tolerance and efficacy in phase I and IIa clinical trials. This highlights the antimicrobial drug approval landscape is changing and why the efforts of smaller pharmaceutical companies, biotech and studies in academic groups like this one are important for the introduction of new antimicrobials in to clinical trials.

Clinical trials may be a longer term goal for the peptides in this study, but further modifications of the peptides and investigations in to the mechanism of action of some of the identified peptides with enhanced TIs is warranted.

7.5 Recombinant peptide production

As discussed in chapter 6 (section 6.1), one of the limitations of this study is the cost of peptide synthesis. Progress was made with the expression system as detectable quantities of Smp24 were being produced but difficulties were faced

with the purification. Challenges have been faced in the expression of antimicrobial peptides, with protein yield varying substantially between AMPs and the chosen bacterial expression system. Song *et al*., (2014) report yields of 0.6 mg/L of the AMP Dermaseptin S4 whilst Chen *et al.*, (2015) report yields of 35 mg/L of plectasin highlighting a degree of variability between the recombinant production of AMPs (Song *et al.* 2014, Chen *et al.* 2015).

The future of this work would be to optimise the purification strategy by performing column chromatography as opposed to the batch purification discussed in chapter 6 (section 6.6). Purification in column format would minimise the loss of product and of agarose beads, which in turn would reduce the financial cost of the work. The antimicrobial, haemolytic and cytotoxic activity of the purified product would be assessed both with and without the FLAG-tag to determine the effect of the fusion tag on the mechanism of action. The activity of FLAG-tagged products can be retained without cleavage of the tag (Fu *et al.* 2019). Wu *et al*., (2013) investigated the *in vitro* antimicrobial activity of the AMP thanatin(S) both with and without a FLAG tag. Both AMPs demonstrated antimicrobial activity and it was determined the FLAG-tag had little effect on the antimicrobial activity of thanatin(S). If the activity of Smp24 could be retained without cleavage of the tag, this would create a more streamlined process in the laboratory and result in a reduced risk of losing peptide yield during additional processes. Additionally, the recombinant system would enable the creation of a library of genes for expression of mutated Smp24 peptides to further investigate the relationship between structure and function.

7.6 Improving the stability of AMPs

One of the major disadvantages of natural AMPs is susceptibility to proteolytic degradation which dominates the pharmacokinetic profile (Travkova *et al.* 2017). In general, AMPs possessing low molecular weights and high positive charges are inherently bactericidal and prone to proteolytic degradation *in vivo* (Wibowo and Zhao 2019). Increasing the stability of AMPs by reducing susceptibility to proteolysis is a major goal for AMP improvement, as it would be

beneficial for practical application and their production through biotechnology (Zhu *et al.* 2017a).

The incorporation of $_{D}$-amino acids ($_{D}$-AAs) in to the AMP structure is a strategy which can enhance the therapeutic application of AMPs. The incorporation of $_{D}$-AAs can increase stability, provide resistance to enzymatic degradation and reduce haemolytic activity whilst preserving the bioactive properties of peptides. However, including $_{D}$-AAs in to peptide chain can be difficult to synthesise and may result in the loss of the secondary structure. Additionally the incorporation of $_{D}$-AAs is also likely incompatible with recombinant production techniques (Cardoso *et al.* 2018). Hong *et al*., (1999) produced 6 analogues of the AMP KLSK which incorporated $_{D}$-AAs in to the structure. The study concluded the incorporation of $_{D}$-lysine at the N- and C- terminal regions of the peptide had little effect on the helical content and thus the peptide retained its antimicrobial activity whilst demonstrating enhanced stability and increased resistance from proteolytic degradation by serine proteases. The incorporation of $_{D}$-lysine in the central region of the peptide resulted in complete loss of both the helical content and antimicrobial activity (Hong *et al.* 1999). Single substitutions of asparginine^{4}, glycine^{8}, alanine^{10} and leucine^{18} for $_{D}$-lysine residues of ascaphin-8, an AMP derived from the skin of the American tailed frog *Ascaphus truei*, produced peptides which retained the antimicrobial activity of native ($_{L}$-) ascaphin-8 but demonstrated reduced haemolytic activity (Michael Conlon *et al.* 2008). Other studies have replaced $_{L}$-amino acids with their respective $_{D}$- enantiomers. Modification of temporin L (TL) to include $_{D}$-enantiomers produced peptides which retained antimicrobial activity and generally demonstrated reduced haemolytic activity (Grieco *et al.* 2012).

The incorporation of $_{D}$-amino acids in to the chain of Smp24 (particularly the S3K modification) using a similar methodology to that used by Grieco *et al.,* (2012) for the modification of TL would be an interesting strategy to adopt. The inclusion of $_{D}$-lysine at position 3 (Smp24 S3$_{D}$-K) could be investigated to determine if the $_{D}$-enantiomer retains the antimicrobial activity of Smp24 S3K and demonstrates reduced haemolytic activities as shown by the inclusion of $_{D}$-AAs in other studies. (Hong *et al.* 1999, Grieco *et al.* 2012). This strategy would be adopted for all of the peptides in this study which demonstrated enhanced therapeutic indices

(TIs), which are S3K, F4A, D23F and S24K modifications of Smp24 (to produce $F4_{D}$-A, $D23_{D}$-F and $S24_{D}$-K) and W3A, W5A and W14A modifications of Smp43 (to produce $W3_{D}$-A, $W5_{D}$-A and $W14_{D}$-A). The peptides would be characterised in terms of antimicrobial, cytotoxicity and haemolytic activity under the same conditions used in this study to enable direct comparisons between the $_{D}$- and $_{L}$-enantiomers. The structure of the peptides would be assessed by performing circular dichroism (CD) spectroscopy to determine if the inclusion of $_{D}$-enantiomers affected the helical content of the peptides when compared with the native $_{L}$-peptides. The stability of the peptides would also be assessed, this could be achieved via the addition of trypsin and quenching the reaction at different time points and characterising the peptides by reversed phase high performance liquid chromatography (RP-HPLC) (Najjar *et al.* 2017).

7.7 Higher resolution structural biology approaches

Protein structure determination by nuclear magnetic resonance (NMR) is a continually evolving technology which enables the dynamics of proteins to be quantitatively characterised and the relevance for function to be elucidated. NMR is unique among the structure-determination approaches in its ability to provide kinetic insights in to protein dynamics without requiring modification of the protein (Arthanari *et al.* 2019).

The α-helical structure of Smp24, Smp24 S3K, Smp24 K7F and Smp43 have been determined by CD spectroscopy. NMR would enable differences in the helical content of the peptides to be determined, by enabling the visualisation of the helical content between amino acid residues. As *ab-initio* modelling of the peptides has been used to support the link between structure and function, NMR could be utilised to provide experimental data on the structural changes which have arisen due to single amino acid substitutions (Imamura *et al.* 2008).

Solid-state NMR can provide information on the 3D conformation of the peptide as well as the mode of interaction with model lipid membranes. The utilisation of NMR could enable the identification of the biophysical properties of critical residues which mediate interactions between the AMPs and the membrane (Li *et*

al. 2017). Elucidating the mechanism of interaction between AMPs and lipid bilayers can require extensive computational resources and provide an experimental challenge, as such, the interactions of AMPs with micelles is often used as an alternative methodology. This technique enables longer simulations and permits the monitoring of biological phenomena of longer time scales (Khandelia and Kaznessis 2005). This methodology would be particularly interesting to adopt to investigate the structural and membrane interaction changes between native Smp24 and the single amino acid modifications which resulted in potently increased and drastically reduced antimicrobial activity. The utilisation of NMR to understand the relationship between structure and function could also aid the future design of more potent peptides.

Conclusions

The development of novel antimicrobials with less susceptibility to bacterial resistance is of high importance. In this thesis, modified scorpion venom-derived antimicrobial peptides have been produced which show enhanced therapeutic profiles when compared with native AMPs. These modified peptides are interesting candidates for further investigations to aid the drug discovery approach. A system for recombinant production of AMPs in *E. coli* has been developed and with further optimisation this could be a useful tool for large-scale AMP production in the laboratory. When combined with the optimised site-directed mutagenesis methodology, this will enable a library of mutant peptides to be produced and further screening (such as cytotoxicity assessment against primary cell lines and proteolytic stability) to be assessed. The utilisation of an SDM approach would enable virtually limitless modified peptides to be produced at an extremely low cost. The power of directed or even random substitutions could be huge and result in a greater understanding of the structure-function relationship of Smp24 and thus the optimisation of a molecule for therapeutic application.

References

Abbas, S. and Stevens, M.P., 2018. The Role of the Hospital Epidemiologist in Antibiotic Stewardship. *Medical Clinics of North America*, 102 (5), 873–882.

Abdel-Rahman, M.A., Harrison, P.L., and Strong, P.N., 2015. Snapshots of scorpion venomics. *Journal of Arid Environments*, 112, 170–176.

Abdel-Rahman, M.A., Quintero-Hernandez, V., and Possani, L.D., 2013. Venom proteomic and venomous glands transcriptomic analysis of the Egyptian scorpion Scorpio maurus palmatus (Arachnida: Scorpionidae). *Toxicon*, 74, 193–207.

Abraham, S., Juel, H.B., Bang, P., Cheeseman, H.M., Dohn, R.B., Cole, T., Kristiansen, M.P., Korsholm, K.S., Lewis, D., Olsen, A.W., McFarlane, L.R., Day, S., Knudsen, S., Moen, K., Ruhwald, M., Kromann, I., Andersen, P., Shattock, R.J., and Follmann, F., 2019. Safety and immunogenicity of the chlamydia vaccine candidate CTH522 adjuvanted with CAF01 liposomes or aluminium hydroxide: a first-in-human, randomised, double-blind, placebo-controlled, phase 1 trial. *The Lancet Infectious Diseases*, 0 (0).

Ageitos, J.M., Sánchez-Pérez, A., Calo-Mata, P., and Villa, T.G., 2017. Antimicrobial peptides (AMPs): Ancient compounds that represent novel weapons in the fight against bacteria. *Biochemical Pharmacology*, 133, 117–138.

Aghapour, Z., Gholizadeh, P., Ganbarov, K., Bialvaei, A.Z., Mahmood, S.S., Tanomand, A., Yousefi, M., Asgharzadeh, M., Yousefi, B., and Kafil, H.S., 2019. Molecular mechanisms related to colistin resistance in Enterobacteriaceae. *Infection and drug resistance*, 12, 965–975.

Agyei, D. and Danquah, M.K., 2011. Industrial-scale manufacturing of pharmaceutical-grade bioactive peptides. *Biotechnology Advances*, 29 (3), 272–277.

Ahmad, M. and Khan, A.U., 2019. Global economic impact of antibiotic resistance: A review. *Journal of Global Antimicrobial Resistance*.

Al-Qarawi, A.A. and Mousa, H.M., 2004. Lipid concentrations in erythrocyte membranes in normal, starved, dehyrated and rehydrated camels (Camelus dromedarius), and in normal sheep (Ovis aries) and goats (Capra hircus) ARTICLE IN PRESS. *Journal of Arid Environments*, 59, 675–683.

Albur, M.S., Noel, A., Bowker, K., and MacGowan, A., 2015. The combination of

colistin and fosfomycin is synergistic against NDM-1-producing Enterobacteriaceae in in vitro pharmacokinetic/pharmacodynamic model experiments. *International Journal of Antimicrobial Agents*, 46 (5), 560–567.

Alencar-Silva, T., Braga, M.C., Oliveira, G., Santana, S., Saldanha-Araujo, F., Pogue, R., Campos Dias, S., Franco, O.L., and Carvalho, J.L., 2018. Breaking the frontiers of cosmetology with antimicrobial peptides. *Biotechnology Advances*, 36, 2019–2031.

Alge, C.S., Hauck, S.M., Priglinger, S.G., Kampik, A., and Ueffing, M., 2006. Differential Protein Profiling of Primary versus Immortalized Human RPE Cells Identifies Expression Patterns Associated with Cytoskeletal Remodeling and Cell Survival. *Journal of Proteome Research*, 5 (4), 862–878.

Alumran, A., Hou, X.-Y., and Hurst, C., 2013. Assessing the overuse of antibiotics in children with URTIs in Saudi Arabia: development of the parental perception on antibiotics scale (PAPA scale). *Journal of epidemiology and global health*, 3 (1), 3–10.

Alvarado-Gomez, E., Perez-Diaz, M., Valdez-Perez, D., Ruiz-Garcia, J., Magana-Aquino, M., Martinez-Castanon, G., and Martinez-Gutierrez, F., 2018. Adhesion forces of biofilms developed in vitro from clinical strains of skin wounds. *Materials Science and Engineering C*, 82, 336–344.

Anderson, B.J., 2008. Paracetamol (Acetaminophen): mechanisms of action. *Pediatric Anesthesia*, 18 (10), 915–921.

Andersson, D.I., Hughes, D., and Kubicek-Sutherland, J.Z., 2016. Mechanisms and consequences of bacterial resistance to antimicrobial peptides. *Drug Resistance Updates*, 26, 43–57.

Andreoli, T.E., Bangham, J.A., and Tosteson, D.C., 1967. The Formation and Properties of Thin Lipid Membranes from HK and LK Sheep Red Cell Lipids. *The Journal of General Physiology*, 50, 1729–1749.

Andrews, J.M., 2001. Determination of minimum inhibitory concentrations. *Journal of Antimicrobial Chemotherapy*, 48 (suppl_1), 5–16.

Aoki, W. and Ueda, M., 2013. Characterization of Antimicrobial Peptides toward the Development of Novel Antibiotics. *Pharmaceuticals (Basel, Switzerland)*, 6 (8), 1055–81.

Apostolakos, I. and Piccirillo, A., 2018. A review on the current situation and challenges of colistin resistance in poultry production. *Avian Pathology*, 47

(6), 546–558.

Armengol-Porta, M., Tenorio-Abreu, A., Bandt, D., Coleman, D.C., Gavier-Widen, D., Hotzel, H., Kinnevey, P., Lazaris, A., Peters, M., Rangstrup-Christensen, L., Schlotter, K., Shore, A.C., Ehricht, R., and Monecke, S., 2016. In vitro activity of ceftaroline against mecC-positive MRSA isolates. *Journal of Global Antimicrobial Resistance*, 5, 3–6.

Aronson, J.K., 2016. Bacitracin. *In*: *Meyler's Side Effects of Drugs*. 807–808.

Arthanari, H., Takeuchi, K., Dubey, A., and Wagner, G., 2019. Emerging solution NMR methods to illuminate the structural and dynamic properties of proteins This review comes from a themed issue on Biophysical and com-putational methods. *Current Opinion in Structural Biology*, 58, 294–304.

Ashcheulova, D.O., Efimova, L. V, Lushchyk, Y., Yantsevich, A. V, Baikov, A.N., and Pershina, A.G., 2018. Production of the recombinant antimicrobial peptide UBI 18-35 in Escherichia coli. *Protein Expression and Purification*, 143, 38–44.

Bacanlı, M. and Başaran, N., 2019. Importance of antibiotic residues in animal food. *Food and Chemical Toxicology*, 125, 462–466.

Bae, J.-S., Jeong, J.-M., Nam, B.-H., Kim, J.-W., Park, J.Y., and Park, C.-I., 2018. Gene expressions and biological activities of two novel antimicrobial peptides (AMPs) isolated from leucocytes of the rock bream, Oplegnathus fasciatus. *Aquaculture*, 495, 35–43.

Bandaranayake, A.D. and Almo, S.C., 2014. Recent advances in mammalian protein production. *FEBS letters*, 588 (2), 253–60.

Barksdale, S.M., Hrifko, E.J., Myung, E., Chung, -Chul, and Van Hoek, M.L., 2016. Peptides from American alligator plasma are antimicrobial against multi-drug resistant bacterial pathogens including Acinetobacter baumannii. *BMC Microbiology*, 1–14.

Bartlett, J.G., 2017. Bezlotoxumab-A New Agent for Clostridium difficile Infection.

Bell, G. and Gouyon, P.H., 2003. Arming the enemy: The evolution of resistance to self-proteins. *Microbiology*, 149 (6), 1367–1375.

Bendesky, A., Menéndez, D., and Ostrosky-Wegman, P., 2002. Is metronidazole carcinogenic? *Mutation Research/Reviews in Mutation Research*, 511 (2), 133–144.

Bessalle, R., Haas, H., Goria, A., Shalit, I., and Fridkin, M., 1992. Augmentation of the antibacterial activity of magainin by positive-charge chain extension.

Antimicrobial agents and chemotherapy, 36 (2), 313–317.

Bittencourt, C.R., de Oliveira Farias, E.A., Bezerra, K.C., Véras, L.M.C., Silva, V.C., Costa, C.H.N., Bemquerer, M.P., Silva, L.P., Souza de Almeida Leite, J.R. de, and Eiras, C., 2016. Immobilization of cationic antimicrobial peptides and natural cashew gum in nanosheet systems for the investigation of anti-leishmanial activity. *Materials Science and Engineering: C*, 59, 549–555.

Blair, J.M., Richmond, G.E., and Piddock, L.J., 2014. Multidrug efflux pumps in Gram-negative bacteria and their role in antibiotic resistance. *Future Microbiology*, 9 (10), 1165–1177.

Bluhm, M.E.C., Knappe, D., and Hoffmann, R., 2015. Structure-activity relationship study using peptide arrays to optimize Api137 for an increased antimicrobial activity against Pseudomonas aeruginosa. *European journal of medicinal chemistry*, 103, 574–582.

Bobone, S., Roversi, D., Giordano, L., De Zotti, M., Formaggio, F., Toniolo, C., Park, Y., and Stella, L., 2012. The Lipid Dependence of Antimicrobial Peptide Activity Is an Unreliable Experimental Test for Different Pore Models. *Biochemistry*, 51 (51), 10124–10126.

Bot, C.T. and Prodan, C., 2010. Quantifying the membrane potential during E. coli growth stages. *Biophysical Chemistry*, 146 (2–3), 133–137.

Brandenburg, K.S., Weaver, A.J., Qian, L., You, T., Chen, P., Karna, S.L.R., Fourcaudot, A.B., Sebastian, E.A., Abercrombie, J.J., Pineda, U., Hong, J., Wienandt, N.A., Leung, K.P., and Leung, K.P., 2019. Development of Pseudomonas aeruginosa Biofilms in Partial-Thickness Burn Wounds Using a Sprague-Dawley Rat Model. *Journal of burn care & research : official publication of the American Burn Association*, 40 (1), 44–57.

Brogden, K.A., 2005. Antimicrobial peptides: pore formers or metabolic inhibitors in bacteria? *Nature reviews. Microbiology*, 3 (3), 238–50.

Brown, D., 2015. Antibiotic resistance breakers: can repurposed drugs fill the antibiotic discovery void? *Nature Reviews Drug Discovery*, 14 (12), 821–832.

Butler, M.S., Blaskovich, M.A., Owen, J.G., and Cooper, M.A., 2016. Old dogs and new tricks in antimicrobial discovery. *Current Opinion in Microbiology*, 33, 25–34.

Campoccia, D., Montanaro, L., and Arciola, C.R., 2013. A review of the biomaterials technologies for infection-resistant surfaces. *Biomaterials*, 34 (34), 8533–8554.

Canton, R., Chouinard, L., and Tarragó, C., 2018. A review of the antibacterial activity of ozenoxacin. *Future Microbiology*, 13 (6s), 1–2.

Cardoso, M.H., C ˆ andido, E.S., Oshiro, K.G., Rezende, S.B., Franco, vio L., and Applications in Biomedicine, P., 2018. Peptides containing D-amino acids and retro-inverso peptides: General applications and special focus on antimicrobial peptides.

Champak Chatterjee, Moushumi Paul, Lili Xie, A., and Donk*, W.A. van der, 2005. Biosynthesis and Mode of Action of Lantibiotics. *Chemical reviews*, 105 (2), 633–684.

Chart, H., Smith, H.R., La Ragione, R.M., and Woodward, M.J., 2000. An investigation into the pathogenic properties of Escherichia coli strains BLR, BL21, DH5alpha and EQ1. *Journal of Applied Microbiology*, 89 (6), 1048–1058.

Chen, X., Shi, J., Chen, R., Wen, Y., Shi, Y., Zhu, Z., Guo, S., and Li, L., 2015. Molecular chaperones (TrxA, SUMO, Intein, and GST) mediating expression, purification, and antimicrobial activity assays of plectasin in *Escherichia coli*. *Biotechnology and Applied Biochemistry*, 62 (5), 606–614.

Chen, Y., Gong, Q., Song, M., Lai, J., Sun, J., and Liu, Y., 2019. Identification and characterization of three novel antimicrobial peptides from Acipenser dabryanus. *Fish and Shellfish Immunology*, 88, 207–216.

Chen, Y., Mant, C.T., Farmer, S.W., Hancock, R.E.W., Vasil, M.L., and Hodges, R.S., 2005. Rational Design of -Helical Antimicrobial Peptides with Enhanced Activities and Specificity/Therapeutic Index. *Journal of Biological Chemistry*, 280 (13), 12316–12329.

Chew, K.L., La, M.-V., Lin, R.T.P., and Teo, J.W.P., 2017. Colistin and Polymyxin B Susceptibility Testing for Carbapenem-Resistant and mcr-Positive Enterobacteriaceae: Comparison of Sensititre, MicroScan, Vitek 2, and Etest with Broth Microdilution. *Journal of Clinical Microbiology*, 55 (9), 2609–2616.

Choi, I.S., Lee, Y.J., Wi, Y.M., Kwan, B.S., Jung, K.H., Hong, W.P., and Kim, J.M., 2016. Predictors of mortality in patients with extensively drug-resistant Acinetobacter baumannii pneumonia receiving colistin therapy. *International Journal of Antimicrobial Agents*, 48 (2), 175–180.

Chopra, I., Schofield, C., Everett, M., O'Neill, A., Miller, K., Wilcox, M., Frère, J.-M., Dawson, M., Czaplewski, L., Urleb, U., and Courvalin, P., 2008. Treatment of health-care-associated infections caused by Gram-negative

bacteria: a consensus statement. *The Lancet Infectious Diseases*.

Ciumac, D., Gong, H., Hu, X., and Ren Lu, J., 2019. Membrane targeting cationic antimicrobial peptides. *Journal of Colloid and Interface Science*, 537, 163–185.

Cociancich, S., Goyffon, M., Bontems, F., Bulet, P., Bouet, F., Menez, A., and Hoffmann, J., 1993. Purification and Characterization of a Scorpion Defensin, a 4kDa Antibacterial Peptide Presenting Structural Similarities with Insect Defensins and Scorpion Toxins. *Biochemical and Biophysical Research Communications*, 194 (1), 17–22.

Cole, C., Barber, J.D., and Barton, G.J., 2008. The Jpred 3 secondary structure prediction server. *Nucleic Acids Research*, 36 (Web Server), W197–W201.

Conway, S.P., Pond, M.N., Watson, A., Etherington, C., Robey, H.L., and Goldman, M.H., 1997. *Intravenous colistin sulphomethate in acute respiratory exacerbations in adult patients with cystic fibrosis One patient withdrew because of severe weakness and dizziness. All other adverse Patients with a previous hypersensitivity re*. Thorax.

Corey, G.R., McKinnell, J.A., and Rybak, M.J., 2019. Delafloxacin in Acute Bacterial Skin and Skin Structure Infections. *Clinical Infectious Diseases*, 68 (Supplement_3), S191–S192.

Corzo, G., Escoubas, P., Villegas, E., Barnham, K.J., He, W., Norton, R.S., and Nakajima, T., 2001. Characterization of unique amphipathic antimicrobial peptides from venom of the scorpion Pandinus imperator. *Biochem. J*, 359, 35–45.

Corzo, G., Villegas, E., Gómez-Lagunas, F., Possani, L.D., Belokoneva, O.S., and Nakajima, T., 2002. Oxyopinins, large amphipathic peptides isolated from the venom of the wolf spider Oxyopes kitabensis with cytolytic properties and positive insecticidal cooperativity with spider neurotoxins. *The Journal of biological chemistry*, 277 (26), 23627–37.

Costa, F., Carvalho, I.F., Montelaro, R.C., Gomes, P., and Martins, M.C.L., 2011. Covalent immobilization of antimicrobial peptides (AMPs) onto biomaterial surfaces. *Acta Biomaterialia*, 7 (4), 1431–1440.

Cotter, P.D., Hill, C., and Ross, R.P., 2005. Food Microbiology: Bacteriocins: developing innate immunity for food. *Nature Reviews Microbiology*, 3 (10), 777–788.

Cowley, N.L., Forbes, S., Amézquita, A., McClure, P., Humphreys, G.J., and

McBain, A.J., 2015. Effects of Formulation on Microbicide Potency and Mitigation of the Development of Bacterial Insusceptibility. *Applied and environmental microbiology*, 81 (20), 7330–8.

D'Costa, V.M., King, C.E., Kalan, L., Morar, M., Sung, W.W.L., Schwarz, C., Froese, D., Zazula, G., Calmels, F., Debruyne, R., Golding, G.B., Poinar, H.N., and Wright, G.D., 2011. Antibiotic resistance is ancient. *Nature*, 477 (7365), 457–61.

Dai, C., Ma, Y., Zhao, Z., Zhao, R., Wang, Q., Wu, Y., Cao, Z., and Li, W., 2008. Mucroporin, the first cationic host defense peptide from the venom of Lychas mucronatus. *Antimicrobial agents and chemotherapy*, 52 (11), 3967–72.

Daniele-Silva, A., Machado, R.J.A., Monteiro, N.K.V., Estrela, A.B., Santos, E.C.G., Carvalho, E., Araújo Júnior, R.F., Melo-Silveira, R.F., Rocha, H.A.O., Silva-Júnior, A.A., and Fernandes-Pedrosa, M.F., 2016. Stigmurin and TsAP-2 from Tityus stigmurus scorpion venom: Assessment of structure and therapeutic potential in experimental sepsis. *Toxicon*, 121, 10–21.

Dathe, M., Wieprecht, T., Nikolenko, H., Handel, L., Maloy, W.L., MacDonald, D.L., Beyermann, M., and Bienert, M., 1997. Hydrophobicity, hydrophobic moment and angle subtended by charged residues modulate antibacterial and haemolytic activity of amphipathic helical peptides. *FEBS Letters*, 403 (2), 208–212.

Datta, A., Kundu, P., and Bhunia, A., 2015. Designing potent antimicrobial peptides by disulphide linked dimerization and N-terminal lipidation to increase antimicrobial activity and membrane perturbation: Structural insights into lipopolysaccharide binding. *Journal of colloid and interface science*, 461, 335–345.

Dean, S.N., Bishop, B.M., and van Hoek, M.L., 2011. Natural and synthetic cathelicidin peptides with anti-microbial and anti-biofilm activity against Staphylococcus aureus. *BMC Microbiology*, 11 (1), 114.

Dennison, S., Wallace, J., Harris, F., and Phoenix, D., 2005. Amphiphilic α-Helical Antimicrobial Peptides and Their Structure / Function Relationships. *Protein & Peptide Letters*, 12 (1), 31–39.

Dennison, S.R. and Phoenix, D.A., 2014. Susceptibility of sheep, human, and pig erythrocytes to haemolysis by the antimicrobial peptide Modelin 5. *European Biophysics Journal*, 43 (8–9), 423–432.

DiNubile, M.J., 2016. Noninferior Antibiotics: When Is 'Not Bad' 'Good Enough'?

Open forum infectious diseases, 3 (3), ofw110.

Donato, M.T., Tolosa, L., and Gómez-Lechón, M.J., 2015. Culture and Functional Characterization of Human Hepatoma HepG2 Cells. Humana Press, New York, NY, 77–93.

Durand, G.A., Raoult, D., and Dubourg, G., 2019. Antibiotic discovery: history, methods and perspectives. *International Journal of Antimicrobial Agents*, 53, 371–382.

Durão, P., Balbontín, R., and Gordo, I., 2018. Evolutionary Mechanisms Shaping the Maintenance of Antibiotic Resistance. *Trends in microbiology*, 25 (8), 677–691.

Echols, R.M., 2011. Understanding the regulatory hurdles for antibacterial drug development in the post-Ketek world. *Annals of the New York Academy of Sciences*, 1241 (1), 153–161.

Edwards, I.A., Elliott, A.G., Kavanagh, A.M., Zuegg, J., Blaskovich, M.A.T., and Cooper, M.A., 2016. Contribution of Amphipathicity and Hydrophobicity to the Antimicrobial Activity and Cytotoxicity of β-Hairpin Peptides. *ACS Infectious Diseases*, 2 (6), 442–450.

Einhauer, A. and Jungbauer, A., 2001. *The FLAGe peptide, a versatile fusion tag for the purification of recombinant proteins*. J. Biochem. Biophys. Methods.

Eisenberg, D., Weiss, R.M., Terwilliger, T.C., and Wilcox, W., 1982. *Hydrophobic Moments and Protein Structure*. Chem. Soc.

Epand, R.F., Wang, G., Berno, B., and Epand, R.M., 2009. Lipid segregation explains selective toxicity of a series of fragments derived from the human cathelicidin LL-37. *Antimicrobial agents and chemotherapy*, 53 (9), 3705–14.

Epand, R.M. and Epand, R.F., 2009. Lipid domains in bacterial membranes and the action of antimicrobial agents. *Biochimica et Biophysica Acta (BBA) - Biomembranes*, 1788 (1), 289–294.

Falcao, C.B., de La Torre, B.G., Pérez-Peinado, C., Barron, a. E., Andreu, D., and Rádis-Baptista, G., 2014. Vipericidins: a novel family of cathelicidin-related peptides from the venom gland of South American pit vipers. *Amino Acids*, 2561–2571.

Fan, L., Sun, J., Zhou, M., Zhou, J., Lao, X., Zheng, H., and Xu, H., 2016. DRAMP: a comprehensive data repository of antimicrobial peptides. *Scientific Reports*, 6 (1), 24482.

Fernandez, D.I., Gehman, J.D., and Separovic, F., 2008. Membrane interactions

of antimicrobial peptides from Australian frogs. *BBA - Biomembranes*, 1788, 1630–1638.

Field, D., Begley, M., O'Connor, P.M., Daly, K.M., Hugenholtz, F., Cotter, P.D., Hill, C., and Ross, R.P., 2012. Bioengineered Nisin A Derivatives with Enhanced Activity against Both Gram Positive and Gram Negative Pathogens. *PLoS ONE*, 7 (10), e46884.

Fjell, C.D., Hiss, J.A., Hancock, R.E.W., and Schneider, G., 2011. Designing antimicrobial peptides: form follows function. *Nature Reviews Drug Discovery*, 11 (January).

Fosgerau, K. and Hoffmann, T., 2015. Peptide therapeutics : current status and future directions §. *Drug Discovery Today*, 20 (1), 122–128.

Fox, J.L., 2013. Antimicrobial peptides stage a comeback. *Nature Biotechnology*, 31 (5), 379–382.

Fu, J., Liu, W., Cui, H., Song, C., Liu, Y., and Wei, L., 2019. Characterization and functional analysis of liver-expressed antimicrobial peptide-2 (LEAP-2) in Pelodiscus sinensis.

Galar, A., Muñoz, P., Valerio, M., Cercenado, E., García-González, X., Burillo, A., Sánchez-Somolinos, M., Juárez, M., Verde, E., and Bouza, E., 2018. Current use of daptomycin and systematic therapeutic drug monitoring: Clinical experience in a tertiary care institution R. *International Journal of Antimicrobial Agents*, 53, 40–48.

Gauldie, J., Hanson, J.M., RUMJANEK, F.D., Shiploni, R.A., and Vernon, C.A., 1976. The Peptide Components of Bee Venom. *European Journal of Biochemistry*, 61 (2), 369–376.

Gerace, E. and Moazed, D., 2015. Affinity Pull-Down of Proteins Using Anti-FLAG M2 Agarose Beads. *Laboratory Methods in Enzymology: Protein Part D*, 559, 99–110.

Gleason, N.J., Vostrikov, V. V, Greathouse, D. V, and Koeppe, R.E., 2013. Buried lysine, but not arginine, titrates and alters transmembrane helix tilt. *Proceedings of the National Academy of Sciences of the United States of America*, 110 (5), 1692–5.

Gottler, L.M. and Ramamoorthy, A., 2009. Structure, membrane orientation, mechanism, and function of pexiganan — A highly potent antimicrobial peptide designed from magainin. *Biochimica et Biophysica Acta (BBA) - Biomembranes*, 1788 (8), 1680–1686.

Graham, J.P., Boland, J.J., and Silbergeld, E., 2007. Growth promoting antibiotics in food animal production: an economic analysis. *Public Health Reports*, 122, 78–87.

Grangeasse, C., Stülke, J., and Mijakovic, I., 2015. Regulatory potential of post-translational modifications in bacteria. *Frontiers in microbiology*, 6, 500.

Greig, S.L., 2016. Obiltoxaximab: First Global Approval. *Drugs*, 76 (7), 823–830.

Grieco, P., Carotenuto, A., Auriemma, L., Saviello, M.R., Campiglia, P., Gomez-Monterrey, I.M., Marcellini, L., Luca, V., Barra, D., Novellino, E., and Mangoni, M.L., 2012. The effect of D-amino acid substitution on the selectivity of temporin L towards target cells: Identification of a potent anti-Candida peptide ☆ , ☆☆.

Hackel, M.A., Lomovskaya, O., Dudley, M.N., Karlowsky, J.A., and Sahm, D.F., 2018. In Vitro Activity of Meropenem-Vaborbactam against Clinical Isolates of KPC-Positive Enterobacteriaceae. *Antimicrobial Agents and Chemotherapy*, 62 (1), e01904-17.

Hancock, R.E., 1997. Peptide antibiotics. *The Lancet*, 349 (9049), 418–422.

Hancock, R.E.W., 1999. Host Defence (Cationic) Peptides. *Drugs*, 57 (4), 469–473.

Hancock, R.E.W. and Lehrer, R., 1998. Cationic peptides: a new source of antibiotics. *Trends in Biotechnology*, 16 (2), 82–88.

Harris, F., Dennison, S., and Phoenix, D., 2009. Anionic Antimicrobial Peptides from Eukaryotic Organisms. *Current Protein & Peptide Science*, 10 (6), 585–606.

Harrison, P.L., Abdel-Rahman, M.A., Miller, K., and Strong, P.N., 2014. Antimicrobial peptides from scorpion venoms. *Toxicon : official journal of the International Society on Toxinology*, 88, 115–37.

Harrison, P.L., Abdel-Rahman, M.A., Strong, P.N., Tawfik, M.M., and Miller, K., 2016. Characterisation of three alpha-helical antimicrobial peptides from the venom of Scorpio maurus palmatus. *Toxicon*, 117, 30–36.

Harrison, P.L., Heath, G.R., Johnson, B.R.G., Abdel-Rahman, M.A., Strong, P.N., Evans, S.D., and Miller, K., 2016. Phospholipid dependent mechanism of smp24, an α-helical antimicrobial peptide from scorpion venom. *Biochimica et Biophysica Acta (BBA) - Biomembranes*, 1858 (11), 2737–2744.

Haugen, H.S., Kristiansen, P.E., Fimland, G., and Nissen-Meyer, J., 2008. Mutational analysis of the class IIa bacteriocin curvacin A and its orientation

in target cell membranes. *Applied and environmental microbiology*, 74 (21), 6766–73.

Hayami, M., Okabe, A., Kariyama, R., Abe, M., and Kanemasa, Y., 1979. Lipid Composition of *Staphylococcus aureus* and Its Derived L-forms. *Microbiology and Immunology*, 23 (6), 435–442.

Hazam, P.K., Goyal, R., and Ramakrishnan, V., 2019. Peptide based antimicrobials: Design strategies and therapeutic potential. *Progress in Biophysics and Molecular Biology*, 142, 10–22.

Heath, G.R., Harrison, P.L., Strong, P.N., Evans, S.D., and Miller, K., 2018. Visualization of diffusion limited antimicrobial peptide attack on supported lipid membranes. *Soft matter*, 14 (29), 6146–6154.

Henly, E.L., Dowling, J.A.R., Maingay, J.B., Lacey, M.M., Smith, T.J., and Forbes, S., 2019. Biocide Exposure Induces Changes in Susceptibility, Pathogenicity, and Biofilm Formation in Uropathogenic Escherichia coli. *Antimicrobial agents and chemotherapy*, 63 (3), 1–15.

Hernández-Aponte, C.A., Silva-Sanchez, J., Quintero-Hernández, V., Rodríguez-Romero, A., Balderas, C., Possani, L.D., and Gurrola, G.B., 2011. Vejovine, a new antibiotic from the scorpion venom of Vaejovis mexicanus. *Toxicon*, 57 (1), 84–92.

Hicks, R.P., Abercrombie, J.J., Wong, R.K., and Leung, K.P., 2013. Antimicrobial peptides containing unnatural amino acid exhibit potent bactericidal activity against ESKAPE pathogens. *Bioorganic & medicinal chemistry*, 21 (1), 205–14.

Hilpert, K., Elliott, M.R., Volkmer-Engert, R., Henklein, P., Donini, O., Zhou, Q., Winkler, D.F.H., and Hancock, R.E.W., 2006. Sequence Requirements and an Optimization Strategy for Short Antimicrobial Peptides. *Chemistry & Biology*, 13, 1101–1107.

Holak, T.A., Engstroem, A., Kraulis, P.J., Lindeberg, G., Bennich, H., Jones, T.A., Gronenborn, A.M., and Clore, G.M., 1988. The solution conformation of the antibacterial peptide cecropin A: a nuclear magnetic resonance and dynamical simulated annealing study. *Biochemistry*, 27 (20), 7620–7629.

Hollmann, A., Martínez, M., Noguera, M.E., Augusto, M.T., Disalvo, A., Santos, N.C., Semorile, L., and Maffía, P.C., 2016. Role of amphipathicity and hydrophobicity in the balance between hemolysis and peptide-membrane interactions of three related antimicrobial peptides. *Colloids and Surfaces B:*

Biointerfaces, 141, 528–536.

Hong-Ling, Y., Zhi-Qiang, S., Xuan, L., and Yi, K., 2016. *Chinese Journal of Natural Medicines Two novel antimicrobial peptides from skin venoms of spadefoot toad Megophrys minor*.

Hong, S.Y., Oh, J.E., and Lee, K.-H., 1999. *Effect of D-Amino Acid Substitution on the Stability, the Secondary Structure, and the Activity of Membrane-Active Peptide*. BIOCHEM PHARMACOL.

Hu, X. and Tam, K., 2017. Biomembrane mimics and their roles in anti-bacterial drug discovery. *ADMET and DMPK*, 5 (1), 9.

Huang, H.W., 2000. Action of Antimicrobial Peptides: Two-State Model †. *Biochemistry*, 39 (29), 8347–8352.

Huang, X., Gao, C., Zhao, Q., and Li, C., 2015. Antimicrobial characterization of site-directed mutagenesis of porcine beta defensin 2. *PloS one*, 10 (2), e0118170.

Imamura, T., Yamamoto, N., Tamura, A., Murabayashi, S., Hashimoto, S., Shimada, H., and Taguchi, S., 2008. NMR based structure-activity relationship analysis of an antimicrobial peptide, thanatin, engineered by site-specific chemical modification: Activity improvement and spectrum alteration.

Irazazabal, L.N., Porto, W.F., Ribeiro, S.M., Casale, S., Humblot, V., Ladram, A., and Franco, O.L., 2016. Selective amino acid substitution reduces cytotoxicity of the antimicrobial peptide mastoparan. *Biochimica et Biophysica Acta (BBA) - Biomembranes*, 1858 (11), 2699–2708.

Iregui, A., Khan, Z., Malik, S., Landman, D., and Quale, J., 2019. Emergence of Delafloxacin-Resistant Staphylococcus aureus in Brooklyn, NY. *Clinical Infectious Diseases*.

Isabelle, F., Damien, S., Florence, R., Sylvie, M., Annick, C., Alhassane, D., Christine, M., Luc, T., and Garde Véronique, L., 2018. Occurrence and persistence of biofilms on cared chronic wounds: A large multicentric clinical study. *Wound Medicine*, 23, 28–34.

Jacobs, R.E. and White, S.H., 1989. The Nature of Hydrophobic Binding of Small Peptides at the Bilayer Interface: Implications for the Insertion of Transbilayer Helices. *Biochemistry*, 28, 3421–3437.

Jagus, R.J., Gerschenson, L.N., and Ollé Resa, C.P., 2016. Chapter 49 – Combinational Approaches for Antimicrobial Packaging: Natamycin and

Nisin. *In*: *Antimicrobial Food Packaging*. 599–608.

Saint Jean, K.D., Henderson, K.D., Chrom, C.L., Abiuso, L.E., Renn, L.M., and Caputo, G.A., 2018. Effects of Hydrophobic Amino Acid Substitutions on Antimicrobial Peptide Behavior. *Probiotics and Antimicrobial Proteins*, 10 (3), 408–419.

Jenssen, H., Hamill, P., and Hancock, R.E.W., 2006. Peptide Antimicrobial Agents. *Clinical Microbiology Reviews*, 19 (3), 491–511.

Jeong, H., Kim, H.J., and Lee, S.J., 2015. Complete Genome Sequence of Escherichia coli Strain BL21. *Genome announcements*, 3 (2).

Jiang, Z., Vasil, A.I., Hale, J.D., Hancock, R.E.W., Vasil, M.L., and Hodges, R.S., 2008. Effects of net charge and the number of positively charged residues on the biological activity of amphipathic alpha-helical cationic antimicrobial peptides. *Biopolymers*, 90 (3), 369–83.

Jiang, Z., Vasil, A.I., Vasil, M.L., and Hodges, R.S., 2014. "Specificity Determinants" Improve Therapeutic Indices of Two Antimicrobial Peptides Piscidin 1 and Dermaseptin S4 Against the Gram-negative Pathogens Acinetobacter baumannii and Pseudomonas aeruginosa. *Pharmaceuticals (Basel, Switzerland)*, 7 (4), 366–91.

Juba, M.L., Porter, D.K., Williams, E.H., Rodriguez, C.A., Barksdale, S.M., and Bishop, B.M., 2015. Helical cationic antimicrobial peptide length and its impact on membrane disruption. *Biochimica et biophysica acta*, 1848 (5), 1081–91.

Kang, S.-J., Kim, D.-H., Mishig-Ochir, T., and Lee, B.-J., 2012. Animicrobial Peptides: Their Physicochemical Properties and Therapeutic Application. *Archives of Pharmaceutical Research*, 35 (3), 409–413.

Kang, W., Liu, H., Ma, L., Wang, M., Wei, S., Sun, P., Jiang, M., Guo, M., Zhou, C., and Dou, J., 2017a. Effective antimicrobial activity of a peptide mutant Cbf-14-2 against penicillin-resistant bacteria based on its unnatural amino acids. *European Journal of Pharmaceutical Sciences*, 105, 169–177.

Kang, W., Liu, H., Ma, L., Wang, M., Wei, S., Sun, P., Jiang, M., Guo, M., Zhou, C., and Dou, J., 2017b. Effective antimicrobial activity of a peptide mutant Cbf-14-2 against penicillin-resistant bacteria based on its unnatural amino acids. *European Journal of Pharmaceutical Sciences*.

Karakonstantis, S. and Kalemaki, D., 2019. Antimicrobial overuse and misuse in the community in Greece and link to antimicrobial resistance using

methicillin-resistant S. aureus as an example. *Journal of Infection and Public Health*, 12, 460–464.

Kaushik, D., Rathi, S., and Jain, A., 2011. Ceftaroline: a comprehensive update. *International Journal of Antimicrobial Agents*, 37, 389–395.

Kempf, I., Jouy, E., and Chauvin, C., 2016. Colistin use and colistin resistance in bacteria from animals.

Kennedy, P., Brammah, S., and Wills, E., 2010. Burns, biofilm and a new appraisal of burn wound sepsis. *Burns*, 36, 49–56.

Khameneh, B., Diab, R., Ghazvini, K., and Fazly Bazzaz, B.S., 2016. Breakthroughs in bacterial resistance mechanisms and the potential ways to combat them. *Microbial Pathogenesis*, 95, 32–42.

Khandelia, H. and Kaznessis, Y.N., 2005. Molecular dynamics simulations of helical antimicrobial peptides in SDS micelles: what do point mutations achieve? *Peptides*, 26 (11), 2037–49.

Kim, C.-H., Go, H.-J., Oh, H.Y., Park, J.B., Lee, T.K., Seo, J.-K., Elphick, M.R., and Park, N.G., 2018. Identification of a novel antimicrobial peptide from the sea star Patiria pectinifera. *Developmental and comparative immunology*, 86 (2018), 203–213.

Kim, M.K., Kang, H.K., Ko, S.J., Hong, M.J., Bang, J.K., Seo, C.H., and Park, Y., 2018. Mechanisms driving the antibacterial and antibiofilm properties of Hp1404 and its analogue peptides against multidrug-resistant Pseudomonas aeruginosa. *Scientific Reports*, 8 (1), 1763.

Kim, S.-K. and Lee, J.-H., 2016. Biofilm dispersion in Pseudomonas aeruginosa. *Journal of Microbiology*, 54 (2), 71–85.

Koehbach, J., 2017. Structure-Activity Relationships of Insect Defensins. *Frontiers in Chemistry*, 5, 45.

Koehbach, J. and Craik, D.J., 2019. The Vast Structural Diversity of Antimicrobial Peptides. *Trends in Pharmacological Sciences*, 40 (7), 516–528.

Kokryakov, V.N., Harwig, S.S.L., Panyutich, E.A., Shevchenko, A.A., Aleshinab, G.M., Shamovab, O. V, Kornevab, H.A., and Lehrera, R.I., 1993. Protegrins: leukocyte antimicrobial peptides that combine features of corticostatic defensins and tachyplesins. *FEBS*, 327 (2), 231–236.

Kuddus, M.R., Rumi, F., Tsutsumi, M., Takahashi, R., Yamano, M., Kamiya, M., Kikukawa, T., Demura, M., and Aizawa, T., 2016. Expression, purification and characterization of the recombinant cysteine-rich antimicrobial peptide

snakin-1 in Pichia pastoris. *Protein expression and purification*, 122, 15–22.

Kyte, J. and Doolittle, R.F., 1982. A simple method for displaying the hydropathic character of a protein. *Journal of Molecular Biology*, 157 (1), 105–132.

Laaris, N., Sun, Y., and Chai, T., 2012. 494 CHARACTERIZATION OF RESTING MEMBRANE POTENTIAL IN RAT AND HUMAN BLADDER UROTHELIAL CELLS. *Journal of Urology*, 187 (4), e202.

Lai, R., Zheng, Y.-T., Shen, J.-H., Liu, G.-J., Liu, H., Lee, W.-H., Tang, S.-Z., and Zhang, Y., 2002. Antimicrobial peptides from skin secretions of Chinese red belly toad Bombina maxima. *Peptides*, 23 (3), 427–435.

Lakshmaiah Narayana, J. and Chen, J.-Y., 2015. Antimicrobial peptides: Possible anti-infective agents. *Peptides*, 72, 88–94.

de Latour, F.A., Amer, L.S., Papanstasiou, E.A., Bishop, B.M., and Hoek, M.L. van, 2010. *Antimicrobial activity of the Naja atra cathelicidin and related small peptides*. Biochemical and Biophysical Research Communications.

Laxminarayan, R., Duse, A., Wattal, C., Zaidi, A.K.M., Wertheim, H.F.L., Sumpradit, N., Vlieghe, E., Hara, G.L., Gould, I.M., Goossens, H., Greko, C., So, A.D., Bigdeli, M., Tomson, G., Woodhouse, W., Ombaka, E., Peralta, A.Q., Qamar, F.N., Mir, F., Kariuki, S., Bhutta, Z.A., Coates, A., Bergstrom, R., Wright, G.D., Brown, E.D., and Cars, O., 2013. Antibiotic resistance—the need for global solutions. *The Lancet Infectious Diseases*, 13 (12), 1057–1098.

Le, C.-F., Fang, C.-M., and Sekaran, S.D., 2017. Intracellular Targeting Mechanisms by Antimicrobial Peptides. *Antimicrobial agents and chemotherapy*, 61 (4).

Lee, D.G., Kim, H.N., Park, Y., Kim, H.K., Choi, B.H., Choi, C.-H., and Hahm, K.-S., 2002. Design of novel analogue peptides with potent antibiotic activity based on the antimicrobial peptide, HP (2–20), derived from N-terminus of Helicobacter pylori ribosomal protein L1. *Biochimica et Biophysica Acta (BBA) - Proteins and Proteomics*, 1598 (1–2), 185–194.

Lee, E.Y., Lee, M.W., and Wong, G.C.L., 2019. Modulation of toll-like receptor signaling by antimicrobial peptides. *Seminars in Cell and Developmental Biology*, 88, 173–184.

Lee, M.-R., Raman, N., Gellman, S.H., Lynn, D.M., and Palecek, S.P., 2017. Incorporation of β-Amino Acids Enhances the Antifungal Activity and Selectivity of the Helical Antimicrobial Peptide Aurein 1.2. *ACS Chemical*

Biology, 12 (12), 2975–2980.

Li, C. and Arakawa, T., 2019. Feasibility of circular dichroism to study protein structure at extreme concentrations. *International Journal of Biological Macromolecules*, 132, 1290–1295.

Li, C. and Salditt, T., 2006. Structure of magainin and alamethicin in model membranes studied by x-ray reflectivity. *Biophysical journal*, 91 (9), 3285–300.

Li, J., Koh, J.-J., Liu, S., Lakshminarayanan, R., Verma, C.S., and Beuerman, R.W., 2017. Membrane Active Antimicrobial Peptides: Translating Mechanistic Insights to Design. *Frontiers in Neuroscience*, 11, 73.

Li, W., Sani, M.-A., Jamasbi, E., Otvos, L., Hossain, M.A., Wade, J.D., and Separovic, F., 2016. Membrane interactions of proline-rich antimicrobial peptide, Chex1-Arg20, multimers. *Biochimica et Biophysica Acta (BBA) - Biomembranes*, 1858 (6), 1236–1243.

Li, Z., Hu, P., Wu, W., and Wang, Y., 2019a. Peptides with therapeutic potential in the venom of the scorpion Buthus martensii Karsch. *Peptides*, 115, 43–50.

Li, Z., Hu, P., Wu, W., and Wang, Y., 2019b. Peptides with therapeutic potential in the venom of the scorpion Buthus martensii Karsch. *Peptides*, 115, 43–50.

Lim, K. and Leong, S.S.J., 2018. Antimicrobial Coating Development Based on Antimicrobial Peptides. *Handbook of Antimicrobial Coatings*, 22, 509–532.

de Lima, D.C., Alvarez Abreu, P., de Freitas, C.C., Santos, D.O., Borges, R.O., Dos Santos, T.C., Mendes Cabral, L., Rodrigues, C.R., and Castro, H.C., 2005. Snake Venom: Any Clue for Antibiotics and CAM? *Evidence-based complementary and alternative medicine : eCAM*, 2 (1), 39–47.

Lin, Q., Deslouches, B., Montelaro, R.C., and Di, Y.P., 2018. Prevention of ESKAPE pathogen biofilm formation by antimicrobial peptides WLBU2 and LL37. *International Journal of Antimicrobial Agents*, 52, 667–672.

Lipinski, C.A., Dominy, B.W., and Feeney, P.J., 1997. *drug delivery reviews Experimental and computational approaches to estimate solubility and permeability in drug discovery and development settings*. Advanced Drug Delivery Reviews.

Liu, G.J., Simpson, A.M., Swan, M.A., Tao, C., Tuch, B.E., Crawford, R.M., Jovanovic, A., and Martin, D.K., 2003. ATP-sensitive potassium channels

induced in liver cells after transfection with insulin cDNA and the GLUT 2 transporter regulate glucose-stimulated insulin secretion. *The FASEB journal : official publication of the Federation of American Societies for Experimental Biology*, 17 (12), 1682–1684.

Livermore, D.M., Meunier, D., Hopkins, K.L., Doumith, M., Hill, R., Pike, R., Staves, P., and Woodford, N., 2018. Activity of ceftazidime/avibactam against problem Enterobacteriaceae and Pseudomonas aeruginosa in the UK, 2015–16. *Journal of Antimicrobial Chemotherapy*, 73 (3), 648–657.

Lohner, K. and Hilpert, K., 2016. Antimicrobial peptides. *Biochimica et biophysica acta*.

Longo, L.G., de Sousa, V.S., Kraychete, G.B., Justo-da-Silva, L.H., Rocha, J.A., Superti, S. V, Bonelli, R.R., Martins, I.S., and Moreira, B.M., 2019. Journal Pre-proof Colistin resistance emerges in pandrug-resistant Klebsiella pneumoniae epidemic clones in Rio de Janeiro, Brazil. *International Journal of Antimicrobial Agents Rio de Janeiro*.

Lutgring, J.D., 2019. Carbapenem-resistant Enterobacteriaceae: An emerging bacterial threat. *Seminars in Diagnostic Pathology*, 36, 182–186.

Lyukmanova, E.N., Shenkarev, Z.O., Schulga, A.A., Ermolyuk, Y.S., Mordvintsev, D.Y., Utkin, Y.N., Shoulepko, M.A., Hogg, R.C., Bertrand, D., Dolgikh, D.A., Tsetlin, V.I., and Kirpichnikov, M.P., 2007a. Bacterial expression, NMR, and electrophysiology analysis of chimeric short/long-chain alpha-neurotoxins acting on neuronal nicotinic receptors. *The Journal of biological chemistry*, 282 (34), 24784–91.

Lyukmanova, E.N., Shenkarev, Z.O., Schulga, A.A., Ermolyuk, Y.S., Mordvintsev, D.Y., Utkin, Y.N., Shoulepko, M.A., Hogg, R.C., Bertrand, D., Dolgikh, D.A., Tsetlin, V.I., and Kirpichnikov, M.P., 2007b. Bacterial expression, NMR, and electrophysiology analysis of chimeric short/long-chain α-neurotoxins acting on neuronal nicotinic receptors. *Journal of Biological Chemistry*, 282 (34), 24784–24791.

Ma, W., Zhang, D., Li, G., Liu, J., He, G., Zhang, P., Yang, L., Zhu, H., Xu, N., and Liang, S., 2017. Antibacterial mechanism of daptomycin antibiotic against Staphylococcus aureus based on a quantitative bacterial proteome analysis. *Journal of Proteomics*, 150, 242–251.

MacFadden, D.R., Bogoch, I.I., Brownstein, J.S., Daneman, N., Fisman, D., German, M., and Khan, K., 2015. A passage from India: Association between

air traffic and reported cases of New Delhi Metallo-beta-lactamase 1 from 2007 to 2012. *Travel medicine and infectious disease*, 13 (4), 295–9.

MacGowan, Alasdair Macnaughton, E., 2017. Antibiotic Resistance. *Medicine*, 45 (10), 622–628.

Machado, R.J.A., Estrela, A.B., Nascimento, A.K.L., Melo, M.M.A., Torres-Rêgo, M., Lima, E.O., Rocha, H.A.O., Carvalho, E., Silva-Junior, A.A., and Fernandes-Pedrosa, M.F., 2016. Characterization of TistH, a multifunctional peptide from the scorpion Tityus stigmurus: Structure, cytotoxicity and antimicrobial activity. *Toxicon*, 119, 362–370.

Macià, M.D., Luis Del Pozo, J., Díez-Aguilar, M., and Guinea, J., 2018. Microbiological diagnosis of biofilm-related infections. *Enfermedades Infecciosas y Microbiología Clínica*, 36 (6), 375–381.

Maeda, Y., Li, H., Yaoita, E., Yamamoto, T., Zhang, Y., Magdeldin, S., Yokoyama, M., Enany, S., Yoshida, Y., Fujinaka, H., Sasaki, S., and Xu, B., 2012. Murine colon proteome and characterization of the protein pathways. *BioData Mining*, 5 (1).

Mahlapuu, M., Håkansson, J., Ringstad, L., and Björn, C., 2016a. Antimicrobial Peptides: An Emerging Category of Therapeutic Agents. *Frontiers in cellular and infection microbiology*, 6 (194), 1–12.

Mahlapuu, M., Håkansson, J., Ringstad, L., and Björn, C., 2016b. Antimicrobial Peptides: An Emerging Category of Therapeutic Agents. *Frontiers in cellular and infection microbiology*, 6, 194.

Malanovic, N. and Lohner, K., 2016. Gram-positive bacterial cell envelopes: The impact on the activity of antimicrobial peptides. *Biochimica et biophysica acta*, 1858 (5), 936–46.

Manzo, G., Ferguson, P.M., Gustilo, V.B., Ali, H., Bui, T.T., Drake, A.F., Atkinson, R.A., Batoni, G., Lorenz, C.D., Phoenix, D.A., and Mason, A.J., 2018. Minor sequence modifications in temporin B cause drastic changes in antibacterial potency and selectivity by fundamentally altering membrane activity. *Scientific Reports*, 9 (1385).

Marr, A.K., Gooderham, W.J., and Hancock, R.E., 2006. Antibacterial peptides for therapeutic use: obstacles and realistic outlook. *Current opinion in pharmacology*, 6 (5), 468–72.

Martins, J.T., Cerqueira, M.A., Souza, B.W.S., Carmo Avides, M. do, and Vicente, A.A., 2010. Shelf Life Extension of Ricotta Cheese Using Coatings of

Galactomannans from Nonconventional Sources Incorporating Nisin against *Listeria monocytogenes*. *Journal of Agricultural and Food Chemistry*, 58 (3), 1884–1891.

Mates, S.M., Patel, L., Kaback, H.R., Mandel, L.J., Milazzo, J.J., Edberg, S.C., and Miller, M.H., 1982. *Membrane potential and gentamicin uptake in Staphylococcus aureus*.

Matsuzaki, K., 2009. Control of cell selectivity of antimicrobial peptides. *Biochimica et Biophysica Acta - Biomembranes*, 1788 (8), 1687–1692.

McCubbin, G.A., Praporski, S., Piantavigna, S., Knappe, D., Hoffmann, R., Bowie, J.H., Separovic, F., and Martin, L.L., 2011. QCM-D fingerprinting of membrane-active peptides. *European Biophysics Journal*, 40 (4), 437–446.

McEwen, S.A. and Collignon, P.J., 2018. Antimicrobial Resistance: a One Health Perspective. *Microbiology Spectrum*, 6 (2).

Mckerrow, J.H. and Lipinski, C.A., 2017. The rule of five should not impede anti-parasitic drug development. *International Journal for Parasitology*, 7, 248–249.

Meincken, M., Holroyd, D.L., and Rautenbach, M., 2005. Atomic force microscopy study of the effect of antimicrobial peptides on the cell envelope of Escherichia coli. *Antimicrobial agents and chemotherapy*, 49 (10), 4085–92.

Memariani, H., Shahbazzadeh, D., Ranjbar, R., Behdani, M., Memariani, M., and Pooshang Bagheri, K., 2016. Design and characterization of short hybrid antimicrobial peptides from pEM-2, mastoparan-VT1, and mastoparan-B. *Chemical Biology & Drug Design*.

Memariani, H., Shahbazzadeh, D., Sabatier, J.-M., Memariani, M., Karbalaeimahdi, A., and Bagheri, K.P., 2016. *Mechanism of action and in vitro activity of short hybrid antimicrobial peptide PV3 against Pseudomonas aeruginosa*. Biochemical and Biophysical Research Communications.

Meng, D.-M., Dai, H.-X., Gao, X.-F., Zhao, J.-F., Guo, Y.-J., Ling, X., Dong, B., Zhang, Z.-Q., and Fan, Z.-C., 2016. Expression, purification and initial characterization of a novel recombinant antimicrobial peptide Mytichitin-A in Pichia pastoris. *Protein Expression and Purification*, 127, 35–43.

Miao, V., Oise Coë Ffet-Legal, M.-F., Brian, P., Brost, R., Penn, J., Whiting, A., Martin, S., Ford, R., Parr, I., Bouchard, M., Silva, C.J., Wrigley, S.K., and Baltz, R.H., 2005. Daptomycin biosynthesis in Streptomyces roseosporus:

cloning and analysis of the gene cluster and revision of peptide stereochemistry. *Microbiology*, 151, 1507–1523.

Michael Conlon, J., Galadari, S., Raza, H., and Condamine, E., 2008. Design of Potent, Non-Toxic Antimicrobial Agents Based Upon the Naturally Occurring Frog Skin Peptides, Ascaphin-8 and Peptide XT-7. *Chemical Biology & Drug Design*, 72 (1), 58–64.

Mihajlovic, M. and Lazaridis, T., 2010. Antimicrobial peptides in toroidal and cylindrical pores. *Biochimica et biophysica acta*, 1798 (8), 1485–93.

Mihajlovic, M. and Lazaridis, T., 2012. Charge distribution and imperfect amphipathicity affect pore formation by antimicrobial peptides. *Biochimica et Biophysica Acta*, 1818, 1274–1283.

Mirski, T., Niemcewicz, M., Bartoszcze, M., Gryko, R., and Michalski, A., 2017. Utilisation of peptides against microbial infections – a review. *Annals of Agricultural and Environmental Medicine*, 25 (2), 205–210.

Miteva, M., Andersson, M., Karshikoff, A., and Otting, G., 1999. Molecular electroporation: a unifying concept for the description of membrane pore formation by antibacterial peptides, exemplified with NK-lysin. *FEBS Letters*, 462 (1–2), 155–158.

Miyashita, M., Kitanaka, A., Yakio, M., Yamazaki, Y., Nakagawa, Y., and Miyagawa, H., 2017. Complete de novo sequencing of antimicrobial peptides in the venom of the scorpion Isometrus maculatus. *Toxicon*, 139, 1–12.

Momin, M.A.M., Thien, S.J., Krittaphol, W., and Das, S.C., 2017. Simultaneous HPLC assay for pretomanid (PA-824), moxifloxacin and pyrazinamide in an inhaler formulation for drug-resistant tuberculosis. *Journal of Pharmaceutical and Biomedical Analysis*, 135, 133–139.

Moore, A.J., Beazley, W.D., Bibby, M.C., and Devine, D.A., 1996. Antimicrobial activity of cecropins. *Journal of Antimicrobial Chemotherapy*, 37 (6), 1077–1089.

Mosley, J.F., Smith, L.L., Parke, C.K., Brown, J.A., Wilson, A.L., Gibbs, L. V, and Gibbs, L. V., 2016. Ceftazidime-Avibactam (Avycaz): For the Treatment of Complicated Intra-Abdominal and Urinary Tract Infections. *P & T : a peer-reviewed journal for formulary management*, 41 (8), 479–83.

Müller, P., Pomorski, T., Porwoli, S., Tauber, R., and Herrmann, A., 1996. Transverse movement of spin-labeled phospholipids in the plasma membrane of a hepatocytic cell line (HepG2): Implications for biliary lipid

secretion. *Hepatology*, 24 (6), 1497–1503.

Münzker, L., Oddo, A., and Hansen, P.R., 2017. Chemical Synthesis of Antimicrobial Peptides. Humana Press, New York, NY, 35–49.

Mygind, P.H., Fischer, R.L., Schnorr, K.M., Hansen, M.T., Sönksen, C.P., Ludvigsen, S., Raventós, D., Buskov, S., Christensen, B., De Maria, L., Taboureau, O., Yaver, D., Elvig-Jørgensen, S.G., Sørensen, M. V., Christensen, B.E., Kjærulff, S., Frimodt-Moller, N., Lehrer, R.I., Zasloff, M., and Kristensen, H.-H., 2005. Plectasin is a peptide antibiotic with therapeutic potential from a saprophytic fungus. *Nature*, 437 (7061), 975–980.

Naafs, M.A., 2018. The Antimicrobial Peptides: Ready for Clinical Trials? *Biomedical Journal of Science and Technology*, 7 (4).

Najjar, K., Erazo-Oliveras, A., Brock, D.J., Wang, T.-Y., and Pellois, J.-P., 2017. An l- to d-Amino Acid Conversion in an Endosomolytic Analog of the Cell-penetrating Peptide TAT Influences Proteolytic Stability, Endocytic Uptake, and Endosomal Escape. *The Journal of biological chemistry*, 292 (3), 847–861.

Nakatsuji, T. and Gallo, R.L., 2012. Antimicrobial peptides: old molecules with new ideas. *The Journal of investigative dermatology*, 132 (3 Pt 2), 887–95.

Newton, K.A., Clench, M.R., Deshmukh, R., Jeyaseelan, K., and Strong, P.N., 2007. Mass fingerprinting of toxic fractions from the venom of the Indian red scorpion,Mesobuthus tamulus: biotope-specific variation in the expression of venom peptides. *Rapid Communications in Mass Spectrometry*, 21 (21), 3467–3476.

Ng, I.-S., Ye, C., Zhang, Z., Lu, Y., and Jing, K., 2014. Daptomycin antibiotic production processes in fed-batch fermentation by Streptomyces roseosporus NRRL11379 with precursor effect and medium optimization. *Bioprocess and Biosystems Engineering*, 37 (3), 415–423.

Nguyen, F., Starosta, A.L., Arenz, S., Sohmen, D., Dönhöfer, A., and Wilson, D.N., 2014. Tetracycline antibiotics and resistance mechanisms. *Biological Chemistry*, 395 (5), 559–75.

Nie, B., Ao, H., Zhou, J., Tang, T., and Yue, B., 2016. Biofunctionalization of titanium with bacitracin immobilization shows potential for anti-bacteria, osteogenesis and reduction of macrophage inflammation. *Colloids and Surfaces B: Biointerfaces*, 145, 728–739.

Nomura, K., Ferrat, G., Nakajima, T., Darbon, H., Iwashita, T., and Corzo, G.,

2005. Induction of Morphological Changes in Model Lipid Membranes and the Mechanism of Membrane Disruption by a Large Scorpion-Derived Pore-Forming Peptide. *Biophysical Journal*, 89 (6), 4067–4080.

O'Toole, G.A., 2011. Microtiter dish biofilm formation assay. *Journal of visualized experiments : JoVE*, (47).

Oddo, A., Nyberg, N.T., Frimodt-Møller, N., Thulstrup, P.W., and Hansen, P.R., 2015. The effect of glycine replacement with flexible ω-amino acids on the antimicrobial and haemolytic activity of an amphipathic cyclic heptapeptide. *European journal of medicinal chemistry*, 102, 574–81.

Ong, Z.Y. and Wiradharma, N., 2014. Strategies employed in the design and optimization of synthetic antimicrobial peptide amphiphiles with enhanced therapeutic potentials. *Advanced Drug Delivery Reviews*, 78, 28–45.

Opal, S., File, T.M., van der Poll, T., Tzanis, E., Chitra, S., and McGovern, P.C., 2019. An Integrated Safety Summary of Omadacycline, a Novel Aminomethylcycline Antibiotic. *Clinical Infectious Diseases*, 69 (Supplement_1), S40–S47.

Ortiz, E., Gurrola, G.B., Schwartz, E.F., and Possani, L.D., 2015. Scorpion venom components as potential candidates for drug development. *Toxicon : official journal of the International Society on Toxinology*, 93, 125–35.

Pal, I., Brahmkhatri, V.P., Bera, S., Bhattacharyya, D., Quirishi, Y., Bhunia, A., and Atreya, H.S., 2016. Enhanced stability and activity of an antimicrobial peptide in conjugation with silver nanoparticle. *Journal of Colloid and Interface Science*, 483, 385–393.

Pan, C., Kumar, C., Bohl, S., Klingmueller, U., and Mann, M., 2009. Comparative Proteomic Phenotyping of Cell Lines and Primary Cells to Assess Preservation of Cell Type-specific Functions. *Molecular & Cellular Proteomics*, 8 (3), 443–450.

Panteleev, P. V, Bolosov, I.A., Balandin, S. V, and Ovchinnikova, T. V, 2015. Design of antimicrobial peptide arenicin analogs with improved therapeutic indices. *Journal of peptide science : an official publication of the European Peptide Society*, 21 (2), 105–13.

Papp-Wallace, K.M., Endimiani, A., Taracila, M.A., and Bonomo, R.A., 2011. Carbapenems: past, present, and future. *Antimicrobial agents and chemotherapy*, 55 (11), 4943–60.

Park, S.-C., Kim, J.-Y., Shin, S.-O., Jeong, C.-Y., Kim, M.-H., Shin, S.Y., Cheong,

G.-W., Park, Y., and Hahm, K.-S., 2006. Investigation of toroidal pore and oligomerization by melittin using transmission electron microscopy. *Biochemical and Biophysical Research Communications*, 343, 222–228.

Parrino, B., Schillaci, D., Carnevale, I., Giovannetti, E., Diana, P., Cirrincione, G., and Cascioferro, S., 2019. Synthetic small molecules as anti-biofilm agents in the struggle against antibiotic resistance. *European Journal of Medicinal Chemistry*, 161, 154–178.

Pedron, C.N., Der, M., Torres, T., Aparecida, J., Lima, S., Silva, P.I., Dias Silva, F., and Oliveira, V.X., 2017. Novel designed VmCT1 analogs with increased antimicrobial activity. *European Journal of Medicinal Chemistry*, 126, 456–463.

Pedron, C.N., de Oliveira, C.S., da Silva, A.F., Andrade, G.P., da Silva Pinhal, M.A., Cerchiaro, G., da Silva Junior, P.I., da Silva, F.D., Torres, M.D.T., and Oliveira, V.X., 2019. The effect of lysine substitutions in the biological activities of the scorpion venom peptide VmCT1. *European Journal of Pharmaceutical Sciences*, 136.

Peleg, A.Y., Jara, S., Monga, D., Eliopoulos, G.M., Moellering, R.C., and Mylonakis, E., 2009. Galleria mellonella as a model system to study Acinetobacter baumannii pathogenesis and therapeutics. *Antimicrobial agents and chemotherapy*, 53 (6), 2605–9.

Penn, J., Li, X., Whiting, A., Latif, M., Gibson, T., Silva, C.J., Brian, P., Davies, J., Miao, V., Wrigley, S.K., and Baltz, R.H., 2006. Heterologous production of daptomycin in Streptomyces lividans. *Journal of Industrial Microbiology & Biotechnology*, 33 (2), 121–128.

Perez-Iratxeta, C. and Andrade-Navarro, M.A., 2008. K2D2: Estimation of protein secondary structure from circular dichroism spectra. *BMC Structural Biology*, 8 (1), 25.

Peri, A.M., Doi, Y., Potoski, B.A., Harris, P.N.A., Paterson, D.L., and Righi, E., 2019. Antimicrobial treatment challenges in the era of carbapenem resistance. *Diagnostic Microbiology and Infectious Disease*, 94, 413–425.

Perrin, B.S., Fu, R., Cotten, M.L., and Pastor, R.W., 2016. Simulations of Membrane-Disrupting Peptides II: AMP Piscidin 1 Favors Surface Defects over Pores. *Biophysical journaln*, 111 (6), 1258–1266.

Perron, G.G., Zasloff, M., and Bell, G., 2006. Experimental evolution of resistance to an antimicrobial peptide. *Proceedings. Biological sciences*, 273 (1583),

251–6.

Peschel, A. and Sahl, H.-G., 2006. The co-evolution of host cationic antimicrobial peptides and microbial resistance. *Nature Reviews Microbiology*, 4 (7), 529–536.

Peters, B.M., Shirtliff, M.E., and Jabra-Rizk, M.A., 2010. Antimicrobial peptides: primeval molecules or future drugs? *PLoS pathogens*, 6 (10), e1001067.

Poole, K., 2005. Efflux-mediated antimicrobial resistance. *Journal of Antimicrobial Chemotherapy*, 56 (1), 20–51.

Quesada, A., Ugarte-Ruiz, M., Iglesias, M.R., Porrero, M.C., Martínez, R., Florez-Cuadrado, D., Campos, M.J., García, M., Píriz, S., Sáez, J.L., and Domínguez, L., 2016. Detection of plasmid mediated colistin resistance (MCR-1) in Escherichia coli and Salmonella enterica isolated from poultry and swine in Spain. *Research in Veterinary Science*, 105, 134–135.

Ramírez-Carreto, S., Jiménez-Vargas, J.M., Rivas-Santiago, B., Corzo, G., Possani, L.D., Becerril, B., and Ortiz, E., 2015. Peptides from the scorpion Vaejovis punctatus with broad antimicrobial activity. *Peptides*, 73, 51–59.

Rathinakumar, R., Walkenhorst, W.F., and Wimley, W.C., 2009. Broad-Spectrum Antimicrobial Peptides by Rational Combinatorial Design and High-Throughput Screening: The Importance of Interfacial Activity. *Journal of the American Chemical Society*, 131 (22), 7609–7617.

Reeks, T.A., Fry, B.G., and Alewood, P.F., 2015. Privileged frameworks from snake venom. *Cellular and molecular life sciences : CMLS*, 72 (10), 1939–58.

Reißer, S., Strandberg, E., Steinbrecher, T., and Ulrich, A.S., 2014. 3D hydrophobic moment vectors as a tool to characterize the surface polarity of amphiphilic peptides. *Biophysical journal*, 106 (11), 2385–94.

Rhouma, M., Beaudry, F., and Letellier, A., 2016. Resistance to colistin: what is the fate for this antibiotic in pig production? *International Journal of Antimicrobial Agents*.

Rodríguez, A., Villegas, E., Montoya-Rosales, A., Rivas-Santiago, B., and Corzo, G., 2014a. Characterization of Antibacterial and Hemolytic Activity of Synthetic Pandinin 2 Variants and Their Inhibition against Mycobacterium tuberculosis. *PLoS ONE*, 9 (7), e101742.

Rodríguez, A., Villegas, E., Montoya-Rosales, A., Rivas-Santiago, B., and Corzo, G., 2014b. Characterization of antibacterial and hemolytic activity of

synthetic pandinin 2 variants and their inhibition against Mycobacterium tuberculosis. *PloS one*, 9 (7), e101742.

Rodvold, K.A., 2019. Introduction: lefamulin and pharmacokinetic/pharmacodynamic rationale to support the dose selection of lefamulin. *Journal of Antimicrobial Chemotherapy*, 74 (Supplement_3), iii2–iii4.

Rončević, T., Vukičević, D., Krce, L., Benincasa, M., Aviani, I., Maravić, A., and Tossi, A., 2019. BBA-Biomembranes Selection and redesign for high selectivity of membrane-active antimicrobial peptides from a dedicated sequence/function database. *BBA-Biomembranes*, 1861, 827–834.

Rossi, F., Girardello, R., Cury, A.P., Di Gioia, T.S.R., Almeida, J.N. de, and Duarte, A.J. da S., 2017. Emergence of colistin resistance in the largest university hospital complex of São Paulo, Brazil, over five years. *The Brazilian Journal of Infectious Diseases*, 21 (1), 98–101.

Sader, H.S., Fedler, K.A., Rennie, R.P., Stevens, S., and Jones, R.N., 2004. Omiganan Pentahydrochloride (MBI 226), a Topical 12-Amino-Acid Cationic Peptide: Spectrum of Antimicrobial Activity and Measurements of Bactericidal Activity. *Antimicrobial Agents and Chemotherapy*, 48 (8), 3112.

Sader, H.S., Rhomberg, P.R., Farrell, D.J., and Jones, R.N., 2015. Differences in potency and categorical agreement between colistin and polymyxin B when testing 15,377 clinical strains collected worldwide. *Diagnostic Microbiology and Infectious Disease*, 83, 379–381.

Saier, M.H., 2006. Protein Secretion Systems in Gram-Negative Bacteria Gram-negative bacteria possess many protein secretion-membrane insertion systems that apparently evolved independently. *Microbe*, 1 (9), 414–419.

Samy, R.P., Sethi, G., and Lim, L.H.K., 2016. A brief update on potential molecular mechanisms underlying antimicrobial and wound-healing potency of snake venom molecules. *Biochemical Pharmacology*, 115, 1–9.

Samy, R.P., Thwin, M.M., Stiles, B.G., Satyanarayana-Jois, S., Chinnathambi, A., Zayed, M.E., Alharbi, S.A., Siveen, K.S., Sikka, S., Kumar, A.P., Sethi, G., and Lim, L.H.K., 2015. Novel phospholipase A2 inhibitors from python serum are potent peptide antibiotics. *Biochimie*, 111, 30–44.

Sánchez, S. and Demain, A.L., 2017. The amazing world of antibiotics. *Biochemical Pharmacology*, 133, 1–3.

Sandhu, R., Wei, D., Sharma, M., and Xu, L., 2019. An N-terminal Flag-tag

impairs TPP1 regulation of telomerase function. *Biochemical and Biophysical Research Communications*, 512, 230–235.

Santos-Beneit, F., Ordóñez-Robles, M., and Martín, J.F., 2017. Glycopeptide resistance: Links with inorganic phosphate metabolism and cell envelope stress. *Biochemical Pharmacology*, 133, 74–85.

Sasaki, F., Okuno, T., Saeki, K., Min, L., Onohara, N., Kato, H., Shimizu, T., and Yokomizo, T., 2012. A high-affinity monoclonal antibody against the FLAG tag useful for G-protein-coupled receptor study. *Analytical Biochemistry*, 425, 157–165.

Schittek, B., Hipfel, R., Sauer, B., Bauer, J., Kalbacher, H., Stevanovic, S., Schirle, M., Schroeder, K., Blin, N., Meier, F., Rassner, G., and Garbe, C., 2001. Dermcidin: a novel human antibiotic peptide secreted by sweat glands. *Nature Immunology*, 2 (12), 1133–1137.

Schmidtchen, A., Pasupuleti, M., and Malmsten, M., 2014. Effect of hydrophobic modifications in antimicrobial peptides. *Advances in Colloid and Interface Science*, 205, 265–274.

Schurer, N., Kohne, A., Schliep, V., Barlag, K., and Goerz, G., 1993. Lipid composition and synthesis of HaCaT cells, an immortalized human keratinocyte line, in comparison with normal human adult keratinocytes. *Experimental Dermatology*, 2 (4), 179–185.

Selsted, M.E., Novotnytll, M.J., Morris, W.L., Tang, Y.-Q., Smith, W., and Cullor, J.S., 1992. Indolicidin, a Novel Bactericidal Tridecapeptide Amide from Neutrophils*. *Journal of Biological Chemistry*, 267 (7), 4292–4295.

Semreen, M.H., El-Gamal, M.I., Abdin, S., Alkhazraji, H., Kamal, L., Hammad, S., El-Awady, F., Waleed, D., and Kourbaj, L., 2018. Recent updates of marine antimicrobial peptides. *Saudi Pharmaceutical Journal*, 26, 396–409.

Sengupta, D., Leontiadou, H., Mark, A.E., and Marrink, S.-J., 2008. Toroidal pores formed by antimicrobial peptides show significant disorder. *Biochimica et biophysica acta*, 1778, 2308–2317.

Shaeer, K.M., Zmarlicka, M.T., Chahine, E.B., Piccicacco, N., and Cho, J.C., 2019. Plazomicin: A Next-Generation Aminoglycoside. *Pharmacotherapy*, 39 (1), 77–93.

Shah, P., Hsiao, F.S.-H., Ho, Y.-H., and Chen, C.-S., 2016. The proteome targets of intracellular targeting antimicrobial peptides. *Proteomics*, 16 (8), 1225–1237.

Shai, Y., 1999. Mechanism of the binding, insertion and destabilization of phospholipid bilayer membranes by α-helical antimicrobial and cell non-selective membrane-lytic peptides. *Biochimica et Biophysica Acta (BBA) - Biomembranes*, 1462 (1–2), 55–70.

Shai, Y., 2002. Mode of action of membrane active antimicrobial peptides. *Biopolymers*, 66 (4), 236–48.

Sharma, H. and Nagaraj, R., 2015. Chapter 3 – Structure–Activity Relationships in the Host-Defense Antimicrobial Peptides Defensins. *In*: *Studies in Natural Products Chemistry*. 69–97.

Singh, A., Upadhyay, V., Upadhyay, A.K., Singh, S.M., and Panda, A.K., 2015. Protein recovery from inclusion bodies of Escherichia coli using mild solubilization process. *Microbial cell factories*, 14, 41.

Singha, P., Locklin, J., and Handa, H., 2017. A review of the recent advances in antimicrobial coatings for urinary catheters. *Acta Biomaterialia*, 50, 20–40.

Sinha, M.S. and Kesselheim, A.S., 2016. Regulatory Incentives for Antibiotic Drug Development: A Review of Recent Proposals.

Smith, J.R., Ning, Y., and Pereira-Smith, O.M., 1992. Why are transformed cells immortal? Is the process reversible? *The American Journal of Clinical Nutrition*, 55 (6), 1215S-1221S.

Sohlenkamp, C. and Geiger, O., 2016. Bacterial membrane lipids: diversity in structures and pathways. *FEMS Microbiology Reviews*, 40 (1), 133–159.

Solomkin, J.S., Gardovskis, J., Lawrence, K., Montravers, P., Sway, A., Evans, D., and Tsai, L., 2018. IGNITE4: Results of a Phase 3, Randomized, Multicenter, Prospective Trial of Eravacycline vs Meropenem in the Treatment of Complicated Intraabdominal Infections. *Clinical Infectious Diseases*.

Song, C., Weichbrodt, C., Salnikov, E.S., Dynowski, M., Forsberg, B.O., Bechinger, B., Steinem, C., de Groot, B.L., Ulrich, Z., and Zeth, K., 2013. Crystal structure and functional mechanism of human antimicrobial membrane channel. *PNAS*, 110 (12), 4586–4591.

Song, D., Chen, Y., Li, X., Zhu, M., and Gu, Q., 2014. HETEROLOGOUS EXPRESSION AND PURIFICATION OF DERMASEPTIN S4 FUSION IN *Escherichia coli* AND RECOVERY OF BIOLOGICAL ACTIVITY. *Preparative Biochemistry and Biotechnology*, 44 (6), 598–607.

Stepanenko, A.A. and Kavsan, V., 2012. Immortalization and malignant

transformation of eukaryotic cells. *Cytology and Genetics*, 46 (2), 96–129.

Stewart, P.S. and Costerton, J.W., 2001. Antibiotic resistance of bacteria in biofilms. *The Lancet*, 358 (9276), 135–138.

Stott, J.B., Povstyan, O. V, Carr, G., Barrese, V., and Greenwood, I.A., 2015. G-protein βγ subunits are positive regulators of Kv7.4 and native vascular Kv7 channel activity: Supporting Information. *PNAS*, 112 (20), 6497–6502.

Takahashi, H., Caputo, G.A., Vemparala, S., and Kuroda, K., 2017. Synthetic Random Copolymers as a Molecular Platform To Mimic Host-Defense Antimicrobial Peptides. *Bioconjugate Chemistry*, 28 (5), 1340–1350.

Talbot, G.H., Bradley, J., Edwards, J.E., Gilbert, D., Scheld, M., and Bartlett, J.G., 2006. Bad Bugs Need Drugs: An Update on the Development Pipeline from the Antimicrobial Availability Task Force of the Infectious Diseases Society of America. *Clinical Infectious Diseases*, 42 (5), 657–668.

Tang, S.S., Apisarnthanarak, A., and Hsu, L.Y., 2014. Mechanisms of ??-lactam antimicrobial resistance and epidemiology of major community- and healthcare-associated multidrug-resistant bacteria. *Advanced Drug Delivery Reviews*, 78, 3–13.

Tanhaiean, A., Azghandi, M., Razmyar, J., Mohammadi, E., and Hadi Sekhavati, M., 2018a. Recombinant production of a chimeric antimicrobial peptide in E. coli and assessment of its activity against some avian clinically isolated pathogens. *Microbial Pathogenesis*, 122, 73–78.

Tanhaiean, A., Azghandi, M., Razmyar, J., Mohammadi, E., and Hadi Sekhavati, M., 2018b. Recombinant production of a chimeric antimicrobial peptide in E. coli and assessment of its activity against some avian clinically isolated pathogens. *Microbial Pthogenesis*, 122, 73–78.

Taute, H., Bester, M.J., Neitz, A.W.H., and Gaspar, A.R.M., 2015. Investigation into the mechanism of action of the antimicrobial peptides Os and Os-C derived from a tick defensin. *Peptides*, 71, 179–87.

Taylor, S.D. and Palmer, M., 2016. The action mechanism of daptomycin. *Bioorganic & medicinal chemistry*, 24, 6253–6268.

Teixeira, V., Feio, M.J., Rivas, L., De La Torre, B.G., Andreu, D., Coutinho, A., and Bastos, M., 2010. Influence of Lysine N ε-Trimethylation and Lipid Composition on the Membrane Activity of the Cecropin A-Melittin Hybrid Peptide CA(1-7)M(2-9) †. *Journal of Physical Chemistry*, 114, 16198–16208.

Torcato, I.M., Huang, Y.-H., Franquelim, H.G., Gaspar, D., Craik, D.J., Castanho,

M.A.R.B., and Troeira Henriques, S., 2013. Design and characterization of novel antimicrobial peptides, R-BP100 and RW-BP100, with activity against Gram-negative and Gram-positive bacteria. *Biochimica et Biophysica Acta (BBA) - Biomembranes*, 1828 (3), 944–955.

Torres, M.D.T., Sothiselvam, S., Lu, T.K., and de la Fuente-Nunez, C., 2019. Peptide Design Principles for Antimicrobial Applications. *Journal of Molecular Biology*.

Tossi, A., Sandri, L., and Giangaspero, A., 2000a. Amphipathic, ?-helical antimicrobial peptides. *Biopolymers*, 55 (1), 4–30.

Tossi, A., Sandri, L., and Giangaspero, A., 2000b. Amphipathic, α-helical antimicrobial peptides. *Biopolymers*, 55 (1), 4–30.

Travkova, O.G., Moehwald, H., and Brezesinski, G., 2017. The interaction of antimicrobial peptides with membranes. *Advances in Colloid and Interface Science*, 247, 521–532.

Uematsu, N. and Matsuzaki, K., 2000. *Polar Angle as a Determinant of Amphipathic a-Helix-Lipid Interactions: A Model Peptide Study*. Biophysical Journal.

Valdez-Velazquéz, L.L., Romero-Gutierrez, M.T., Delgado-Enciso, I., Dobrovinskaya, O., Melnikov, V., Quintero-Hernández, V., Ceballos-Magaña, S.G., Gaitan-Hinojosa, M.A., Coronas, F.I., Puebla-Perez, A.M., Zamudio, F., De la Cruz-García, I., Vázquez-Vuelvas, O.F., Soriano-Hernandez, A.D., and Possani, L.D., 2016. Comprehensive analysis of venom from the scorpion Centruroides tecomanus reveals compounds with antimicrobial, cytotoxic, and insecticidal activities. *Toxicon : official journal of the International Society on Toxinology*, 118, 95–103.

Vaneperen, A.S. and Segreti, J., 2016. Empirical therapy in Methicillin-resistant Staphylococcus Aureus infections: An Up-To-Date approach.

Ventola, C.L., 2015. The antibiotic resistance crisis: part 1: causes and threats. *P & T : a peer-reviewed journal for formulary management*, 40 (4), 277–83.

Viens, A.M. and Littmann, J., 2015. Is Antimicrobial Resistance a Slowly Emerging Disaster? *Public health ethics*, 8 (3), 255–265.

Walia, K., Sharma, M., Vijay, S., and Shome, B.R., 2019. Understanding policy dilemmas around antibiotic use in food animals & offering potential solutions. *The Indian journal of medical research*, 149 (2), 107–118.

Walker, J. and Moore, G., 2015. Pseudomonas aeruginosa in hospital water

systems: biofilms, guidelines, and practicalities. *Journal of Hospital Infection*, 89 (4), 324–327.

Wang-Kan, X., Blair, J.M.A., Chirullo, B., Betts, J., La Ragione, R.M., Ivens, A., Ricci, V., Opperman, T.J., and Piddock, L.J. V, 2017. Lack of AcrB Efflux Function Confers Loss of Virulence on Salmonella enterica Serovar Typhimurium. *mBio*, 8 (4), e00968-17.

Wanmakok, M., Orrapin, S., Intorasoot, A., and Intorasoot, S., 2018. Expression in Escherichia coli of novel recombinant hybrid antimicrobial peptide AL32-P113 with enhanced antimicrobial activity in vitro. *Gene*, 671, 1–9.

Wellington, E.M.H., Boxall, A.B.A., Cross, P., Feil, E.J., Gaze, W.H., Hawkey, P.M., Johnson-Rollings, A.S., Jones, D.L., Lee, N.M., Otten, W., Thomas, C.M., and Williams, A.P., 2013. The role of the natural environment in the emergence of antibiotic resistance in Gram-negative bacteria. *The Lancet*, 13, 155–165.

Wibowo, D. and Zhao, C.-X., 2019. Recent achievements and perspectives for large-scale recombinant production of antimicrobial peptides. *Applied Microbiology and Biotechnology*, 103 (2), 659–671.

Wilkening, S., Stahl, F., Bader, A., and Prough, R.A., 2003. Comparison of primary human hepatocytes and hepatoma cell line Hepg2 with regard to their biotransformation properties. *Drug metabolism and disposition: the biological fate of chemicals*, 31 (8), 1035–42.

Willcox, M.D.P., Hume, E.B.H., Aliwarga, Y., Kumar, N., and Cole, N., 2008. A novel cationic-peptide coating for the prevention of microbial colonization on contact lenses. *Journal of Applied Microbiology*, 105 (6), 1817–1825.

Williams, J.F. and Worely, S.D., 2000. Infection-Resistant Nonleachable Materials for Urologic Devices. *Journal of Endourology*, 14 (5), 395–400.

Wimley, W.C., 2010. Describing the mechanism of antimicrobial peptide action with the interfacial activity model. *ACS chemical biology*, 5 (10), 905–17.

De Winter, J.C.F., 2013. Using the Student's t-test with extremely small sample sizes, 18 (10).

Wright, G.D., 2005. Bacterial resistance to antibiotics: Enzymatic degradation and modification. *Advanced Drug Delivery Reviews*, 57, 1451–1470.

Wu, M., Maier, E., Benz, R., and Hancock, R.E.W., 1999. Mechanism of Interaction of Different Classes of Cationic Antimicrobial Peptides with Planar Bilayers and with the Cytoplasmic Membrane of Escherichia coli †.

Biochemistry, 38, 7235–7242.

Wu, T., Tang, D., Chen, W., Huang, H., Wang, R., and Chen, Y., 2013. Expression of antimicrobial peptides thanatin(S) in transgenic Arabidopsis enhanced resistance to phytopathogenic fungi and bacteria.

Wurm, F.M., 2004. Production of recombinant protein therapeutics in cultivated mammalian cells. *Nature Biotechnology*, 22 (11), 1393–1398.

Xiao, H., Shao, F., Wu, M., Ren, W., Xiong, X., Tan, B., and Yin, Y., 2015. The application of antimicrobial peptides as growth and health promoters for swine. *Journal of Animal Science and Biotechnology*, 6 (1), 19.

Yandek, L.E., Pokorny, A., Florén, A., Knoelke, K., Langel, U., and Almeida, P.F.F., 2007. Mechanism of the cell-penetrating peptide transportan 10 permeation of lipid bilayers. *Biophysical journal*, 92 (7), 2434–44.

Yang, N., Wang, X., Teng, D., Mao, R., Hao, Y., Zong, L., Feng, X., and Wang, J., 2016. Modification and characterization of a new recombinant marine antimicrobial peptide N2. *Process Biochemistry*, 51, 734–739.

Yang, X., Wang, Y., Lee, W.-H., and Zhang, Y., 2013. Antimicrobial peptides from the venom gland of the social wasp Vespa tropica. *Toxicon*, 74, 151–157.

Ye, J., Zhao, H., Wang, H., Bian, J., and Zheng, R., 2010. A defensin antimicrobial peptide from the venoms of Nasonia vitripennis. *Toxicon*, 56 (1), 101–106.

Yeaman, M.R. and Yount, N.Y., 2003. Mechanisms of Antimicrobial Peptide Action and Resistance, 55 (1), 27–55.

Yidong, G., Bo, W., Yongxia, G., Wen, L., Xiaoli, Z., Xiaofeng, H., Jianghua, Y., D, G.Y., X, G.Y., L, Z.X., F, H.X., and H, Y.J., 2017. Occurrence and Fate of Antibiotics in the Aqueous Environment and Their Removal by Constructed Wetlands in China: A review. *Pedosphere*, 27 (1), 42–51.

Yoo, J. and Cui, Q., 2008. Does Arginine Remain Protonated in the Lipid Membrane? Insights from Microscopic pKa Calculations. *Biophysical Journal*, 94 (8), L61–L63.

Young, S.A., Desbois, A.P., Coote, P.J., and Smith, T.K., 2019. Characterisation of Staphylococcus aureus lipids by nanoelectrospray ionisation tandem mass spectrometry (nESI-MS/MS). *bioRxiv*, 593483.

Yu, H., Li, H., Gao, D., Gao, C., and Qi, Q., 2015. Secretory production of antimicrobial peptides in Escherichia coli using the catalytic domain of a cellulase as fusion partner. *Journal of Biotechnology*, 214, 77–82.

Yuan, Y., Zai, Y., Xi, X., Ma, C., Wang, L., Zhou, M., Shaw, C., and Chen, T., 2019. A novel membrane-disruptive antimicrobial peptide from frog skin secretion against cystic fibrosis isolates and evaluation of anti-MRSA effect using Galleria mellonella model. *BBA - General Subjects*, 1863, 849–856.

Zasloff, M., 1987. Magainins, a class of antimicrobial peptides from Xenopus skin: isolation, characterization of two active forms, and partial cDNA sequence of a precursor. *Proceedings of the National Academy of Sciences of the United States of America*, 84 (15), 5449–53.

Zasloff, M., 2002. Antimicrobial peptides of multicellular organisms. *Nature*, 415 (6870), 389–395.

Zhang, Y., Algburi, A., Wang, N., Kholodovych, V., Oh, D.O., Chikindas, M., and Uhrich, K.E., 2017. Self-assembled cationic amphiphiles as antimicrobial peptides mimics: Role of hydrophobicity, linkage type, and assembly state. *Nanomedicine: Nanotechnology, Biology and Medicine*, 13 (2), 343–352.

Zhao, H., Sood, R., Jutila, A., Bose, S., Fimland, G., Nissen-Meyer, J., and Kinnunen, P.K.J., 2006. Interaction of the antimicrobial peptide pheromone Plantaricin A with model membranes: Implications for a novel mechanism of action. *Biochimica et Biophysica Acta (BBA) - Biomembranes*, 1758 (9), 1461–1474.

Zhou, H., Fang, J., Tian, Y., and Lu, X.Y., 2014. Mechanisms of nisin resistance in Gram-positive bacteria. *Annals of Microbiology*, 64 (2), 413–420.

Zhu, M., Liu, P., and Niu, Z.-W., 2017a. A perspective on general direction and challenges facing antimicrobial peptides. *Chinese Chemical Letters*, 28, 703–708.

Zhu, M., Liu, P., and Niu, Z.-W., 2017b. A perspective on general direction and challenges facing antimicrobial peptides. *Chinese Chemical Letters*, 28 (4), 703–708.

Zhu, S. and Gao, B., 2013. Evolutionary origin of β-defensins. *Developmental and comparative immunology*, 39 (1–2), 79–84.

Zhu, S., Peigneur, S., Gao, B., Umetsu, Y., Ohki, S., and Tytgat, J., 2014. Experimental Conversion of a Defensin into a Neurotoxin: Implications for Origin of Toxic Function. *Molecular Biology and Evolution*, 31 (3), 546–559.

Zhu, X., Dong, N., Wang, Z., Ma, Z., Zhang, L., Ma, Q., and Shan, A., 2014. Design of imperfectly amphipathic α-helical antimicrobial peptides with enhanced cell selectivity. *Acta biomaterialia*, 10 (1), 244–57.

Appendix

Growth curve analysis of *E. coli* BL21 λDE3 containing the Smp24 vector. Once bacterial growth reached mid-log phase (approximately 0.6 OD_{600}) isopropyl-1-thio-β-D-galactopyranoside (IPTG) was added to varying concentrations (0.025mM to 2mM) and the growth was observed by recording the OD_{600} every 20 minutes over 18 hours. Data presents the average of three replicates. As shown in the appendix 1, upon addition of IPTG, the growth rate of *E. coli* was reduced, thus suggesting energy was spent on protein production with less energy available for bacterial growth.

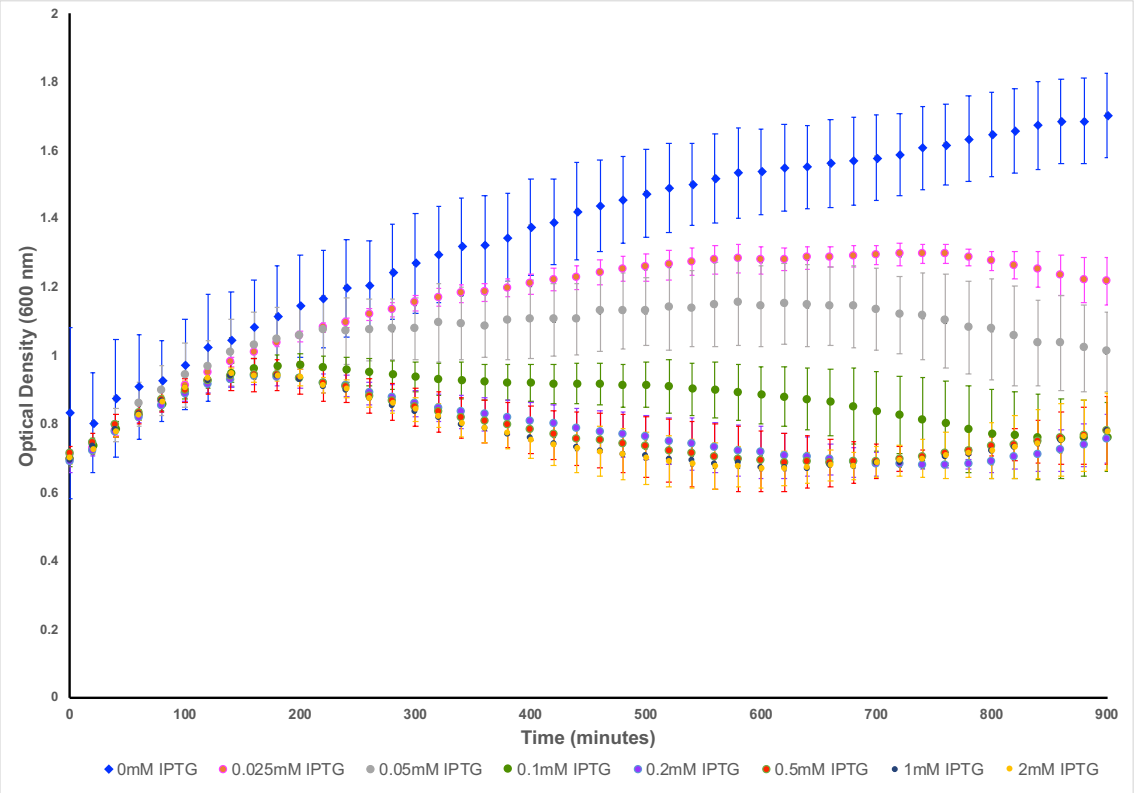

Appendix 1: Growth rate of *E. coli* BL21 λDE3 upon addition of varying concentrations of IPTG